

Supramolecular dendritic architectures

Citation for published version (APA):

Broeren, M. A. C. (2005). *Supramolecular dendritic architectures*. [Phd Thesis 1 (Research TU/e / Graduation TU/e), Chemical Engineering and Chemistry]. Technische Universiteit Eindhoven.
<https://doi.org/10.6100/IR598845>

DOI:

[10.6100/IR598845](https://doi.org/10.6100/IR598845)

Document status and date:

Published: 01/01/2005

Document Version:

Publisher's PDF, also known as Version of Record (includes final page, issue and volume numbers)

Please check the document version of this publication:

- A submitted manuscript is the version of the article upon submission and before peer-review. There can be important differences between the submitted version and the official published version of record. People interested in the research are advised to contact the author for the final version of the publication, or visit the DOI to the publisher's website.
- The final author version and the galley proof are versions of the publication after peer review.
- The final published version features the final layout of the paper including the volume, issue and page numbers.

[Link to publication](#)

General rights

Copyright and moral rights for the publications made accessible in the public portal are retained by the authors and/or other copyright owners and it is a condition of accessing publications that users recognise and abide by the legal requirements associated with these rights.

- Users may download and print one copy of any publication from the public portal for the purpose of private study or research.
- You may not further distribute the material or use it for any profit-making activity or commercial gain
- You may freely distribute the URL identifying the publication in the public portal.

If the publication is distributed under the terms of Article 25fa of the Dutch Copyright Act, indicated by the "Taverne" license above, please follow below link for the End User Agreement:

www.tue.nl/taverne

Take down policy

If you believe that this document breaches copyright please contact us at:

openaccess@tue.nl

providing details and we will investigate your claim.

Supramolecular Dendritic Architectures

Supramolecular Dendritic Architectures

PROEFSCHRIFT

ter verkrijging van de graad van doctor aan de Technische Universiteit Eindhoven, op gezag van de Rector Magnificus, prof.dr.ir. C.J. van Duijn, voor een commissie aangewezen door het College voor Promoties in het openbaar te verdedigen op donderdag 8 december 2005 om 16.00 uur

door

Martinus Adrianus Cornelis Broeren

geboren te Nijmegen

Dit proefschrift is goedgekeurd door de promotor:

prof.dr. E.W. Meijer

Copromotor:

dr.ir. M.H.P. van Genderen

This research has been financially supported by the Council for Chemical Sciences of the Netherlands Organization for Scientific Research (NWO-CW).

Omslagontwerp: Koen Pieterse, Maarten Broeren en Jan-Willem Luiten (JWL Producties)

Druk: Universiteitsdrukkerij, Technische Universiteit Eindhoven

CIP-DATA LIBRARY TECHNISCHE UNIVERSITEIT EINDHOVEN

Broeren, Martinus A.C.

Supramolecular dendritic architectures / by Martinus A.C. Broeren. –
Eindhoven : Technische Universiteit Eindhoven, 2005.

Proefschrift. – ISBN 90-386-2947-8

NUR 913

Subject headings: dendritic polymers ; polyamines / supramolecular chemistry / inclusion compounds / drug delivery systems / NMR spectroscopy / combinatorial chemistry ; dynamic libraries

Trefwoorden: dendrimeren ; polyaminen / supramoleculaire chemie / inkapseling / medicijnafgifte ; formuleringen / NMR-spectroscopie / host-guest chemie / massaspectrometrie / combinatoriële chemie ; dynamische bibliotheken

“Maar de schapen hadden hem wel iets anders geleerd, iets wat nog veel belangrijker was: dat er een taal bestond die iedereen begreep en die de jongen gedurende heel die tijd gebruikt had om de zaak te doen floreren. Dat was de taal van de geestdrift, van de dingen die je doet met hart en ziel, op zoek naar iets wat je wilt of waar je in gelooft.”

P. Coelho
De alchemist

Voor mijn ouders

Contents

Chapter 1. Dendrimers in supramolecular chemistry	1
1.1 Introduction	1
1.2 The synthesis and conformation of dendrimers	2
1.3 Binding valency	5
1.4 Dendritic host–guest systems	6
1.4.1 Aspecific binding.....	6
1.4.2 Monovalent binding.....	7
1.4.3 Multiple monovalent interactions - no cooperativity.....	10
1.4.4 Cooperativity in multiple monovalent interactions	15
1.5 Aim and scope of this thesis.....	20
1.6 References	23
Chapter 2. The synthesis, characterization and 3D-structure of supramolecular dendritic architectures	27
2.1 Introduction	28
2.2 Synthesis of host molecules, guest molecules and complexes	29
2.2.1 Synthesis of the dendritic hosts	29
2.2.2 Synthesis of carboxylic acid guests	30
2.2.3 Synthesis of phosphonic acid guests.....	32
2.2.4 Synthesis of sulfonic acid guests	33
2.2.5 General preparation of dendritic host–guest complexes.....	33
2.3 Chirality as a probe for the packing density of non-covalently bound guests to dendrimers.....	35
2.3.1 Introduction	35
2.3.2 Synthesis of the guest molecule.....	37
2.3.3 Analysis of the complex	38
2.3.4 Conclusions	40
2.4 The 3-dimensional structure of dendritic host–guest complexes	40
2.4.1 Introduction	40
2.4.2 X-ray diffraction	41
2.4.3 Molecular dynamics simulations	43
2.4.4 Conclusions	45
2.5 Experimental section.....	45
2.6 References	52

Chapter 3. Supramolecular dendritic architectures in the gas phase **55**

3.1 Introduction.....	56
3.2 The Quadrupole Time-of-Flight (Q/TOF) Instrument.....	57
3.3 Gas phase studies of dendritic host–guest complexes.....	59
3.3.1 Influence of acid strength, molecular weight and loading.....	59
3.3.2 Oligo-peptide complexes.....	65
3.4 Chloroform vs the gas phase.....	68
3.5 Gas phase simulations.....	71
3.6 Conclusions.....	73
3.7 Experimental section.....	74
3.8 Appendix: The kinetic model.....	75
3.9 References.....	77

Chapter 4. Supramolecular dendritic architectures in chloroform **79**

4.1 Introduction.....	80
4.2 The location of guests in supramolecular dendritic aggregates determined by ^1H - ^1H NOESY spectroscopy.....	81
4.3 Multi-component host–guest chemistry of carboxylic and phosphonic acid based guests with dendritic hosts.....	85
4.3.1 Designing the system.....	85
4.3.2 Introduction of the ^{13}C -label.....	86
4.3.3 Analysis of the complexes by ^1H NMR techniques.....	87
4.3.4 Complexation observed by ^{13}C NMR.....	90
4.3.5 Complexation observed by ^{31}P NMR.....	93
4.3.6 Quantitative analysis of binding.....	95
4.3.7 Exchange.....	96
4.3.8 Interpretation of the NMR data.....	97
4.3.9 Dynamic light scattering.....	100
4.4 Conclusions.....	101
4.5 Experimental section.....	103
4.6 Appendix.....	105
4.7 References.....	107

Chapter 5. Supramolecular dendritic architectures in water **109**

5.1 Introduction.....	110
5.2 The preparation of supramolecular dendritic architectures in water.....	111
5.3 Stability of the aggregates.....	115
5.4 The structure of dendritic host–guest complexes in water.....	117
5.5 ^{13}C NMR and ^{31}P NMR complexation studies in D_2O	122
5.5.1 Oligoethylene glycol guests.....	122

5.5.2 Guest molecules with MRI labels.....	127
5.5.3 Peptide guest molecules.....	128
5.6 Overall conclusions.....	130
5.7 Epilogue.....	132
5.8 References.....	133
Summary.....	135
Samenvatting.....	137
Curriculum Vitae.....	139
List of publications.....	140
Dankwoord.....	141

Chapter 1

Dendrimers in supramolecular chemistry

1.1 INTRODUCTION

The field of supramolecular chemistry has been defined as “chemistry beyond the covalent bond”, and aims to understand how molecules specifically interact with other molecules, resulting in more complex structures that exert a certain function.^{1, 2} The most beautiful examples of supramolecular chemistry are found in living systems. Most, if not all, biological functions are controlled by the non-covalent interactions between molecules that play a role in signal transduction, the selective transport of ions or small molecules, the generation and storage of energy and replication.³ These tremendously complicated processes have in common that they often occur through multiple interactions. Non-covalent interactions such as electrostatic interactions, van der Waals forces, hydrophobic interactions, hydrogen bonding, metal coordination or π - π stacking interactions are individually much weaker than covalent bonds, but can collectively form highly specific and strong interactions.⁴ In order to construct multicomponent supramolecular assemblies analogous to assemblies found in the natural world, a fundamental understanding of multiple, non-covalent interactions is required.⁵ In the design of functional, multicomponent supramolecular architectures, dendrimers can play an important role.

Dendrimers are well-defined, highly-branched macromolecules that emanate from a central core.^{6, 7} After the first reports of highly branched molecules, Maciejewski⁸ and De Gennes⁹ presented a theoretical discussion of dendritic molecules as ideal container molecules (hosts) for smaller molecules (guests). It was recognized that dendrimers, due to their branched structure and tendency to form spherical objects at higher generation, have localized micro-environments or cavities similar to the active site of enzymes. In addition, the discrete number and high concentration of end groups allow the preparation of scaffolds with multiple ligands or recognition sites. It is the combination of these properties that makes dendrimers ideal molecules for the formation of well-defined, multicomponent supramolecular assemblies and gives the opportunity to investigate multiple binding events in great detail.

In this chapter, the synthesis and properties of dendrimers are discussed, followed by their role in the field of host-guest chemistry.¹⁰⁻¹³

1.2 THE SYNTHESIS AND CONFORMATION OF DENDRIMERS

Ideally, dendrimers are perfectly monodisperse macromolecules with a regular and highly branched structure. These macromolecules are produced in an iterative sequence of reaction steps, in which each repetition of steps results in a new generation. This can either be done from core to periphery (the divergent method)¹⁴ or from periphery to core (the convergent method).¹⁵ Vögtle was the first to report a synthetic route to branched structures.¹⁶ The first dendritic structures that have received widespread attention are Tomalia's "PAMAM" dendrimers^{17, 18} and Newkome's "arborol" dendrimers,¹⁹ both synthesized divergently. On the basis of the work of Vögtle, divergently prepared poly(propylene imine) dendrimers (PPI dendrimers) were reported at a later date by Mühlaupt²⁰ and de Brabander.²¹ The convergent method was introduced by Fréchet and Hawker^{22, 23} through the synthesis of poly(benzylether) dendrimers. The four families of dendrimers are depicted in figure 1.1.

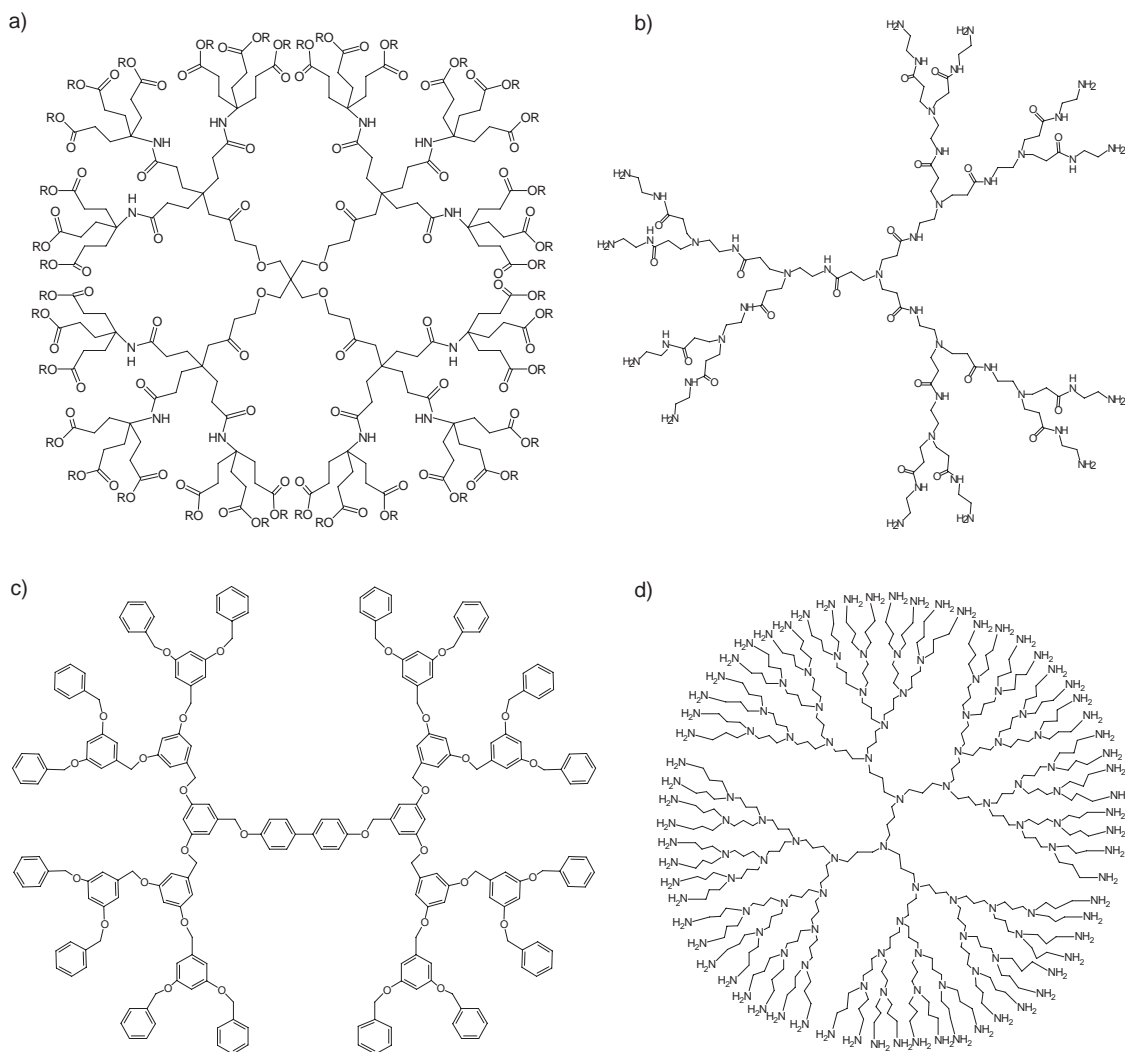


Figure 1.1 a) Newkome's arborols b) Tomalia's poly(amidoamine) dendrimers (PAMAMs) c) Fréchet's polyether dendrimers d) the poly(propylene imine) dendrimers.

The strength of the convergent synthesis lies in the possibility to purify the dendrons after each coupling step. Furthermore, all kinds of functional groups can be incorporated at the periphery, branches or core of the dendrimer, making this synthetic methodology very suitable for “tailor-made” dendrimers with specific properties. However, these steps are elaborate and therefore not suitable for large-scale production. Only two classes of dendrimers are commercially available, poly(amidoamine) dendrimers and poly(propylene imine) dendrimers. The synthesis of the latter starts with a double Michael addition with acrylonitrile to both primary amines of 1,4-diaminobutane followed by a Raney/Co catalysed hydrogenation of the 4 nitrile endgroups to the corresponding amines. A repetition of these steps results in the formation of the 2nd, 3rd, 4th and 5th generation poly(propylene imine) dendrimer. Due to the large number of reactions that are performed on a single molecule, the presence of a small number of statistical defects cannot be avoided. Where the 3rd generation dendrimer is virtually defect free, the 5th generation shows a purity of 23%, with a polydispersity of 1.002.²⁴

The primary amines at the periphery can be used for further modification of the dendrimer. The properties of the entities attached to the periphery of dendrimers, together with the branched architectures of the dendrimer itself, determine its overall size, shape and function.^{6, 7, 14, 25} The synthesis and properties of dendrimers for specific applications have been reported extensively, and include fields like medicinal chemistry,²⁶⁻²⁸ catalysis,²⁹ and light harvesting and photo induced processes.³⁰ Applications in the field of host–guest chemistry with dendrimers include enzyme mimetics,³¹ drug delivery³² and catalysis.³³

There has been significant controversy about the shape of dendrimers, and the placement of their chain ends either at the “periphery” of the globular macromolecule or back-folded within its branches.^{14, 25} A variety of calculations and measurements have suggested backfolding of the chain ends, while others confirmed the end groups to be at the periphery. Most dendrimers have been shown to be flexible, whereas some of the largest seem to be more rigid. In general, dendrimers are globular macromolecules that acquire significant rigidity only at high generation. This is also determined by the dendrimer end group. High generation dendrimers with large, bulky end groups are much more rigid than dendrimers with flexible end groups. This was demonstrated by Meijer and coworkers with a study of functionalized dendrimers at the air–water interface (Figure 1.2).³⁴

A poly(propylene imine) dendrimer was modified with long alkyl chains, resulting in a dendritic structure with a hydrophilic interior and hydrophobic end groups. The dendrimer can only interact with the water surface through the hydrophilic interior of the structure, and not through the hydrophobic chain ends. As a result, the dendrimer changes shape from a globular structure — the structure favored in non-polar solvents — to a flattened conformation in which the dendrimer interior maximizes its association with the water surface and the hydrophobic end groups are forced upward and away from the water surface. The same experiment performed with the more bulky

adamantyl groups at the periphery of the poly(propylene imine) dendrimer did not result in stable monolayers due to the more rigid character of the dendrimer.

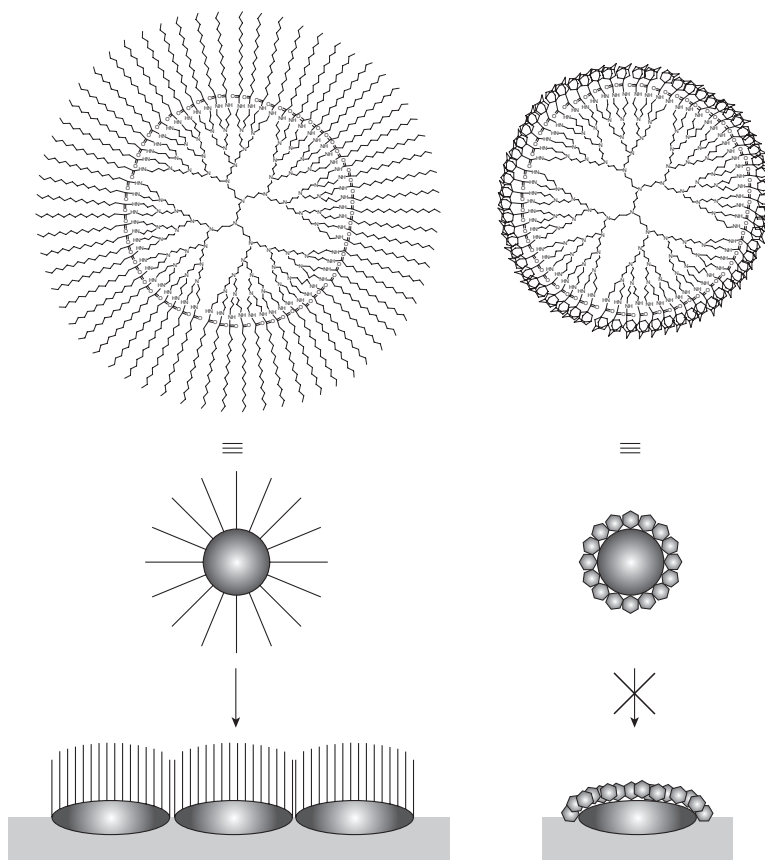


Figure 1.2 A PPI dendrimer modified with alkyl chains is flexible enough to refold in such a way that its interior is able to interact with a water surface, while the hydrophobic tails face upward (left). The more bulky adamantyl dendrimers are much more rigid, and cannot form stable monolayers (right).

The question of the existence of cavities within dendrimers has also been raised frequently. The fact that molecules have been encapsulated inside dendrimers proves the presence of cavities, but this does not mean that dendrimers have a permanent and rigid cavity. Most dendrimers are flexible enough to encapsulate a guest, especially when favorable interactions exist. Overall, the conformation is determined by the free energy, and dendrimers react to their environment to minimize their free energy. In a good solvent, a dendrimer may be fully extended and adopt a spherical shape. In a bad solvent or in the absence of solvent, the volume collapses and the resulting structure is determined by the flexibility of the dendrimer, the interactions between its various components, and the interactions with other molecules. Depending on the conditions used, the cavities can be filled up by end groups, solvent molecules, or guests.

Before examples of host–guest systems based on dendrimers are discussed, it is important to clearly define the different modes of binding that can be present between a ligand and a receptor, as well as the role of cooperativity in binding events with a multivalent guest and/or host. This is done in the following section.

1.3 BINDING VALENCY

The valency of a molecule is defined as the number of separate binding events a molecule can form with another particle through ligand–receptor interactions.⁴ Both a receptor and a ligand can be monovalent or multivalent, giving rise to three different types of binding (Figure 1.3). A monovalent ligand that binds to a monovalent receptor results in a monovalent complex. When multiple monovalent ligands bind to a multivalent receptor, multiple monovalent complexes occur. The simultaneous binding of multiple ligands of one entity to multiple receptors of another results in a multivalent interaction. Multivalent interactions can be much stronger than monovalent interactions due to the statistical and chelate effect.^{27, 35, 36}

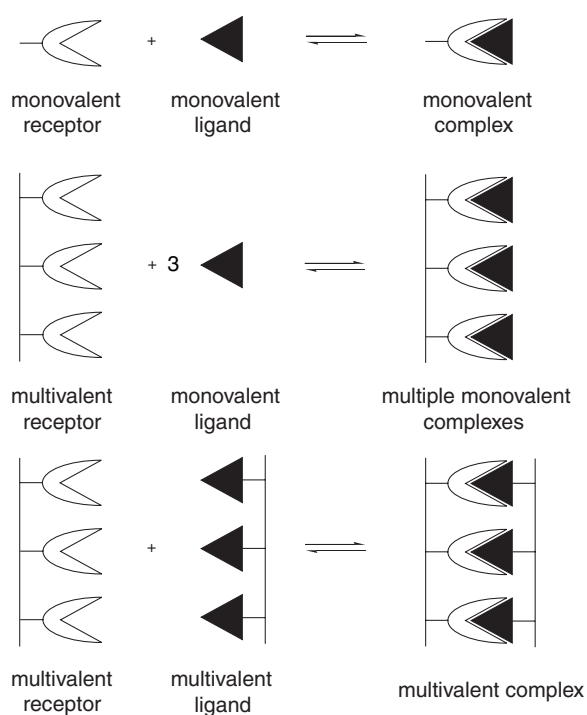


Figure 1.3 *The three modes of binding between monovalent and multivalent ligands and receptors.*

An important aspect in these three binding modes is cooperativity, which is defined as the influence of the binding of a ligand to a receptor site on the binding strength of subsequent ligands to free receptor sites. For the situation of multiple monovalent interactions, cooperativity has been defined unambiguously, and can be determined mathematically by the analysis of a Scatchard or Hill plot. A well-known example from biology is the binding of oxygen to hemoglobin, which has four receptor sites. In this specific case, the binding of the first oxygen molecule increases the binding strength of hemoglobin toward the subsequent oxygen molecules. The assessment of cooperativity in synthetic systems, e.g. the binding of multiple, monovalent guests to a multivalent dendrimer, can be performed in an identical fashion.

In multivalent interactions, cooperativity also plays an important role. In biology, several models have been derived to assess cooperativity, for example in the helix-to-coil transition of polypeptides or the formation or melting of DNA duplexes.^{37, 38} However, in synthetic systems cooperativity has not been defined clearly and is a source of much confusion. The presence of both inter- and intramolecular interactions, together with all kinds of symmetry effects that have to be considered, make the assessment of cooperativity in multivalent systems very difficult. Furthermore, cooperativity is often claimed when multiple interactions between a ligand and a receptor site take place. Almost always, the binding between a receptor site and a ligand takes place via multiple interactions. When these interactions take place all at once, it is not really possible to speak about multiple binding events, and therefore about cooperativity. The result is a monovalent interaction. When the multiple interactions do not take place all at once, the binding of the receptor and the ligand can be described as multivalent. In this case it is the chelate effect, and not cooperativity, that is found frequently.

Dendrimers, being multivalent molecules, are ideal building blocks to analyze multiple monovalent and multivalent interactions. The following sections give an overview of the field of host–guest chemistry with dendrimers, with a focus on multiple, monovalent interactions. First, aspecific binding of guests to dendrimers is briefly described. Subsequently, specific binding of monovalent guests to single and multiple binding sites on the dendrimer are described. The mathematical background for the assessment of cooperativity is discussed. Cooperativity has only been demonstrated in a few cases, which will be discussed in more detail.

1.4 DENDRITIC HOST–GUEST SYSTEMS

1.4.1 Aspecific binding

The ability of dendrimers to entrap the simplest guests molecules around, i.e. solvent molecules, was first recognized by Seebach et al.³⁹ Very stable complexes, called “clathrates”, were formed between chiral dendrimers and several solvent molecules like tetrachloromethane, ethyl acetate and 1,4-dioxane. The dendrimers could only be freed from their guests by prolonged heating of the complexes at reduced pressure. A year later, the physical entrapment of “real” guests inside dendrimers was demonstrated by Jansen and Meijer.^{40, 41} Small molecules with some affinity for the tertiary amines of poly(propylene imine) dendrimers were present during the functionalization of the periphery of the dendrimer with bulky Boc-protected amino acids. The resulting highly dense, hydrogen-bonded shell prohibited guests from diffusing out of the dendrimer, resulting in a dendritic container also known as the “dendritic box”.

Guests can be encapsulated by dendrimers through a variety of interactions. Hydrophobic dendrimers with a hydrophilic periphery, like the unimolecular micelles of Newkome⁴² and

Fréchet^{43, 44} are able to encapsulate hydrophobic guests in water through hydrophobic interactions. Poly(amidoamine) dendrimers generated from a diaminododecane core with polar primary amine end groups provided a hydrophobic environment for the hydrophobic dye Nile Red in water.⁴⁵ Even the much more hydrophilic poly(propylene imine) dendrimer is able to encapsulate hydrophobic guests in water, but the encapsulation efficiency is strongly dependent on the pH of the aqueous phase. At a pH above 10, the dendrimer is only partly protonated, and pyrene prefers to be in the less polar microenvironment of the dendrimer. When the pH is lowered, the primary and tertiary amines get protonated, and pyrene is expelled to the aqueous phase.⁴⁶ The affinity of poly(propylene imine) dendrimers with polar endgroups to hydrophobic guests is enhanced by acid–base interactions, as has been demonstrated by Baars and Meijer.⁴⁷ A binding constant of $5 \times 10^5 \text{ M}^{-1}$ for Rose Bengal was obtained in buffered aqueous media at pH 7. Other examples of guest binding in water include the binding of ions to hydrophilic dendrimers.⁴⁸⁻⁵¹

When the periphery of dendrimers is modified with hydrophobic groups, the dendrimers become soluble in organic solvents and behave as inverted micelles.^{52, 53} These dendrimers can be used to efficiently extract anionic dyes⁵³ and ions⁵⁴ from water into organic solvents like dichloromethane, toluene and supercritical CO₂.⁵⁵

The incorporation of specific recognition sites into dendrimers enables more detailed studies on the binding between a guest and a host, and on how the binding is influenced by the structure of the dendrimer. The following paragraph discusses the binding of monovalent guests to monovalent dendritic hosts.

1.4.2 Monovalent binding

Diederich developed dendrimers with a cyclophane recognition site for small steroids and aromatic guests (Figure 1.4).^{56, 57} Due to the water-soluble dendritic wedges, the whole structure becomes water-soluble, while the guests bind to the hydrophobic cyclophane interior via π – π interactions. The structure can be compared to a globular protein with a hydrophobic active site buried inside the molecule.

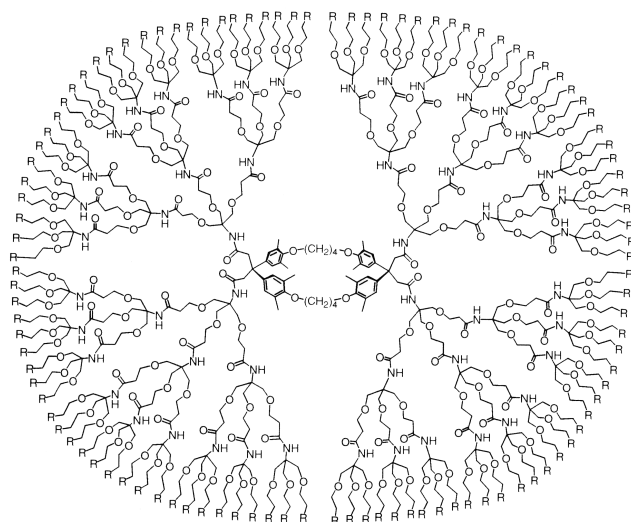


Figure 1.4 Diederich's dendrophane.

The influence of the dendritic architecture on the accessibility of a recognition site in the core has been nicely illustrated by Aida and coworkers.^{58, 59} They prepared Fréchet-type dendrimers with a single zinc porphyrin core, and found that the morphology of the dendrimer changes from open to closed as the generation is increased from 1 to 5 (Figure 1.5). This was confirmed with binding experiments to dendritic imidazoles. The higher the generation of the dendritic host, the lower the association constant of the guest. For the largest guest, a reduction in the association constant from $3.6 \times 10^4 \text{ M}^{-1}$ to $2.4 \times 10^2 \text{ M}^{-1}$ (150 fold decrease) was observed. Since then, several other examples of site isolation have been reported.^{30, 31, 60}

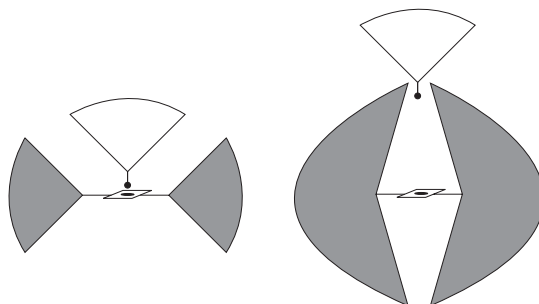


Figure 1.5 Schematic representation of the principle of site isolation, described by Aida *et al.* For low generation dendritic wedges (gray), the bulky imidazole guest (white) is able to coordinate to the zinc porphyrin core. When the dendritic host becomes more bulky, the binding is hampered.

Zimmerman and coworkers were among the first to prepare dendritic hosts with single hydrogen bonding units at the core.^{61, 62} Dendritic hosts with naphthyridine units at their core could hydrogen bond to complementary benzamidinium guests, though no difference in hydrogen bond strength was observed with respect to model compounds indicating that the micro-environment inside the dendrimer is similar to the solvent. In many other examples, the micro-environment inside dendrimers has shown to be clearly different from the solvent. A recent example comes from the

work of Kaifer. Electrochemical measurements performed on the redox-active center of Newkome-type dendrons modified with a viologen derivative indicated that the micropolarity near the focal point (Figure 1.6) increases with increasing generation.⁶³

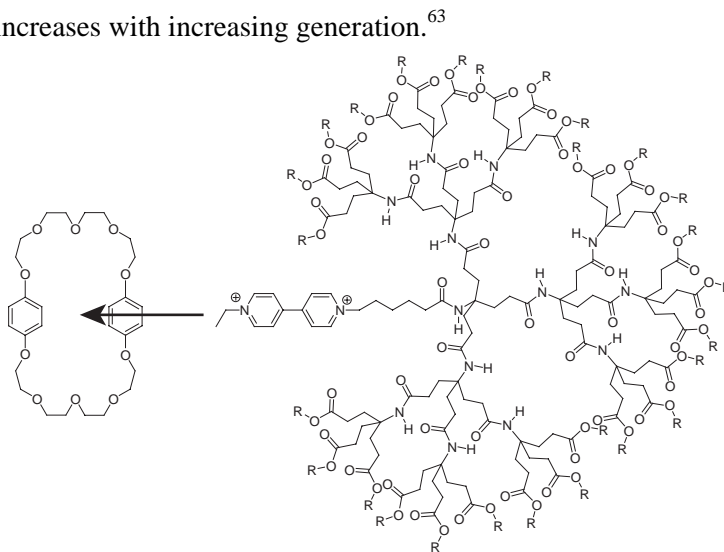


Figure 1.6 Binding of a third generation Newkome-type dendrimer with a viologen unit at the core to a crown ether. The binding is negatively influenced by the size of the dendrimer.

However, the binding to bis-*p*-phenylene-34-crown-8 appeared to be strongly dependent on the dendrimer size, and a decrease of the association constant for higher generation dendrimers in acetone was found. This is most likely due to steric hindrance of the dendritic architecture. On the other hand, no significant difference in binding was observed for increasing generations of Fréchet-type dendrimers modified with a viologen unit at the core. Several other reports from this group discuss the interaction between a dendrimer with a single recognition site and a receptor.⁶⁴⁻⁶⁷

Almost all examples of dendrimers containing a single recognition site in the core are based on existing ligand and receptor motifs. Recently, the group of Zimmerman demonstrated that it is also possible to create hosts for specific guests via another way: molecular imprinting.^{68, 69} The approach comprises three steps: 1) the covalent attachment of dendrons with polymerizable end groups to the template with cleavable bonds, 2) cross-linking of the dendron end groups, and 3) removal of the template. In the specific example shown in figure 1.7, porphyrin was used as the template molecule. The alkene endgroups were cross-linked using the Grubbs catalyst, and the resulting cross-linked structure was treated with potassium hydroxide in tetrahydrofuran to remove the porphyrin template. The hydrolysis reaction results in 8 additional –OH groups, and therefore does not result in an ideal imprint of the template porphyrin itself. However, it has shown to be an effective binding site for closely related porphyrins. Binding studies of several porphyrin molecules to the dendritic host indicated selective and tight binding with apparent association constants around 10^5 M^{-1} in toluene. Furthermore, porphyrins that cannot interact at all four binding contacts in the host did not show any binding under the conditions used in the study (Figure 1.7b). In a similar manner, the recognition of amines was investigated.^{70, 71}

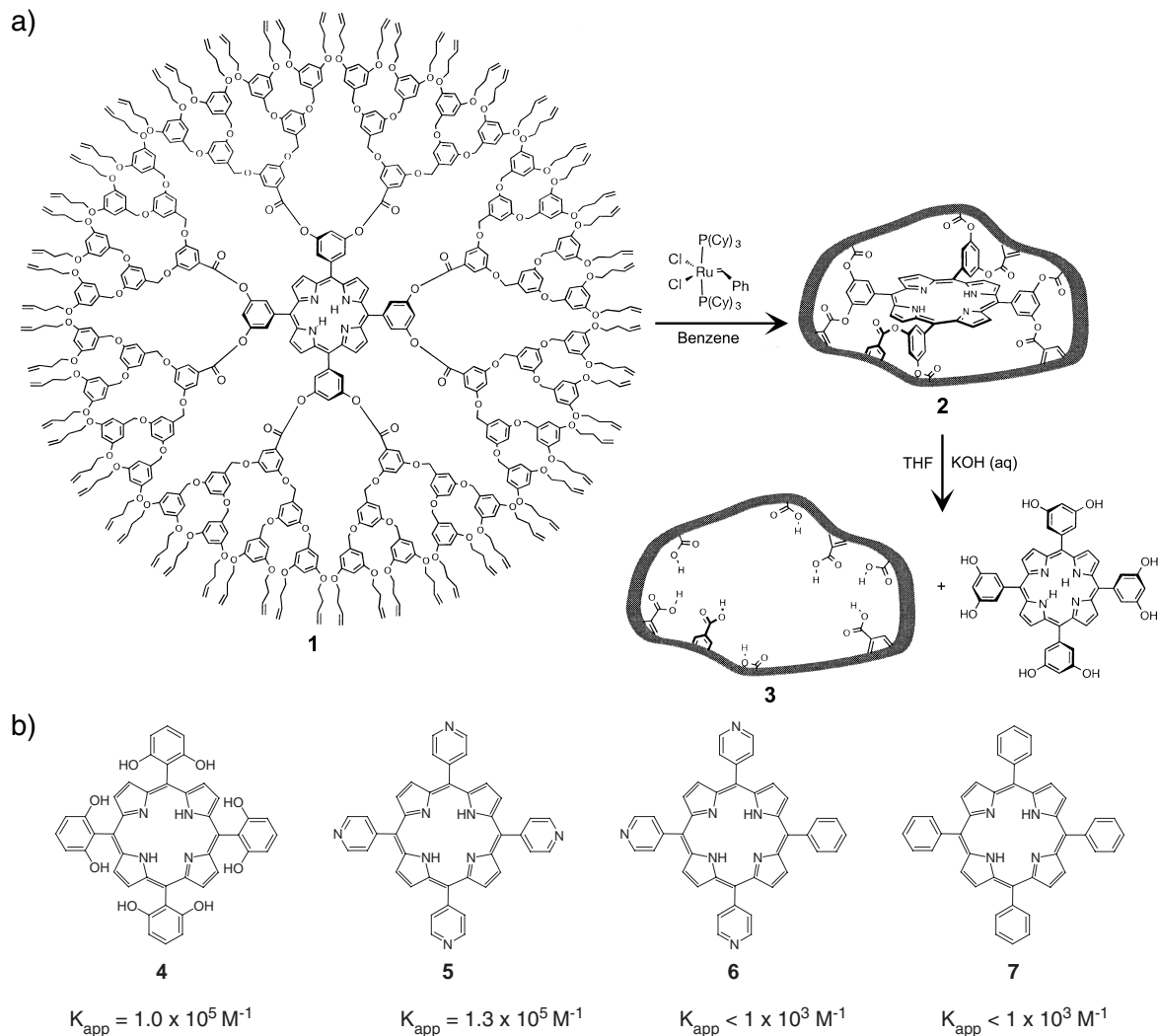


Figure 1.7 a) The preparation of imprinted dendrimer **3**. Polymerisation of porphyrin dendrimer **1** results in the formation of molecule **2**. The porphyrin core is removed under basic conditions resulting in imprinted structure **3**. b) Different porphyrin molecules interact strongly with **3**, but only when the guest can interact via the original four binding contacts (compare guest **4** and **5** versus guest **6** and **7**).

Overall, we can conclude that the complexation of guests to dendrimers with single binding sites can be investigated in great detail. Three species can be present in solution: free ligand, free receptor and the complex, and via spectroscopic techniques the concentrations of these species can be determined. In the following section, this aspect is evaluated for the situation of multiple monovalent complexes.

1.4.3 Multiple monovalent interactions - no cooperativity

It is important to realize that all host–guest systems are dynamic. Though supramolecular aggregates consisting of multiple monovalent interactions are often displayed in a static picture, the binding between a host and a guest is a dynamic process and exchange takes place constantly. The actual supramolecular aggregates present in solution are determined by the concentrations of guest

and host and the association constant between binding site and ligands. When the concentration and association constant are known, and non-cooperative binding is assumed (the binding of a guest does not influence the binding of another guest), it is possible to determine the degree of complexation.⁷² For a simple, monovalent complex this phenomenon is easy to be visualized. However, for multiple, monovalent complexes, many different complexes can be present, which makes it more difficult to describe the real situation adequately. An example is given in table 1.1, which shows how the number of bound and free guests is influenced by the association constant between a ligand and a receptor. In this specific theoretical example, the dendrimer contains 32 identical binding sites to which 32 guests are added at a dendrimer concentration of 1 mM. The degree of complexation is here defined as the ratio between the number of bound guests versus the total number of guests. Here, no cooperativity is assumed.

Table 1.1 Calculations of the number of bound guest, free guest and the degree of complexation (θ) for increasing association constants, in the situation of a dendrimer containing 32 binding sites together with 32 guests at a concentration of 1 mM of dendrimer.

Association constant (M^{-1})	Guest/host ratio	Number of bound guests	Number of free guests	Degree of complexation (θ)
10^1	32	6.5	25.5	0.20
10^2	32	18.4	17.6	0.57
10^3	32	26.8	5.2	0.84
10^4	32	30.3	1.7	0.95
10^5	32	31.4	0.6	0.98
10^6	32	31.8	0.2	0.99

The calculations show that in order to get complexation of most ligands to the dendrimer, the association constant must be quite high (around 10^4 – 10^5 M^{-1} at a dendrimer concentration of 1 mM). When the association constant becomes lower, the dendrimer will only be partly functionalized by the guests. Furthermore, the degree of complexation is an average value, meaning that a distribution of host–guest complexes is present in solution, ideally a binomial distribution. These aspects must be taken into account in the evaluation of multiple monovalent complexes. In the following examples of multiple, monovalent interactions, no cooperativity has been assumed.

An example of multiple, monovalent interactions can be found in a very interesting recent paper by Aida et al.⁷³ The group synthesized several porphyrin dendrimers that are able to host multiple, chiral bidentate guests (Figure 1.8). Interestingly, the RR and SS enantiomers of the guest give strong (and opposite) signals in circular dichroism (CD) spectra upon complexation to the dendritic hosts. The *meso*-guest binds equally strong, but does obviously not give any chiroptical response.

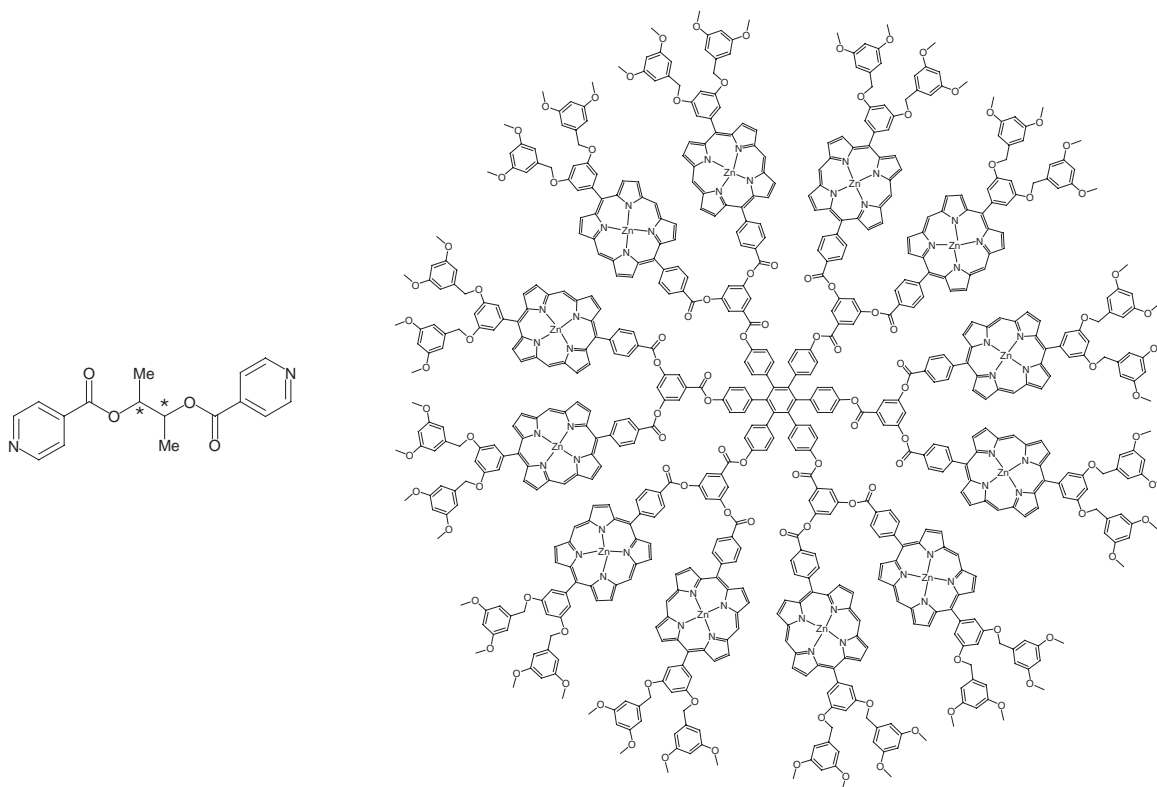


Figure 1.8 Example of a dendrimer appended with zinc porphyrin units (right), that is able to host multiple bidentate guests (left).

Reinhoudt and Huskens investigated the binding of urea–adamantyl functionalized poly(propylene imine) dendrimers with β -cyclodextrin in aqueous media (Figure 1.9).⁷⁴ All five dendrimer generations are insoluble in water, even at low pH. The addition of a slight excess of β -cyclodextrin relative to the number of adamantyl endgroups resulted in solubilization of the dendrimers at low pH. This is due to the complexation of the hydrophobic adamantyl groups to the hydrophobic interior of the β -cyclodextrin cavity.

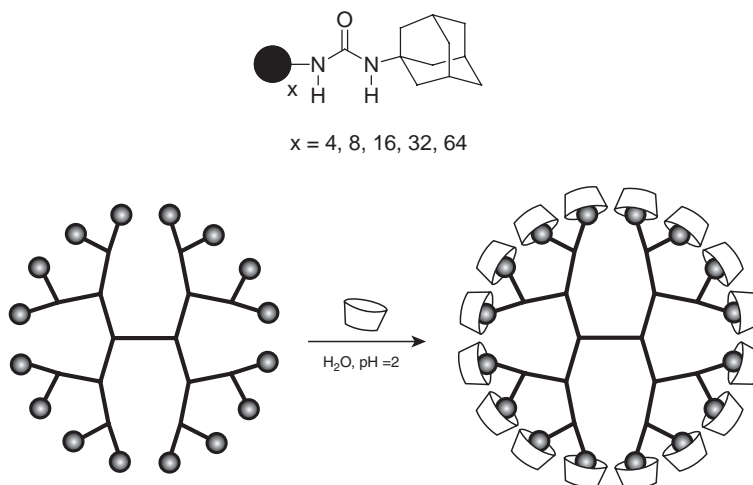


Figure 1.9 Top: The urea–adamantyl dendrimers used by Reinhoudt *et al.* The black disk represents the dendritic interior. Bottom: Schematic representation of the complexation of β -cyclodextrin to the third generation urea–adamantyl dendrimer in water, resulting in solubilization of the dendritic structure.

The hydrophilic outside of the β -cyclodextrin molecules renders the complete structure hydrophilic, resulting in solubilization of the dendritic structure in water. ^1H NMR titration experiments demonstrated that in case of generation 1 to 4, all adamantyl groups are bound to β -cyclodextrin. For the fifth generation dendrimer, incomplete complexation was observed due to steric congestion of the β -cyclodextrin molecules at the periphery of the dendrimer. These results were confirmed with calculations of the outer surface of the dendrimer, which is larger than the total surface occupied by the β -cyclodextrin molecules for generation 1 to 4, but not for generation 5. Association constants of the binding of neutral adamantyl derivatives to β -cyclodextrin in water are around 10^5 – 10^6 M^{-1} . These high values, in combination with the bad solubility of the dendrimers in water, drive the binding of β -cyclodextrin molecules to the dendrimer to full complexation.

The groups of Kaifer⁷⁵ and Kim⁷⁶ have reported similar supramolecular dendritic structures, based on the binding of cobaltocenium units to β -cyclodextrin, and the binding of doubly charged diaminobutane to cucurbituril respectively.

The binding of multiple guests to the interior of dendrimers has recently been reported by Stoddart et al.⁷⁷ Two dendrimers containing 9 and 21 viologen units in their branches have been prepared and analysed (Figure 1.10). The dicationic viologens are known to interact with crown ethers, but can also bind to the dianionic dye eosin in dichloromethane. Eosin has an intense fluorescence band, which is completely quenched upon complexation to the viologen unit. A titration experiment of dioctylviologen to eosin in dichloromethane indicated a strong 1:1 complex with an association constant $> 10^6$ M^{-1} .

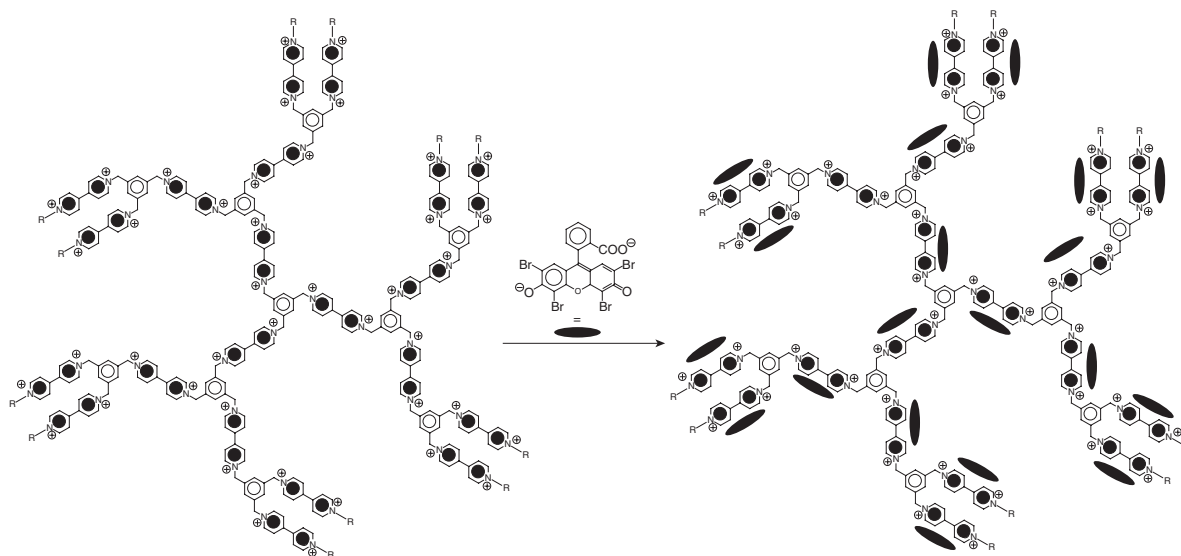


Figure 1.10 The dendritic structure reported by Stoddart et al., with 21 viologen moieties in its branches. All viologens are able to strongly bind eosin molecules in dichloromethane.

When eosin is titrated to the dendrimers in dichloromethane, the fluorescence band of eosin remains absent until more than one eosin molecule per viologen is present. This demonstrates that the binding is strong, and that all eosin molecules are bound to the dendrimer at this concentration.

Crooks and coworkers reported the binding of fatty acids onto the surface of amine terminated poly(amidoamine) dendrimers (Figure 1.11).⁷⁸ A solution of 1% dodecanoic acid in toluene is able to extract a fourth generation amine terminated PAMAM dendrimer from water into the organic phase. This corresponds to 70–80 molecules of acid per dendrimer. The fatty acids assemble around the dendrimer based on acid–base interactions with the primary amines of the dendrimer, resulting in an aggregate that resembles an inverted micelle with a relatively hydrophilic core and a hydrophobic periphery. Like the inverted micelles, the supramolecular aggregate is able to extract hydrophobic dyes into the organic phase. The binding of the acids is obviously not very specific, and complexation to the inner tertiary amines of the dendrimer cannot be excluded. This was confirmed with IR-measurements at higher ratios of dodecanoic acid per dendrimer, indicating that the inner tertiary amines are protonated as well.⁷⁹

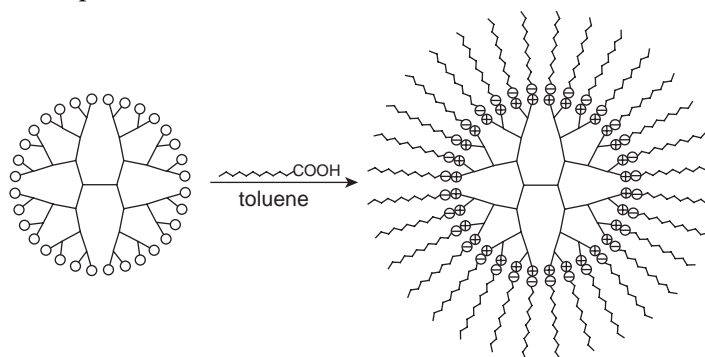


Figure 1.11 The formation of a supramolecular inverted micelle in toluene, described by Crooks and coworkers.

Meijer and coworkers used poly(propylene imine) dendrimers modified with urea–adamantyl end groups to bind ureido–acetic acid guests in chloroform. The combination of an acid–base interaction between the tertiary amines of the dendrimer and the acidic headgroups of the guests together with hydrogen bonding between the urea groups of guest and host (Figure 1.12) resulted in binding of the guests.

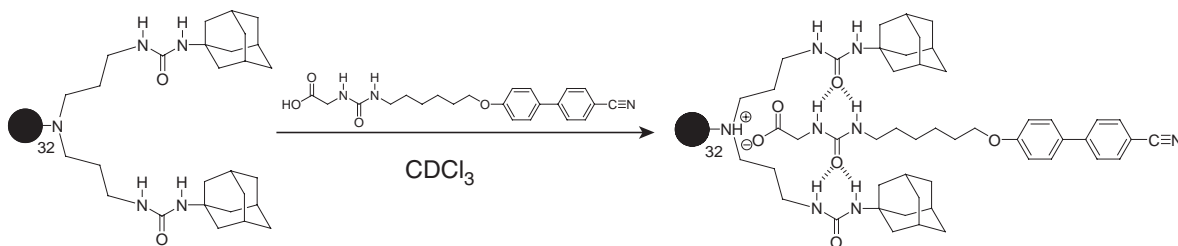


Figure 1.12 The complexation of ureido–acetic acid guests to a fifth generation poly(propylene imine) dendrimer based on a combination of acid–base and hydrogen bonding interactions. The black disk represents the dendritic framework.

It was found that the binding stoichiometry was close to 1 guest per 2 endgroups, suggesting that complexation only took place at the periphery of the dendrimer. This was confirmed with ^1H – ^1H NOESY experiments, which indicated a close proximity between the headgroups of the guests

and the periphery of the dendrimer. The association constant for the binding of a cyano-biphenyl guest (Figure 1.12) to the dendrimer appeared to be around 10^5 M^{-1} in chloroform, which indicates that only the fully modified dendrimer is present in solution at a concentration of 1 mM.

Specific binding based on hydrogen bonding has been reported by Dirksen et al.⁸⁰ The periphery of four generations of poly(propylene imine) dendrimers was modified with Hamilton receptors, which bind to barbiturate guests due to multiple hydrogen bonding interactions (Figure 1.13).

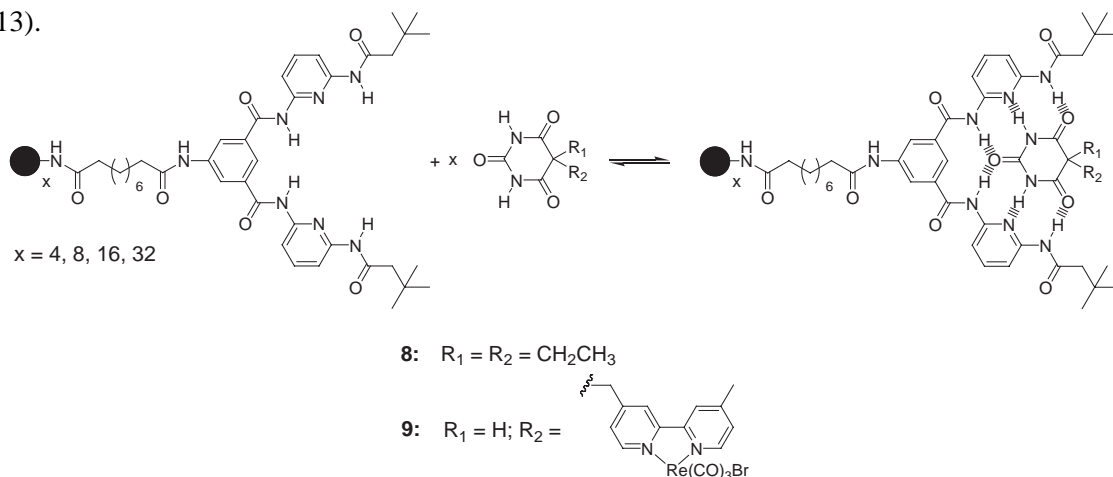


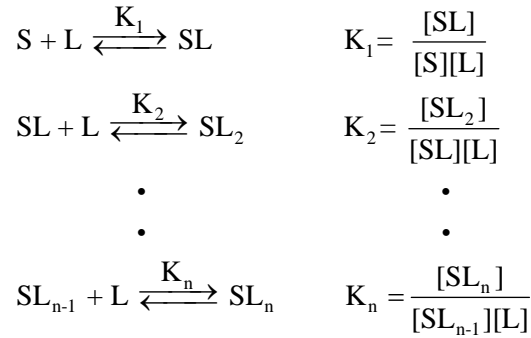
Figure 1.13 The binding of Barbital (**8**) and a bipyridine modified barbiturate guest (**9**) to Hamilton-receptors at the periphery of poly(propylene imine) dendrimers. The black disk represents the dendritic framework.

The binding of two guests, Barbital (**8**), and a bipyridine modified barbiturate guest (**9**) was investigated. The association constants of **8** and **9** to a single Hamilton receptor in chloroform were determined via ^1H NMR titrations to be $1.4 \times 10^3 \text{ M}^{-1}$ and $1.5 \times 10^5 \text{ M}^{-1}$, respectively. The difference in association constant could be assigned to the ability of guest **9** to undergo a keto–enol–enolate tautomerism, which positively influences the binding to the receptor. This difference in binding constant has been illustrated in a competition experiment, which showed that guest **9** can substitute guest **8** from the dendrimer.

In all the above-described examples, no cooperativity has been assumed or observed. The following section describes some examples in which cooperative binding is investigated.

1.4.4 Cooperativity in multiple monovalent interactions

The assessment of cooperativity in supramolecular systems has only been performed in a number of cases. In most cases non-cooperativity has been assumed, meaning that the receptor sites on a macromolecule all behave independently and do not influence each other. Cooperativity arises when the binding of a ligand to a site increases the affinity of another ligand for a site. If the influence is negative, the binding is said to be anticooperative. Scheme 1.1 displays the general equilibrium equations for the binding of n monovalent ligands (L) to a multivalent substrate (S).



Scheme 1.1 The general equilibrium equations for the binding of monovalent ligands L to a multivalent substrate S with n recognition sites.

In the case of non-cooperativity, it is not so that all K -values are equal.^{38, 72} Though the binding is equal for each step at the microscopic level, each complex SL_i (with $i = 1, 2, \dots, n$) has a certain number of isomers. At the macroscopic level no discrimination is being made between these isomers, and the macroscopic equilibrium constants K_i simply take these isomers together. Therefore, the macroscopic K -values decrease according to statistical values in the situation of no cooperativity. The ratio between subsequent K -values is given in equation 1.1.

$$\frac{K_{i+1}}{K_i} = \frac{i(n-i)}{(i+1)(n-i+1)} \quad (1.1)$$

For example, the ratios between the macroscopic association constants for a substrate that can bind three ligands ($n = 3$) correspond to $K_1:K_2:K_3 = 3:1:1/3$. When the individual K -values decrease more strongly than these statistical values, the binding is anticooperative. When they decrease less strongly than these statistical values, or increase, the binding is cooperative.

The individual K -values can only be determined when the concentrations of all the components in the system are known. Often only the fractions of free and bound ligand can be determined. Then, cooperativity can be assessed by an analysis of the Scatchard or Hill plot. In case of non-cooperative binding, the fraction of bound ligands θ can be described as a function of the microscopic association constant K_{ass} and the ligand concentration according to equation 1.2. This equation can be rearranged into equation 1.3.

$$\theta = \frac{K_{ass}[L]}{1 + K_{ass}[L]} \quad (1.2)$$

$$\frac{\theta}{[L]} = K_{ass} - \theta K_{ass} \quad (1.3)$$

In a Scatchard plot, $\theta/[L]$ is plotted versus θ . This gives a slope of $-K_{ass}$ and an intercept on the θ -axis of unity. When a concave graph is obtained and not a straight line, the system is anticooperative. A convex graph indicates cooperative behavior. Equation 1.2 can be rearranged into equation 1.4:

$$\log \left(\frac{\theta}{1-\theta} \right) = \log K_{ass} + \log [L] \quad (1.4)$$

When $\log(\theta/(1-\theta))$ is plotted against $\log([L])$, a straight line with a slope of unity should be obtained for the situation of no cooperativity. The binding is anticooperative for a slope < 1 and cooperative for a slope > 1 .

Gibson and co-workers have evaluated cooperativity in the binding of several dibenzo-24-crown-8 derivatives to 1,3,5-tris(p-benzylammoniummethylphenyl)benzene tri(hexafluorophosphate) (**10**).⁸¹ First, the binding to DB24C8 (**11**) was investigated (Figure 1.14). Interestingly, the aromatic protons at the core of **3** appeared to be different for **10**, **10·11₁**, **10·11₂** and **10·11₃**. From the concentrations of these species K_1 – K_3 could be determined in acetonitrile, and non-cooperative behavior was found as the ratios between $K_1:K_2:K_3$ appeared to be $3:1:1/3$ ($440:140:41 \text{ M}^{-1}$ respectively). The Scatchard plot gave a straight line, also indicating that no cooperativity was taking place (Figure 1.15). Similar results were obtained in deuterated acetone. When the crown ethers were modified with a first, second and third generation Fréchet-type dendron, the self-assembly appeared to be cooperative in acetone (Figure 1.15).

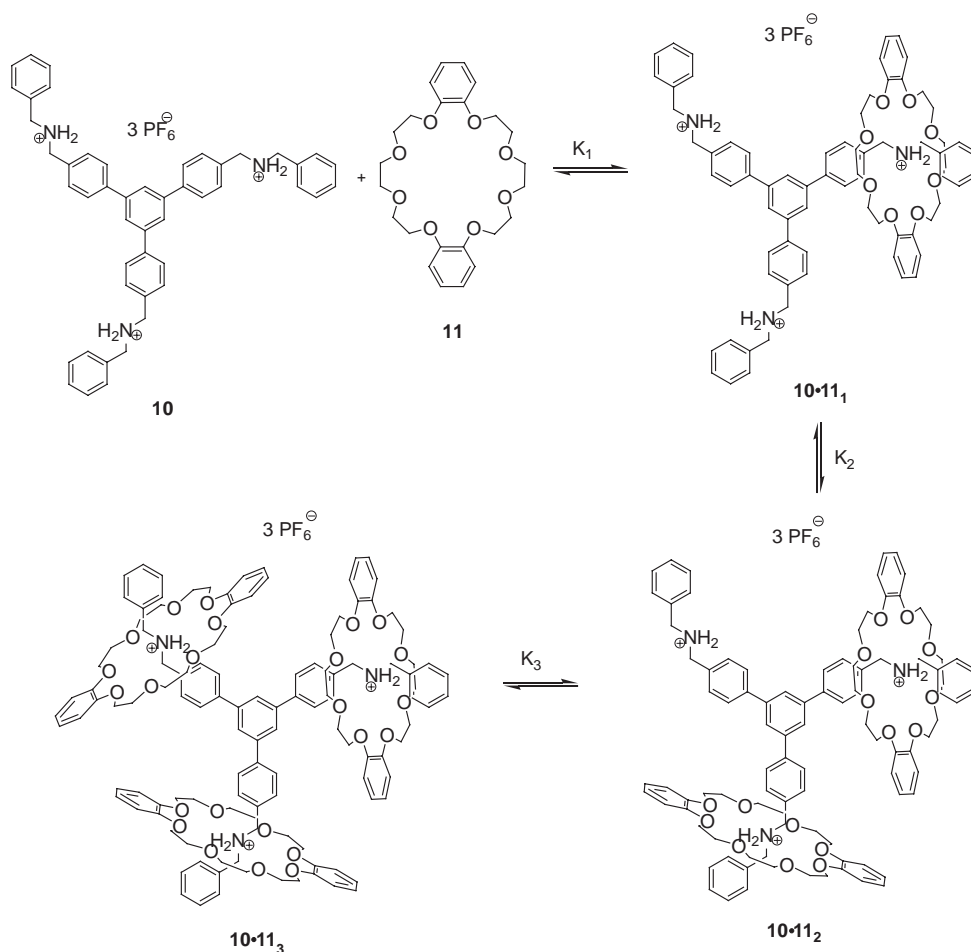


Figure 1.14 The stepwise binding of **11** to the quaternary ammonium sites on **10**.⁸¹

The ratios of the individual association constants exceeded the expected statistical ratios, and Scatchard analysis clearly showed convex graphs, corresponding to cooperative binding. The extent of cooperativity also increased as the size of the dendron increased. This has been attributed to the dendron's ability to shield the ionic core of **3** from the solvent.

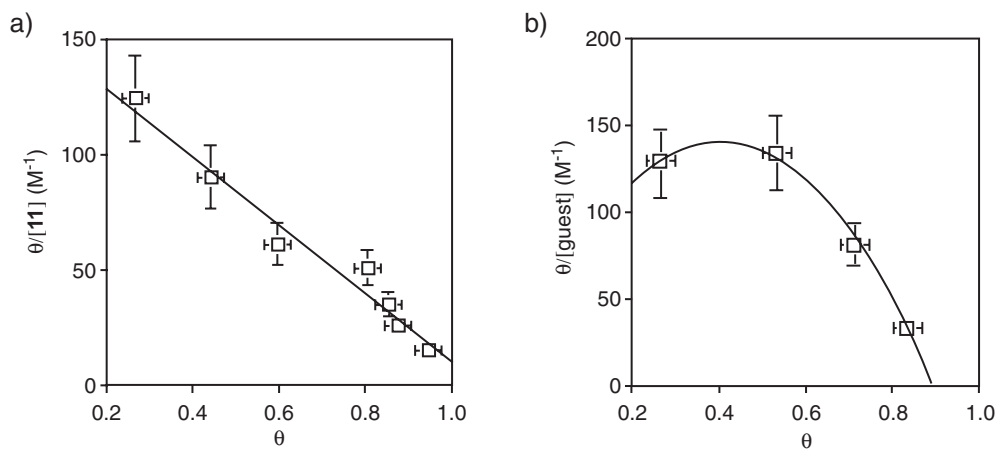


Figure 1.15 a) Scatchard plot for the binding of guest **11** to host **10** in acetonitrile. A linear behavior is obtained, indicating that no cooperativity takes place. b) Scatchard plot for the binding of a DB24C8 derivative modified with a third generation Fréchet-type dendron in acetone. The convex graph indicates that the binding is cooperative.

In another study from the same group, the periphery of a first and third generation poly(propylene imine) dendrimer was modified with dibenzo-24-crown-8 moieties.⁸² The association with dicationic bipyridyl derivatives was studied in acetone. For both generations of dendrimers, the association with the guests appeared to be anticooperative. The Scatchard plots were concave, and the Hill plots had a slope smaller than unity (Figure 1.16). The results were not unexpected. Back folding of the end groups, intramolecular hydrogen bonding and repulsive electrostatic interactions could explain the behavior. The influence of folding was further investigated by protonation of the tertiary amines of the dendrimer via addition of an equivalent amount of trifluoroacetic acid. Interestingly, the Scatchard plot for the third generation dendrimer became linear, indicative of non-cooperative binding. An association constant of $70 \pm 8 \text{ M}^{-1}$ was determined, in agreement with the binding to model compounds.

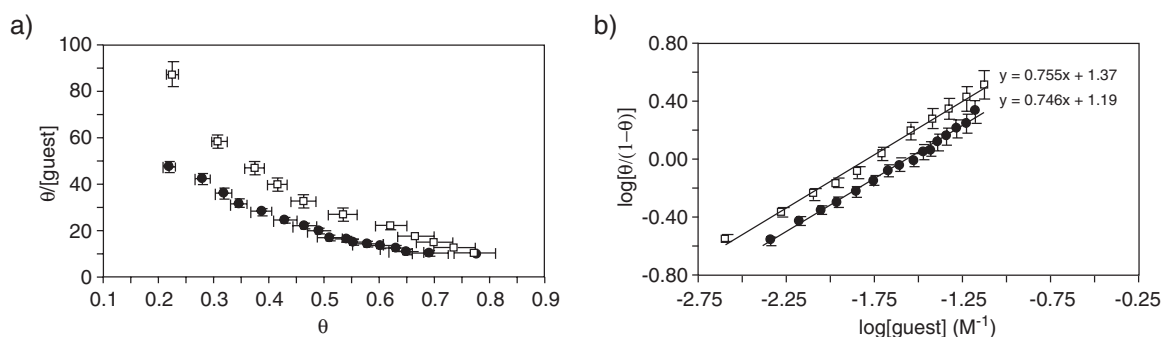


Figure 1.16 a) Scatchard plots of the binding of bipyridyl guests to a first (\square) and third generation (\bullet) crown ether dendrimer. The concave shape indicates that the binding is anticooperative. The Hill plot (b) also shows anticooperative behavior, as the slope of both graphs is < 1 .

Not many other groups have reported the cooperative binding of monovalent ligands to multivalent hosts. The groups of Lehn⁸³ and Hirsch⁸⁴ have reported the cooperative binding of cyanuric acid guests to ditopic and tritopic Hamilton receptors, based on a Scatchard plot and the computer program Chem-Equili. However, no experimental data have been reported in the articles.

Cooperativity has been described in multivalent interactions,⁴ but as discussed in section 1.3 the assessment is not straightforward, as a distinction has to be made between the first binding event, which is intermolecular, and the subsequent binding events, which are pseudo-intramolecular.⁸⁵ This results in different dimensions for the first and subsequent association constants, which cannot easily be compared. The assessment of cooperativity cannot be done based on the analysis of Scatchard or Hill plots in case of multivalent interactions. Other methods need to be used, like the model derived by Huskens et al.⁸⁶ for the thermodynamics of multivalent host–guest interactions at interfaces or the model derived by Ercolani⁸⁵ for the assessment of cooperativity in self-assembly.

1.5 AIM AND SCOPE OF THIS THESIS

The supramolecular chemistry of dendrimers and their multiple monovalent interactions are of great interest to understand complex multicomponent systems. Within this field, the methodology designed in our group to modify the periphery of dendrimers in a non-covalent manner (Figure 1.12) contains a number of very intriguing features. First of all, the binding is dynamic, meaning that the system has the ability to interchange between a number of supramolecular rearrangements, depending on the type of guests and conditions used. Secondly, the guests are bound to the periphery, which allows them to interact with their environment. They are able to participate in all kinds of recognition events while bound to the dendritic scaffold, which is especially interesting for biomedical applications like drug delivery, targeting and the specific binding to biologically active molecules or surfaces. For these applications, the complexes should be stable in water.

Therefore, a fundamental understanding of the factors that govern binding between host and guest is essential. Much is unknown about this system. The three-dimensional structure of the complex, the location of the guests, the stability of the complexes, the actual mode of binding, exchange phenomena and the dependency of these aspects on solvent polarity are not well understood. Also the existence of (anti)cooperativity in the multiple monovalent interactions is not known. These questions will need to be addressed in order to reach the ultimate goal of this system, a dynamic library in water. The concept is schematically depicted in figure 1.17. First, the hydrophobic dendrimer is solubilized by hydrophilic guests to render the complex water-soluble. When several guest molecules are added that contain a specific recognition motive for a site on a substrate, all kinds of statistical combinations of guests bound to the dendrimers will be present (Figure 1.17, middle).

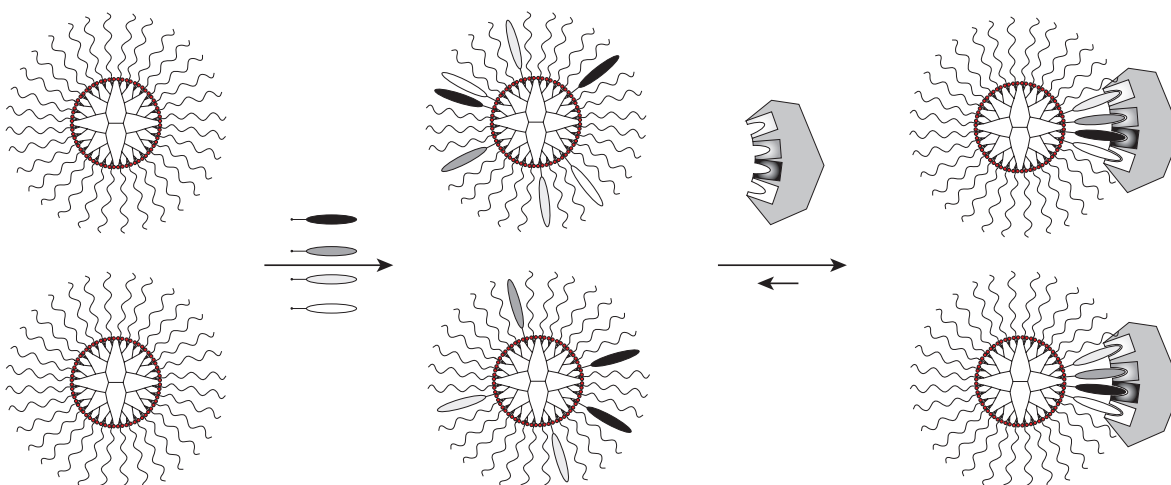


Figure 1.17 Schematic representation of the concept of a supramolecular dynamic library in water.

If these guests are still able to exert their function while bound to the dendrimer, addition of the substrate to the complexes should result in a shift of the equilibrium into the direction of the best binding sequence of guests to the complex due to multivalent binding (Figure 1.17, right). Fixation of the supramolecular aggregate would give a tightly binding ligand for the substrate, not obtained via multistep covalent synthesis, but via multistep *non*-covalent synthesis.

Clearly, the dynamic library is not a reality yet. This thesis describes the results obtained in order to get a fundamental understanding of the factors that govern binding between guest and host, and to bring the dynamic library in water a step closer to reality. In **chapter 2**, the synthesis of guest and host molecules is described. Furthermore, the mobility of the end groups of guests non-covalently bound to dendrimers has been investigated, and the three-dimensional structure of dendritic host–guest complexes is investigated by a crystal structure analysis of model compounds together with molecular dynamics simulations. **Chapter 3** discusses the analysis of supramolecular aggregates with mass spectrometry. The stability of dendritic host–guest complexes has been determined by collision induced dissociation, and these results have been linked to the binding of guest molecules in chloroform. This aspect has been investigated in detail with NMR spectroscopy in **chapter 4**. The location of the guest molecules has been determined with ^1H – ^1H NOESY NMR, and the binding of carboxylic and phosphonic acid guests has been investigated by ^{13}C NMR and ^{31}P NMR. Finally, in **chapter 5** a supramolecular synthesis is described to make stable complexes in water. The resulting aggregates have been studied with a number of techniques, and the exchange with functional guest molecules is investigated.

Throughout the course of this thesis, it will become clear that the binding of guests to the adamantyl dendrimer is not easily portrayed in a single scheme, like in figure 1.18a. Several other interactions can take place, for example binding to the inner tertiary amines of the dendrimer, especially by phosphonic acid guest molecules (figure 1.18b). On top of that, the binding is dynamic, and not static.

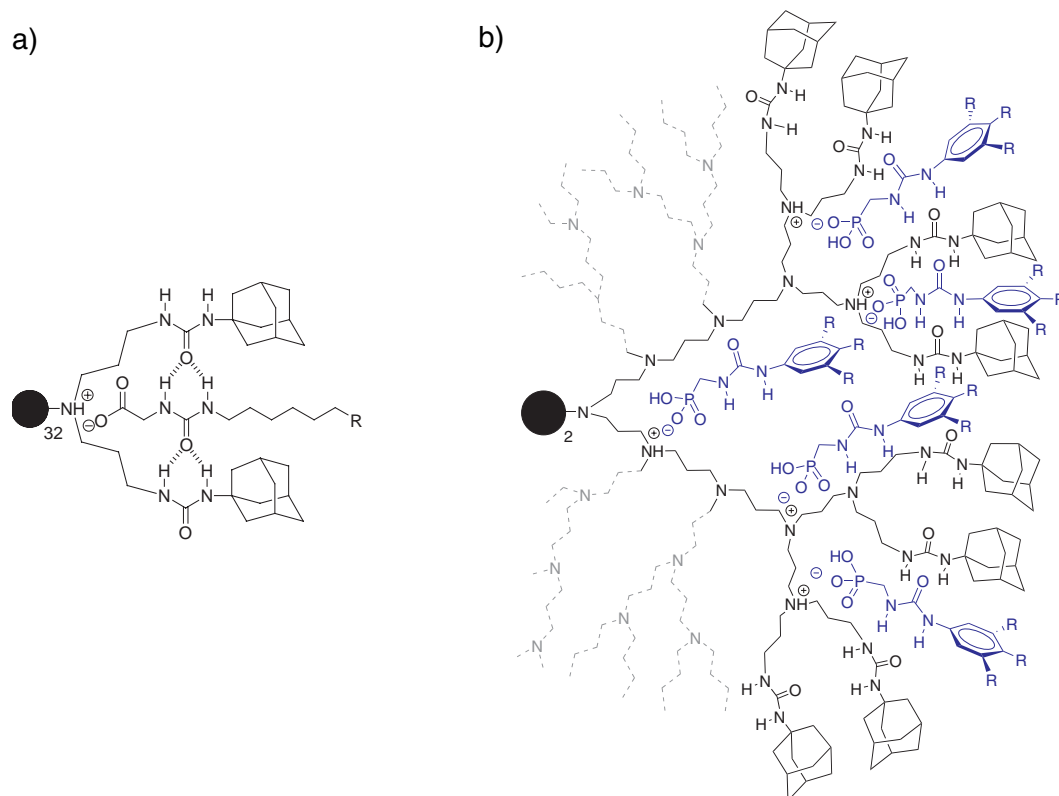


Figure 1.18 a) Schematic representation of the dendritic host–guest complex. b) Complexation of phosphonic acid guests to the interior of the urea–adamantyl dendrimer.

Though not very realistic, the representation of figure 1.18a is very convenient to describe the supramolecular host–guest complex. Throughout this thesis, the picture of figure 1.18a is used, but as a schematic and simplified representation of the more complex, dynamic supramolecular dendritic aggregates, like in figure 1.18b.

1.6 REFERENCES

- 1 J.-M. Lehn, *Supramolecular Chemistry — Concepts and Perspectives*, VCH, Weinheim, **1995**.
- 2 J. L. Atwood, J. E. D. Davies, D. M. MacNicol, F. Vögtle, J.-M. Lehn, *Comprehensive Supramolecular Chemistry, Vol. 9*, Pergamon, Oxford, **1996**.
- 3 L. Stryer, *Biochemistry*, 4 ed., W. H. Freeman and Company New York, **1995**.
- 4 M. Mammen, S.-K. Chio, G. M. Whitesides, *Angew. Chem. Int. Ed.* **1998**, *37*, 2755-2794.
- 5 J. D. Badjic, A. Nelson, S. J. Cantrill, W. B. Turnbull, J. F. Stoddart, *Acc. Chem. Res.* **2005**, ACS ASAP.
- 6 G. R. Newkome, C. N. Moorefield, F. Vögtle, *Dendrimers and Dendrons; Concepts, Synthesis, Applications*, Wiley-VCH, Weinheim, Germany, **2001**.
- 7 J. M. J. Fréchet, D. A. Tomalia, *Dendrimers and other dendritic polymers*, John Wiley & Sons, Ltd., **2001**.
- 8 M. Maciejewski, *J. Macromol. Sci., Chem.* **1982**, *A17*, 689-703.
- 9 P. G. De Gennes, H. Hervet, *J. Phys. Lett. Fr.* **1983**, *44*, 351-360.
- 10 F. Zeng, S. C. Zimmerman, *Chem. Rev.* **1997**, *97*, 1681-1712.
- 11 S. C. Zimmerman, L. J. Lawless, *Top. Curr. Chem.* **2001**, *217*, 95-120.
- 12 M. W. P. L. Baars, E. W. Meijer, *Top. Curr. Chem.* **2000**, *210*, 131-182.
- 13 D. K. Smith, A. R. Hirst, C. S. Love, J. G. Hardy, S. V. Brignell, B. Huang, *Prog. Polym. Sci.* **2005**, *30*, 220-293.
- 14 A. W. Bosman, H. M. Janssen, E. W. Meijer, *Chem. Rev.* **1999**, *99*, 1665-1688.
- 15 S. M. Grayson, J. M. J. Fréchet, *Chem. Rev.* **2001**, *101*, 3819-3867.
- 16 E. Buhleier, W. Wehner, F. Vögtle, *Synthesis* **1978**, 155-158.
- 17 D. A. Tomalia, H. Baker, J. Dewald, M. Hall, G. Kallos, S. Martin, J. Roeck, J. Ryder, P. Smith, *Polym. J. (Tokyo)* **1985**, *17*, 117-132.
- 18 D. A. Tomalia, H. Baker, J. Dewald, M. Hall, G. Kallos, S. Martin, J. Roeck, J. Ryder, P. Smith, *Macromolecules* **1986**, *19*, 2466-2468.
- 19 G. R. Newkome, Z. Yao, G. R. Baker, V. K. Gupta, *J. Org. Chem.* **1985**, *50*, 2003-2004.
- 20 C. Wörner, R. Mülhaupt, *Angew. Chem. Int. Ed. Engl.* **1993**, *32*, 1306-1308.
- 21 E. M. M. de Brabander-van den Berg, E. W. Meijer, *Angew. Chem. Int. Ed. Engl.* **1993**, *32*, 1308-1311.
- 22 C. Hawker, M. J. Fréchet, *J. Chem. Soc., Chem. Commun.* **1990**, 1010-1013.
- 23 C. J. Hawker, J. M. J. Fréchet, *J. Am. Chem. Soc.* **1990**, *112*, 7638-7647.
- 24 J. C. Hummelen, J. L. J. Van Dongen, E. W. Meijer, *Chem. Eur. J.* **1997**, *3*, 1489-1493.
- 25 J. M. J. Fréchet, *Proc. Natl. Acad. Sci. USA* **2002**, *99*, 4782-4787.
- 26 L. L. Kiessling, L. E. Strong, J. E. Gestwicki, *Annu. Rep. Med. Chem.* **2000**, *35*, 321-330.
- 27 J. E. Gestwicki, C. W. Cairo, L. E. Strong, K. A. Oetjen, L. L. Kiessling, *J. Am. Chem. Soc.* **2002**, *124*, 14922-14933.
- 28 U. Boas, P. M. H. Heegaard, *Chem. Soc. Rev.* **2004**, *33*, 43-63.
- 29 D. Astruc, F. Chardac, *Chem. Rev.* **2001**, *101*, 2991-3023.
- 30 D.-L. Jiang, T. Aida, *Prog. Polym. Sci.* **2005**, *30*, 403-422.
- 31 C. Liang, J. M. J. Fréchet, *Prog. Polym. Sci.* **2005**, *30*, 385-402.
- 32 E. R. Gillies, J. M. J. Fréchet, *Drug Discovery Today* **2005**, *10*, 35-43.
- 33 R. van de Coevering, R. J. M. Klein Gebbink, G. van Koten, *Prog. Polym. Sci.* **2005**, *30*, 474-490.

- 34 A. P. H. J. Schenning, C. Elissen-Roman, J.-W. Weener, M. W. P. L. Baars, S. J. Van der Gaast, E. W. Meijer, *J. Am. Chem. Soc.* **1998**, *120*, 8199-8208.
- 35 D. A. Mann, L. L. Kiessling, in *Glycochemistry. Principles, Synthesis and Applications* (Eds.: P. G. Wang, C. R. Bertozzi), Marcel Dekker: New York, **2001**, pp. 221-277.
- 36 D. A. Fulton, S. J. Cantrill, J. F. Stoddart, *J. Org. Chem.* **2002**, *67*, 7968-7981.
- 37 W. Saenger, *Principles of Nucleic Acid Structure*, Springer-Verlag New York, **1984**.
- 38 K. E. van Holde, W. C. Johnson, P. Shing Ho, *Principles of Physical Biochemistry*, Prentice-Hall, Inc., **1998**.
- 39 D. Seebach, J. M. Lapierre, K. Skobridis, G. Greiveldinger, *Angew. Chem. Int. Ed. Engl.* **1994**, *33*, 440-442.
- 40 J. F. G. A. Jansen, E. M. M. de Brabander van den Berg, E. W. Meijer, *Science* **1994**, *266*, 1226-1229.
- 41 J. F. G. A. Jansen, E. W. Meijer, E. M. M. de Brabander-van den Berg, *J. Am. Chem. Soc.* **1995**, *117*, 4417-4418.
- 42 G. R. Newkome, C. N. Moorefield, G. R. Baker, M. J. Saunders, S. H. Grossman, *Angew. Chem. Int. Ed. Engl.* **1991**, *30*, 1178-1180.
- 43 C. J. Hawker, K. L. Wooley, J. M. J. Fréchet, *J. Chem. Soc., Perkin Trans. 1* **1993**, 1287-1297.
- 44 C. J. Hawker, K. L. Wooley, J. M. J. Fréchet, *J. Am. Chem. Soc.* **1993**, *115*, 4375-4376.
- 45 D. M. Watkins, Y. Sayed-Sweet, J. W. Klimash, N. J. Turro, D. A. Tomalia, *Langmuir* **1997**, *13*, 3136-3141.
- 46 G. Pistolis, A. Malliaris, D. Tsiourvas, C. M. Paleos, *Chem. Eur. J.* **1999**, *5*, 1440-1444.
- 47 M. W. P. L. Baars, R. Kleppinger, M. H. J. Koch, S.-L. Yeu, E. W. Meijer, *Angew. Chem. Int. Ed.* **2000**, *39*, 1285-1288.
- 48 M. F. Ottaviani, S. Bossmann, N. J. Turro, D. A. Tomalia, *J. Am. Chem. Soc.* **1994**, *116*, 661-671.
- 49 M. F. Ottaviani, F. Montalti, N. J. Turro, D. A. Tomalia, *J. Phys. Chem. B* **1997**, *101*, 158-166.
- 50 A. W. Bosman, A. P. H. J. Schenning, R. A. J. Janssen, E. W. Meijer, *Chem. Ber. Recl.* **1997**, *130*, 725-728.
- 51 M. Zhao, L. Sun, R. M. Crooks, *J. Am. Chem. Soc.* **1998**, *120*, 4877-4878.
- 52 S. Stevelmans, J. C. M. v. Hest, J. F. G. A. Jansen, D. A. F. J. Van Boxtel, E. M. M. de Berg, E. W. Meijer, *J. Am. Chem. Soc.* **1996**, *118*, 7398-7399.
- 53 Y. Sayed-Sweet, D. M. Hedstrand, R. Spinder, D. A. Tomalia, *J. Mater. Chem.* **1997**, *7*, 1199-1205.
- 54 M. W. P. L. Baars, P. E. Froehling, E. W. Meijer, *Chem. Commun.* **1997**, 1959-1960.
- 55 A. I. Cooper, J. D. Londono, G. Wignall, J. B. McClain, E. T. Samulski, J. S. Lin, A. Dobrynin, M. Rubinstein, A. L. C. Burke, J. M. J. Fréchet, J. M. DeSimone, *Nature* **1997**, *389*, 368-371.
- 56 S. Mattei, P. Wallimann, B. Kenda, W. Amrein, F. Diederich, *Helv. Chim. Acta* **1997**, *80*, 2391-2417.
- 57 F. Diederich, B. Felber, *Proc. Natl. Acad. Sci. USA* **2002**, *99*, 4778-4781.
- 58 R. H. Jin, T. Aida, S. Inoue, *J. Chem. Soc., Chem. Commun.* **1993**, 1260-1262.
- 59 Y. Tomoyose, D.-L. Jiang, R.-H. Jin, T. Aida, T. Yamashita, K. Horie, E. Yashima, Y. Okamoto, *Macromolecules* **1996**, *29*, 5236-5238.
- 60 S. Hecht, J. M. J. Fréchet, *Angew. Chem. Int. Ed.* **2001**, *40*, 74-91.
- 61 Y. Wang, F. Zeng, S. C. Zimmerman, *Tetrahedron Lett.* **1997**, *38*, 5459-5462.
- 62 S. C. Zimmerman, Y. Wang, P. Bharathi, J. S. Moore, *J. Am. Chem. Soc.* **1998**, *120*, 2172-2173.
- 63 W. Ong, J. Grindstaff, D. Sobransingh, R. Toba, J. M. Quintela, C. Peinador, A. E. Kaifer, *J. Am. Chem. Soc.* **2005**, *127*, 3353-3361.

- 64 C. M. Cardona, J. Alvarez, A. E. Kaifer, T. D. McCarley, S. Pandey, G. A. Baker, N. J. Bonzagni, F. V. Bright, *J. Am. Chem. Soc.* **2000**, *122*, 6139-6144.
- 65 C. M. Cardona, T. D. McCarley, A. E. Kaifer, *J. Org. Chem.* **2000**, *65*, 1857-1864.
- 66 W. Ong, A. E. Kaifer, *Angew. Chem. Int. Ed.* **2003**, *42*, 2164-2167.
- 67 W. Ong, M. Gomez-Kaifer, A. E. Kaifer, *Chem. Commun.* **2004**, 1677-1683.
- 68 S. C. Zimmerman, M. S. Wendland, N. A. Rakow, I. Zharov, K. S. Suslick, *Nature* **2002**, *418*, 399-403.
- 69 S. C. Zimmerman, I. Zharov, M. S. Wendland, N. A. Rakow, K. S. Suslick, *J. Am. Chem. Soc.* **2003**, *125*, 13504-13518.
- 70 J. B. Beil, S. C. Zimmerman, *Chem. Commun.* **2004**, 488-489.
- 71 E. Mertz, S. L. Elmer, A. M. Balija, S. C. Zimmerman, *Tetrahedron* **2004**, *60*, 11191-11204.
- 72 K. A. Connors, *Binding Constants*, John Wiley & Sons, Inc., **1987**.
- 73 W.-S. Li, D.-L. Jiang, Y. Suna, T. Aida, *J. Am. Chem. Soc.* **2005**, *127*, 7700-7702.
- 74 J. J. Michels, M. W. P. L. Baars, E. W. Meijer, J. Huskens, D. N. Reinhoudt, *J. Chem. Soc., Perkin Trans. 2* **2000**, 1914-1918.
- 75 B. Gonzalez, C. M. Casado, B. Alonso, I. Cuadrado, M. Moran, Y. Wang, A. E. Kaifer, *Chem. Commun.* **1998**, 2569-2570.
- 76 J. W. Lee, Y. H. Ko, S.-H. Park, K. Yamaguchi, K. Kim, *Angew. Chem. Int. Ed.* **2001**, *40*, 746-749.
- 77 F. Marchioni, M. Venturi, A. Credi, V. Balzani, M. Belohradsky, A. M. Elizarov, H.-R. Tseng, J. F. Stoddart, *J. Am. Chem. Soc.* **2004**, *126*, 568-573.
- 78 V. Chechik, M. Zhao, R. M. Crooks, *J. Am. Chem. Soc.* **1999**, *121*, 4910-4911.
- 79 V. Chechik, M. Zhao, R. M. Crooks, *J. Am. Chem. Soc.* **1999**, *121*, 4910-4911; supporting information.
- 80 A. Dirksen, U. Hahn, F. Schwanke, M. Nieger, J. N. H. Reek, F. Vögtle, L. De Cola, *Chem. Eur. J.* **2004**, *10*, 2036-2047.
- 81 H. W. Gibson, N. Yamaguchi, L. Hamilton, J. W. Jones, *J. Am. Chem. Soc.* **2002**, *124*, 4653-4665.
- 82 J. W. Jones, W. S. Bryant, A. W. Bosman, R. A. J. Janssen, E. W. Meijer, H. W. Gibson, *J. Org. Chem.* **2003**, *68*, 2385-2389.
- 83 V. Berl, M. Schmutz, M. J. Krische, R. G. Khoury, J.-M. Lehn, *Chem. Eur. J.* **2002**, *8*, 1227-1244.
- 84 A. Franz, W. Bauer, A. Hirsch, *Angew. Chem. Int. Ed.* **2005**, *44*, 1564-1567.
- 85 G. Ercolani, *J. Am. Chem. Soc.* **2003**, *125*, 16097-16103.
- 86 J. Huskens, A. Mulder, T. Auletta, C. A. Nijhuis, M. J. W. Ludden, D. N. Reinhoudt, *J. Am. Chem. Soc.* **2004**, *126*, 6784-6797.

Chapter 2

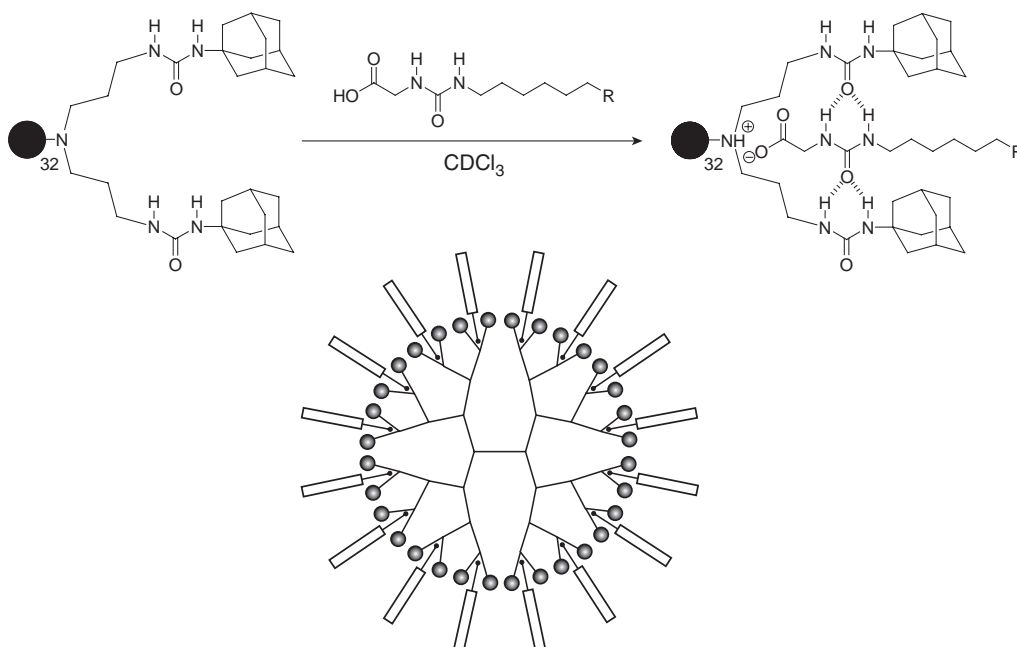
The synthesis, characterization and 3D-structure of supramolecular dendritic architectures*

ABSTRACT: *In this chapter the synthesis and characterization of supramolecular dendritic architectures are introduced. Herein, urea–adamantyl dendrimer hosts are brought together with different acid–urea guest molecules. Synthetic strategies for the preparation of carboxylic acid, phosphonic acid and sulfonic acid based guest molecules are described. Using these methodologies, several guests and model compounds have been prepared. To obtain guest molecules with a good solubility in a broad range of solvents, including water, two oligoethylene glycol containing guests have been prepared with a carboxylic acid and a phosphonic acid headgroup. A carboxylic acid guest molecule containing an N-t-Boc-L-phenylalanine group has been synthesized to shed light on the mobility of the end groups of guest molecules non-covalently bound to dendrimers. Optical rotation experiments show that the conformational freedom at the dangling ends of guest molecules non-covalently attached to dendrimers does not change significantly upon complexation. Crystal structures of guest molecules and model compounds imply that the guest and host can interact in many different ways, next to hydrogen bonding between the urea groups and acid–base interactions between the acid group of the guest and the tertiary amine of the dendrimer. Molecular dynamics simulations are in nice agreement with the crystal structures, and show that the 3D-structure of dendritic host–guest systems is much more complex than the two-dimensional pincer model described in the beginning of this chapter.*

* Part of this work has been published: M.A.C. Broeren, B.F.M. de Waal, J.L.J. van Dongen, M.H.P. van Genderen, E.W. Meijer, *Org. Biomol. Chem.* **2004**, 3, 281-285. T.C. Chang, K. Pieterse, M.A.C. Broeren, H. Kooijman, A.L. Spek, P.A.J. Hilbers, E.W. Meijer, *J. Am. Chem. Soc.*, submitted for publication.

2.1 INTRODUCTION

In our group, a dendritic host–guest system has been developed in which multiple, monovalent guest molecules can bind to a dendritic scaffold. The binding of the guests to poly(propylene imine) dendrimers modified with urea–adamantyl groups occurs through acid–base interactions between the acidic headgroup of the guest and a tertiary amine of the dendrimer, in combination with hydrogen bonding between the urea groups of the guest and the host (Scheme 2.1).¹ The first studies on this host–guest system indicated that 1) the binding between the guest and host is directed to the periphery of the dendrimer as a result of the hydrogen bonding interactions, and 2) the stoichiometry of binding comes close to one guest per two end groups. These observations have resulted in the so-called “pincer model”, which proposes that each two end groups of the dendrimer can act as an individual binding site for ureido–acetic acid guest molecules (Scheme 2.1).



Scheme 2.1 Top: the pincer model. The acid–base interaction between the guest and host is driven to the most outward tertiary amine of the dendrimer due to the additional hydrogen bonding interactions at the periphery of the dendrimer. Bottom: schematic representation of the dendritic host–guest complex for a 4th generation dendrimer with full complexation to all binding sites.

NMR spectroscopy is a useful tool to investigate the binding between the guest and host in a qualitative fashion. Characteristic changes in the ¹H NMR spectrum are indicative of the acid–base interaction and hydrogen bonding. ¹H–¹H NOESY NMR gives information about the proximity of guests to the dendritic host, and T₁ measurements are indicative of changes in the mobility of the dendritic periphery and/or the head groups of the guests. These techniques have also been used in the analysis of several other types of guest molecules that have been prepared, like guest molecules

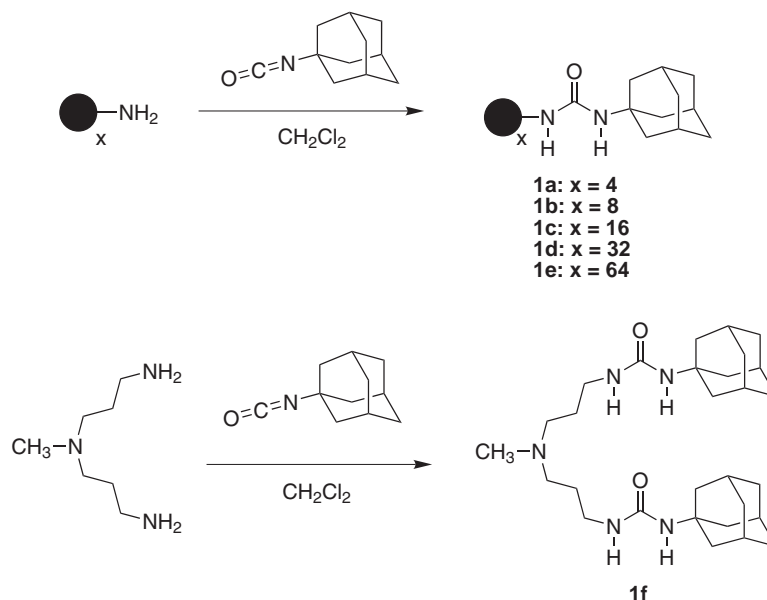
that contain a phosphonic or sulfonic acid headgroup. Pittelkow and Christensen found that these guests bind stronger to the dendritic host, presumably due to the greater acid strength.^{2,3}

This chapter starts with the synthesis of the dendritic hosts and several guest molecules that are used throughout this thesis. Next to guest molecules with a carboxylic acid headgroup, the synthesis of guest molecules that contain a phosphonic acid or sulfonic acid head group is described. Subsequently, the preparation of the dendritic host–guest complexes is described. In section 2.3, the complexation of a guest molecule that contains an *N*-*t*-Boc-L-phenylalanine unit has been investigated, and optical rotation measurements have been used to investigate the mobility of the end groups of the guest while non-covalently bound to the dendrimer. In section 2.4, information on the 3D structure of dendritic host–guest complexes is obtained via the analysis of crystal structures of model compounds in combination with molecular dynamics simulations. The results are compared to the pincer model, and indicate that the binding between guest and host is more complex than initially assumed.

2.2 SYNTHESIS OF HOST MOLECULES, GUEST MOLECULES AND COMPLEXES

2.2.1 Synthesis of the dendritic hosts

The synthesis of urea–adamantyl modified poly(propylene imine) dendrimers is straightforward. When poly(propylene imine) dendrimers are reacted with 1-adamantyl isocyanate in dichloromethane under an argon atmosphere, urea–adamantyl dendrimers are obtained in good yields (Scheme 2.2). Precipitation in ether results in the pure product.^{4,5}



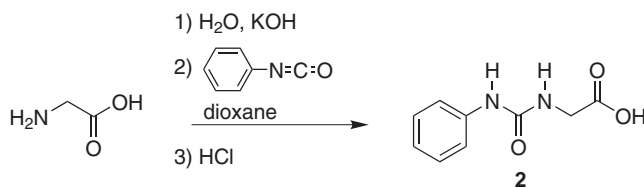
Scheme 2.2 The synthesis of urea–adamantyl dendrimers **1a–1e** and model compound **1f**.

The 1st, 2nd, 3rd, 4th and 5th generation urea–adamantyl dendrimer are designated as **1a–1e** respectively, and this notation is maintained throughout the thesis. Molecule **1f** has been used as a

model compound, and represents a single binding site for a guest on urea–adamantyl dendrimers. “Pincer molecule” **1f** can be obtained in a good yield by the reaction of bis(propylamine)methylamine with two equivalents of 1-adamantyl isocyanate in dichloromethane, followed by a recrystallization from ethanol.

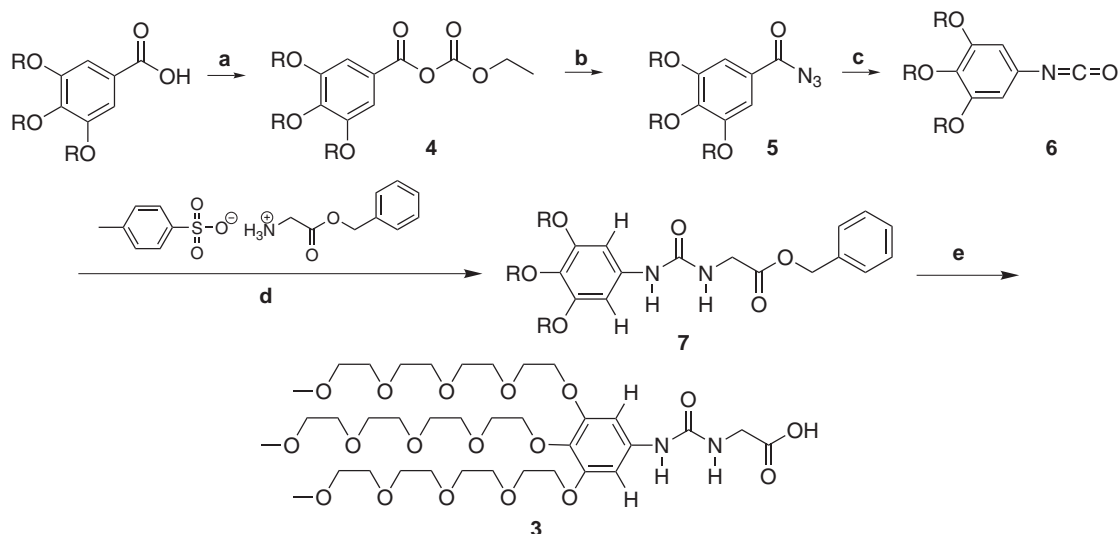
2.2.2 Synthesis of carboxylic acid guests

The starting material for all ureido–acetic acid guest molecules is glycine. The guest molecule of interest is obtained when the amine of glycine is converted into a urea group. In the case of 2-phenylureido–acetic acid (**2**), the reaction is performed by the addition of an excess of phenylisocyanate in dioxane to an alkaline solution of glycine in water (Scheme 2.3).⁶ Under these conditions a lot of symmetrical urea is formed as a side product, but it precipitates while the desired product remains soluble. Filtration and acidification of the filtrate results in precipitation of the desired product. The procedure is only useful for hydrophobic guests that precipitate in water upon acidification.



Scheme 2.3 The synthesis of 2-phenylureido–acetic acid (**2**).

When the acid group of glycine is protected as an ester the molecule becomes soluble in most organic solvents, which improves the overall reaction yield as hydrolysis of the isocyanate is limited due to the absence of water. Furthermore, side reactions on the carboxylic acid group are prevented. Guest molecule **3** has been prepared from the benzyl ester of glycine (Scheme 2.4). As a starting material for the oligoethylene glycol part, 3,4,5-tri(tetra-ethyleneoxy)benzoic acid was used, which was synthesized according to a described procedure.⁷ This acid is reacted with ethylchloroformate in THF with triethylamine to afford the mixed anhydride (**4**). The mixture is added to a solution of sodium azide in water, and extractions with dichloromethane result in acylazide derivative **5**. The acylazide can subsequently be converted to the isocyanate **6** via the Curtius rearrangement in refluxing toluene. Isocyanate **6** is reacted with glycine benzyl ester toluene-4-sulfonate. Triethylamine is added to liberate the free amine.



Scheme 2.4 The synthesis of guest **3**. $R = (\text{CH}_2\text{CH}_2\text{O})_4\text{CH}_3$. Reagents and conditions: a) ethylchloroformate, THF, $N(\text{Et})_3$ b) NaN_3 , H_2O c) toluene, reflux d) CH_2Cl_2 , triethylamine e) $t\text{-BuOH}$, H_2O , H_2 , Pd/C.

The sequence of reaction steps can be nicely followed by IR-spectroscopy due to the unique frequencies of the azide and isocyanate groups in the IR-spectrum (Figure 2.1).

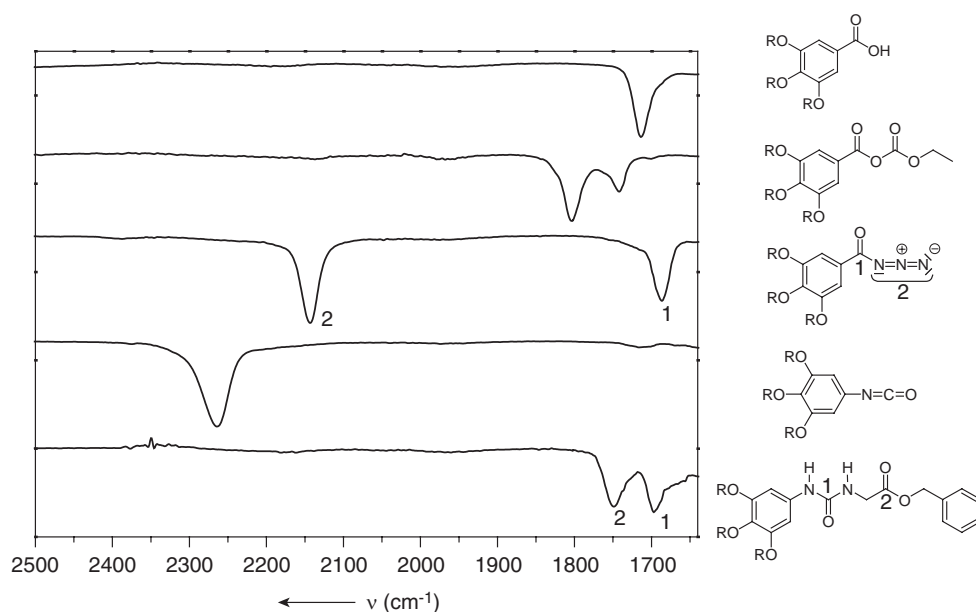
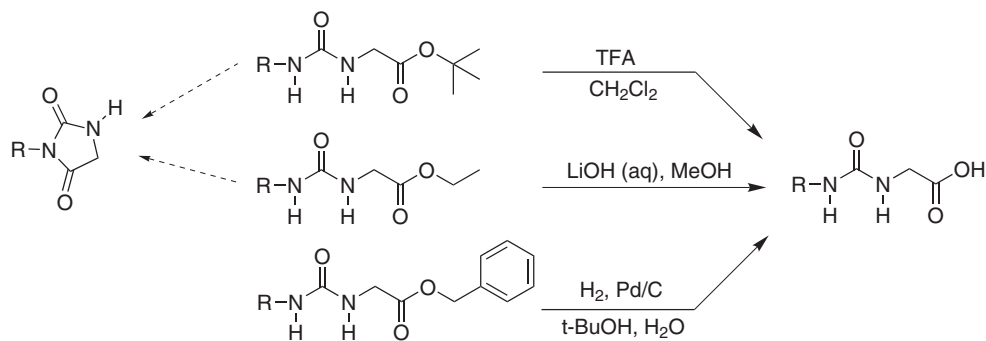


Figure 2.1 The ATR-IR spectra show the conversion of the acid functionality into the isocyanate via the acylazide, and subsequently into the urea group after reaction with the amine of glycine.

Ester **7** can be purified using column chromatography. Finally, the benzyl ester is converted into guest **3** by catalytic hydrogenolysis with H_2 -gas and Pd/C as a catalyst. Due to the oligoethylene glycol tails, guest **3** has a very good solubility in a broad range of solvents, including water.

The benzyl ester has shown to be the best protective group for carboxylic acid guests (Scheme 2.5). Other esters, like t -butyl esters or ethyl esters can be used but occasionally give rise to hydantoin formation.

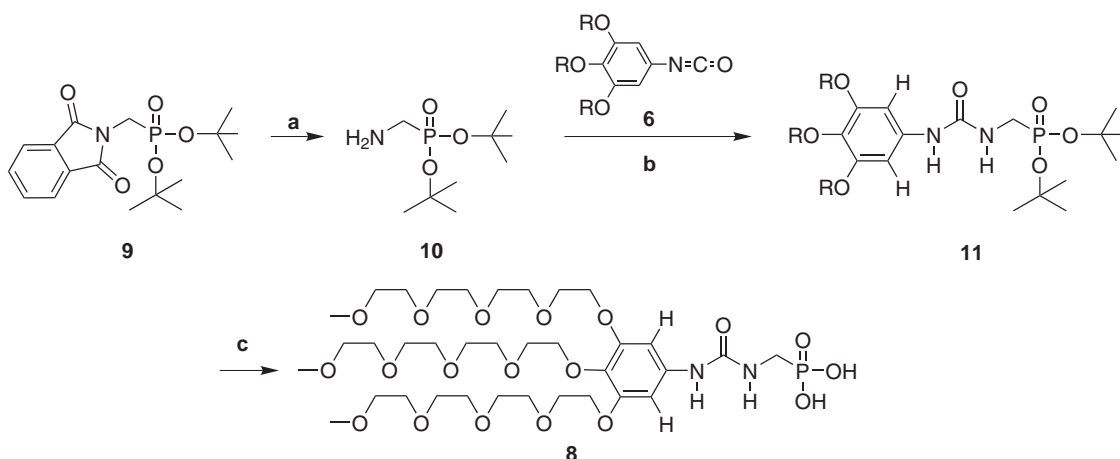


Scheme 2.5 Deprotection of *t*-butyl, ethyl and benzyl esters results in the free carboxylic acid, but hydantoin formation (left) can occur under basic and acidic conditions.

The deprotection of benzyl esters by catalytic hydrogenolysis is mild, fast and least susceptible to hydantoin formation.⁸

2.2.3 Synthesis of phosphonic acid guests

The starting materials for ureidomethylphosphonic acids are phthalimidomethyl phosphonate esters. Removal of the phthalimide group with hydrazine affords the primary amine, which can be coupled to an isocyanate to give the urea group. Deprotection of the ester results in the ureidomethylphosphonic acid. In the synthesis of guest **8** (Scheme 2.6), di-*t*-butyl(phthalimidomethyl)phosphonate (**9**) has been used as the starting material, which has been synthesized according to a modified literature procedure.⁹



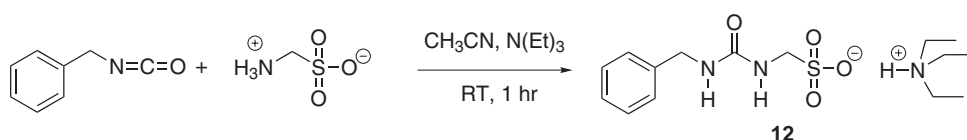
Scheme 2.6 The synthesis of phosphonic acid guest **8**. Reagents and conditions: (a) H_2NNH_2 , EtOH (b) CH_2Cl_2 (c) TFA, CH_2Cl_2 .

Treatment of with **9** with hydrazine results in amine **10**, which is immediately used for reaction with isocyanate **6**. Product **11** can be purified using column chromatography, and treatment with TFA to remove the *t*-butyl groups results in pure **8**. Interestingly, the deprotection step only goes to

completion under acidic conditions. The reaction with base stops when the first ester is deprotected.¹⁰⁻¹³

2.2.4 Synthesis of sulfonic acid guests

Ureidomethylsulfonic acids can be prepared from aminomethanesulfonic acid. Due to the strong acidity of sulfonic acids no good protective groups are available, which makes the synthesis of ureidomethylsulfonic acids less straightforward. Garrigues and Mulliez have prepared several ureidomethylsulfonic acids by reacting an excess of isocyanate with aminomethane sulfonic acid in a pyridine/water mixture.¹⁴ This procedure is far from ideal as it results in large amounts of symmetrical urea. This can be improved by performing the reaction in an acetonitrile/triethylamine mixture (Scheme 2.7).



Scheme 2.7 The synthesis of ureidomethylsulfonic acid guest **12**.

Addition of the isocyanate to this solution results in full conversion to the desired product within two hours. Evaporation of the solvent gives the product as the triethylammonium salt. Unfortunately, the synthesis of a sulfonic acid guest modified with oligoethylene glycol tails similar to guests **3** and **8** was not successful.

2.2.5 General preparation of dendritic host–guest complexes

The dendritic host–guest complexes are generally prepared by dissolving dendrimer and guest together in chloroform at a dendrimer concentration around 1 mM. In most experiments the stoichiometry of one guest per two end groups is maintained, which is the theoretical amount to get full complexation of the guest to the peripheral tertiary amines of the dendrimer. When the solubility of the guest in chloroform is low, e.g. in the case of guest **13**, **14** and **15** (depicted in scheme 2.8 and synthesized by M. Pittelkow and J.B. Christensen),^{2, 15} sonication and heating of the chloroform solution in the presence of dendrimer is necessary to solubilize the guest. Most frequently the guest can be driven into solution by the dendrimer, but the number of guests that can be solubilized by the dendrimer clearly depends on its solubility in chloroform.

The sulfonic acid guest requires an additional step, as it is present as either a pyridinium or a triethylammonium salt. Addition of these salts to the dendrimer in chloroform immediately results in the formation of pyridine or triethylamine, deduced from the smell (!). This indicates that the

2.3 CHIRALITY AS A PROBE FOR THE PACKING DENSITY OF NON-COVALENTLY BOUND GUESTS TO DENDRIMERS

2.3.1 Introduction

The chirality of dendritic macromolecules has been a topic of interest since the first report of Denkewalter in 1981.¹⁶ Chiral units can be built in dendrimers at different positions, e.g. the core, the branching points or the periphery, resulting in different architectures that have been the subject of numerous studies.¹⁷⁻²⁰ In our group the periphery of a fifth generation poly(propylene imine) dendrimer was modified with *N*-*t*-Boc-L-phenylalanine, resulting in the so-called “dendritic box”. It was found that the periphery forms a dense shell and that small molecules can be encapsulated inside the dendrimer.²¹ This dense-shell behavior was reflected in the chiroptical properties of the dendritic box. The specific optical rotation of DAB-*dendr*-(NH-*t*-Boc-L-Phe)_x, **16a–16e** (Figure 2.2), vanishes to zero on going from the first generation with 4 end groups ($[\alpha]_D^{20} = -11$, $c = 1$, CHCl₃)²² to the fifth generation dendrimer with 64 end groups ($[\alpha]_D^{20} = -0.1$, $c = 1$, CHCl₃).¹⁹ For other bulky Boc-protected amino acids, a similar effect was observed. Though never completely understood, the vanishing optical rotation was explained by the rigid character of the shell that does not enable all end groups to adopt their most favorable conformation. Since this particular end group possesses a strongly conformation-dependent optical rotation, the presence of many different conformations in the shell results in averaging of the optical rotation. In addition, dendrimers with amide–acetal end groups, which do not possess a conformation-dependent optical rotation, exhibited the same optical rotation for all generations.¹⁹

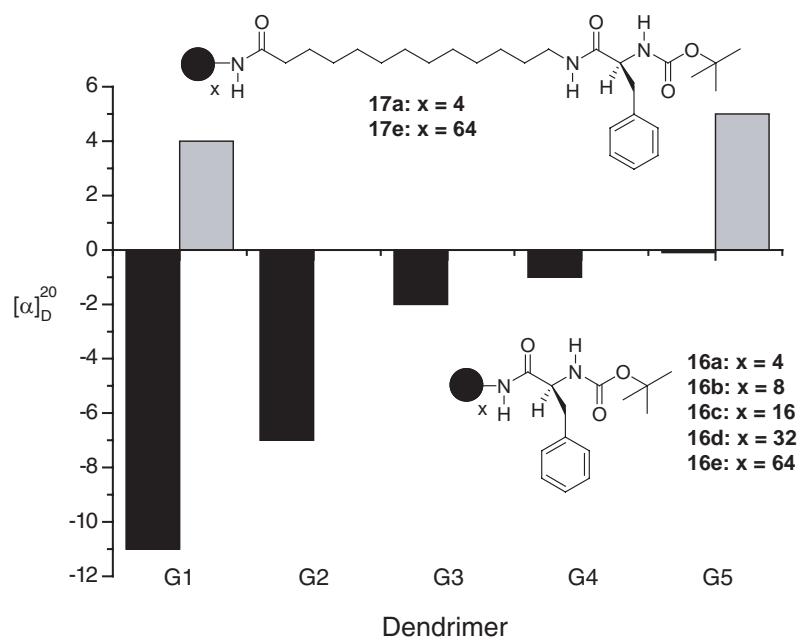
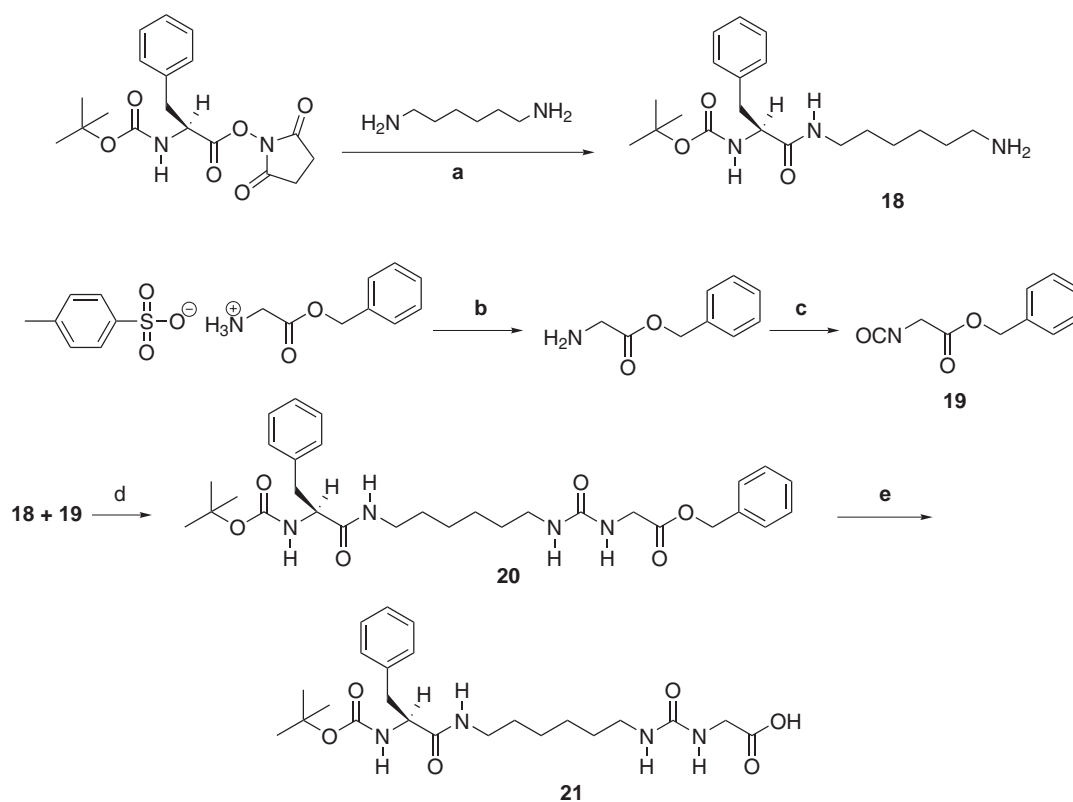


Figure 2.2 Optical rotation values of spacer armed dendrimers **17a** and **17e** in comparison to the values for the dendritic box (**16a–16e**).

This issue was further investigated by introduction of a C₁₂ alkyl spacer between the N-*t*-Boc-L-phenylalanine unit and the dendrimer surface.¹⁹ The alkyl spacer played a crucial role in the specific optical rotation obtained for dendrimer **17a** and **17e** (Figure 2.2), revealing a constant value of approximately $[\alpha]_D^{20} = +4$. This is in sharp contrast to the values found for the dendritic box analogs and supports the idea that the conformational freedom of the N-*t*-Boc-L-phenylalanine unit is reflected in the optical rotation.

We are now interested to investigate the conformational freedom of end groups that are non-covalently attached to dendrimers more thoroughly. T₁-relaxation measurements already gave some indication that the local mobility of the dangling end of guest molecules remains unperturbed.⁵ On the other hand, T₁-relaxation measurements also showed that at the dendrimer periphery the mobility decreases. We have used N-*t*-Boc-L-phenylalanine as a chiral probe to investigate the conformational freedom of the dangling ends of guest molecules. Therefore, an N-*t*-Boc-L-phenylalanine containing guest molecule has been synthesized (Scheme 2.9). The chiroptical properties of the complex of this guest with different generations of urea–adamantyl dendrimers have been studied in chloroform and have been compared to the chiroptical properties of both the dendritic box and spacer armed dendrimers **17a** and **17e**.

2.3.2 Synthesis of the guest molecule



Scheme 2.9 Synthesis of *N*-*t*-Boc-*L*-phenylalanine containing guest **23**. a) CH_2Cl_2 , 12 h, b) 2.4 M NaOH (aq), CH_2Cl_2 , c) CH_2Cl_2 , di-*t*-butyl-tricarbonate, 0.5 h, d) CH_2Cl_2 , 2 h, e) Pd/C catalyst (10%), *t*-butanol: H_2O 1/1 (v.v.), 4 h.

Guest **21** was synthesized starting from *N*-*t*-Boc-*L*-phenylalanine-*N*-hydroxysuccinimide ester and 1,6-hexanediamine. By use of a large excess of 1,6-hexanediamine, the mono-functionalized amine is formed as the main product. The purified amine **18** was converted to ester **20** via isocyanate **19**. This isocyanate is formed starting from *p*-toluenesulfonyl glycine benzyl ester. First the salt was washed with a NaOH-solution to liberate the free amine and subsequently the amine was in situ converted to isocyanate **19** using di-*t*-butyl-tricarbonate. Addition of amine **18** to isocyanate **19** resulted in pure ester **20** after column chromatography. Catalytic hydrogenation using Pd/C as a catalyst resulted in acid **21**. All compounds could be obtained in good yields and were characterized by ^1H NMR, ^{13}C NMR, ATR-IR spectroscopy and MALDI-TOF mass spectrometry.

2.3.3 Analysis of the complex

Guest molecule **23** is barely soluble in chloroform. However, upon addition of 4, 8 and 32 equivalents of **23** to second, third and fifth-generation urea–adamantyl dendrimer respectively, a clear solution is obtained. The resulting complexes are stable and can be characterized with ^1H NMR (Figure 2.3).

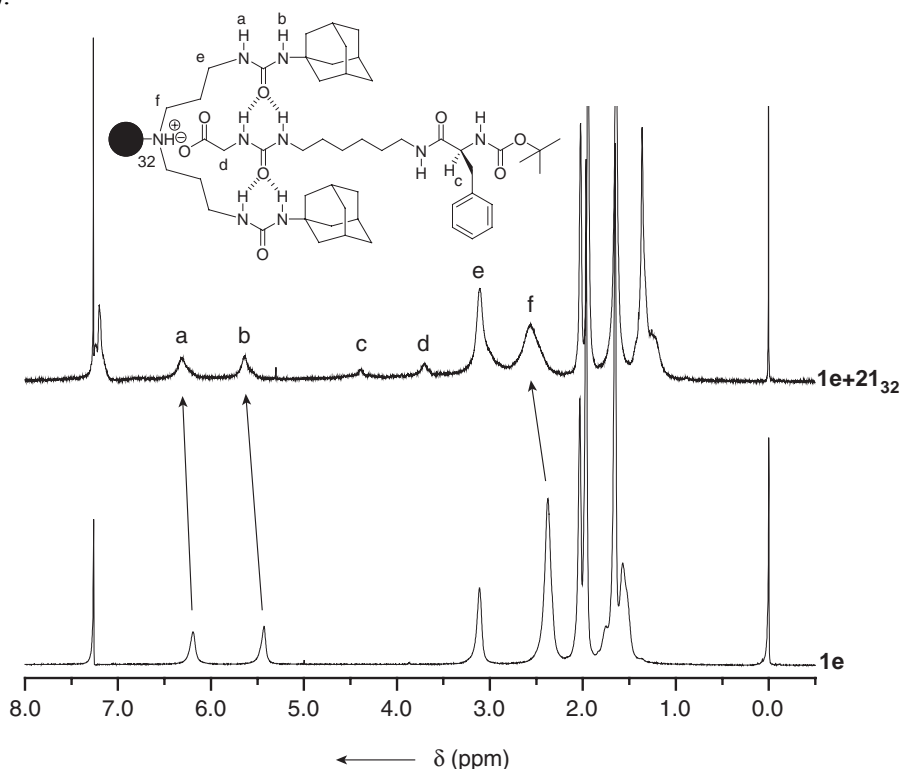


Figure 2.3 ^1H NMR spectra of dendrimer **1e** and the complex **1e+21**₃₂. The changes upon complexation are indicated with arrows.

^1H NMR measurements of the complexes reveal a downfield shift of both the urea protons of the dendrimer (signals **a** and **b**) and the methylene protons adjacent to the tertiary amine of the outermost shell (signal **f**) in all cases, as depicted for the **1e+21**₃₂ complex in figure 2.3. This is indicative of hydrogen bonding between the urea groups of guest and host and protonation of the tertiary amines of the dendrimer. Due to the poor solubility of **21** in chloroform, it was dissolved in deuterated 1,1,2,2-tetrachloroethane and a ^1H NMR spectrum was obtained at high temperature (120 °C). This spectrum was used to assign signals **c** and **d** of the **1e+21**₃₂ complex. ^1H - ^1H NOESY measurements of the **1e+21**₃₂ complex have been performed in CDCl_3 to investigate the location of the guest molecules. The spectrum depicted in figure 2.4 shows NOE interactions between the ureido–acetic acid part of **21** and the methylene protons next to the tertiary amines of dendrimer **1e**. The low solubility of guest **21** and the clear indication of complexation with ^1H NMR spectroscopy point to a high apparent association constant.

T_1 -relaxation measurements in chloroform for methylene protons **f** give values of 0.84 s for pure **1e** and 1.05 s for **1e+21₃₂**, which is in agreement with earlier measurements. This is an indication that the periphery of the dendrimer becomes more rigid upon complexation of the guest. Of course, it would be interesting to compare T_1 values of the dangling ends of the guest upon binding to **1e**. Unfortunately, for chiral proton **c** this appeared to be very difficult due to its low signal intensity. The signal of the Boc-group overlaps with the dendrimer, making it unsuitable for reliable T_1 -measurements. However, the optical rotation can be monitored easily and gives information about the mobility of the dangling end. It can be compared to values found for the covalently modified dendrimers, as well as with free guest **21**.

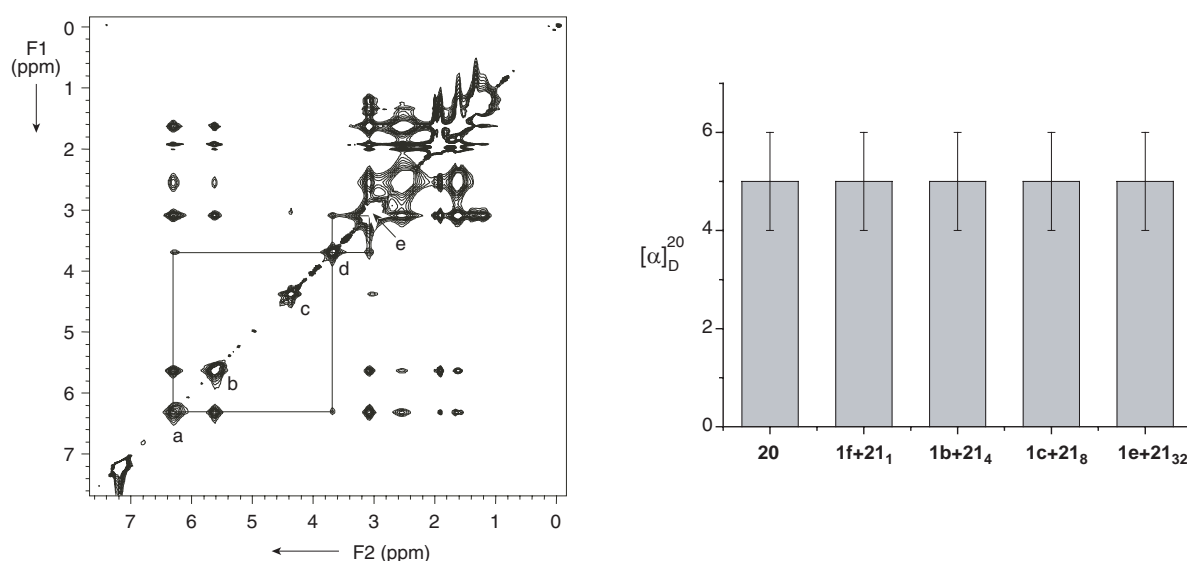


Figure 2.4 ^1H - ^1H NOESY spectrum of **1e+21₃₂** (left) and the optical rotation measurements performed on the complexes of different generations of the urea-adamantyl dendrimer with guest **21** (right).

Optical rotation measurements were performed in chloroform to investigate the chiroptical properties of the complexes formed. In all cases the concentration of **21** was kept constant at 10 mg/mL ($c = 1$), so the number of chiral groups is constant in all samples. The different generations of dendrimer or pincer were added in such an amount, that a stoichiometry of one guest per two endgroups was present. This means that theoretically all the guest molecules can bind to the peripheral tertiary amines of the host. The results are depicted in figure 2.4. Compound **20** was taken as a reference (chosen because of the poor solubility of **21** in chloroform) and gives a value of $[\alpha]_{\text{D}}^{20} = 5 \pm 1$. This value is also found for all host–guest complexes. This is comparable to spacer-armed dendrimers **17a** and **17e** and can be explained, as the amount of chiral groups present is approximately equal in all cases.²³

The results show a different behavior than measurements performed on the dendritic box, in which the optical rotation decreased from $[\alpha]_{\text{D}}^{20} = -11$ to -0.1 in going from the first to the fifth

generation dendrimer (Figure 2.2), but are in agreement with the spacer-armed dendrimers **17a** and **17e**. These results indicate that the local conformational freedom of the N-*t*-Boc-L-phenylalanine part of the guest molecules is not severely disturbed upon complexation and is comparable to the molecular motion of molecules covalently attached to dendrimers via a spacer.

2.3.4 Conclusions

An N-*t*-Boc-L-phenylalanine containing guest molecule has been synthesized, and ^1H NMR and ^1H - ^1H NOESY spectroscopy have revealed that this molecule is able to form a complex in chloroform with poly(propylene imine) dendrimers functionalized with urea–adamantyl end groups. T_1 -measurements have shown that the dendrimer periphery becomes more rigid when guest molecules bind to the dendrimer due to complexation, but optical rotation measurements on the complexes of different generations reveal a constant value. These results indicate that while the dendrimer periphery rigidifies upon complexation with guest molecules, the conformational freedom at the dangling ends of guest molecules non-covalently attached to dendrimers does not change significantly upon complexation. We have to take into account that the supramolecular complex is a dynamic system and the dynamics can influence the conformational freedom of the dangling end groups. On top of that, the chiral center is connected to the ureido-acetic acid binding site of the guest via a C_6 spacer, which also allows for more possibilities of reorganization. However, no change at all is observed in the specific optical rotation, which is in sharp contrast with the dendritic box dendrimers. This indicates that the mobility must be significantly different from the covalently modified dendritic box analogs.

The results obtained do not give information about the exact structure of the complexes. In order to obtain information about the different types of interaction that can take place between the dendritic host and guests, crystal structure analysis of model compounds together with molecular dynamics simulations have been performed. This is discussed in the next section.

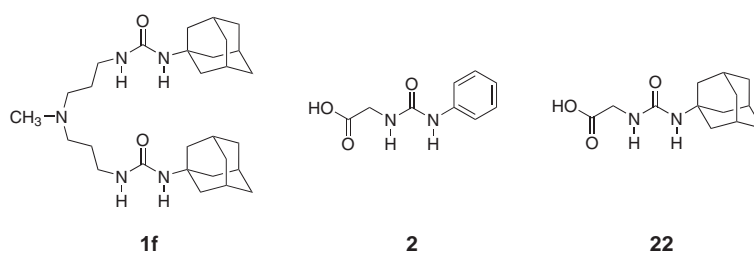
2.4 THE 3-DIMENSIONAL STRUCTURE OF DENDRITIC HOST–GUEST COMPLEXES

2.4.1 Introduction

Although dendrimers are esthetically appealing structures, often drawn perfectly symmetrical on paper, their three-dimensional structure is very complex. Steric hindrance, electrostatic interactions, hydrogen bonding and hydrophobic interactions are just some of the aspects that influence the size and shape of the molecule. Complexation of guest molecules to dendrimers does not make the shape of the resulting aggregate easier. On top of that, the dendritic host–guest complex is dynamic, and the noncovalent interactions holding the components together are constantly broken and reformed. These interactions cannot be easily portrayed in a single

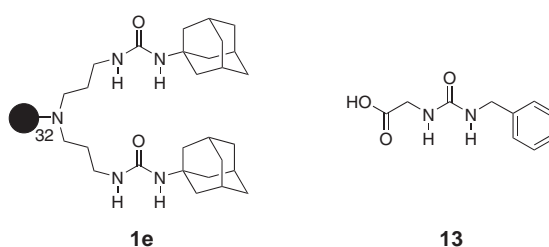
scheme. Still, in the design of new supramolecular dendritic structures it is of great importance to know which interactions govern the binding between guest and dendrimer, and how this affects the overall structure. This has been investigated by an analysis of the crystal packing structures of several model compounds, performed by dr. Theresa Chang of our group, in combination with molecular dynamics simulations, performed by dr. ir. Koen Pieterse (Biomodeling and Bioinformatics group, Eindhoven University of Technology, Eindhoven, The Netherlands)

With X-ray diffraction from single crystals, molecular structure can be resolved to the atomic level. However, single crystals of dendritic structures are difficult to come by.²⁴ Therefore, X-ray quality single crystals have been obtained of pincer molecule **1f** (Scheme 2.10) that resembles the binding site of the dendrimer, as well as single crystals of guest molecule **2** and **22**.



Scheme 2.10 The model compounds used in this study.

Co-crystals of pincer–guest complexes were also attempted but without success, indicative that a guest sandwiched between the arms of a pincer is not necessarily a favored structure. Molecular dynamics (MD) simulations of the 5th generation urea–adamantyl dendrimer **1e** were performed using NAMD. The simulations were conducted both with and without guest **13** in a ratio of 1 guest per 2 endgroups (Scheme 2.11).



Scheme 2.11 The dendrimer and guest used in the molecular dynamics simulations.

The acid–base reactions of these guests with the basic dendrimers were simulated as acid–base interactions (i.e. electrostatic interactions) consistent with the gas phase.

2.4.2 X-ray diffraction

The packing structures of the adamantyl pincer show that the pincer is quite flexible (Figure 2.5). Two polymorphs were found in crystals grown from the same solvent system. These packing

structures show that the adamantyl group prevents intra-pincer hydrogen bonding between urea groups. Hydrogen bonding is observed between pincers, forming infinite hydrogen bond stacks in both polymorphs with urea groups rotated by 90° relative to each other.

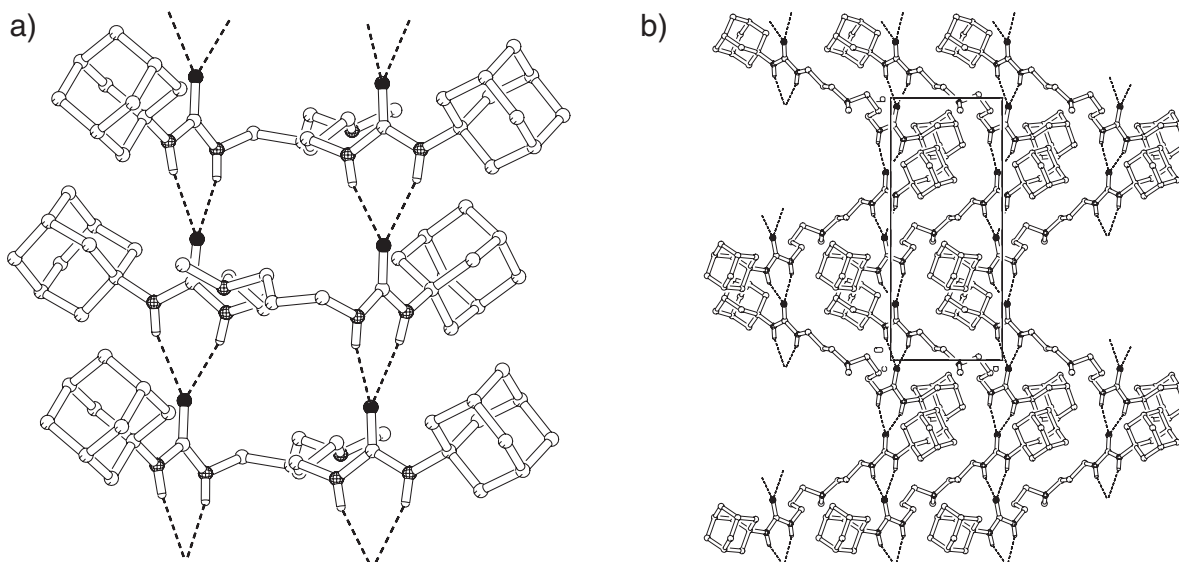


Figure 2.5 Solid-state superstructure of two polymorphs (a) and (b) of the adamantyl pincer.

Crystal structures of phenyl guest **2** result in a columnar packing structure (Figure 2.6a). An infinite hydrogen-bonding stack is formed with guest molecules rotated 180° relative to the ones above and below. Hydrogen bonding between the OH of the carboxylic acid group and the carbonyl oxygen of the urea group link these columns together (Figure 2.6b). No π - π stacking interactions were observed.

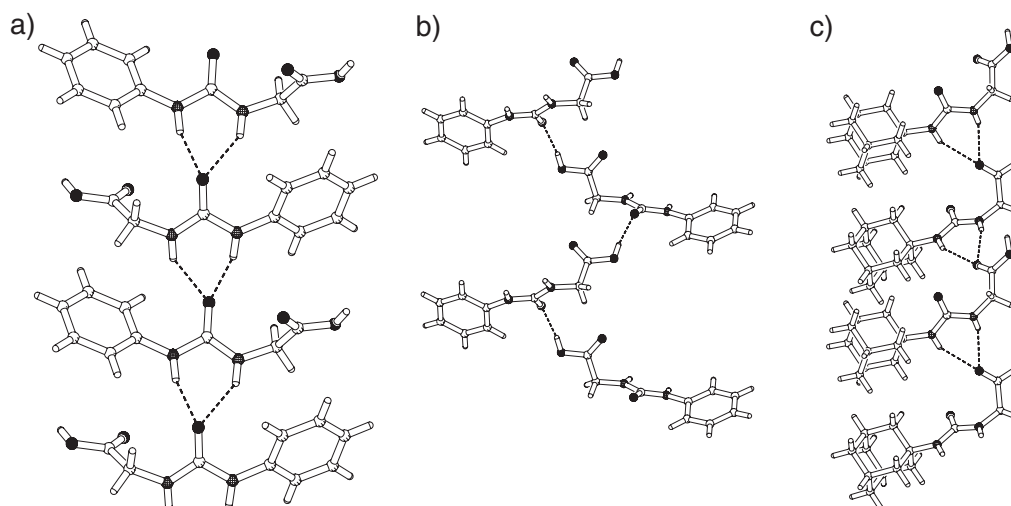


Figure 2.6 a) Phenyl guest **2** forms infinite stacks via urea-urea hydrogen bonding. b) The stacks are linked to other stacks via urea-acid bonds. c) Adamantyl guest **22** forms columns via hydrogen bonding between urea NH groups with acid carbonyl groups.

The crystal structure of adamantyl guest **22** (Figure 2.6c) is in agreement with what was observed in case of the adamantyl pincer **1f** and guest **2**. The bulky adamantyl groups prevent intramolecular urea–urea bonds so that hydrogen bonds are formed between the urea moiety and the carboxylic acids of adjacent guest molecules instead.

From the crystal structures we can conclude that there are several other types of interactions possible within and between the molecules, next to the urea–urea hydrogen bond and acid–base interaction displayed in scheme 2.1. Although no co-crystals have been obtained, it is conceivable to believe that the same interactions take place between a pincer molecule and a guest, and between a dendrimer and a guest. In fact, all the secondary interactions found in the crystal structures are also present in the molecular dynamics simulations and conceivably contribute to the overall complexity of the system.

2.4.3 Molecular dynamics simulations

Molecular dynamics simulations performed on the 5th generation urea–adamantyl with and without 32 equivalents of guest **13** result in the structures depicted in figure 2.7.

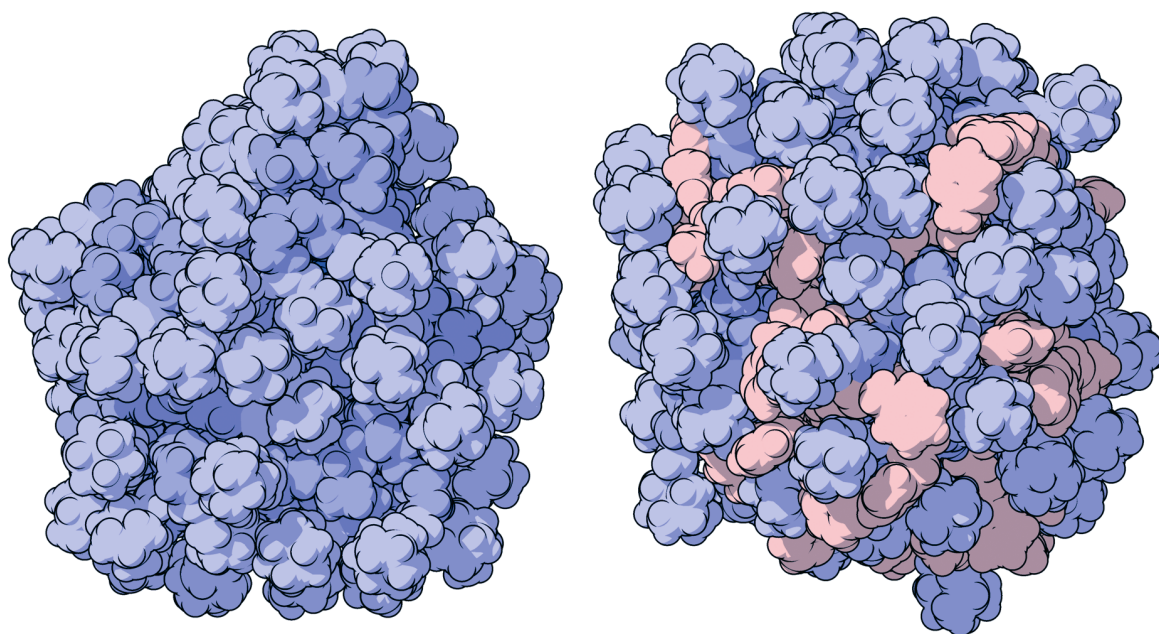


Figure 2.7 Space-filled representations of dendrimer **1e** (left) and the complex of **1e** with 32 equivalents of **13** (right).

The peripheral adamantyl groups are light blue, while the dendritic framework is darker blue. The guest is pink. In case of the bare dendrimer, the end groups do not completely shield the dendrimer interior, as large parts of the dendritic framework are visible. When the guests bind to the dendrimer, the structures seem to look a bit more globular. Both structures look very chaotic, and it is clear that the binding of the guests is far more complicated than the pincer model described in the

beginning of this chapter. The chaotic nature of the host–guest complexes makes it difficult to visualize what exactly is happening in the dendrimer. A stick representation of the complex of **1e** with 32 equivalents of **13** has been depicted in figure 2.8 to more clearly show how the guests and host interact.

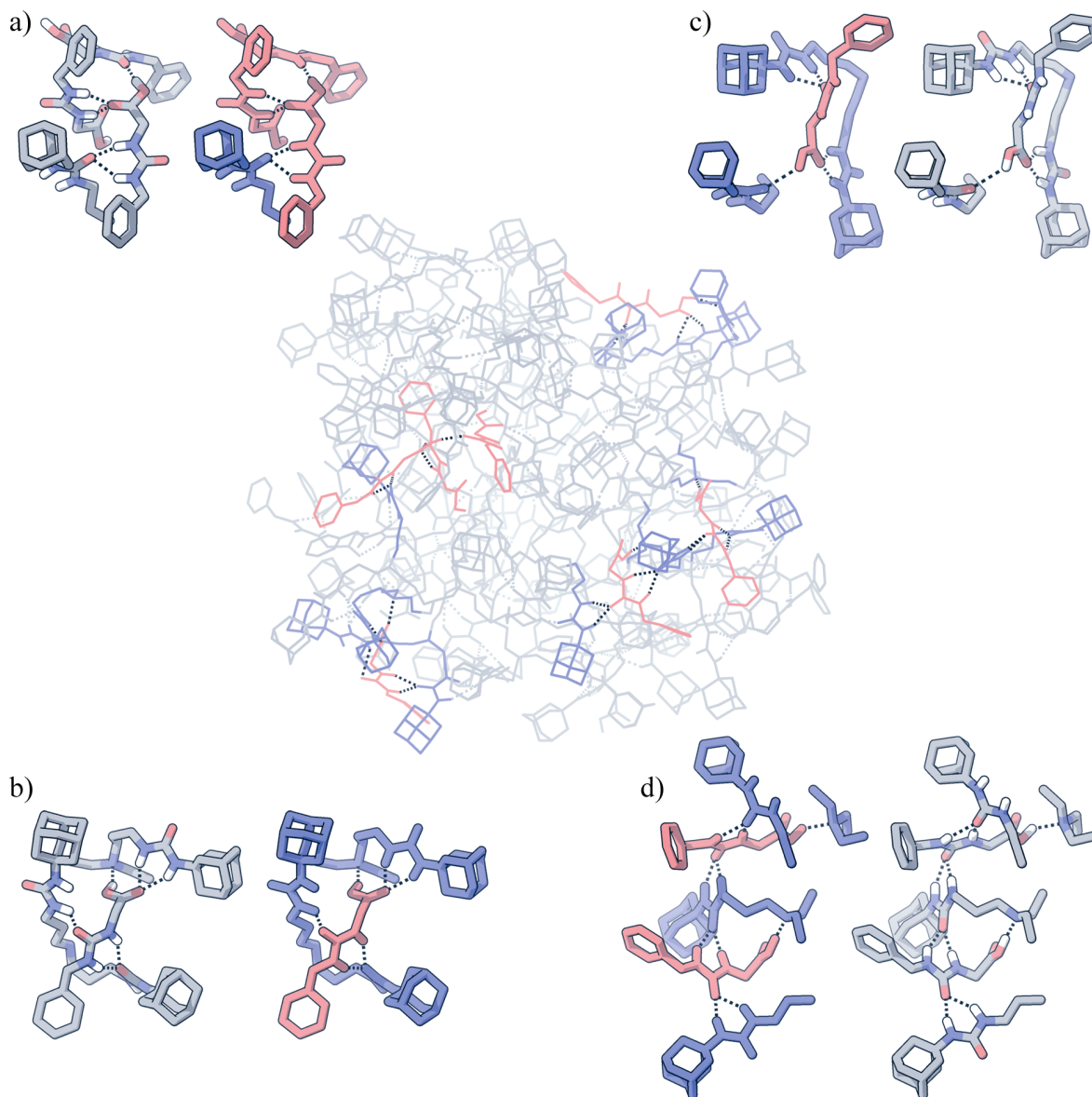


Figure 2.8 Simulation snapshot of dendrimer **1e** together with 32 equivalents of guest **13** (middle). Four parts (a-d) are highlighted that represent the different ways a guest (red) interacts with either the dendrimer (blue) or with other guests. The stick representations colored by atom type make clear which atoms are involved in hydrogen bonding. Hydrogen bonding is indicated with dashed lines.

There are vast numbers of ways a guest molecule can bind to the dendrimer, oftentimes via multiple interactions to different parts of the dendrimer. The examples shown in figure 2.8b, 2.8c and 2.8d illustrate the typical interactions found in such a dendrimer–guest complex. Sometimes interactions between guests are observed (Figure 2.8a).

Guest molecules do bind to the pincer-like moiety in the dendrimer as designed, although not in the way shown in scheme 2.1. In figure 2.8d we see a urea stack composed of alternating guests and pincer arms, but each time the molecule rotates relative to the urea stack as a result of either steric reasons or reorientation of the molecule to optimize interactions with another part of the dendrimer. As a result of steric repulsions arising from the bulky adamantyl groups, urea–urea bonds found in simulations regarding adamantyl–urea dendrimers (with or without guests) exhibit torsion angles centered around 90° as was found in all crystal structures containing adamantyl–urea groups.

In figure 2.8b, a guest molecule forms urea–urea hydrogen bonds with both arms of a pincer, but again the guest is rotated 90° to the arms of the pincer. The guest also binds using acid–base and hydrogen bonding interactions to another pincer via its carboxylic acid group. Figure 2.8c shows that the guest forms a urea–urea bond with one arm of the pincer and binds to the urea group of other arm via a hydrogen bond with the carboxylic acid carbonyl oxygen. The acidic proton of the guest also interacts with a carbonyl oxygen from another part of the dendrimer.

2.4.4 Conclusions

Crystal structures of model compounds and molecular dynamics simulations of dendrimer–guest complexes are in nice agreement and give insights on how guests interact with adamantyl–urea dendrimers. There is not one clear way the guest molecules bind to the dendrimer, but usually multiple interactions with different parts of the dendrimer are formed. The resulting 3D-structure is clearly more complex than the two-dimensional pincer model described in scheme 2.1.

It is important to stress that crystal structures of model compounds and simulations of dendrimer–guest complexes in vacuum can be different from dendrimer–guest complexes in solution. It has become clear that, in order get a better understanding of the way in which dendrimer and guest interact, new analytical techniques are required that shed light on the structures in solution. This is the topic of the upcoming chapters.

2.5 EXPERIMENTAL SECTION

General

All solvents used were provided by Biosolve and of p.a. quality. *N*-*t*-Boc-L-phenylalanine-*N*-hydroxysuccinimide ester (Sigma), *p*-toluenesulfonyl glycine benzyl ester (Fluka) and 1,6-hexanediamine (Janssen Chimica) were used as received. Standard ¹H NMR, ¹³C NMR and ¹H-¹H COSY spectra were recorded at 25 °C on a Varian Gemini 300 or Varian Mercury 400 MHz spectrometer. Chemical shifts are given in ppm (δ) relative to tetramethylsilane (0 ppm). IR-spectra have been obtained on a Perkin Elmer Spectrum One ATR-FT-IR machine. MALDI-TOF MS spectra were measured on a Perspective DE Voyager spectrometer utilising an α-cyano-4-hydroxycinnamic acid matrix. Optical rotation experiments performed on

the complexes with guest **23** were conducted on a Pleuger Optical Activity polarimeter and a Jasco DIP-370 digital polarimeter. All samples had a concentration of 10 mg/mL of guest molecule. The NMR relaxation time experiments and the 2D NMR ^1H - ^1H NOESY experiments were carried out on a Varian Unity Inova 500 spectrometer operating at 500.618 MHz and equipped with a 5-mm 500 SW/PFG probe from Varian. Spectra were referenced to TMS and were obtained at 25 °C. Prior to Fourier-transformation, the f1 and f2 data points were processed with a squared shifted sinebell weighing function (for f1: sb = -0.13 and sbs = -0.13; for f2, sb1 = -0.065 and sbs1 = -0.065). A mixing time of 0.1 s was used. Spin-lattice relaxation time (T_1) measurements were conducted using a standard ^1H inversion recovery experiment supplied by Varian.

Bis[3-(1-adamantyl-1,3-ureido)propyl]methylamine (1f)

To a solution of bis(propylamine)methylamine (1.45 g, 10 mmol) in dry dichloromethane (50 mL) was added 1-adamantylisocyanate (3.9 g, 22 mmol). The solution was stirred for 24 h under an argon atmosphere. The resulting white precipitate was filtered off and washed with dichloromethane. Recrystallisation from ethanol yielded pure **1f** as a white solid (4.49 g, 90%). ^1H NMR (DMSO- d_6): δ = 5.66 (t, 1H, CH_2NH), 5.47 (s, 1H, Ad-NH), 2.93 (q, 4H, CH_2NH), 2.22 (t, 4H, CH_2N), 2.01 (s, 3H, CH_3), 1.98 (s, 6H, H-3), 1.85 (s, 12H, H-2), 1.59 (s, 12H, H-4), 1.44 (m, 4H, $\text{CH}_2\text{CH}_2\text{CH}_2$). ^{13}C NMR ($\text{CDCl}_3+\text{CD}_3\text{OD}$): δ = 26.8 ($\text{CH}_2\text{CH}_2\text{CH}_2$), 29.4 (C-3), 36.3 (C-4), 37.7 (CH_2NH), 41.7 (CH_3), 42.2 (C-2), 50.3 (C-1), 54.5 (CH_2N), 158.5 (NHC(O)NH).

Benzyl 2-((3,4,5-Tris(2-(2-(2-methoxyethoxy)-ethoxy)-ethoxy))phenylureido) acetate (7)

To a solution of 3,4,5-tri(tetraethyleneoxy)benzoic acid (2.9 g, 3.9 mmol) and triethylamine (1.11 mL, 8.0 mmol) in 20 mL of THF was dropwise added a solution of ethylchloroformate (0.77 mL, 8.0 mmol) in 3 mL of THF at 0°C. Stirring was continued overnight at room temperature. The resulting mixture was added dropwise to a solution of sodium azide (5.2 g, 80 mmol) in 15 mL of water at 0°C. The solution was diluted with 10 mL of water and stirred for two hours at room temperature, and subsequently extracted with methylene chloride (4 x 50 mL). The combined organic layers were dried over MgSO_4 and evaporated in vacuo. Thorough drying over P_2O_5 afforded a pale, yellow oil (2.5 g, 3.3 mmol), which was identified to be acylazide **5** based on FT-IR-spectroscopy. Part of the acyl azide (1.0 g, 1.3 mmol) was redissolved in toluene (20 mL) and heated under reflux for 2.5 h. Evaporation of the solvent in vacuo resulted in a yellow oil (FT-IR-spectroscopy confirmed full conversion into isocyanate **6**) which was redissolved in freshly distilled methylenechloride (10 mL). To this solution was added glycine benzyl ester p-toluenesulfonic acid (472 mg, 1.4 mmol) and triethylamine (mL, 1.4 mmol). The solution was stirred for two hours and 10 mL of dichloromethane was added to the mixture. The organic phase was washed with 1 M KHSO_4 (aq, 2 times 20 mL) and saturated NaHCO_3 (aq, 2 times 20 mL), dried over MgSO_4 and subsequently the solvent was removed in vacuo. The residue was purified using column chromatography (flash silica, dichloromethane/methanol 95/5 v.v. and dimethoxyethane/pentane, 85/15 v.v.) resulting in pure **10** (0.76 g, 71%). ^1H NMR (CDCl_3): δ = 7.97 (s, 1H, ArNH), 7.31 (m, 5H, PhH), 6.76 (s, 2H, ArH), 6.28 (br t, 1H, NHCH_2), 5.12 (s, 2H, PhCH_2O), 4.04 (m, 8H, ArOCH_2 {6} + $\text{CH}_2\text{C}(\text{O})\text{O}$ {2}), 3.8-3.4 (m, 42 H, $\text{OCH}_2\text{CH}_2\text{O}$), 3.15(s, 3H, CH_3), 3.14 (s, 6H, CH_3). ^{13}C NMR (CDCl_3): 170.15 (C(O)O), 155.3 (NHC(O)NH), 151.8 (ArC_3'), 135.3, 135.0 (PhC_{ipso} , ArC_4'), 132.4 (ArC_1'), 127.9, 127.7, 127.63 (PhCH), 98.0 (ArC_2'), 71.7-67.9 ($\text{OCH}_2\text{CH}_2\text{O}$), 66.0 (CH_2 -benzyl), 58.24

(CH₃), 58.21 (2 x OCH₃), 41.21 (CH₂C(O)O). ATR-IR: ν (cm⁻¹) = 3359.5, 2873.0, 1748.5, 1697.0, 1605.7, 1552.4, 1503.9, 1455.9, 1422.4, 1350.3, 1294.3, 1186.0, 1098.0, 946.4, 847.7. MALDI-TOF MS: calc. m/z 902.46, found [M+H]⁺: 903.24, [M+Na]⁺: 925.24.

2-((3,4,5-Tris(2-(2-(2-(2-methoxyethoxy)-ethoxy)-ethoxy)-ethoxy))-phenylureido)acetic acid (3)

Through a solution of ester **10** (320 mg, 0.35 mmol) and Pd/C catalyst (20 mg, load: 10%) in a mixture of *t*-butanol and water (6 mL, 1/1 v.v.), N₂-gas was bubbled for 10 minutes. The solution was placed in a low pressure Parr apparatus and shaken at room temperature for 4 h at a H₂-gas pressure of 50 psi. The solution was filtered over a Whatman glass microfibre filter and the solvent was removed in vacuo. Thorough drying over P₂O₅ in vacuo resulted in 260 mg (0.32 mmol, 91%) of pure **11**. ¹H NMR (CDCl₃): δ = 8.14 (s, 1H, ArNH), 6.75 (s, 2H, ArH), 6.33 (br t, 1H, NHCH₂), 4.06 (m, 6H, ArOCH₂), 4.0-3.52 (m, 44H, OCH₂CH₂O {42} + CH₂C(O)OH {2}), 3.36 (s, 3H, CH₃), 3.35 (s, 6H, CH₃). ¹³C NMR (CDCl₃): δ = 172.4 (C(O)OH), 156.1 (NHC(O)NH), 152.2 (ArC₃), 135.3 (ArC₄), 133.1 (ArC₁), 99.0 (ArC₂), 72.1, 71.7, 71.6, 70.3-70.0, 69.4, 68.3 (OCH₂CH₂O), 58.7 (OCH₃), 58.6 (2 x OCH₃), 41.6 (CH₂C(O)O). ATR-IR: ν (cm⁻¹) = 3356.9, 2873.8, 1741.4, 1697.0, 1604.7, 1553.3, 1504.1, 1455.5, 1422.4, 1349.5, 1294.2, 1199.5, 1094.5, 945.3, 846.9, 755.5. MALDI-TOF MS: calc. m/z 812.42, found [M+Na]⁺: 835.29.

Di-tert-butyl(phthalimidomethyl)phosphonate (9)

Bromomethyl phthalimide (Acros) was recrystallised from heptane/ethyl acetate (2:1 v/v) prior to use. Di-tert-butyl phosphite (Lancaster) was stored on activated molsieves (3 Å) in a refrigerator. Potassium bis(trimethylsilyl)amide (\geq 95 %; Fluka) was used as received. Potassium bis(trimethylsilyl)amide (11.35 g; 56.9 mmol) was dissolved in freshly distilled THF (200 mL) under an argon gas atmosphere. It was cooled on an ice/water bath and magnetically stirred. Then di-tert-butyl phosphite (10.76 g; 55.4 mmol) was added and the clear solution was stirred for 50 minutes. A solution of bromomethyl phthalimide (13.30 g; 55.4 mmol) in 70 mL THF was added dropwise during 40 minutes. Stirring was continued for 1 hour with external ice/water bath cooling. The ice bath was removed and the turbid mixture was stirred for 2 hours at room temperature. The mixture was concentrated in vacuo yielding a brown syrup. This material redissolved in 200 mL of dichloromethane. The organic layer was washed with 200 mL of water and 200 mL of brine (2 times). The organic layer was dried on anhydrous sodium sulfate. After evaporation of the solvent, the product was refluxed for 10 minutes with 50 mL of pentane. After stirring for 2 hours at room temperature, the mixture was filtered and washed with 50 mL of pentane, resulting in 15.2 g yellow solid. The product was dissolved in 10 mL dichloromethane, and subsequently 30 mL flash silica was added and evaporated. The resulting powder was put on a flash silica column. Flash chromatography was performed starting with a gradient of hexane/ethyl acetate from 4:2 v/v to 4:3 v/v. to give pure **9** as a white powder in a yield of 9.1 g (25.7 mmol, 46%). ¹H NMR (CDCl₃): δ = 7.86, 7.72 (dd, 4H, ArH), 3.99 (d, 2H, CH₂, ²J_{H-P} = 11 Hz), 1.30 (s, 18H, CH₃). ¹³C NMR (CDCl₃): δ = 167.13 (C(O)), 134.19, 132.31, 123.48 (ArC), 84.00 (C(CH₃)₃), 37.80 (CH₂, ¹J_{C-P} = 161 Hz), 30.43 (CH₃). ³¹P NMR (CDCl₃): δ = 9.8. Elemental analysis: Calc. for C₁₇H₂₄NO₅P: C, 57.79; H, 6.85; N, 3.96%, found C, 57.74; H, 6.61; N, 4.06%.

Di-tert-butyl{(3,4,5-Tris{2-(2-[2-methoxyethoxy]-ethoxy)-ethoxy})-phenylureido} methane phosphonate (11)

To a solution of di-tert-butyl(phthalimidomethyl)phosphonate (**9**, 1.2 g, 3.4 mmol) in 10 mL of ethanol was added 0.5 mL of hydrazine monohydrate (0.51 g, 10.2 mmol). The mixture was stirred for 24 hours under an argon atmosphere. The solvent was removed in vacuo, 50 mL of dichloromethane was added and the suspension was stirred for ten minutes. Subsequently the suspension was filtered and the dichloromethane in the filtrate was removed in vacuo to give pure **10** as a slightly yellow oil (0.76 g, 100%). $^1\text{H NMR}$ (CDCl_3): $\delta = 2.71$ (2H, d, $^2J_{\text{H-P}} = 9$ Hz, CH_2), 1.40 (18H, s, CH_3). Immediately after liberation of amine **10**, 0.6 g (2.7 mmol) of **10** was added to a solution of 1.9 g (2.6 mmol) of crude isocyanate **6** in 5 mL of distilled dichloromethane. After stirring for two hours 20 mL of dichloromethane was added. The organic phase was washed with 1 M KHSO_4 (aq) (2 times 20 mL) and saturated NaHCO_3 (aq) (2 times 20 mL) and subsequently dried with MgSO_4 . The dichloromethane was removed in vacuo and column chromatography (flash silica, dichloromethane/methanol 95/5 v.v. to 90/10 v.v. and dimethoxyethane/pentane 85/15 v.v.) was performed to obtain pure **11** as a slightly yellow oil (1.3 g, 52%). $^1\text{H NMR}$ (CDCl_3): $\delta = 7.79$ (s, 1H, ArNH), 6.82 (s, 2H, ArH), 5.92 (br t, 1H, NHCH_2), 4.10 (m, 6H, ArOCH_2), 3.82-3.42 (m, 44 H, $\text{OCH}_2\text{CH}_2\text{O}$ {42} + CH_2P {2}), 3.37 (s, 9H, OCH_3), 1.51 (s, 18H, $\text{C}(\text{CH}_3)_3$). $^{13}\text{C NMR}$ (CDCl_3): $\delta = 155.3$ (d, $\text{NHC}(\text{O})\text{NH}$, $^3J_{\text{C-P}} = 9$ Hz), 152.2 (ArC_3), 135.7 (ArC_4), 133.0 (ArC_1), 98.4 (ArC_2), 83.1 (d, $\text{C}(\text{CH}_3)_3$, $^2J_{\text{C-P}} = 9$ Hz), 72.0, 71.5, 70.8, 70.4, 70.3-70.0, 69.3, 68.4 ($\text{OCH}_2\text{CH}_2\text{O}$), 58.6 (OCH_3), 38.4 (d, CH_2P , $J_{\text{C-P}} = 165$ Hz), 30.2 ($\text{C}(\text{CH}_3)_3$). $^{31}\text{P NMR}$ (CDCl_3): $\delta = 15.4$. ATR-IR: ν (cm^{-1}) = 3348.99, 2873.59, 1698.31, 1605.63, 1552.30, 1504.50, 1455.81, 1423.12, 1370.25, 1350.03, 1302.70, 1211.41, 1099.31, 1038.67, 982.68, 847.54. MALDI-TOF MS: calc. m/z 960.52, found $[\text{M}+\text{H}]^+$: 960.30, $[\text{M}+\text{Na}]^+$: 983.30.

{(3,4,5-Tris{2-(2-[2-methoxyethoxy]-ethoxy)-ethoxy})phenylureido}-methane phosphonic acid (8)

To a solution of 0.8 g (0.8 mmol) of phosphonate ester **11** in 3 mL of dichloromethane was added 3 mL of trifluoroacetic acid. The solution was stirred for 3 hours and the solvent was removed in vacuo. The sample was redissolved in dichloromethane that was again removed in vacuo. Subsequently the sample was connected to a high vacuum until $^{19}\text{F NMR}$ indicated that no more TFA ($\delta = -77$ ppm) was present, resulting in 0.68 g of pure **8** (96%). $^1\text{H NMR}$ (CDCl_3): $\delta = 9.50$, 8.05 (br s, 2H, $\text{NHC}(\text{O})\text{NH}$), 6.68 (s, 2H, ArH), 4.05 (m, 6H, ArOCH_2), 3.8-3.51 (m, 44 H, $\text{OCH}_2\text{CH}_2\text{O}$ {42} + CH_2P {2}), 3.36 (s, 3H, CH_3), 3.34 (s, 6H, CH_3). $^{13}\text{C NMR}$ (CDCl_3): $\delta = 157.0$ ($\text{NHC}(\text{O})\text{NH}$, d, $^3J_{\text{C-P}} = 4$ Hz), 152.5 (ArC_3), 134.9 (ArC_4), 133.8 (ArC_1), 99.6 (ArC_2), 72.3, 71.9, 71.8, 70.6-70.4, 69.7, 68.7 ($\text{OCH}_2\text{CH}_2\text{O}$), 59.0 (CH_3), 58.9 (2 x CH_3), 37.3 (d, CH_2P , $J_{\text{C-P}} = 151$ Hz). $^{31}\text{P NMR}$ (CDCl_3): $\delta = 22.6$. ATR-IR: ν (cm^{-1}) = 3340.52, 2870.48, 1696.3, 1663.6, 1603.8, 1555.8, 1504.3, 1454.2, 1423.5, 1349.7, 1299.4, 1216.8, 1095.5, 1023.1, 936.8, 845.5. HRMS: calculated mass for $[\text{C}_{35}\text{H}_{65}\text{N}_2\text{O}_{19}\text{P} + \text{H}]^+$: 849.3997; found 849.3992.

(3-Benzyl-ureido)-methanesulfonate triethylammonium (12)

Aminomethanesulfonic acid (0.50 g, 4.5 mmol) was dissolved in a mixture of acetonitrile (25 mL) and triethylamine (3 mL). Benzyl isocyanate (0.56 mL, 4.5 mmol) was added to the solution. After three hours of

stirring at room temperature, the solution was evaporated. The residue was redissolved in 5 mL of dichloromethane and precipitated in 100 mL of ether. The solvent was decanted, and the small amount of remaining solvent was removed in vacuo to give pure **12** as a yellow oil (1.5 g, 95%). ¹H NMR (DMSO-d₆): δ = 1.19-1.24 (t, 9H, N(CH₂CH₃)₃), 3.12 (m, 6H, N(CH₂CH₃)₃), 3.88 (d, 2H, CH₂SO₃⁻), 4.24 (d, 2H, PhCH₂), 6.32 (br t, 1H, NHCH₂SO₃⁻), 6.66 (br, 1H, PhCH₂NH), 7.22-7.36 (m, 5H, PhH), 8.80-9.10 (br s, 1H, H⁺N(Et)₃). ¹³C NMR (CDCl₃): δ = 8.3 (H⁺N(CH₂CH₃)₃), 43.3 (PhCH₂), 46.0 (H⁺N(CH₂CH₃)₃), 56.8 (CH₂SO₃⁻), 126.3, 126.8, 128.0, 140.4 (PhC), 158.3 (NHC(O)NH). ATR-IR: ν (cm⁻¹) = 13317, 3028, 2935, 2708, 2509, 2250, 2063, 1679, 1651, 1558, 1496, 1475, 1454, 1401, 1363, 1308, 1216, 1156, 1083, 1062, 1031, 918, 839, 739, 700. MALDI-TOF MS: calc. m/z for [M]⁺: 243.26, found: 243.22.

***N'*-(6-Aminohexyl)-*N*-*t*-Boc-*L*-phenylalaninamide (18)**

To a solution of 60 g (51 mmol) of 1,6-hexanediamine in 120 mL of dichloromethane was added dropwise a solution of 3.62 g (10 mmol) *N*-*t*-Boc-*L*-phenylalanine-*N*-hydroxy-succinimide ester in 200 mL of dichloromethane in 2 hours. Upon addition of the ester a white precipitate started to form. After stirring overnight the reaction mixture was transferred to a separatory funnel and washed with water (6 times 300 mL) and a saturated NaCl solution (once 100 mL). During this procedure the formed precipitate disappeared. The organic phase was dried over Na₂SO₄ and evaporated in vacuo. Column chromatography (50 g SiO₂) starting with CHCl₃/MeOH, 95/5 (v.v.) as an eluent was used to remove the doubly functionalized species from the residue, and subsequently the eluent was changed to CHCl₃/MeOH/N(Et)₃, 90/5/5 v.v. to remove the mono-functionalized species from the column. Evaporation of the solvent in vacuo gave pure amine **18** as a yellow oil (2.5 g, 69%). ATR-IR: ν (cm⁻¹) = 3301.0, 2977.8, 2931.0, 2857.7, 1651.5, 1525.9, 1497.1, 1455.3, 1391.4, 1365.9, 1247.2, 1166.0, 1047.0, 1021.4, 748.7, 698.4. ¹H NMR (DMSO-d₆): δ = 1.05-1.4 (m, 17 H, (CH₃)₃C (9H) + CH₂(CH₂)₄CH₂ (8H)), 2.55 (t, 2H, ³J_{H-H} = 7 Hz, H₂NCH₂), 2.7 (dd, 1H, J_{H'-Ha} = 9.9, ³J_{H'-H''} = 13.6 Hz, PhCH'H''C*), 2.85 (dd, 1H, ²J_{H'-H''} = 13.6 Hz, ³J_{H''-Ha} = 5.1 Hz, PhCH'H''C*), 3.0 (m, 2H, CH₂NHC(O)), 4.05 (pseudo dt, 1H, ³J_{Ha-NH} = 8.8 Hz, ³J_{Ha-H'} = 9.9 Hz, ³J_{Ha-H''} = 5.1 Hz, C*H), 6.8 (d, 1H, ³J_{Ha-NH} = 8.8 Hz, C*HNHC(O)), 7.2 (m, 5H, PhH), 7.8 (br t, 1H, ³J_{NH-CH₂} = 5.5 Hz, CH₂NHC(O)). ¹³C NMR (CDCl₃): δ = 26.42, 26.56 (H₂NCH₂CH₂(CH₂)₂), 28.29 (C(CH₃)₃), 29.27, 33.48 (H₂NCH₂CH₂(CH₂)₂CH₂CH₂), 38.84 (CH₂NHC(O)), 39.33 (ArCCH₂), 42.03 (H₂NCH₂), 56.06 (C*), 80.0 (C(CH₃)₃), 126.87, 128.61, 129.34 (PhCH), 136.95 (PhC_{ipso}), 155.70 (NHC(O)OC(CH₃)₃), 171.03 (NHC(O)C*). MALDI-TOF MS: mw. calc. for [M+H]⁺: 364.25, found 364.17; mw calc. for [M+Na]⁺: 386.24 found 386.16.

***N'*-(6-(benzyloxycarbonylmethyl-1,3-ureido)hexyl)-*N*-*t*-Boc-*L*-phenylalaninamide (20)**

A solution of 1.44 g (14.8 mmol) of *p*-toluenesulfonyl glycine benzyl ester in 150 mL of dichloromethane was washed with 75 mL of a NaOH-solution (2.4 M) and water (2 times 75 mL). Drying of the organic layer with Na₂SO₄ and evaporation of the solvent gave glycine benzyl ester as a slightly yellow oil (0.6 g, 85%). ¹H NMR (CDCl₃): δ = 7.35 (s, 5H, PhH), 5.16 (s, 2H, PhCH₂), 3.46 (s, 2H, CH₂NH₂), 1.42 (s, br, 2H, NH₂). Of this amine 0.446 g (2.7 mmol) in 2 mL of distilled dichloromethane was added to a solution of 0.708 g (2.7 mmol) di-*t*-butyl-tricarbonate in 3 mL of distilled dichloromethane. IR-spectroscopy showed a large peak at 2252.3 cm⁻¹, indicating that the amine was converted to isocyanate **19**. After stirring for half an

hour a solution of 1.0 g (2.8 mmol) of amine **18** in 3 mL of distilled dichloromethane was added. IR-spectroscopy revealed a complete disappearance of the isocyanate peak after two hours. The reaction mixture was subjected to column chromatography (SiO₂, CHCl₃/MeOH, 95/5 v.v.) and precipitation in hexane to obtain pure **20** as a white solid (1.27 g, 85%). Mp: 107–109 °C. $[\alpha]_D^{20} = 5$ (c = 1 in CHCl₃), Calc. for C₃₀H₄₂N₄O₆: C, 64.96; H, 7.63; N, 10.10%, found C, 64.82; H, 7.55; N, 10.14%. ATR-IR: ν (cm⁻¹) = 3317.3, 2931.1, 2858.3, 1732.7, 1687.1, 1645.9, 1562.5, 1521.9, 1455.4, 1439.0, 1390.9, 1365.3, 1290.7, 1232.2, 1200.8, 1168.0, 1024.7, 734.2, 697.0. ¹H NMR (DMSO-d₆): δ = 1.18–1.45 (br m, 8H, CH₂(CH₂)₄CH₂), 1.38 (s, 9H, (CH₃)₃C), 2.7 (dd, 1H, ²J_{H'-H''} = 13.6 Hz, ³J_{H'-H α} = 9.9 Hz, PhCH'H''C*), 2.9 (dd, 1H, ³J_{H''-H α} = 5.0 Hz, ²J_{H'-H''} = 13.6 Hz, PhCH'H''C*), 2.95–3.1 (m, 4H, (CH₂(CH₂)₄CH₂), 3.8 (d, 2H, ³J_{CH₂-NH} = 6.2 Hz, NHCH₂C(O)), 4.1 (pseudo dt, 1H, ³J_{H α -NH} = 8.5 Hz, ³J_{H α -H''} = 5.0 Hz, ³J_{H α -H'} = 9.9 Hz, C*H), 5.1 (s, 2H, PhCH₂O), 6.15 (m, 2H, NHCONH), 6.8 (d, 1H, ³J_{H α -NH} = 8.5 Hz, NHC*), 7.18–7.38 (m, 10H, PhH), 7.8 (br t, 1H, C*(O)NH). ¹³C NMR (CDCl₃): δ = 25.86, 25.91 (CH₂CH₂(CH₂)₂CH₂CH₂), 28.06 (CH₃)₃C), 28.84, 29.75 (CH₂CH₂(CH₂)₂CH₂CH₂), 38.84 (CH₂(CH₂)₄CH₂), 39.54 (PhCH₂C*), 41.93 (CH₂C(O)O), 55.85 (C*), 66.48 (CH₂-benzyl), 79.40 (C(CH₃)₃), 126.42, 127.93, 128.08, 128.12, 128.30, 129.10 (ArCH), 135.21, 136.86 (PhC_{ipso}-benzyl + PhC_{ipso}CH₂C*), 155.56 (NHC(O)O), 158.72 (NHC(O)NH), 171.40 (C(O)O), 171.93 (NHC(O)). MALDI-TOF MS: mw. calc. for [M+Na]⁺ 577.30, found 577.07.

N'-(6-(carboxymethyl-1,3-ureido)hexyl)-*N*-*t*-Boc-*L*-phenyl-alaninamide (**21**)

To a 1/1 v.v. mixture of *t*-butanol and water (50 mL) was added 1.00 g (0.15 mmol) of ester **22** and 40 mg of Pd/C catalyst (load: 10%). Subsequently, N₂-gas was bubbled through the solution for 15 minutes. The flask was put in a Parr-apparatus, and was shaken for 3 hours under H₂-atmosphere (pressure: 50 psi). Subsequently the suspension was filtered to remove the catalyst and the solvent was evaporated in vacuo, to give acid **23** as a white, sticky foam (0.75 g, 89%). Mp: 71–73 °C. Calc. for C₂₃H₃₆N₄O₆: C, 59.47; H, 7.81; N, 12.06%, found C, 59.73; H, 7.94; N, 11.68%. ATR-IR: ν (cm⁻¹) = 3312.3, 2978.7, 2932.9, 2859.8, 1646.6, 1563.3, 1498.3, 1455.3, 1440.3, 1392.6, 1366.7, 1264.9, 1248.0, 1165.4, 699.6. ¹H NMR (DMSO-d₆): δ = 1.18–1.40 (br, 8H, CH₂(CH₂)₄CH₂), 1.29 (s, 9H, (CH₃)₃C), 2.7 (dd, 1H, ³J_{H'-H α} = 9.0 Hz, ²J_{H'-H''} = 13.6 Hz, PhCH'H''C*), 2.9 (dd, 1H, ²J_{H'-H''} = 13.6 Hz, ³J_{H''-H α} = 5.0 Hz, PhCH'H''C*), 2.95–3.1 (m, 4H, (CH₂(CH₂)₄CH₂), 3.63 (d, 2H, ³J_{CH₂-NH} = 5.9 Hz, NHCH₂C(O)), 4.1 (pseudo dt, 1H, ³J_{H α -NH} = 8.8 Hz, ³J_{H α -H'} = 9.0 Hz, ³J_{H α -H''} = 5.0 Hz, C*H), 6.0, 6.1 (t, 2H, ³J_{NH-CH₂} = 5.8 Hz, NHCONH), 6.8 (d, 1H, ³J_{H α -NH} = 8.8 Hz, NHC*), 7.23 (m, 5H, PhH), 7.84 (t, 1H, C*HNHC(O)). ¹³C NMR (DMSO-d₆): δ = 26.34 (CH₂CH₂(CH₂)₂CH₂CH₂), 28.36 (C(CH₃)₃), 29.22, 30.22 (NHC(O)NHCH₂CH₂ + CH₂CH₂NHC(O)C*), 38.01 (CH₂NHC(O)C*), 42.96 (CH₂C(O)OH), 56.01 (C*H), 78.15 (C(CH₃)₃), 126.37, 128.20, 129.40 (PhCH), 138.37 (PhC_{ipso}), 155.36 (NHC(O)O(CH₃)₃), 158.23 (NHC(O)NH), 171.51 (C(O)OH), 173.39 (NHC(O)C*). MALDI-TOF MS: mw. calc. for [M+Na]⁺ 487.25, found 487.09.

2-Adamantylureido-acetic acid (22)

A solution of 2.84 g (16.0 mmol) of 1-adamantylisocyanate in 30 mL of CHCl₃ was put under an argon atmosphere, and 3 mL of triethylamine was added. The solution was cooled with an ice bath and subsequently

3.0 g (23.9 mmol) of glycine methyl ester hydrochloric acid was added. After stirring for three hours in an Argon atmosphere, 250 mL of a 0.1 M HCl-solution was added, and a white precipitate was formed. The mixture was filtered over a glass funnel. The residue was washed with distilled water, and dried in vacuo to give the 1-adamantylurea methyl ester as a white powder (3.5 g, 82%). From this compound 3.0 g (11.3 mmol) was dissolved in 25 mL of H₂O and 25 mL of THF. LiOH.H₂O (3.94 g, 93.9 mmol) was added and the solution was stirred for 24 h. The THF was removed in vacuo, and the solution was acidified with 100 mL of a 1 M HCl-solution. The resulting white precipitate was isolated via filtration, and thorough drying in vacuo resulted in 2.26 g (79%) of pure **25**. ¹H NMR (DMSO-d₆): δ = 1.60 (br s, 6H, H-4), 1.85 (br s, 6H, H-2), 1.98 (br s, 3H, H-3), 3.63 (d, 2H, CH₂, ³J_{NH-CH₂} = 14 Hz), 5.85 (br s, 2H, NHC(O)NH). ¹³C NMR (DMSO-d₆): δ = 29.4 (C-3), 36.5 (C-4), 42.4 (C-2), 41.5 (CH₂), 49.9 (C-1), 157.2 (NHC(O)NH), 173.2 (C(O)OH).

2.6 REFERENCES

- 1 M. W. P. L. Baars, A. J. Karlsson, V. Sorokin, B. F. W. De Waal, E. W. Meijer, *Angew. Chem. Int. Ed.* **2000**, *39*, 4262-4265.
- 2 M. Pittelkow, J. B. Christensen, E. W. Meijer, *J. Polym. Sci., Part A : Polym. Chem.* **2004**, *42*, 3792-3799.
- 3 M. Pittelkow, C. B. Nielsen, M. A. C. Broeren, J. L. J. van Dongen, M. H. P. van Genderen, E. W. Meijer, J. B. Christensen, *Chem. Eur. J.* **2005**, *11*, 5126-5135.
- 4 A. P. H. J. Schenning, C. Elissen-Roman, J.-W. Weener, M. W. P. L. Baars, S. J. Van der Gaast, E. W. Meijer, *J. Am. Chem. Soc.* **1998**, *120*, 8199-8208.
- 5 M. W. P. L. Baars, A. J. Karlsson, V. Sorokin, B. F. W. De Waal, E. W. Meijer, *Angew. Chem. Int. Ed.* **2000**, *39*, 4262-4265.
- 6 P. M. Ivanov, I. G. Pojarlieff, I. B. Blagoeva, C. Jaime, V. T. Angelova, A. H. Koedjikov, *J. Phys. Org. Chem.* **2004**, *17*, 423-430.
- 7 M. W. P. L. Baars, R. Kleppinger, M. H. J. Koch, S.-L. Yeu, E. W. Meijer, *Angew. Chem. Int. Ed.* **2000**, *39*, 1285-1288, supp. info.
- 8 M. Bodanszky, *Principles in peptide synthesis*, 2nd rev. ed., New York: Springer, **1993**.
- 9 J. P. Genêt, J. Uziel, M. Port, A. M. Touzin, S. Roland, S. Thorimbert, S. Tanier, *Tetrahedron Lett.* **1992**, *33*, 77-80.
- 10 H. Christol, M. Levy, C. Marty, *J. Organometal. Chem.* **1968**, *12*, 459-470.
- 11 H. Christol, C. Marty, *J. Organometal. Chem.* **1968**, *12*, 471-478.
- 12 K. S. Narayanan, K. D. Berlin, *J. Am. Chem. Soc.* **1979**, *101*, 109-115.
- 13 K. Maeda, K. Morino, Y. Okamoto, T. Sato, E. Yashima, *J. Am. Chem. Soc.* **2004**, *126*, 4329-4342.
- 14 B. Garrigues, M. Mulliez, *Synthesis* **1988**, 810-813.
- 15 M. A. C. Broeren, J. L. J. v. Dongen, M. Pittelkow, J. B. Christensen, M. H. P. v. Genderen, E. W. Meijer, *Angew. Chem. Int. Ed.* **2004**, *43*, 3557-3562.
- 16 R. G. Denkwalter, J. Kolc, W. J. Lukasavage, *U.S. Pat. 4, 289,872, Sept. 15, 1981*.
- 17 D. Seebach, J. M. Lapierre, K. Skobridis, G. Greiveldinger, *Angew. Chem.* **1994**, *106*, 457-458.
- 18 D. Seebach, P. B. Rheiner, G. Greiveldinger, T. Butz, H. Sellner, *Top. Curr. Chem.* **1998**, *197*, 125-164.
- 19 H. W. I. Peerlings, E. W. Meijer, *Chem. Eur. J.* **1997**, *3*, 1563-1570. In this publication the values for DAB(PA-LPhe)_x should be negative instead of positive.
- 20 J. R. McElhanon, D. V. McGrath, *J. Am. Chem. Soc.* **1998**, *120*, 1647-1656.
- 21 J. F. G. A. Jansen, E. M. M. de Brabander-van den Berg, E. W. Meijer, *Science* **1994**, *266*, 1226-1229.
- 22 The specific optical rotation was originally defined as $[\alpha]_D^{20} = 100 \cdot \alpha / (c \cdot l)$, with c the concentration in grams per 100 mL and l the length of the tube in decimeters. The notation $[\alpha]_D^{20}$ is used to indicate the temperature (20 °C) and the wavelength of the light (D line of a sodium lamp: $\lambda = 589.6$ nm). Nowadays the following equation is used in textbooks, which is slightly different: $[\alpha]_D^{20} = \alpha / (c \cdot l)$. In this case the concentration is given in grams per mL, resulting in the same value for the specific optical rotation. Throughout this chapter the old convention is used, so $c = 1$ refers to a concentration in grams per 100 mL.
- 23 10 mg of **21** results in $1.80 \cdot 10^{-5}$ moles of L-phenylalanine units. 10 mg of **17a** results in $1.96 \cdot 10^{-5}$ moles of moles of L-phenylalanine units, and 10 mg of **17e** results in $1.84 \cdot 10^{-5}$ moles of L-

phenylalanine units. The amount of chiral units that determine the optical rotation are approximately the same.

- 24 A. W. Bosman, M. J. Bruining, H. Kooijman, A. L. Spek, R. A. J. Janssen, E. W. Meijer, *J. Am. Chem. Soc.* **1998**, *120*, 8547-8548.

Chapter 3

Supramolecular dendritic architectures in the gas phase*

ABSTRACT: *Electrospray mass spectrometry has been able to achieve the delicate transfer of supramolecular dendritic architectures from chloroform to the gas phase. For the first time, individual dendritic host–guest complexes have been visualized. Collision induced dissociation (CID) with argon atoms can be used to determine the stability of guest–host complexes in the gas phase, based on the center of mass energy at which 50% of the ion of interest has dissociated. It was found that sulfonic acid guests bind strongest, followed by phosphonic acid guests and carboxylic acid guests. By subjecting an ion to CID that contains two different guest molecules simultaneously attached to one dendrimer, it is possible to determine which guest is most strongly bound to the dendritic host. In this way, it has been shown that the presence of urea groups clearly strengthens the binding to the dendrimer. The results are in agreement with the binding strength of guest molecules in chloroform. Also dendrimer–tripeptide aggregates have been observed. CID showed a weaker binding of peptides that have bulky residues close to the acidic headgroup of the guest, indicating a negative steric effect. Molecular dynamics simulations have shown that it is possible to determine the stability of the host–guest complexes in the gas phase by investigating at which temperature a slowly heated complex is losing guest molecules. The mass spectrometry results are in agreement with the performed molecular dynamics simulations. With the model at hand it might be possible to determine how guest molecules can be designed to come to a stronger binding between guest and host.*

* Part of this work has been published: M.A.C. Broeren, J.L.J. van Dongen, M. Pittelkow, J.B. Christensen, M.H.P. van Genderen, E.W. Meijer, *Angew. Chem. Int. Ed.* **2004**, *43*, 3557-3562. M.A.C. Broeren, J.L.J. van Dongen, M.H.P. van Genderen, E.W. Meijer, *Polym. Mater. Sci. Eng.* **2004**, *91*, 933-934. M. Pittelkow, C.B. Nielsen, M.A.C. Broeren, J.L.J. van Dongen, M.H.P. van Genderen, E.W. Meijer, J.B. Christensen, *Chem. Eur. J.* **2005**, *11*, 5126-5135.

3.1 INTRODUCTION

Mass spectrometry has emerged as one of the most important techniques in the identification of molecules, ranging from single atoms to large polymers and proteins. The enormous evolution in “soft” ionization methods, ion optics, mass accuracy and mass range has made mass spectrometry indispensable in all fields of chemistry and biology. The discovery of Electrospray Ionisation (ESI) by Fenn and coworkers, for which he was awarded the Nobel Prize in Chemistry of 2002, was a breakthrough in the analysis of large and fragile proteins.¹ Electrospray ionization has proven to be best technique to successfully transfer large molecules, like dendrimers² or proteins,^{3,4} from solution to the gas phase. In recent years it has become apparent that the gentle nature of electrospray ionization can also result in the analysis of intact, non-covalent structures.⁵⁻⁷ The coupling of ESI with time-of-flight mass analysis (TOF) has increased the mass-to-charge ratio (m/z) range significantly,⁸ and has enabled mass spectrometric analysis of non-covalent complexes like protein oligomers, small viruses and DNA.⁹⁻¹² Recently, Heck and coworkers have used electrospray mass spectrometry to monitor the formation of supramolecular complexes involved in the GroEl–GroEs chaperonin system.¹³

Also in the field of supramolecular chemistry, electrospray ionizations has been used to analyze non-covalently bound structures, but the number of examples is limited. The major difficulty is to ionize weakly bound, noncovalent species without disrupting their structure. Most hydrogen-bonded aggregates for example decompose in common electrospray solvents such as methanol. Chloroform can be used instead, but this often makes ionization of the aggregate more difficult. In some cases, ion labeling to create “built-in” charges has solved this problem.¹⁴⁻¹⁶ Examples of supramolecular structures analyzed with electrospray mass spectrometry include metallodendrimers, molecular squares and triangles, rosette-type assemblies from barbiturate and melamine subunits, and molecular capsules.¹⁷ Apart from regular mass spectrometry, tandem mass spectrometry can be used to obtain more information about the supramolecular aggregate.

In tandem mass spectrometry (MS/MS), a first analyzer in the mass spectrometer isolates a precursor ion, which subsequently undergoes fragmentation yielding product ions that are analyzed with the second analyzer.¹⁸ One of the most frequently used MS/MS techniques is collision induced dissociation (CID).^{19,20} In CID an ion is accelerated, selected and subsequently collided with neutral gas atoms, e.g. argon, in a collision cell. The mechanism of dissociation of larger molecules or aggregates is not based on a knockout principle, in which a molecule breaks at the position where a gas atom has struck. It is generally accepted that the mechanism of fragmentation is based on a two-step phenomenon.^{19,21,22} First, excitation takes place through collisions, where a fraction of the ion’s kinetic energy is transferred into internal energy. Then, when the internal energy reaches a certain threshold value, dissociation of the excited ion takes place. Through collisions, the ions are actually “heated” until an internal temperature is reached that results in fragmentation. The extent of

fragmentation depends on the internal energy of the excited ion, which in turn is related to the imposed acceleration. CID is mostly used to get structural information from the selected ion. Peptides for example fragment according to specific gas phase reactions. Based on the masses of the fragments, the sequence can be derived.²³ CID can also be performed on ions of noncovalent complexes.²⁴⁻²⁷ In this way, the stability of the complex can be assessed in the gas phase. Although it is tempting to link this stability to the binding strength of the complex in solution, great care must be taken in comparing these results, especially when complexation in water is compared to the gas phase.²⁸⁻³¹

In this chapter, the analysis of dendritic host–guest complexes with mass spectrometry is described. The experiments have been performed on a Q/TOF mass spectrometer, which is briefly described in the following paragraph. The complexation of several guest molecules with the third generation urea–adamantyl dendrimer is investigated. The influence of acid strength, presence of urea groups, molecular weight and loading on the binding strength has been investigated with MS/MS. The results are compared with complexation studies in chloroform and show a remarkable agreement. It has also been possible to observe peptide–dendrimer aggregates, confirming that a statistical mixture of guests bound to the dendrimer is formed. A kinetic model has been derived that is used to get insights into the cooperativity (or anticooperative) in binding of the guests. Molecular dynamics simulations have been used to get more insights into interactions that govern binding between guest and host.

3.2 THE QUADRUPOLE TIME-OF-FLIGHT (Q/TOF) INSTRUMENT³²

The term Q/TOF is used to describe a type of hybrid mass spectrometer system (Figure 3.1) in which a quadrupole analyzer (Q) is used in conjunction with a time-of-flight analyzer (TOF). The use of two analyzers together (hence the term hybrid) provides the advantage to do tandem mass spectrometry.

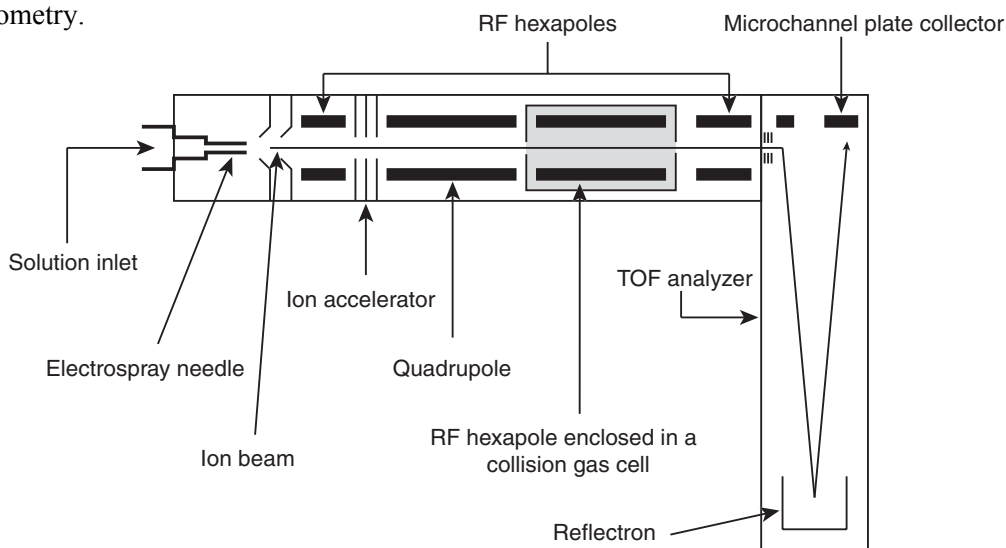


Figure 3.1 Schematic diagram of an orthogonal Q/TOF instrument.

In the Q/TOF, the quadrupole is used in one of two modes to select the ions to be examined, and the TOF analyzer measures the actual mass spectrum. Several hexapole assemblies are used to keep the ions in the desired trajectory. A quadrupole analyser consists of four cylindrical rods placed parallel and opposite to each other (Figure 3.2). To each opposed pair of rods a static and alternating electric field can be applied, which influences the trajectory of the ions that are injected through the rods. In the narrow band pass mode, an ion with a certain m/z value is selected and passed through the rods, while the others strike the poles and are lost. In the wide band pass mode all ions go through the quadrupole.

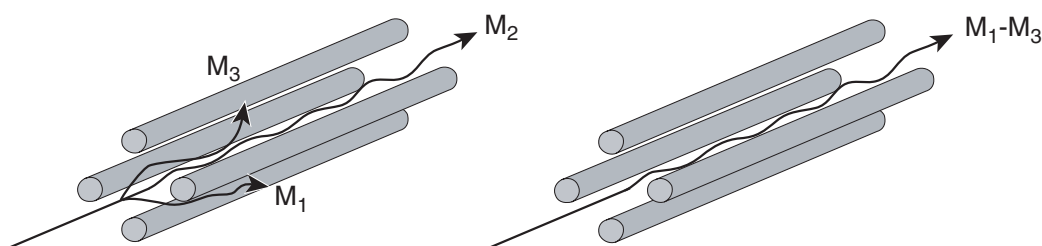


Figure 3.2 Schematic representation of a quadrupole in narrow band pass mode (left) and wide band pass mode (right). In the narrow band pass mode, the ion with m/z M_2 is selected. All other ions collide with the rods.

In case of a regular mass spectrum, the Q/TOF is operated with the quadrupole in wide band-pass mode. All ions generated at the electrospray inlet will pass through the quadrupole and are analyzed in the TOF analyzer. In case of collision induced dissociation, the Q/TOF is operated with the quadrupole in narrow band-pass mode. The ions are first accelerated, giving them a higher kinetic energy, and then injected in the quadrupole. Only the ions of the selected m/z range will leave the quadrupole. These ions enter the collision cell. The selected ions collide with the argon gas atoms and gain sufficient internal energy to fragment. The extent of fragmentation depends on the internal energy of the excited ion, which in turn is related to the kinetic energy of the ion prior to injection into the collision cell. Thus, selected precursor ions are dissociated to give product (fragment) ions. The product ions and unchanged parent ions enter the TOF analyser, and a mass spectrum is obtained.

3.3 GAS PHASE STUDIES OF DENDRITIC HOST–GUEST COMPLEXES

3.3.1 Influence of acid strength, molecular weight and loading

In the study of dendritic aggregates with mass spectrometry, the third generation urea-adamantyl dendrimer **1c** has been used as a host (in this chapter described as **D**, figure 3.3). For poly(propylene imine) dendrimers it is known that the amount of imperfect dendrimer structures increases upon increasing dendrimer generation as a result of side reactions during the divergent synthesis.² This hampers a detailed analysis of the supramolecular complexes with the fourth and fifth generation dendrimer. For the guest molecules the benzyl and ethylene glycol modified guests **2–6** have been used, described in chapter two. In this way the influence of acid strength and molecular weight of the guests can be analysed.

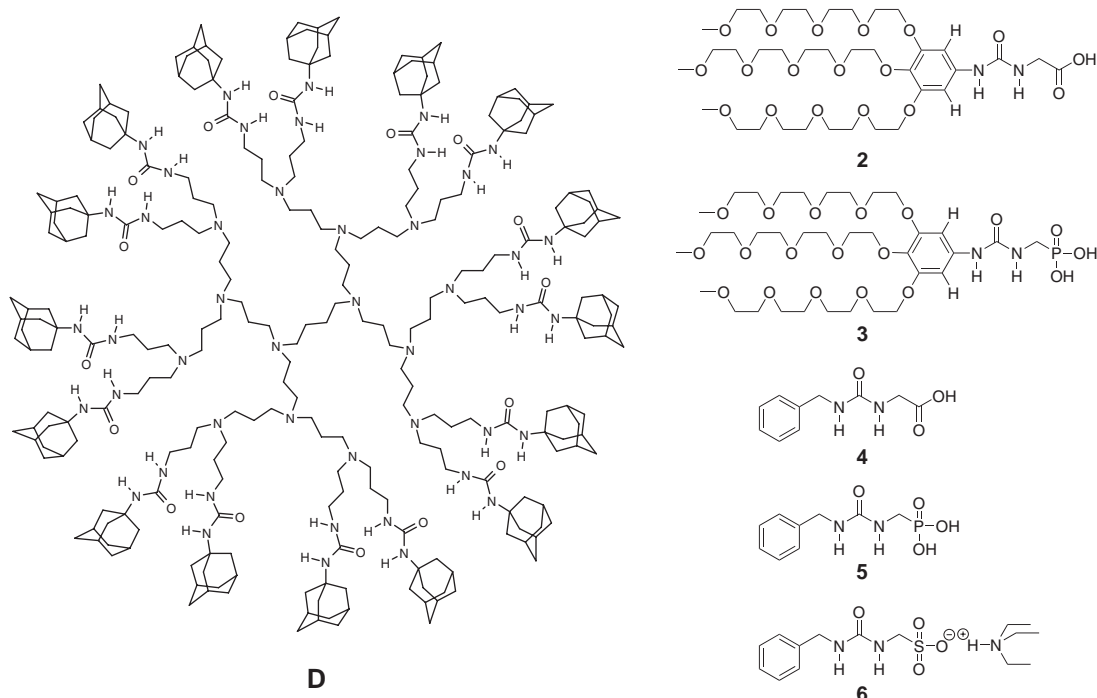


Figure 3.3 The molecules used in this study.

The electrospray mass spectrum of dendrimer **D** mainly gives the 3+ and 4+ ions of the intact molecule, and deconvolution results in the correct mass of 4522 g/mol (Figure 3.4a). The much smaller peak at 4565 g/mol corresponds to the dendrimer that lacks one propylamine unit ($\Delta M = 57.1$). The peak 37 g/mol higher in mass is presumably HCl non-covalently bound to a tertiary amine of the dendrimer, and is observed frequently when chloroform is used as solvent. When a 4-fold excess of guest **5** over **D** in chloroform is injected in the mass spectrometer, clusters of triply and quadruply protonated ions are observed. Deconvolution provides the overall spectrum and, surprisingly, all possible assemblies between **D** and **5** are observed as well as a small portion of free **D** (Figure 3.4d). The 10 major peaks are separated by the mass of **5** ($M = 244$) and are interpreted as x guests **5** bound to **D** (notation used throughout this chapter is $\mathbf{D}\cdot(\mathbf{5}_x)$ with $x = 0-9$). The spectra

prove that the different complexes are indeed formed and are stable enough to be transferred and analysed in the gas phase.

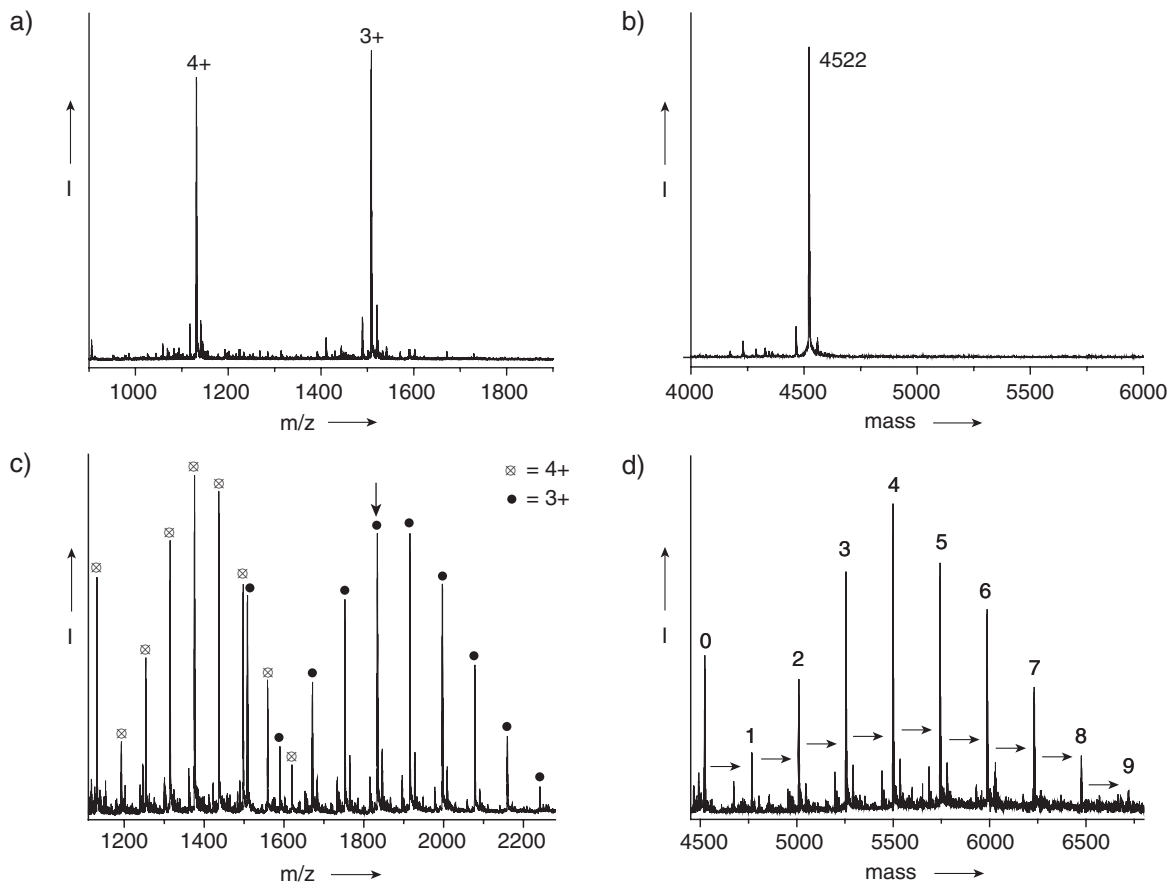


Figure 3.4 Mass spectra of dendrimer **D** before (a) and after (b) deconvolution, and of sample **D+5₄** before (c) and after (d) deconvolution. The mass difference between the peaks after deconvolution matches the mass of guest **5**. In figure 3.4c, the ion indicated with an arrow corresponds to $\mathbf{D}\cdot(\mathbf{5}_4)^{3+}$. This ion is subjected to CID, as depicted in figure 3.5.

It is possible to select one of the assemblies in the quadrupole (e.g. $\mathbf{D}\cdot(\mathbf{5}_4)^{3+}$, figure 3.4c) and subsequently perform a collision induced dissociation experiment. In figure 3.5, a stacked plot of mass spectra obtained with increasing acceleration voltages is given. Going from low to high voltage, the subsequent dissociation of guest **5** is observed, eventually resulting in empty \mathbf{D}^{3+} . The guests are removed as neutral species and only the tri-cationic dendritic complexes are observed. This is a general observation found for all aggregates (**D** with **2–6**), and is independent of the number of guests bound.

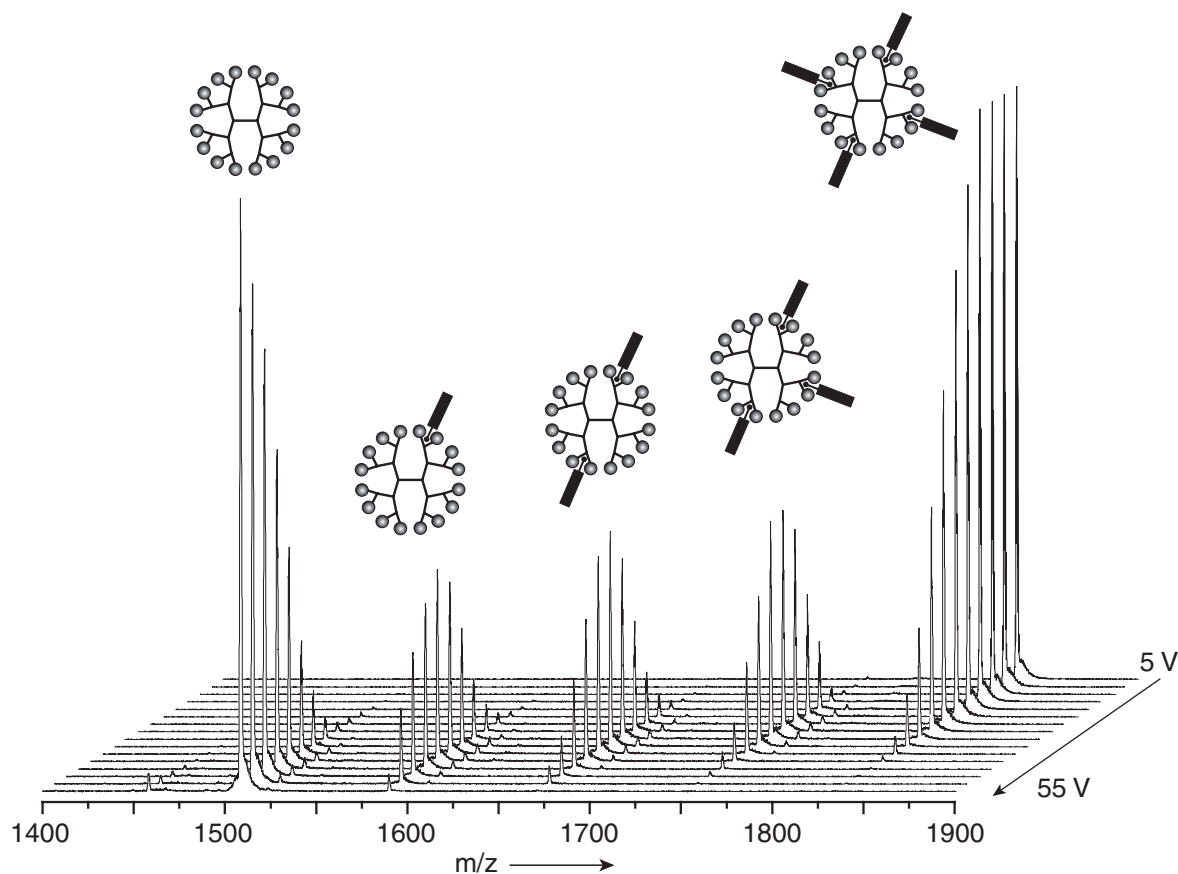


Figure 3.5 CID-experiment performed on $D\bullet(5_4)^{3+}$. The parent ion loses guest molecules as neutral species upon increasing acceleration voltage. Eventually the only ion present is the empty dendrimer D^{3+} .

Due to the multivalent nature of the dendrimer, it is possible to assemble different guests simultaneously to the dendritic host, and to analyze these multi-component ions with mass spectrometry. In this way the binding strength of different guests can be systematically analyzed, since the gain in internal energy as a result of the collisions is distributed over all guests in the same aggregate.

The mass spectrum of **D** with two equivalents of both **4** and **5** shows clusters of peaks that correspond to different combinations of **4** and **5** bound to the dendrimer. The $D\bullet(4_2+5_2)^{3+}$ ion has been selected and subjected to CID (Figure 3.6a). In this way the influence of the acid group can be investigated. Upon increasing acceleration voltage guest **4** dissociates first from the dendrimer. At 20 V $D\bullet(5_2)^{3+}$ is the most abundant ion. A further increase of the acceleration voltage results in dissociation of phosphonic acid guest **5**. This selective dissociation of carboxylic acid guest **4** over phosphonic acid guest **5** is remarkably strong, independent of the combination of the guests attached to the dendrimer, and indicative of a difference in binding strength in the gas phase due to differences in acidity.

This methodology is comparable to the kinetic method developed by Cooks and coworkers, which is a procedure to determine thermochemical information based on the rates of competitive

dissociations of mass selected cluster ions.³³⁻³⁵ Although it is not possible in our case to get quantitative data due to several unknown parameters (see paragraph 3.5) it is in our view valid to compare the binding of different guests to dendrimer **D** in the gas phase in a qualitative manner.

When both **3** and **5** are assembled on the same dendrimer and $\mathbf{D}\cdot(\mathbf{3}_2+\mathbf{5}_2)^{3+}$ is subjected to CID, the small guests are significantly less strongly anchored than the large guests (Figure 3.6b).

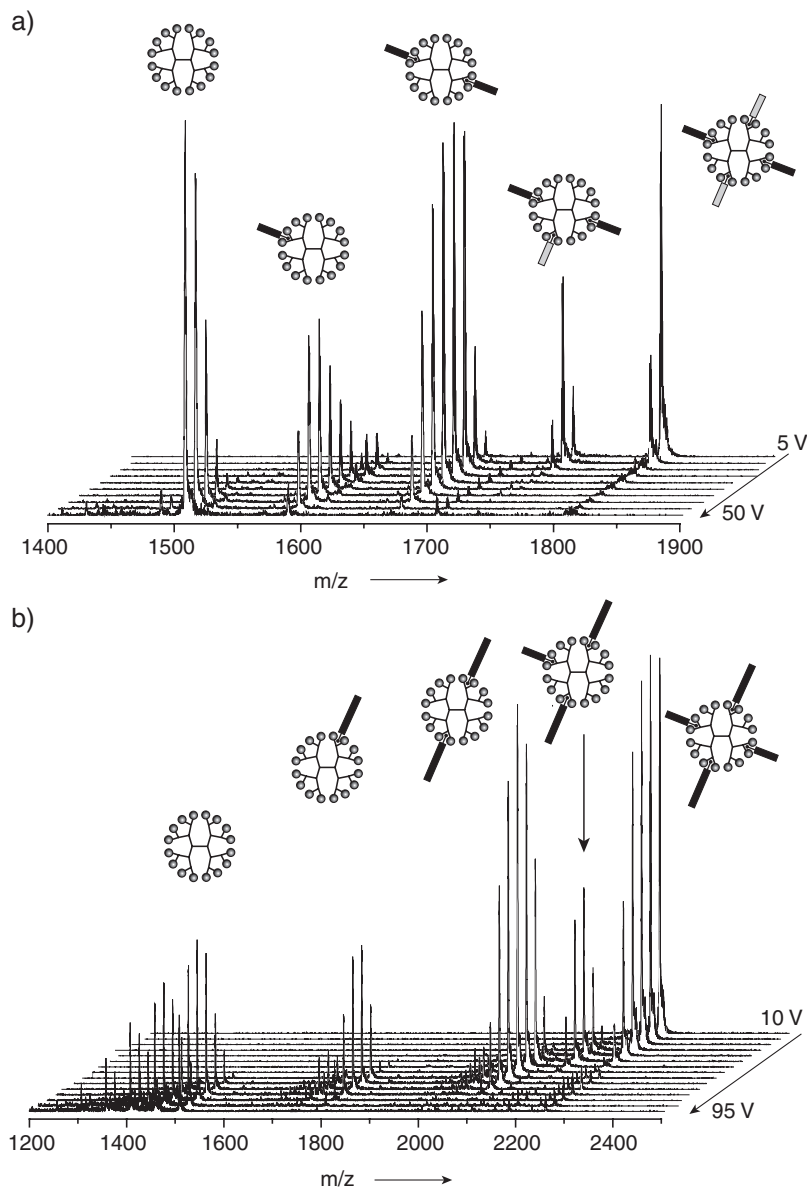


Figure 3.6 a) CID experiment performed on $\mathbf{D}\cdot(\mathbf{4}_2+\mathbf{5}_2)^{3+}$. The carboxylic acid guests **4** (light gray) selectively dissociate before the phosphonic acid guests **5** are removed. b) CID experiment performed on $\mathbf{D}\cdot(\mathbf{3}_2+\mathbf{5}_2)^{3+}$. Phosphonic acid guests **5** (small guest) dissociate first, until only $\mathbf{D}\cdot(\mathbf{3}_2)^{3+}$ is present. Subsequently, guest **3** dissociates. Covalent fragmentation of the dendrimer starts to take place at higher voltages.

In contrast to the gas phase data, the difference in binding strength measured between **3** and **5** with **D** in chloroform is marginal. This discrepancy between solution and gas phase is proposed to be due to additional Van der Waals interactions in the gas phase between the ethylene glycol chains

of **3** and the dendrimer scaffold. In chloroform the chains of the guests are solvated and the association constant is then primarily determined by the acid–urea motif.

Several other peaks emerge during the CID experiment. At high voltages some peaks with $m/z = 50.3$ are observed next to the intact \mathbf{D}^{3+} ion. Small fragments dissociate from the adamantyl dendrimer as neutral species that have a mass of 151 g/mol, which corresponds exactly with adamantyl amine. These fragments also appear when bare \mathbf{D}^{3+} is subjected to CID. Apparently, competition between covalent fragmentation and non-covalent fragmentation starts to occur at these high acceleration potentials, and can even take place simultaneously as dissociation of an adamantyl group is also observed while a guest molecule is still attached to the dendrimer. This can also be used as a measure for the stability of the non-covalent interaction between guest and host.

In order to analyze the data in a more quantitative way we compared the voltage required to reach an ion survival yield of 50% (referred to as I_{50}). However, it is important to stress that when different ions are compared the fraction of kinetic energy that can be converted into internal energy (which causes dissociation) is inversely proportional to the total mass of the ion. In order to compare the CID-experiments, the acceleration voltage has to be converted from the lab frame energy into the center of mass energy, which corrects for these mass differences. This can be done by making use of equation 3.2.

$$E_{lab} = n \cdot V \quad (3.1)$$

$$E_{CM} = E_{lab} \cdot \frac{M_g}{M_g + M_i} \quad (3.2)$$

With:

E_{lab} = lab frame energy (eV)

E_{CM} = center of mass energy (eV)

n = charge of the ion (-)

M_g = molar mass of the collision gas (g/mol)

V = acceleration potential (V)

M_i = molar mass of the parent ion (g/mol)

When the I_{50} -values of $\mathbf{D} \cdot (\mathbf{4}_4)^{3+}$, $\mathbf{D} \cdot (\mathbf{5}_4)^{3+}$ and $\mathbf{D} \cdot (\mathbf{6}_4)^{3+}$ are compared (Figure 3.7a), we observe that phosphonic acid guest **5** binds significantly stronger than carboxylic acid guest **4**. Sulphonic acid guest **6** even binds a bit stronger than **5**, but the difference is small. In the center of mass frame (Figure 3.7b) the results look similar due to the small differences in mass of the guests. Applying this correction, the data for $\mathbf{D} \cdot (\mathbf{4}_x)^{3+}$ and $\mathbf{D} \cdot (\mathbf{5}_x)^{3+}$ come close to the data of the mixed $\mathbf{D} \cdot (\mathbf{4}_2 + \mathbf{5}_2)^{3+}$ aggregate, discussed above. Dendrimers with smaller guest **5** require significantly less voltage than dendrimers with larger guest **3** (Figure 3c). The same trend is observed for **4** versus **2** (not depicted).

Also in the center of mass frame a significant difference remains present between $\mathbf{D}\cdot(5_x)^{3+}$ and $\mathbf{D}\cdot(3_x)^{3+}$, indicating stronger binding of the larger guests **3** (Figure 3.7d).

The influence of the number of guests bound to the dendrimer on the I_{50} -value is not large for guest **5** (in all cases approximately 30 V). A different trend is observed for guest **3**. For $\mathbf{D}\cdot(3_1)^{3+}$ the I_{50} value is 50 V, while for $\mathbf{D}\cdot(3_5)^{3+}$ it is 72 V. At first glance this result suggests a cooperative effect, meaning that the binding strength of guest **3** increases when more guests are bound. However, after correction for the mass of the ions the differences become small in going from $\mathbf{D}\cdot(5_3)^{3+}$ to $\mathbf{D}\cdot(5_7)^{3+}$ and $\mathbf{D}\cdot(3_1)^{3+}$ to $\mathbf{D}\cdot(3_5)^{3+}$ (Figure 3.7d). Actually the I_{50} value decreases slightly upon higher loading of **D** with **3** and **5**. This might indicate anticooperative binding of the guests, but the effect is small.

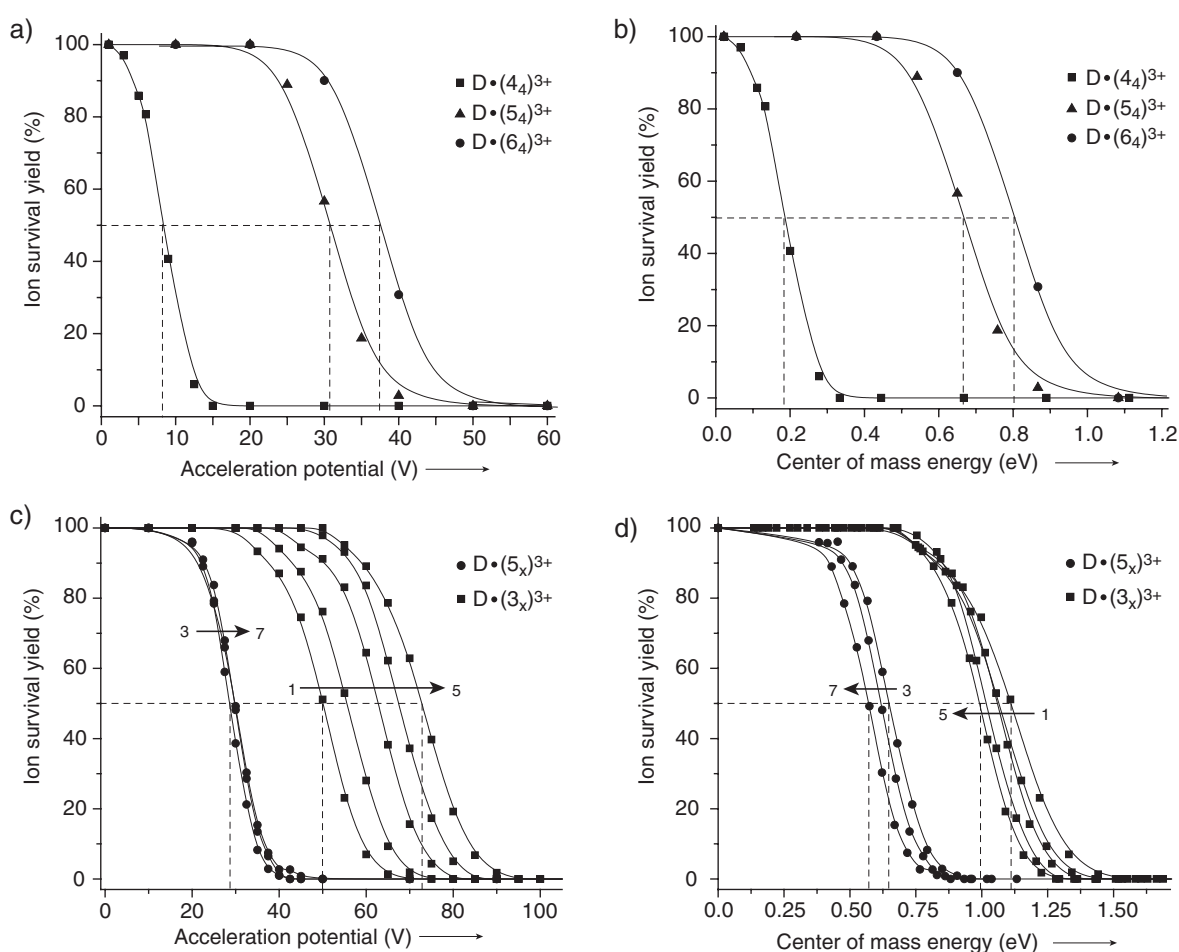


Figure 3.7 a) Influence of the acidic headgroup of guest **4**, **5** and **6** on the stability of the selected complexes. b) Conversion of the acceleration potential depicted in figure a into the center of mass frame. c) Influence of loading and molecular weight of guests **3** and **5** on the stability of the selected complexes. d) Conversion of the acceleration potential depicted in figure c into the center of mass frame.

In order to investigate the relation between the number of guests bound to the dendrimer and ion stability in more detail, we have simulated the distributions of complexes formed during CID via a simple model. The release of guests from a complex due to collisions with argon atoms can be modeled as consecutive reaction steps that are pseudo-first order due to the constant argon

concentration. We have used the $\mathbf{D}\cdot(\mathbf{5}_4)^{3+}$ complex and defined four reaction rate constants (k_1, k_2, k_3, k_4) as parameters. After integrating the rate equations, we can calculate the fractions of the various species ($\mathbf{D}\cdot(\mathbf{5}_4)^{3+}$, $\mathbf{D}\cdot(\mathbf{5}_3)^{3+}$, $\mathbf{D}\cdot(\mathbf{5}_2)^{3+}$, $\mathbf{D}\cdot(\mathbf{5}_1)^{3+}$, and \mathbf{D}^{3+}) as a function of time. The effect the acceleration voltage has on the populations of the different ions in the collision cell has been simulated by looking at the populations of the different complexes at increasing times (see appendix). The best fit of the model with the experimental data is achieved when the k -values increase slightly in value, indicating that the guest molecules dissociate slightly easier when less guest molecules are bound. However, the influence of loading on the stability of the complexes is small and close to statistical dissociation of the guests.

3.3.2 Oligo-peptide complexes

Apart from urea-acetic acid guest molecules, U. Boas demonstrated that tripeptides with a Boc-protected N-terminus and free carboxylic acid could also be assembled around urea-adamantyl dendrimers.³⁶ The urea-urea hydrogen bonding could easily be replaced with urea-amide hydrogen bonding between the dendrimer and the peptide backbone. Next to glycine it was also possible to use other C-terminal amino acids like alanine, phenylalanine or valine.

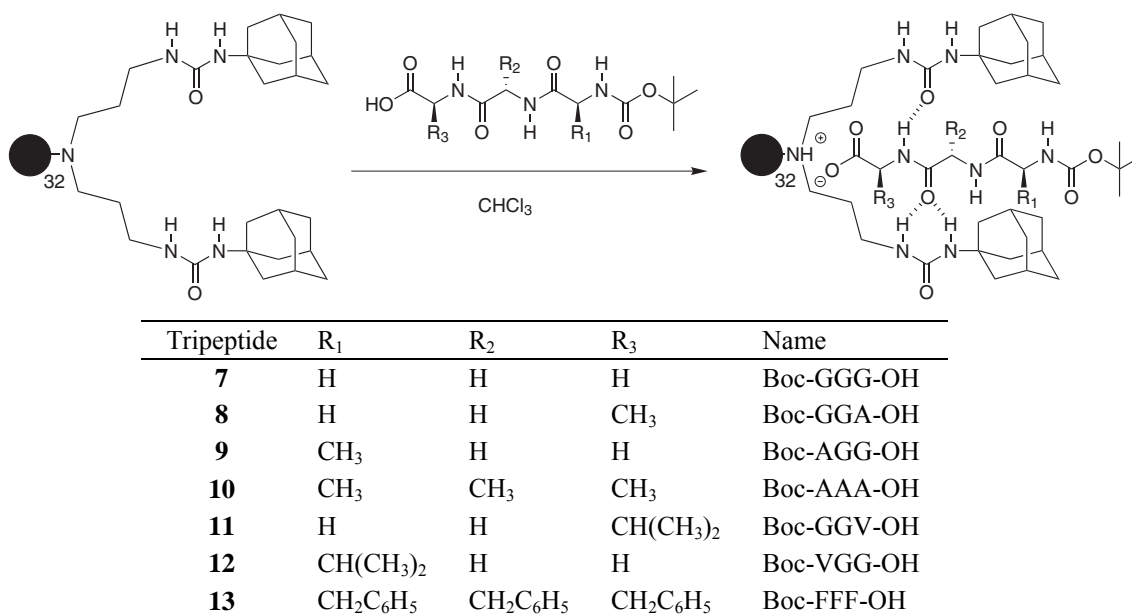


Figure 3.8 The complexation of Boc-protected tripeptides to the dendritic host. Several tripeptides containing glycine (G), alanine (A), phenylalanine (F) and valine (V) have been examined.

The tripeptide-dendrimer aggregates could also be observed with electrospray mass spectrometry from chloroform, as well as mixtures of tripeptides simultaneously anchored to the dendrimer. Figure 3.9a shows a deconvoluted mass spectrum of \mathbf{D} together with Boc-GGG-OH (**7**) and Boc-GGA-OH (**8**). Due to the small difference in mass between the tripeptides, clusters of peaks

appear that correspond to one to five guest molecules bound to the dendrimer. All peaks in the clusters can be assigned to the different possible combinations of guests. Interestingly, complexes of the peptides with the most abundant imperfect dendritic structure, which lacks one propylamine branch, can also be observed (indicated with an asterisk). The clusters of peaks are also observed for mixtures of dendrimer **D** with Boc-GGG-OH (**7**), Boc-GGA-OH (**8**) and Boc-AAA-OH (**10**). When we look at the cluster of 3+ ions that has three guests bound to **D**, 10 different combinations of guests are possible that can all be observed. Two combinations result in an identical mass.

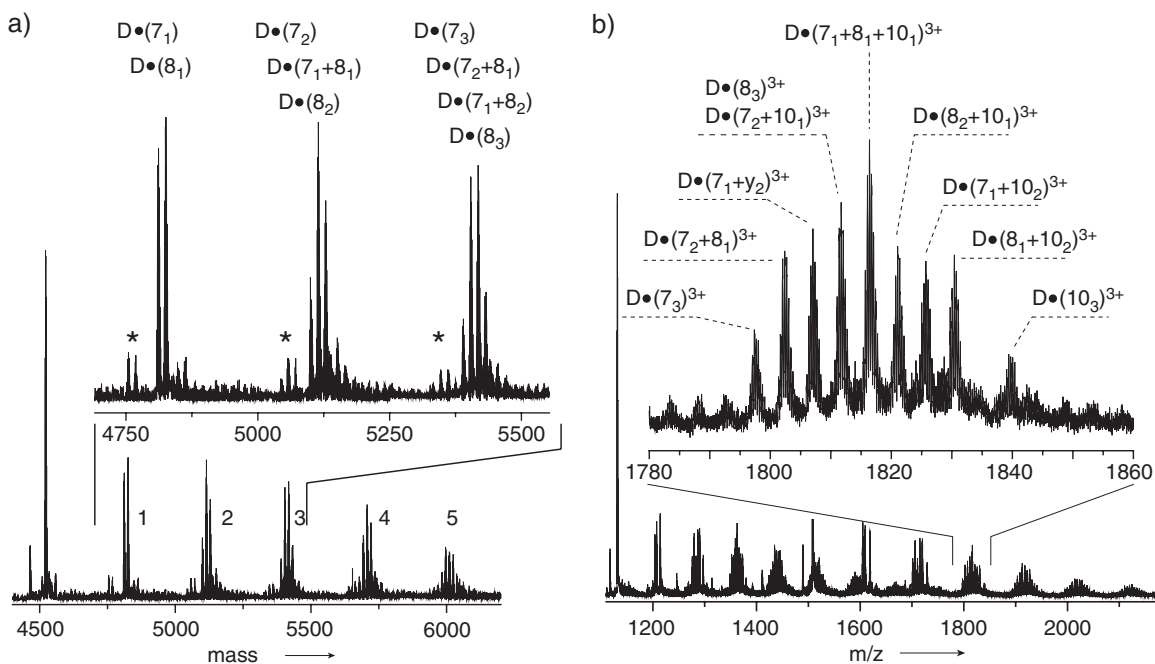


Figure 3.9 a) Deconvoluted mass spectrum of a sample of **D** together with **7** and **8**. b) Mass spectrum of **D** together with **7**, **8** and **10**.

By selecting a specific ion with two different tripeptides, it is possible to investigate the difference in binding affinity. Remarkably, very small structural differences are leading to significant changes in the dissociation. Figure 3.10 for example shows a clear preference for the dissociation of Boc-AAA-OH (**10**) over Boc-GGG-OH (**7**), though the guests differ only by three methyl groups. Steric interference of the methyl groups with the binding motif of the dendrimer could explain the results. On the other hand, the heavier Boc-FFF-OH (**13**) binds significantly stronger than Boc-GGG-OH (**7**) (not depicted). This is a general observation in the CID-experiments. When the mass difference between two guests becomes too large, additional specific interactions like Van Der Waals interactions or π -cation interactions result in stronger binding of the heavier guest. The influence of steric repulsion has been investigated, but in an indirect way.

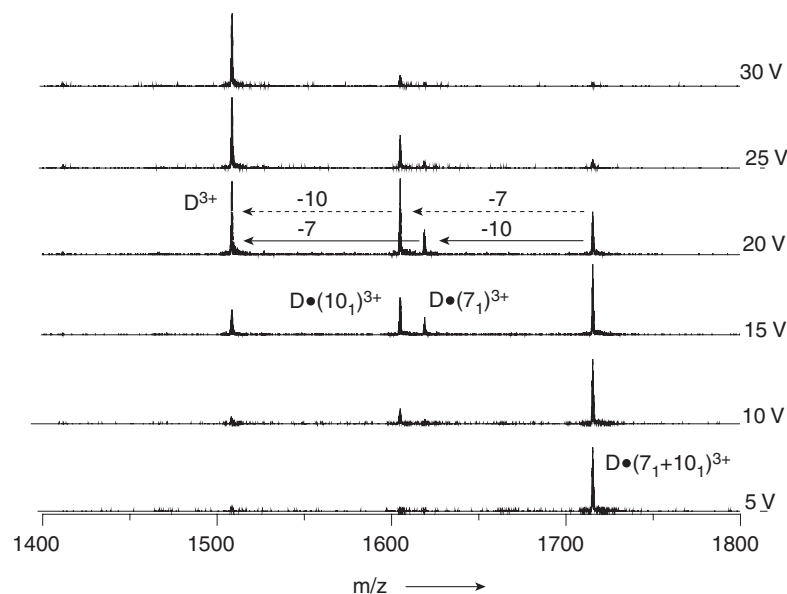


Figure 3.10 CID spectra of *D* with one Boc-GGG-OH (**7**) and one Boc-AAA-OH (**10**) peptide. Two pathways can be envisioned of which the one indicated with the dashed arrows predominates.

Peptides **8** and **9** both consist of one alanine and two glycine amino acids, the alanine being present either at the first or the third position. In case of peptides **11** and **12**, valine is used instead of alanine. Mixtures of these peptides with Boc-GGG-OH have been prepared and the ions containing one guest of each have been examined with CID (Figure 3.11).

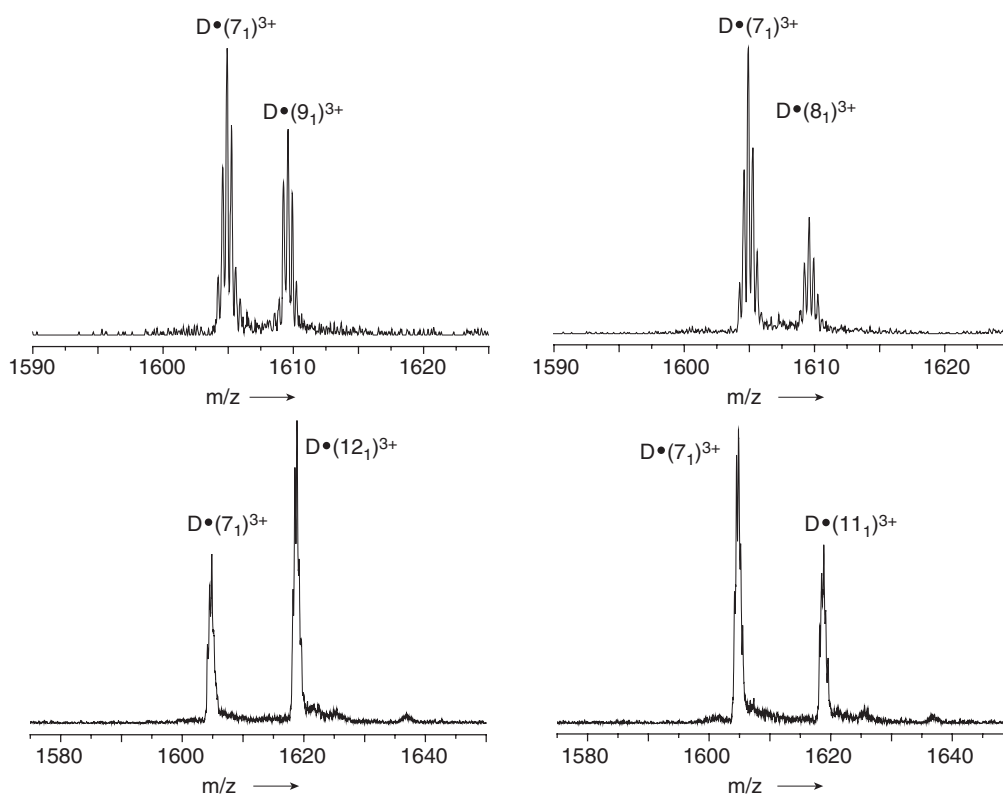


Figure 3.11 Expansions of the middle part of the CID spectra for $D\bullet(7_1+9_1)^{3+}$ at 15 V (a), $D\bullet(7_1+8_1)^{3+}$ at 15 V (b), $D\bullet(7_1+12_1)^{3+}$ at 20 V (c) and $D\bullet(7_1+11_1)^{3+}$ at 20 V (d). In $D\bullet(7_1+12_1)^{3+}$ vs. $D\bullet(7_1+11_1)^{3+}$, the peaks “flip over” in intensity, indicating that **11** binds weaker than **12**.

The spectra look similar to the spectra shown for $\mathbf{D}\cdot(\mathbf{7}_1+\mathbf{10}_1)^{3+}$, but the intensities of the peaks in the middle are slightly different. For $\mathbf{D}\cdot(\mathbf{7}_1+\mathbf{9}_1)^{3+}$ it can be concluded that **9** dissociates slightly easier than **7**, as the intensity of the left peak in figure 3.11a is a bit higher (only the middle part of the mass spectrum is depicted, acceleration potential = 15 V). However, when $\mathbf{D}\cdot(\mathbf{7}_1+\mathbf{8}_1)^{3+}$ is subjected to CID, the difference in intensity becomes more significant, meaning that the location of the CH_3 -group influences the binding to the dendrimer (Figure 3.11b). Apparently, moving the CH_3 -group closer to the acid headgroup of the peptide negatively influences its binding to the dendrimer. The same trend is observed for $\mathbf{D}\cdot(\mathbf{7}_1+\mathbf{11}_1)^{3+}$ vs. $\mathbf{D}\cdot(\mathbf{7}_1+\mathbf{12}_1)^{3+}$ (Figure 3.11c and d). In the case of $\mathbf{D}\cdot(\mathbf{7}_1+\mathbf{12}_1)^{3+}$, guest **7** dissociates easier than guest **12** (as the right-hand peak is a bit higher), while in the case of $\mathbf{D}\cdot(\mathbf{7}_1+\mathbf{11}_1)^{3+}$ it is the other way around. Again, moving the steric group closer to the acid headgroup negatively influences the binding to the dendrimer, and in this case the effect seems to be even bigger. Results with other Boc-protected tripeptides have indicated that the observed trend is valid as long as the mass difference between the peptides is small.

3.4 CHLOROFORM VS THE GAS PHASE

Ever since soft ionisation mass spectrometry has resulted in non-covalently bound complexes in the gas phase, scientists have investigated whether MS/MS experiments could determine the interaction strength of the molecules in solution. Several studies have shown that, with a few exceptions, no agreement exists between gas phase binding and water. The main reason is that electrostatic interactions and dipolar non-covalent interactions are strengthened in the absence of solvent shielding, while hydrophobic interactions become less important in the absence of solvent.³¹ In our case however, we compare the gas-phase experiments to chloroform instead of aqueous media. Chloroform is an aprotic solvent, and a non-competing solvent to acid–base and hydrogen bonding interactions due to the low dielectric constant.³⁷⁻⁴⁰ Therefore, some comparisons between chloroform and the gas phase can be made.

M. Pittelkow and J.B. Christensen have synthesized guest molecules **14–19** and determined the association constants to pincer molecule **P**, a model compound for the binding site on the dendrimer.⁴¹ The 9-methyl-anthracenyl moiety acts as a fluorescent probe. Protonation of the tertiary amine due to complexation results in an increase of the fluorescence intensity of the 9-methyl-anthracenyl unit, and by titration of the guests to the pincer the association constant has been obtained. The 3,4,5-tris-dodecyloxybenzoyl group was used to increase the solubility of the guests in chloroform.

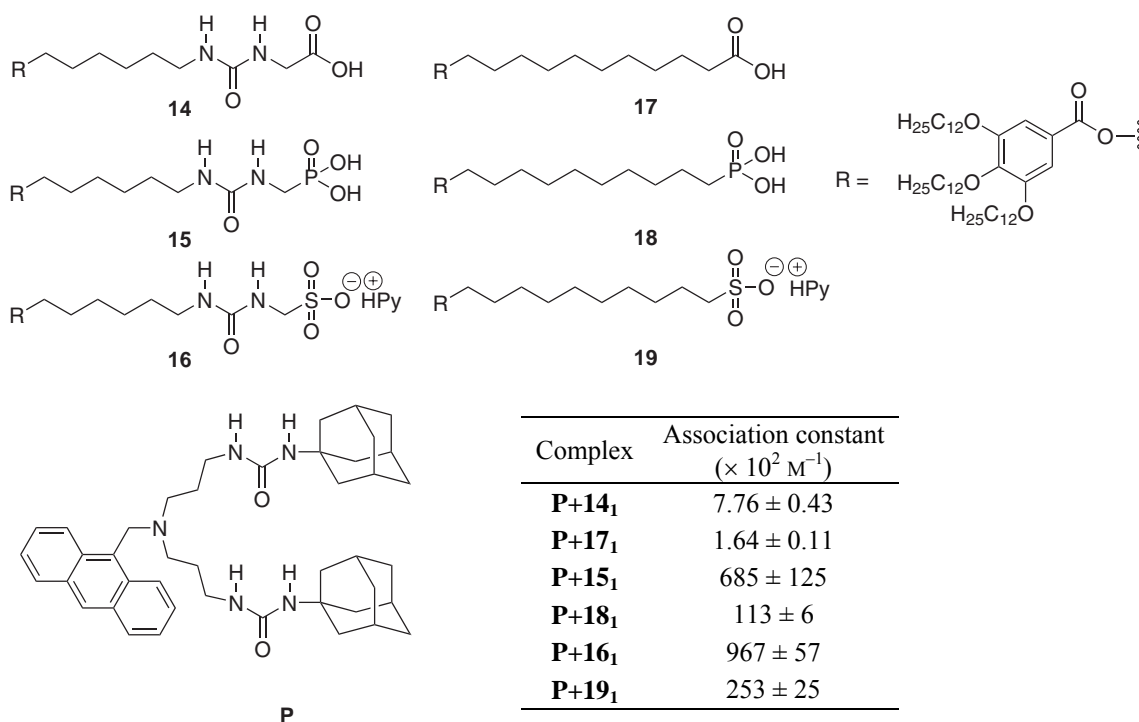


Figure 3.12 The association constants of the complexation of guests **14–19** to pincer **P** in chloroform as determined by fluorescence titration experiments.⁴¹

The results show that a stronger complex is formed upon increasing acid strength. They also show that the presence of the urea group in the guest clearly increases the affinity to the host due to hydrogen bonding. The acid strength of guest **14**, **15** and **16** is somewhat higher than their analogues without urea groups due to the inductive effect of the nitrogen, but this effect plays only a minor role in the increased binding of **14**, **15** and **16**.

The CID-experiments performed on $\mathbf{D}\cdot(4_4)^{3+}$, $\mathbf{D}\cdot(5_4)^{3+}$ and $\mathbf{D}\cdot(6_4)^{3+}$ already showed that the sulfonic acid guests give the most stable complexes to dendrimer **D**, followed by the phosphonic acid guest and the carboxylic acid guest. This is in agreement with the determined association constants. We were interested to see whether the difference in binding between guests that lack or contain the urea group could also be observed by CID mass spectrometry.

First the six different complexes have been made, each consisting of 4 equivalents of guest **14–19** added to **D**. All samples give spectra that show complexation to the dendrimer, indicating that these complexes are stable enough to be observed in the gas phase, except for guest **17**. These results show that for the carboxylic acid guest the presence of the urea group is of crucial importance in order to obtain a complex that is stable enough to survive the transfer from solution to the gas phase. For the phosphonic and sulfonic acid guests, the urea group is apparently not a necessity.

Collision induced dissociation experiments have been performed to determine the relative binding strength of **15** versus **18** and **16** versus **19**, in order to investigate the influence of the urea

groups on the binding strength with **D**. Two samples have been prepared consisting of 2 equivalents of **15** and 2 equivalents of **18** added to **D** in chloroform, and 2 equivalents of **16** and 2 equivalents of **19** added to **D** in chloroform. Both samples gave complexes showing the statistical combinations of guests bound to **D** (not depicted). From the first sample, ion $\mathbf{D}\cdot(\mathbf{15}_1+\mathbf{18}_1)^{3+}$ was selected and subjected to collision induced dissociation. The $\mathbf{D}\cdot(\mathbf{15}_1+\mathbf{18}_1)^{3+}$ ion remains stable until 25 V, but starts to fragment when the voltage is further increased. The first major product of fragmentation is $\mathbf{D}\cdot(\mathbf{15}_1)^{3+}$, which means that **18** dissociates first from the dendrimer as a neutral species and is the weaker binding guest. The dissociation is not 100% selective as the peak of $\mathbf{D}\cdot(\mathbf{18}_1)^{3+}$ is also present, but the intensity of this ion is almost negligible. When the voltage is further increased guest **15** also starts to dissociate, resulting in bare \mathbf{D}^{3+} at roughly 70 V. Clearly the urea groups positively influence binding to the dendrimer. A similar trend is observed for the sulfonic acid guests (Figure 3.13). Collision induced dissociation subjected to $\mathbf{D}\cdot(\mathbf{16}_1+\mathbf{19}_1)^{3+}$ shows that guest **19** dissociates first from the dendrimer, followed by guest **16**. This again indicates that the guest molecule without the urea group is the weaker binding guest in the gas phase, which is in agreement with the fluorescence experiments in chloroform. The amount of covalent fragmentation next to non-covalent fragmentation is huge in case of the sulphonic acid guests. At 85 V **D** has lost 1 to 10 adamantyl groups (!). This shows that the sulfonic acid guests bind stronger than the phosphonic acid guests.

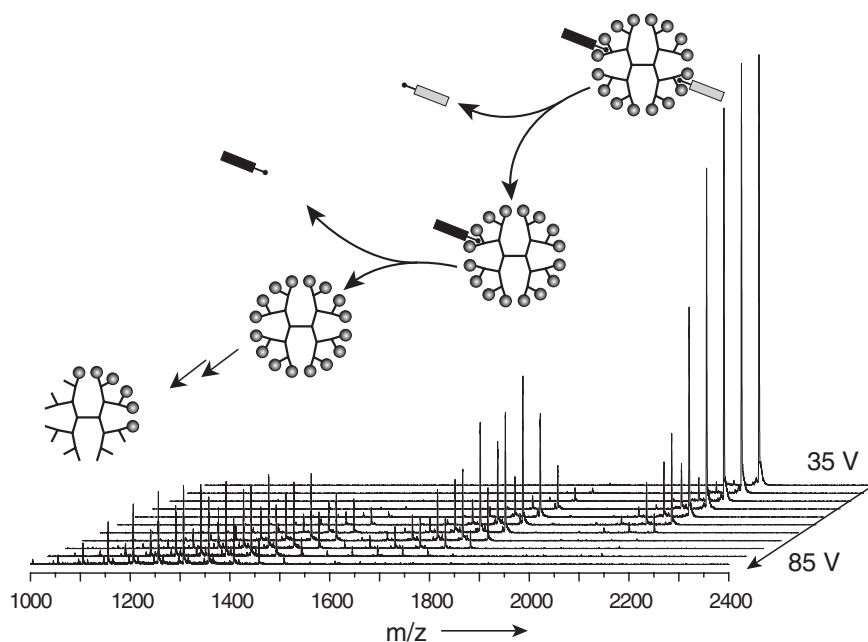


Figure 3.13 CID performed on $\mathbf{D}\cdot(\mathbf{16}_1+\mathbf{19}_1)^{3+}$. Guest **19** is depicted in light gray. Severe covalent fragmentation is observed.

The results described in this section show that the binding between guests and the dendrimer in the gas phase nicely correlates to the binding of model compounds in chloroform. Molecular dynamics (MD) simulations are ideal to study intermolecular interactions in the gas phase. If it is possible to predict how guest molecules bind to the dendrimer in the gas phase using molecular

dynamics simulations, this method could give more insights into how guests interact with the dendrimer. Furthermore MD could be a useful tool in the design of stronger binding guests. Therefore, molecular dynamics simulations have been performed to investigate the stability of dendrimer host–guest systems in the gas phase, which is the subject of the following section.

3.5 GAS PHASE SIMULATIONS

Throughout this chapter we have interpreted the results of the CID experiments in a qualitative way by either looking at the acceleration voltage at which 50% of the parent ion had dissociated (after correction for the mass of the ion), or by looking at the guest that dissociated first from the dendrimer that had two different guests simultaneously anchored.

The correct measure for the stability of ions in the gas phase is not the acceleration voltage. It is also not the center of mass energy, which only corrects for the mass of the ion. It is the internal energy, or the internal temperature of the ion, that needs to reach a certain threshold value for dissociation to occur. Unfortunately, the internal energy of the complexes before they enter the collision cell is not known, and therefore the internal energy of ions in the collision cell cannot be determined. During the electrospray ionization process of complexes to the gas phase, the ions gain internal energy. This internal energy cannot be calculated or estimated and is dependent on many experimental conditions. Apart from this, several other uncertainties during the collision process, like the number of collisions in the collision cell⁴²⁻⁴⁴ and the amount of kinetic energy transferred into internal energy,⁴⁵⁻⁴⁷ hamper a quantitative analysis. On the other hand, it can be assumed that these parameters are fairly constant, as both the mass spectrometric parameters (cone voltage, gas pressure inside collision cell etc.) and the dendritic host (third generation urea–adamantyl dendrimer) have been kept constant throughout all experiments. Therefore, we have chosen the center of mass energy as a relative measure for the internal energy. These values have been compared with the dissociation temperature of several complexes obtained with molecular dynamics simulations.

In molecular dynamics simulations, the motion of atoms in time can be investigated. Newton's equation of motion, $F = m \cdot a$, states that the force acting on a single atom drives its motion. Therefore, by determining the force on an atom at certain time intervals, their position can be calculated. The force on an atom is related to its potential energy, governed by both short-range interactions like bond energies as well as long-range interactions like Van der Waals interactions and electrostatic interactions. Empirical force fields can calculate the potential energy of a system and can be used to study structures, both in solution and in the gas phase.

Complexes of dendrimer **D** with guests **2–5** in the gas phase have been simulated using NAMD 2 with the CHARMM22 force field (an example of such a complex for the fifth generation

urea–adamantyl dendrimer **1e** with 32 equivalents of guest **4** has been shown in chapter 2, figure 2.12). All simulated complexes consisted of four identical guests. The stability of these complexes has been investigated using molecular dynamics simulations by monitoring at which temperature a guest dissociates from the dendrimer when the temperature is gradually increased. Interestingly, the stability of the complexes obtained via molecular dynamics simulations matches quite nicely with the mass spectrometry results. Table 3.1 shows the average dissociation temperature over five simulations at which 50% of the guests (i.e. 2 guests on average) have dissociated from the dendrimer (not to be confused with the I_{50} -value).

Table 3.1 *The stability of the dendrimer–guest complexes according to MD simulations.*

Complex	Dissociation temperature (K)
D•(2₄)³⁺	931 ± 42
D•(3₄)³⁺	977 ± 34
D•(4₄)³⁺	761 ± 30
D•(5₄)³⁺	930 ± 42

The results show that the guest molecules with a phosphonic acid headgroup bind significantly stronger than the guests with a carboxylic acid headgroup, which is in agreement with the mass spectrometry results. They also show that the ethylene glycol tails have a positive effect on the stability of the complexes. A visual inspection of the complexes **D•(2₄)³⁺** and **D•(3₄)³⁺** shows that the ethylene glycol tails interact with the dendrimer to maximize Van der Waals interactions and electrostatic interactions.

It is possible to calculate from the mass spectrometry results the center of mass energy for each complex at which 50% of the guests are dissociated. When the 50% dissociation temperatures shown in table 3.1 are displayed as a function of the center of mass energies, a linear trend is observed (Figure 3.14), signifying the agreement between the experimental results obtained with collision induced dissociation and the molecular dynamics simulations.

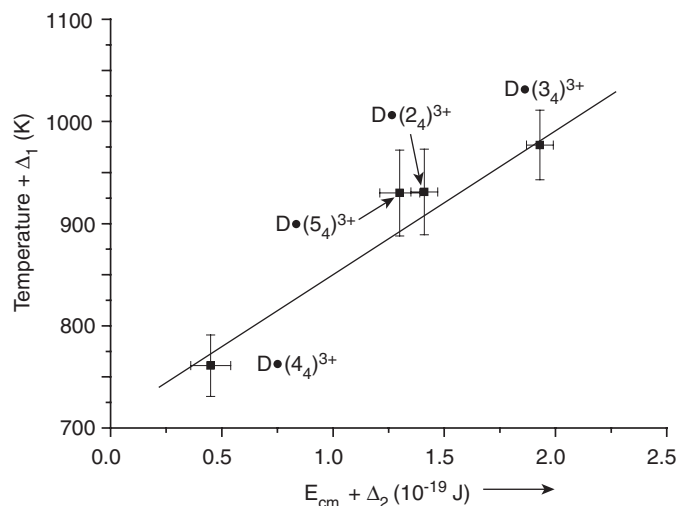


Figure 3.14 Dissociation temperatures of the complexes obtained from MD simulations as a function of the center of mass dissociation energies obtained from the CID experiments. The symbols Δ_1 and Δ_2 indicate that there is an uncertainty in the position of the whole data set in both the x and y direction.

Though the comparison between the experimental data and the simulations should be made with caution due to the assumptions and uncertainties in both techniques, the graph suggests that the molecular dynamics simulations can be used to get an indication of the stability of dendrimer–guest complexes in the gas phase. We believe that the individual positions of the points in the graph with respect to each other is correct, but that the position of the whole data set in the graph is uncertain due to the unknown parameters in both the mass spectrometry experiments and the molecular dynamics simulations. This means that the results can be interpreted qualitatively, but not quantitatively.

3.6 CONCLUSIONS

Electrospray mass spectrometry has shown to be a valuable technique in the analysis of supramolecular dendritic aggregates. The technique has allowed for the first time the visualization of individual dendritic complexes. As almost all host–guest complexes have a unique mass, mass spectrometry has proven to be especially suitable for the study of mixtures of aggregates. Next to the identification of supramolecular dendritic aggregates, the stability of the aggregates can be probed using collision induced dissociation. By subjecting an ion that contains two different guest molecules to CID, it is possible to determine which guest is most strongly bound to the dendritic host. In this way it has been shown that a carboxylic acid guest binds weaker to the dendrimer than a phosphonic acid guest, which binds weaker than a phosphonic acid guest. Also the presence of urea groups has shown to positively influence the binding to the dendrimer. The results are in nice agreement with the association constants obtained on a model system in chloroform, and indicate

that the binding between guest and host in the gas phase corresponds to the binding in chloroform. Molecular dynamics simulations have shown that it is possible to determine the stability of the host–guest complexes in the gas phase by investigating at which temperature a slowly heated complex is losing guest molecules. The mass spectrometry results are in agreement with the performed molecular dynamics simulations, and with the model at hand it might be possible to determine how guest molecules can be designed to come to a stronger binding between guest and host.

As the aggregates are detected in the gas phase, they are not in thermodynamic equilibrium with their environment. It is therefore not possible to determine the association constant between dendrimer and guest. Furthermore, it is questionable whether the aggregates observed with mass spectrometry are an exact representation of the complexes in solution. It is possible that some guest molecules dissociate from the dendrimer during the ionisation process, resulting in different aggregates in the gas phase than in solution. This aspect hampers a detailed analysis of the amount of guests that can bind to the dendrimer. It is also not possible to investigate the binding of guest molecules to higher generation dendrimers, as the fourth and fifth generation urea–adamantyl dendrimer are too polydisperse for these experiments. It would be nice if the results obtained with mass spectrometry could be complemented with results obtained in solution. This has been done, and is the subject of the next chapter.

3.7 EXPERIMENTAL SECTION

The ESI mass spectra of the dendrimer complexes were recorded with a Q/TOF Ultima GLOBAL mass spectrometer (Micromass, Manchester, UK) equipped with a Z-spray source. The samples (10 μ l) were injected in the Flow Injection Analysis (FIA) mode. The HPLC-grade chloroform was pumped with a Shimadzu LC-10ADvp at a flow rate of 30 μ L min^{-1} . Electrospray ionization was achieved in the positive ion mode by application of 5 kV on the needle. The source block temperature was maintained at 60° C and the desolvation gas was heated to 60° C. For the regular mass spectrometry experiments all complexes were prepared by adding 4 equivalents of guest to the dendrimer in a total concentration of 1 mg/ml in chloroform. To 400 μ l of each of these solutions was added 100 μ L of a 1% acetic acid in chloroform solution. For the MS/MS experiments, 2 equivalents of each guest molecule were added to the dendrimer in a total concentration of 1 mg/ml in chloroform. To 400 μ L of these solutions was added 100 μ L of 1% acetic acid in chloroform solution. This mixture was immediately injected in the mass spectrometer. The small amount of acetic acid is used to protonate the dendrimer interior. When no acetic acid is used, no ions are observed in the mass spectrum. When too much acetic acid is used, the solvent destroys the supramolecular aggregate and only bare dendrimer **D** is observed. Under these conditions we use we mostly observe the 4+ and 3+ ions next to small amounts of the 2+ ion. As the 3+ ions are often the predominant species, all MS/MS experiments were performed with this ion. MS/MS experiments performed on the 2+ ion gave different voltages of

dissociation, but never changed the order of dissociation when two different guests were compared while bound to the same dendrimer.

3.8 APPENDIX: THE KINETIC MODEL

We assume dissociation occurs through the following pathway:



A model has been written in the Maple 7 program and is based on five differential equations (3.4–3.8) for pseudo-1st order kinetics (Ar-concentration constant).

$$\frac{\partial}{\partial t} [D\cdot 2_4](t) = -k_1 [D\cdot 2_4](t) \quad (3.4)$$

$$\frac{\partial}{\partial t} [D\cdot 2_3](t) = k_1 [D\cdot 2_4](t) - 0.75 \cdot k_2 [D\cdot 2_3](t) \quad (3.5)$$

$$\frac{\partial}{\partial t} [D\cdot 2_2](t) = 0.75 \cdot k_2 [D\cdot 2_3](t) - 0.50 \cdot k_3 [D\cdot 2_2](t) \quad (3.6)$$

$$\frac{\partial}{\partial t} [D\cdot 2_1](t) = 0.50 \cdot k_3 [D\cdot 2_2](t) - 0.25 \cdot k_4 [D\cdot 2_1](t) \quad (3.7)$$

$$\frac{\partial}{\partial t} [D](t) = 0.25 \cdot k_4 [D\cdot 2_1](t) \quad (3.8)$$

After integrating the rate equations, we can calculate the fractions of the various species as a function of time. In the experiment a higher acceleration voltage yields a higher kinetic energy for the complexes, and this in effect raises the reaction temperature for the release of the guests, i.e. the rate constants are increased, and higher conversions are reached for the same reaction time. We have modeled this in a constant-temperature approach by using longer reaction times to give similarly higher conversions. In other words, the concentrations of the different fractions at a certain *time* simulate the effect of the collision cell. We then tried to approach the distribution of the various species by varying the reaction time in the model, and by changing the k-values. All reaction rate constants were scaled with $k_1 = 1$, and the equations are corrected for the number of pathways in which each complex can lose a guest. We also introduced a factor λ in the model that can decrease or increase consecutive reaction rates (i.e. $k_i = \lambda^{i-1} k_1$). When this λ -value is changed, the fractions of the different complexes change in time.

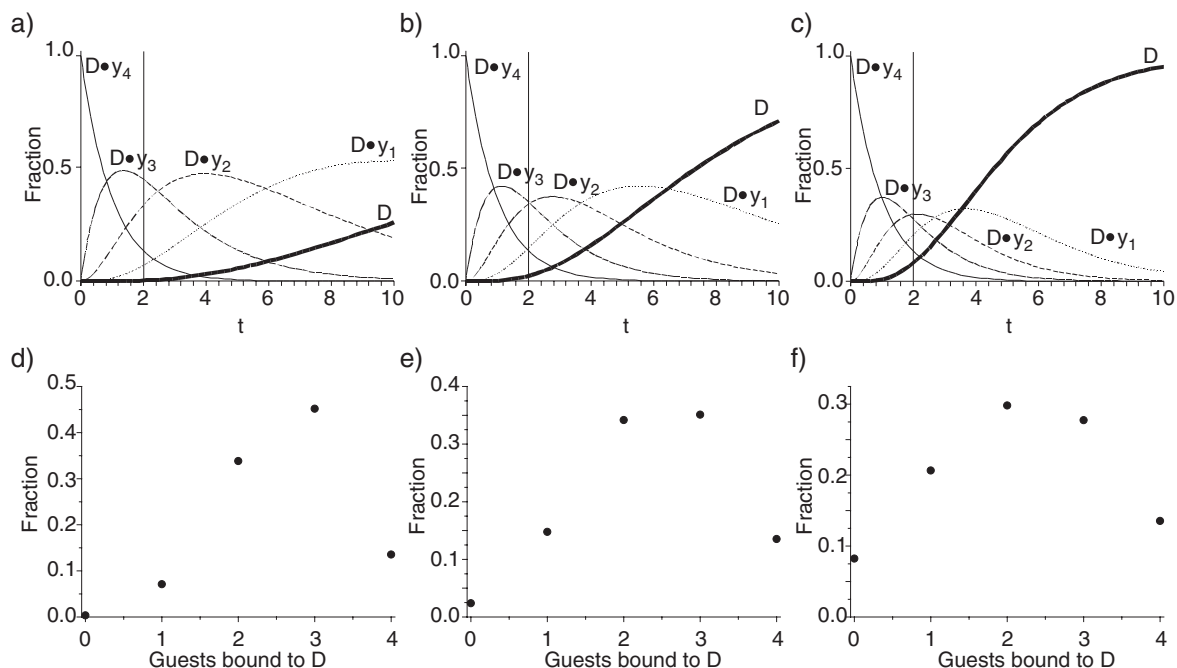


Figure 3.15 Top: The fractions of the different complexes as a function of time for a) decreasing k -values ($\lambda = 0.7$) b) equal k -values ($\lambda = 1.0$) and c) increasing k -values ($\lambda = 1.3$). Bottom: The populations of all the ions at one fixed time ($t = 2$). Upon going from $\lambda = 0.7$ (d) to $\lambda = 1.3$ (f) the populations shift in the direction of empty D (0 guests bound to D).

It was found that the best fit between experimental results (at all different voltages) and the simulated data (at different times for a single λ -value) could be obtained with a λ -value slightly bigger than 1 ($\lambda = 1.3$, see figure 3.16). This could indicate that the guests are a little more tightly bound when other guest molecules are present. However, the effect seems very small and is close to statistical dissociation ($\lambda = 1.0$). Furthermore, no corrections for mass differences are made during the fragmentation process.

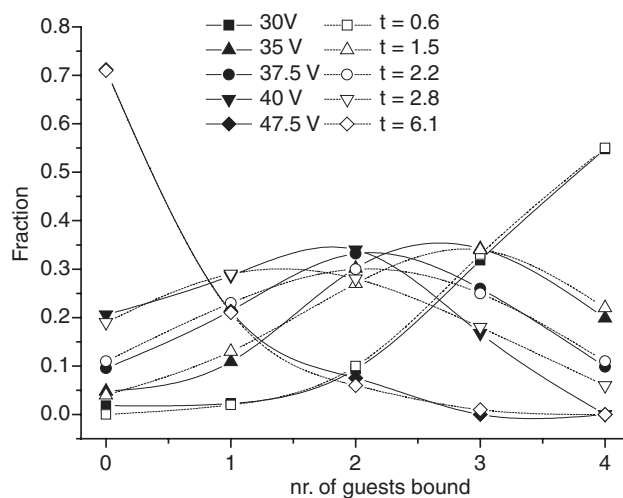


Figure 3.16 The fractions of ions formed during dissociation of $D \cdot (2_4)^{3+}$. Solid symbols represent experimental values and open symbols the corresponding simulated values. The lines are used to guide the eye. The best fit was obtained when a slight increase in the k values from k_1 to k_4 was used. The lines are used to guide the eye.

3.9 REFERENCES

- 1 J. B. Fenn, M. Mann, C. K. Meng, S. F. Wong, C. M. Whitehouse, *Science* **1989**, *246*, 64-71.
- 2 J. C. Hummelen, J. L. J. van Dongen, E. W. Meijer, *Chem. Eur. J.* **1997**, *3*, 1489-1493.
- 3 B. Ganem, Y. T. Li, J. D. Henion, *J. Am. Chem. Soc.* **1991**, *113*, 6294-6296.
- 4 W. J. H. Van Berkel, R. H. H. Van Den Heuvel, C. Versluis, A. J. R. Heck, *Protein Sci.* **2000**, *9*, 435-439.
- 5 J. L. Beck, M. L. Colgrave, S. F. Ralph, M. M. Sheil, *Mass Spectrom. Rev.* **2001**, *20*, 61-87.
- 6 P. Sarni-Manchado, V. Cheynier, *J. Mass Spectrom.* **2002**, *37*, 609-616.
- 7 J. A. E. Kraunsoe, R. T. Aplin, B. Green, G. Lowe, *FEBS Lett.* **1996**, *396*, 108-112.
- 8 A. N. Verentchikov, W. Ens, K. G. Standing, *Anal. Chem.* **1994**, *66*, 126-133.
- 9 J. A. Loo, *Mass Spectrom. Rev.* **1997**, *16*, 1-23.
- 10 C. V. Robinson, *Nature Structural Biology* **2002**, *9*, 505-506.
- 11 R. H. H. van den Heuvel, A. J. R. Heck, *Curr. Opin. Chem. Biol.* **2004**, *8*, 519-526.
- 12 A. J. R. Heck, R. H. H. van den Heuvel, *Mass Spectrom. Rev.* **2004**, *23*, 368-389.
- 13 E. van Duijn, P. J. Bakkes, R. M. A. Heeren, R. H. H. van den Heuvel, H. van Heerikhuizen, S. M. van der Vies, A. J. R. Heck, *Nature Methods* **2005**, *2*, 371-376.
- 14 X. Cheng, Q. Gao, R. D. Smith, E. E. Simanek, M. Mammen, G. M. Whitesides, *J. Org. Chem.* **1996**, *61*, 2204-2206.
- 15 M. Scherer, J. L. Sessler, M. Moini, A. Gebauer, V. Lynch, *Chem. Eur. J.* **1998**, *4*, 152-158.
- 16 P. Timmerman, K. A. Jolliffe, M. C. Calama, J.-L. Weidmann, L. J. Prins, F. Cardullo, B. H. M. Snellink-Ruel, R. H. Fokkens, N. M. M. Nibbering, S. Shinkai, D. N. Reinhoudt, *Chem. Eur. J.* **2000**, *6*, 4104-4115.
- 17 C. A. Schalley, *Mass Spectrom. Rev.* **2001**, *20*, 253-309.
- 18 E. D. Hoffmann, J. Charette, V. Stroobant, *Mass Spectrometry - Principles and Applications*, 1st ed., John Wiley & Sons, **1996**.
- 19 A. K. Shukla, J. H. Futrell, *J. Mass Spectrom.* **2000**, *35*, 1069-1090.
- 20 P. B. Armentrout, *Top. Curr. Chem.* **2003**, *225*, 233-262.
- 21 S. A. McLuckey, D. E. Goeringer, *J. Mass Spectrom.* **1997**, *32*, 461-474.
- 22 J. Laskin, J. H. Futrell, *Mass Spectrom. Rev.* **2005**, *24*, 135-167.
- 23 M. Kinter, N. E. Sherman, *Protein Sequencing and Identification Using Tandem Mass Spectrometry*, John Wiley & Sons, Inc., **2000**.
- 24 C. A. Schalley, T. Müller, P. Linnartz, M. Witt, M. Schäfer, A. Lützen, *Chem. Eur. J.* **2002**, *8*, 3538-3551.
- 25 R. Zadnard, M. Junkers, T. Schrader, T. Grawe, A. Kraft, *J. Org. Chem.* **2003**, *68*, 6511-6521.
- 26 R. Zadnard, A. Kraft, T. Schrader, U. Linne, *Chem. Eur. J.* **2004**, *10*, 4233-4239.
- 27 K. Schug, P. Frycak, N. M. Maier, W. Lindner, *Anal. Chem.* **2005**, *77*, 3660-3670.
- 28 A. Van der Kerk-Van Hoof, A. J. R. Heck, *J. Mass Spectrom.* **1999**, *34*, 813-819.
- 29 V. J. Nesatyy, *J. Mass Spectrom.* **2001**, *36*, 950-959.
- 30 V. J. Nesatyy, *Int. J. Mass Spectrom.* **2002**, *221*, 147-161.
- 31 J. M. Daniel, S. D. Friess, S. Rajagopalan, S. Wendt, R. Zenobi, *Int. J. Mass Spectrom.* **2002**, *216*, 1-27.
- 32 C. G. Herbert, R. A. W. Johnstone, *Mass Spectrometry Basics*, 1st ed., CRC Press, **2003**.
- 33 R. G. Cooks, T. L. Kruger, *J. Am. Chem. Soc.* **1977**, *99*, 1279-1281.
- 34 R. G. Cooks, J. S. Patrick, T. Kotiaho, S. A. McLuckey, *Mass Spectrom. Rev.* **1994**, *13*, 287-339.

- 35 R. G. Cooks, P. S. H. Wong, *Acc. Chem. Res.* **1998**, *31*, 379-386.
- 36 U. Boas, S. H. M. Söntjens, K. J. Jensen, J. B. Christensen, E. W. Meijer, *ChemBioChem* **2002**, *3*, 433-439.
- 37 J. March, M. B. Smith, *March's Advanced Organic Chemistry*, 5th ed., John Wiley & Sons, Inc., **2001**.
- 38 C. Reichardt, *Solvents and Solvent Effects in Organic Chemistry*, 3rd ed., WILEY-VCH Weinheim Germany, **2003**.
- 39 K. M. Dyumaev, B. A. Korolev, *Russ. Chem. Rev.* **1980**, *49*, 1021-1032.
- 40 L. M. Epshtein, A. V. Iogansen, *Russ. Chem. Rev.* **1990**, *59*, 134-151.
- 41 M. Pittelkow, C. B. Nielsen, M. A. C. Broeren, J. L. J. v. Dongen, M. H. P. v. Genderen, E. W. Meijer, J. B. Christensen, *Chem. Eur. J.* **2005**, *11*, 5126-5135.
- 42 Owing to the large number of degrees of freedom in a large molecule, it is very difficult to accurately determine the amount of internal energy that is taken up by a large molecule upon ion collisional activation. Heeren et. al. have determined a transfer efficiency of 4.4% for the pentapeptide Leucine Enkephaline. Most likely, the transfer efficiency is different for our complexes due to the larger and branched structure of the dendritic host-guest complex. See also refs. 19, 46 and 47.
- 43 M. S. Kim, *Int. Jour. Mass Spectrom. Ion Phys.* **1983**, *50*, 189-203.
- 44 J. L. Holmes, *Org. Mass Spectrom.* **1985**, *20*, 169-183.
- 45 The pressure in the collision cell corresponds to approximately 0.8 mTorr ($1 \cdot 10^{-6}$ bar). With a collision cell length of 18.5 mm this means that multiple collisions occur in the collision cell. See also refs. 19, 43 and 44.
- 46 R. M. A. Heeren, K. Vekey, *Rapid Commun. Mass Spectrom.* **1998**, *12*, 1175-1181.
- 47 X. Guo, M. C. Duursma, P. G. Kistemaker, N. M. M. Nibbering, K. Vekey, L. Drahos, R. M. A. Heeren, *J. Mass Spectrom.* **2003**, *38*, 597-606.

Chapter 4

Supramolecular dendritic architectures in chloroform*

ABSTRACT: *A ^1H - ^1H NOESY study is performed on a supramolecular complex of the third generation urea–adamantyl dendrimer with 8 equivalents of a cyanobiphenyl guest. Many cross-peaks are observed between the guest and the periphery of the host, clearly suggesting that the guest molecules are located at the periphery of the dendrimer. Furthermore, a new way to analyze supramolecular dendritic architectures in chloroform is described by making use of ^{13}C NMR and ^{31}P NMR spectroscopy. For this purpose, an ethylene glycol guest modified with a ^{13}C -label at the carboxylic acid position, and an ethylene glycol guest with a phosphonic acid head group have been used. The binding of these guests to urea–adamantyl modified poly(propylene imine) dendrimers has been investigated with ^{13}C NMR and ^{31}P NMR next to 1D and 2D ^1H NMR techniques. Different amounts of the fifth generation dendrimer have been added to the ^{13}C -labeled guest, and the observed chemical shift values in ^{13}C NMR were fitted to a model that assumes non-cooperative binding. An association constant of $400 \pm 95 \text{ M}^{-1}$ is obtained with 41 binding sites per dendrimer. When different amounts of the fifth generation urea–adamantyl dendrimer are added to the phosphonic acid guest, two different signals are observed in ^{31}P NMR. Deconvolution gives the fractions of free and bound guest, resulting in an association constant of $(4 \pm 3) \times 10^4 \text{ M}^{-1}$ and 61 ± 1 binding sites. A statistical analysis shows that the carboxylic acid guest forms a “polydisperse supramolecular aggregate”, while the phosphonic acid guest is able to form a “monodisperse supramolecular aggregate” when the amount of guest is high enough. The NMR results are compared with dynamic light scattering experiments and a remarkable agreement is found. The phosphonic acid guest is able to exchange with the carboxylic acid guest, which is in agreement with the obtained association constants and shows that these techniques can be used to analyze multicomponent dendritic aggregates.*

* Part of this work has been published: D. Banerjee, M.A.C. Broeren, M.H.P. van Genderen, E.W. Meijer, P.L. Rinaldi, *Macromolecules* **2004**, 37, 8313-8318. M.A.C. Broeren, B.F.M. de Waal, M.H.P. van Genderen, H.M.H.F. Sanders, G. Fytas, E.W. Meijer, *J. Am. Chem. Soc.* **2005**, 127, 10334-10343.

4.1 INTRODUCTION

Nuclear magnetic resonance (NMR) spectroscopy has become a powerful technique in the structural and conformational analysis of molecules in solution. From the initial observation of proton magnetic resonance in water¹ and in paraffin,² the discipline has seen an incredible growth as an analytical tool, and has evolved to become the principal analytical technique for research chemists. The usefulness of NMR spectroscopy comes from the fact that it can distinguish different nuclei within a molecule based on their chemical environments. These differences in chemical environment are reflected in the chemical shifts and spin–spin couplings of the nuclei.

Utilization of NMR in biochemistry has shown its potential in the structural analysis of complex macromolecules like proteins. For dendrimers on the other hand, not many studies have been carried out beyond the routine 1D ¹H NMR and ¹³C NMR experiments. The iterative procedure in which dendrimers are prepared results in highly symmetrical structures with many unique, but chemically similar nuclei. This limits the ability to resolve and assign the resonances of all nuclei. Multidimensional NMR experiments can overcome this problem by dispersing resonances in two or three dimensions. For example, HMQC-TOCSY (heteronuclear multiple quantum coherence total correlation spectroscopy) 2D and 3D NMR experiments have been successfully used in the complete assignment of the third generation poly(propylene imine) dendrimer.³ Still, the number of reports that discuss the structure of dendrimers in such detail is limited.^{4, 5} The conformation of dendrimers has mostly been analyzed with ¹H and ¹³C NMR spin-lattice relaxation time (T_1) measurements⁶⁻¹⁰ and NOE experiments.^{3, 5, 11} The degree of protonation of poly(propylene imine) dendrimers in water has been investigated in detail using ¹⁵N NMR.¹²

Apart from the analysis of dendrimers themselves, NMR has frequently been used to investigate the binding of guest molecules to dendrimers in solution, mostly by ¹H NMR titrations experiments.¹³ Often a signal of guest or host shifts or broadens upon complexation, and this can give information about the binding strength and stoichiometry between guest and host. T_1 -relaxation measurements, ¹H-¹H NOESY NMR and ¹H DOSY (diffusion ordered spectroscopy) NMR experiments can also be used to investigate the binding between a guest and a host in solution.¹³⁻¹⁵

In this chapter the analysis of the dendritic host–guest system with NMR spectroscopy is described. In the first part, a detailed analysis is presented on the location of guest molecules in the dendritic structure by making use of 2D NOESY NMR. Prior to interpretation of the NOE contacts, all resonances in the ¹H NMR spectra of the dendrimer and complex were assigned by making use several 2D NMR techniques. The second and major part of the chapter describes our attempts to quantify the binding of carboxylic and phosphonic acid guests to the urea–adamantyl dendrimer by making use of ¹³C NMR and ³¹P NMR. In case of the carboxylic acid guest, a synthetic route is described to prepare ¹³C-labeled ureido–acetic acid headgroups. The NMR results not only give

information about the binding strength of the guests, but also the binding stoichiometry is determined. Furthermore differences in the exchange kinetics are observed for different generations of dendritic hosts. Next to the NMR measurements, dynamic light scattering experiments in chloroform have been performed to exclude the possibility of dendrimer–dendrimer aggregation.

4.2 THE LOCATION OF GUESTS IN SUPRAMOLECULAR DENDRITIC AGGREGATES DETERMINED BY ^1H - ^1H NOESY SPECTROSCOPY

As has been described in the previous chapters, the complexation between urea–adamantyl dendrimers and ureido–acetic acid guests was originally designed to selectively assemble guests at the periphery of the dendrimer. Though the tertiary amines are present in every layer of the dendrimer, the urea groups are only present at the periphery of the molecule. This should enhance complexation and direct the guests to the periphery of the dendrimer. Molecular dynamics simulations and crystal structure analysis have indicated that the guests cannot bind in a ”pincer-like” fashion due to steric reasons (see chapter 2). Although the binding process has appeared to be more complicated than the initial pincer model, it is still possible that guests predominantly bind to the periphery of the dendrimer. This has been examined in detail with ^1H - ^1H NOESY NMR in collaboration with the group of prof. Peter L. Rinaldi (University of Akron, Akron, Ohio)

Because poly(propylene imine) dendrimers are synthesized by the divergent method, defects exist in higher generation dendrimers. In earlier work, unfunctionalized poly(propylene imine) dendrimers of generation 1–4 have been examined by 750 MHz NMR.³ Defects were evident from the NMR spectra of the 4th generation dendrimer, but no obvious defects were found from the NMR spectra of the 3rd or lower generation dendrimers. Therefore the third generation urea–adamantyl dendrimer has been chosen as the host molecule in the ^1H - ^1H NOESY studies. As this dendrimer has 16 endgroups, 8 guests can in theory bind to the peripheral tertiary amines. For the guest, cyanobiphenyl guest molecule **4** has been chosen, which was the first guest used in ^1H - ^1H NOESY studies.¹⁶ This guest is not soluble in chloroform, but can be solubilized by complexation to dendrimer **1c**. The ^1H NMR spectrum of **1c**+**4**₈ in CDCl_3 is depicted in figure 4.1. This notation is deliberately chosen to describe the amount of a certain guest that is added to a certain dendrimer, which is different from the amount of guest that is *bound* to a certain dendrimer like in the case of the complexes observed by mass spectrometry (see chapter 3).

Before looking at any interaction between guest and host, all peaks in the spectra of free dendrimer and complex had to be assigned. All resonances could be assigned by making use of ^{13}C NMR and 2D NMR techniques like ^1H - ^1H TOCSY and ^1H - ^{13}C gHSQC. The downfield shift of the urea-protons of the dendrimer upon addition of the guest is in agreement with the initial findings. The downfield shift of the methylene groups next to the tertiary amines upon protonation is

observed as well. Interestingly, the peaks that correspond to the methylene group next to protonated or unprotonated amines can almost be completely resolved due to the higher resolution at 750 MHz. This is also observed for guest signals 4', 5' and 6', which overlap at lower field strengths.

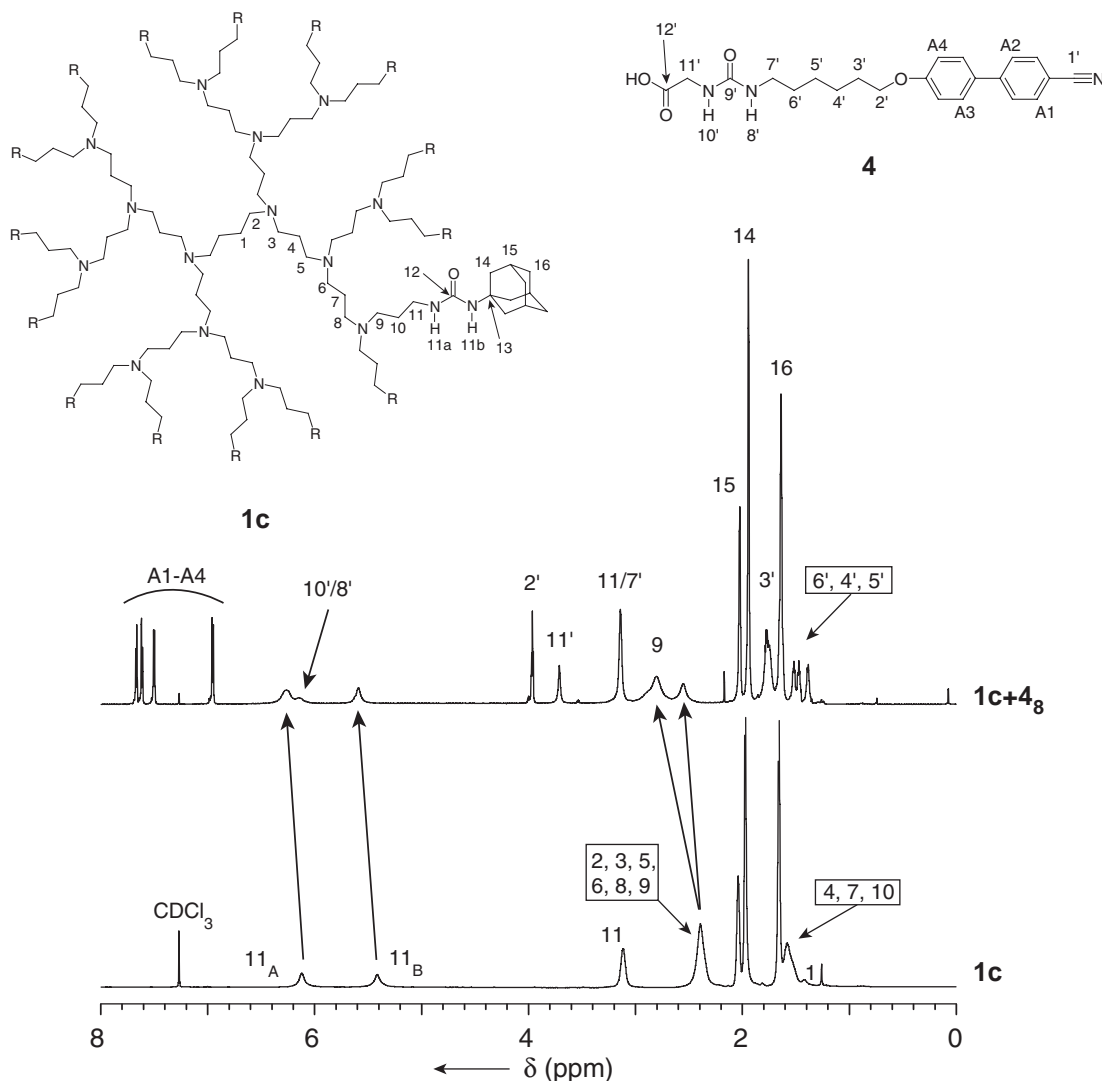


Figure 4.1 The ^1H NMR spectra of dendrimer **1c** and complex **1c+4_g**. The signals corresponding to the protons of dendrimer and guest are indicated.

Segments from the ^1H - ^1H NOESY spectrum of **1c+4_g** (Figures 4.2 and 4.3) are most important in this study as they reveal the specific H–H interactions associated with complexation between the host and guest. Figure 4.2 shows the NOE interactions of the protons bound to the nitrogen atoms in **1c+4_g**. The resonances of urea type N–H protons in the dendrimer ($\text{H}_{11\text{A}}$ and $\text{H}_{11\text{B}}$) apart from showing cross-peaks among themselves (B) also exhibit cross-peaks with the resonances of the other N–H protons (A and C). The only other urea type groups present in the system are the N–H protons ($\text{H}_{10'}$ and $\text{H}_{8'}$) situated at the acidic end of the guest molecules. This is consistent with the close proximity of urea type protons 1 and 2. However, this is not unequivocal evidence as the cross-peaks could be produced by chemical exchange of the amide protons.

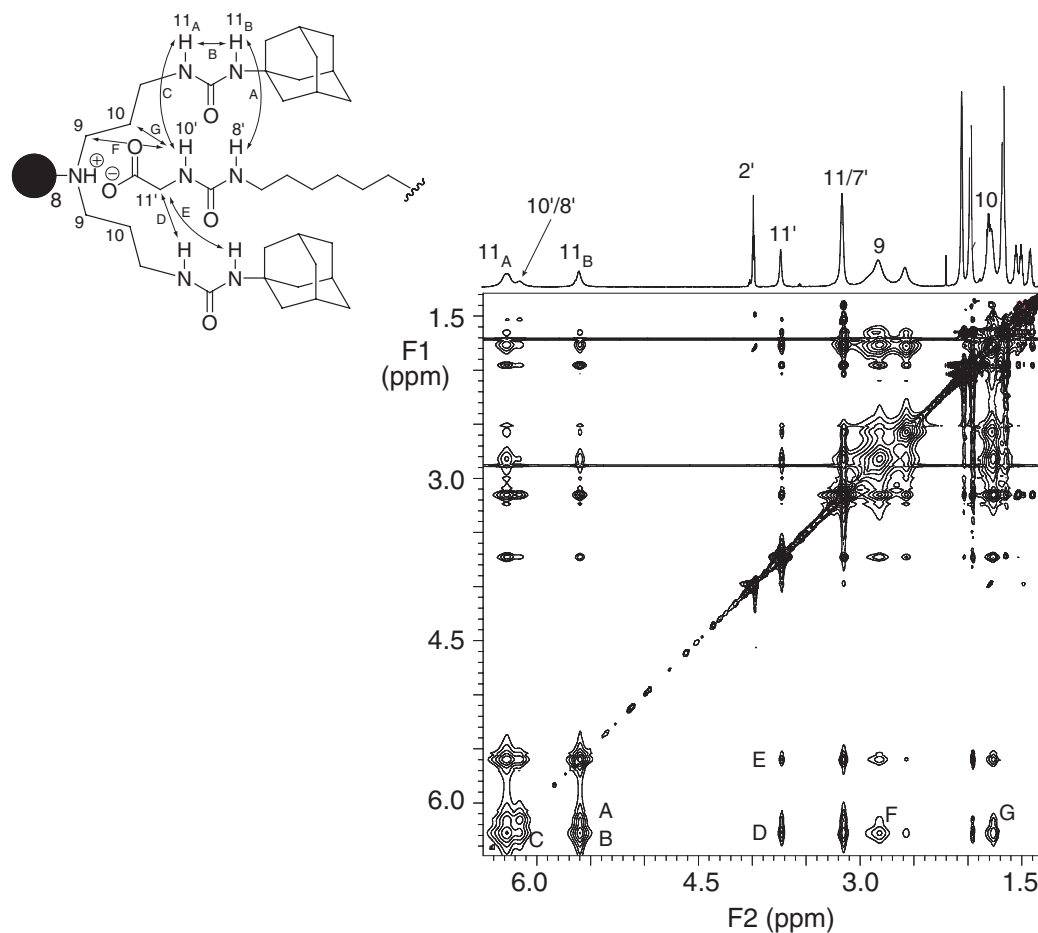


Figure 4.2 750 MHz ^1H - ^1H NOESY spectrum of complex $\mathbf{1c}+4_8$ in CDCl_3 .

The urea proton resonances of $\mathbf{1c}$ also exhibit cross-peaks (D and E) with the resonances of the methylene group situated in between the acidic and urea moiety of the guest ($\text{H}_{11'}$). This is strong evidence for a binding model having the carboxylic acid end groups of the guest molecules encapsulated near the surface of the dendritic host, as they are correlations between non-exchangeable protons on the guest molecule. Cross-peaks F and G are consistent with intermolecular interactions between H_9 and H_{10} respectively of $\mathbf{1c}$, and urea protons ($\text{H}_{8'}$ and $\text{H}_{10'}$) of $\mathbf{4}$. However, it is important to realize that these cross-peaks among N-H protons might also arise from chemical exchange.

Further evidence for complexation is evident from intermolecular NOESY interactions between non-exchangeable protons, shown in the expansion of the 1.3–4.1 ppm region of the NOESY spectrum (Figure 4.3).

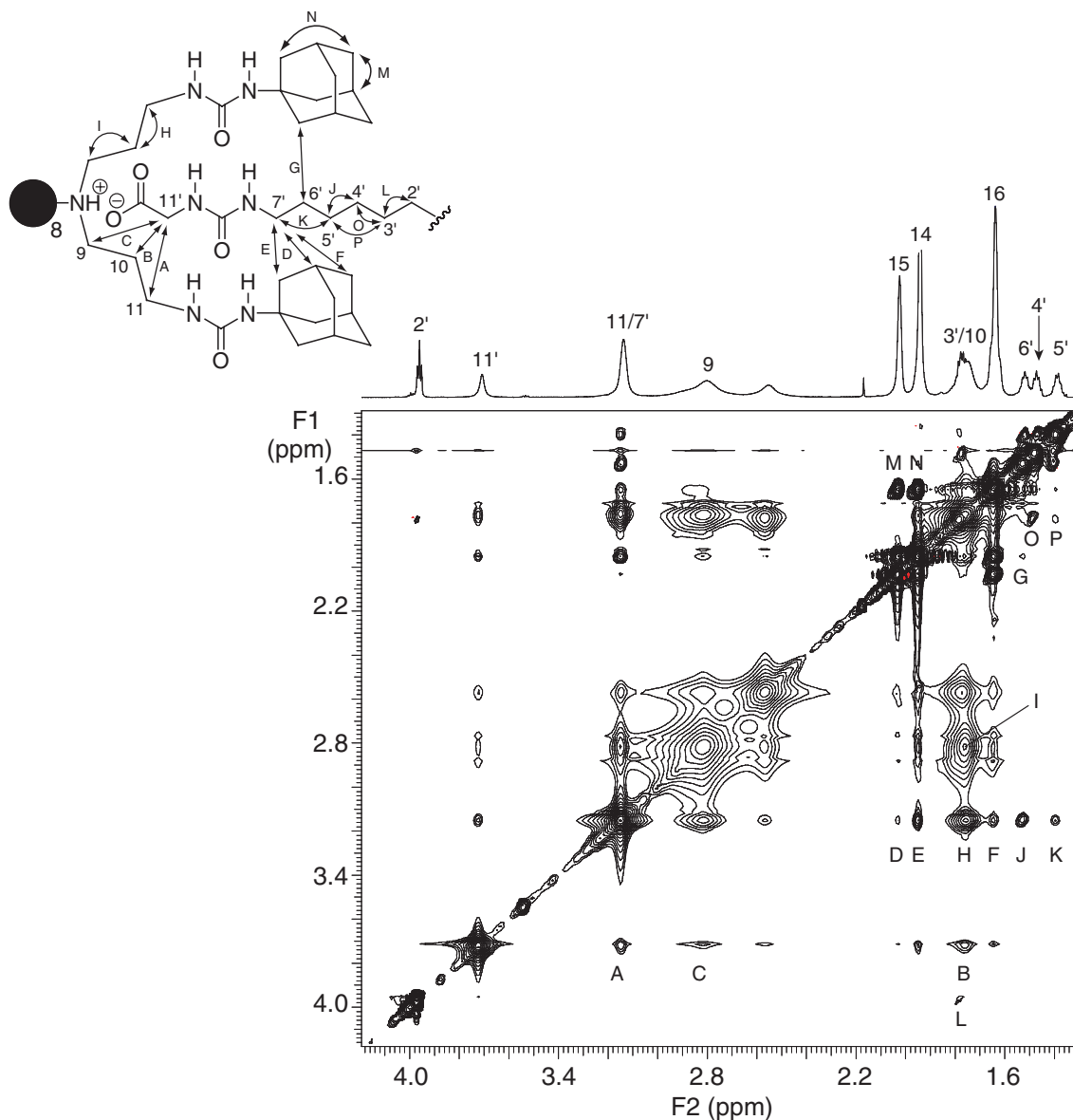


Figure 4.3 Expansion of the high field region from the 750 MHz ^1H - ^1H NOESY spectrum of complex $1\mathbf{c}+4\mathbf{g}$.

This spectrum is expanded to clearly distinguish the closely spaced cross-peaks from one another. Cross-peaks A, B, and C arise from the close proximity of $\text{H}_{11'}$ of $\mathbf{4}$ and the peripheral methylene protons H_{11} , H_{10} , and H_9 of the dendrimer, respectively. In this orientation, the methylene group next to the urea group at the side of the aliphatic spacer of $\mathbf{4}$ ($\text{H}_{7'}$), should approach the adamantyl protons of $1\mathbf{c}$. This intermolecular interaction is confirmed by NOESY cross-peaks D, E, and F between the resonance of $\text{H}_{7'}$ and the resonances of H_{14} , H_{15} , and H_{16} , respectively. Similarly, cross-peak G is evidence for the proximity of H_{14} and $\text{H}_{6'}$. Cross-peaks in this figure, from intramolecular NOE interactions, also support some of the resonance assignments made above. For example, cross-peaks H and I originate from the NOE interactions of H_{10} with H_9 and H_{11} , respectively, consistent with the previous claim that H_{10} is shifted downfield in the complex. Similarly, cross-peaks J and K from the methylene spacers of the guest confirm that one of these

methylene resonances is around 3.15 ppm (H_7). Intramolecular NOESY cross-peaks M and N result from interactions between H_{14} and H_{15} with H_{16} . Finally, cross-peaks L, O, and P result from the interactions among the aliphatic spacers of **4**. Cross-peak L is the only NOE interaction of H_2 , and hence it must be the interaction with the protons on next methylene group in the chain, i.e., H_3 . The H_3 resonance exhibits two other NOESY cross-peaks O and P, of which O is more intense. Cross-peak O is due to interaction with the neighboring methylene H_4 , while the less intense cross-peak P arises from the interaction of H_3 and H_5 .

The results confirm that binding between guest and host occurs primarily via the ureido–acetic acid headgroup of the guest. Although we know that the pincer model is not the most realistic way to portray the binding between guest and host, the many cross-peaks between the peripheral protons of the dendrimer and the protons of the guest clearly suggest that the guests are located at the periphery of the dendrimer.

4.3 MULTI-COMPONENT HOST–GUEST CHEMISTRY OF CARBOXYLIC AND PHOSPHONIC ACID BASED GUESTS WITH DENDRITIC HOSTS

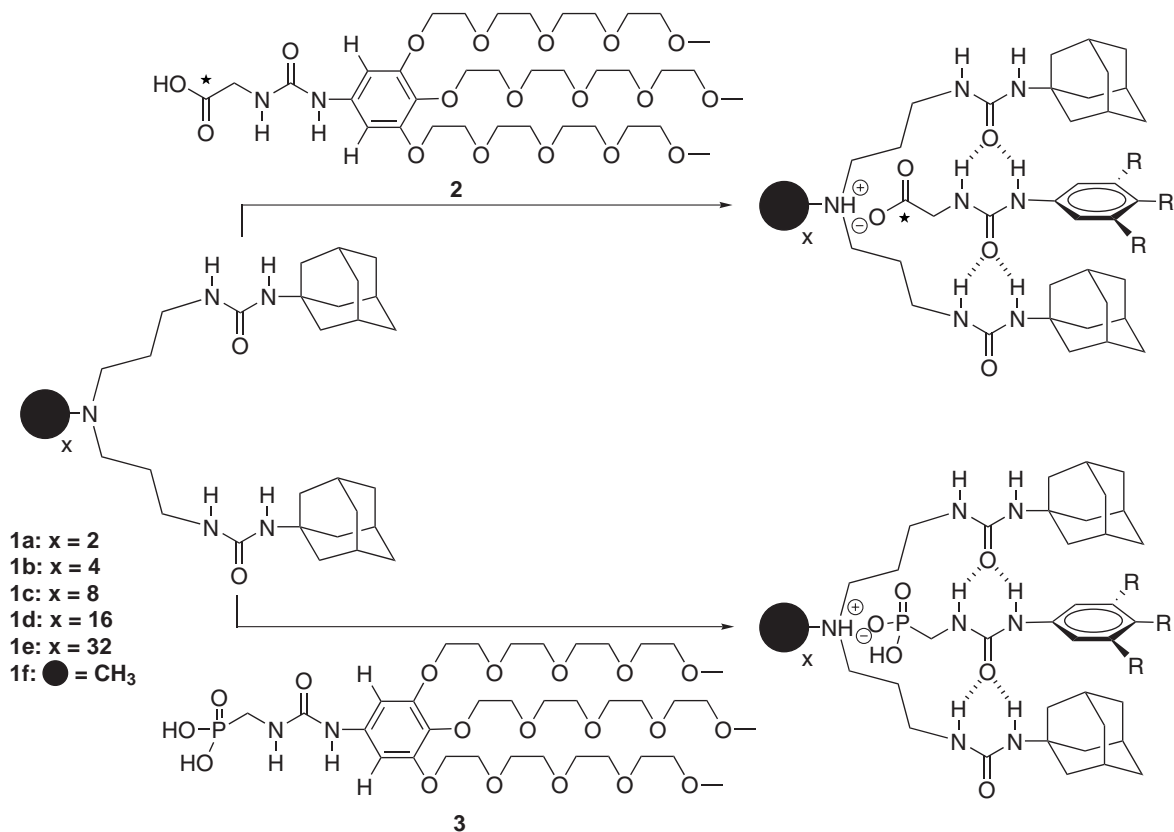
4.3.1 Designing the system

In an apolar aprotic solvent like chloroform, an acid (HA) and a base (B) are usually in equilibrium with a tight ion pair. The formed anion (A^-) and cation (BH^+) are in close proximity of each other due to electrostatic attraction and hydrogen bonding (equation 1), and it is generally believed that no free ions are present in solution.¹⁷⁻³⁴



It is known that both the ^{13}C chemical shift of carboxylic acids and the ^{31}P chemical shift of phosphonic acids are strongly dependent on the pH. In water, the ^{13}C chemical shift of carboxylic acids can shift over 5 ppm downfield when the acid is deprotonated and the carboxylate salt is formed.³⁵⁻³⁹ For phosphonic acids, both upfield and downfield shifts in ^{31}P NMR have been reported upon deprotonation.⁴⁰⁻⁴³ This inspired us to use ^{13}C NMR and ^{31}P NMR as a tool to investigate the binding of ureido–acetic acid and ureido–phosphonic acid type guests to urea–adamantyl dendrimers in chloroform.

In order to make analysis easier and to prevent long measurement times, a ^{13}C -label has been incorporated in the carbonyl group of the acid functionality of the ureido–acetic acid guest molecules. For solubility reasons, ethylene glycol guests **2** and **3**, already described in chapter 2 and 3, have been used in this study (Scheme 4.1).

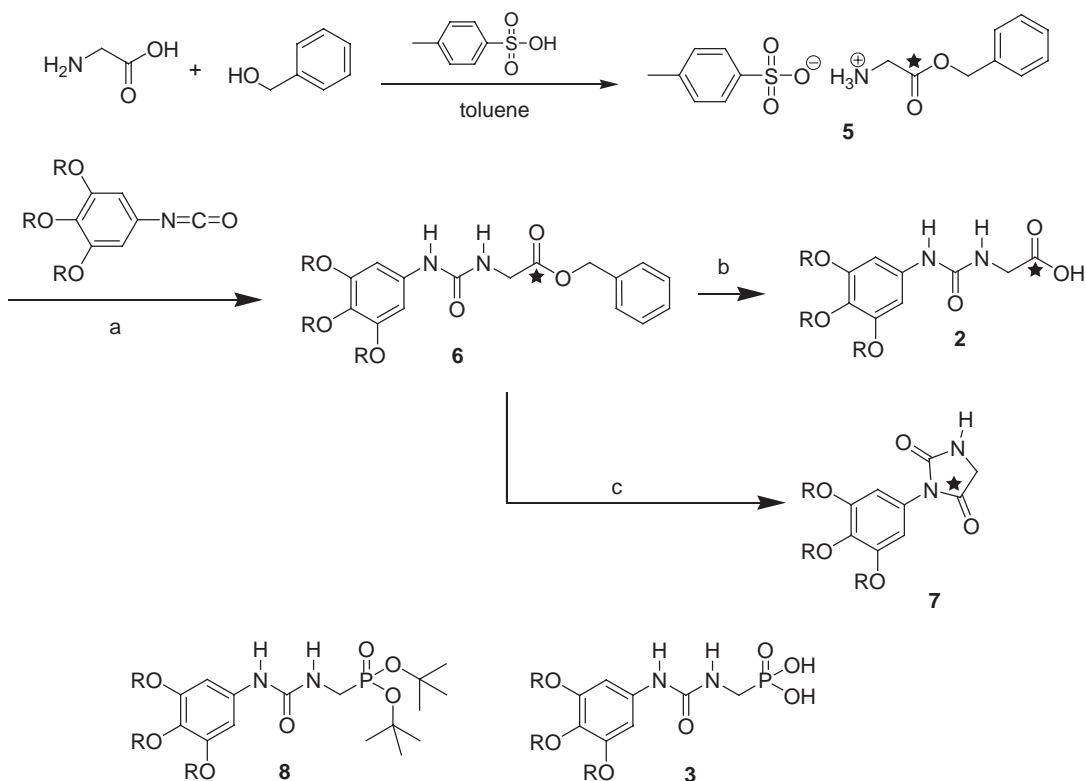


Scheme 4.1 Schematic representation of the molecules used in this study. The ^{13}C -label of the carbonyl group of the carboxylic acid is indicated with an asterisk.

Complexation experiments of both guests have been performed to several dendritic hosts (**1a–1e**), and the experimental results in case of host **1e** were fitted to get an idea of the binding stoichiometry and the association constant. Exchange experiments have been performed in which both guest molecules were simultaneously added to the dendrimer host, in order to investigate the difference in binding strength between guest **2** and **3** in more detail.

4.3.2 Introduction of the ^{13}C -label

The starting material for the ^{13}C -label in guest **2** is the commercially available 1- ^{13}C -glycine (Scheme 4.2). Reaction with benzyl alcohol in toluene in the presence of p-toluenesulfonic acid resulted in the benzyl ester of 1- ^{13}C -glycine as the p-toluenesulfonic acid salt (**5**). A Dean-Stark setup was used to azeotropically remove the water that is formed during the reaction. With this compound in hand, the synthesis of guest **2** has been performed in analogy to the unlabeled ethylene glycol guest described in previous chapters (see scheme 4.2). Ester **6** has to be treated carefully though. A first attempt to purify **6** by a basic workup with 1 M NaOH (aq) resulted in hydantoin **7**. When a saturated NaHCO₃ (aq) is used, this side reaction can be prevented.



Scheme 4.2 The synthesis of ^{13}C -labeled guest **2**. $R = (\text{OCH}_2\text{CH}_2)_4\text{OCH}_3$. a) CH_2Cl_2 , b) $t\text{-BuOH}/\text{H}_2\text{O}$ 1:1 v.v., H_2 , Pd/C c) 1 M NaOH (aq). The ^{13}C -labeled hydantoin side product has also been used in this study, as well as guest **3** and its precursor molecule **8**.

Though initially unwanted, hydantoin **7** was purified and analyzed, and has been used for several control experiments. The synthesis of phosphonic acid guest **3** has already been described in chapter two. Its precursor molecule **8** has been used for several control experiments.

4.3.3 Analysis of the complexes by ^1H NMR techniques

All complexes were prepared in a similar fashion, in which the concentration of the *guest* was kept constant. For both guest **2** and **3**, 10 mg was weighed and an amount of dendrimer was added to obtain the desired guest/host ratio. The compounds were dissolved in 0.5 mL of CDCl_3 and shaken for 5 minutes. Before we investigated the complexation behavior of guest **2** and **3** with ^{13}C NMR and ^{31}P NMR, we have analyzed the complexation to dendrimer **1e** with several ^1H NMR techniques to ascertain that binding occurred. This was done for both guests on a sample with a guest/host ratio of 32, denoted as **1e+2**₃₂ and **1e+3**₃₂.

The observed changes in ^1H NMR upon addition of guest **2** and **3** to dendrimer **1e** are depicted in figure 4.4, and in agreement with earlier findings. The urea signals of guest and host shift downfield due to hydrogen bonding. The signal of the methylene groups next to the tertiary amines of the dendrimer shift partially downfield due to protonation of some of the tertiary amines. Interestingly, the signal of the aromatic protons (F, figure 4.4) of the guest broadens upon addition

to the dendrimer. This effect happens most severely for phosphonic acid guest **3**. Most likely, the broadening is due to a decreased mobility of the headgroup of the guest when it binds to the dendritic macromolecule. This results in an increase of T_2 -relaxation and in a broader signal. When 32 equivalents of **7** or **8** are added to dendrimer **1e**, no changes in the ^1H NMR spectra are observed.

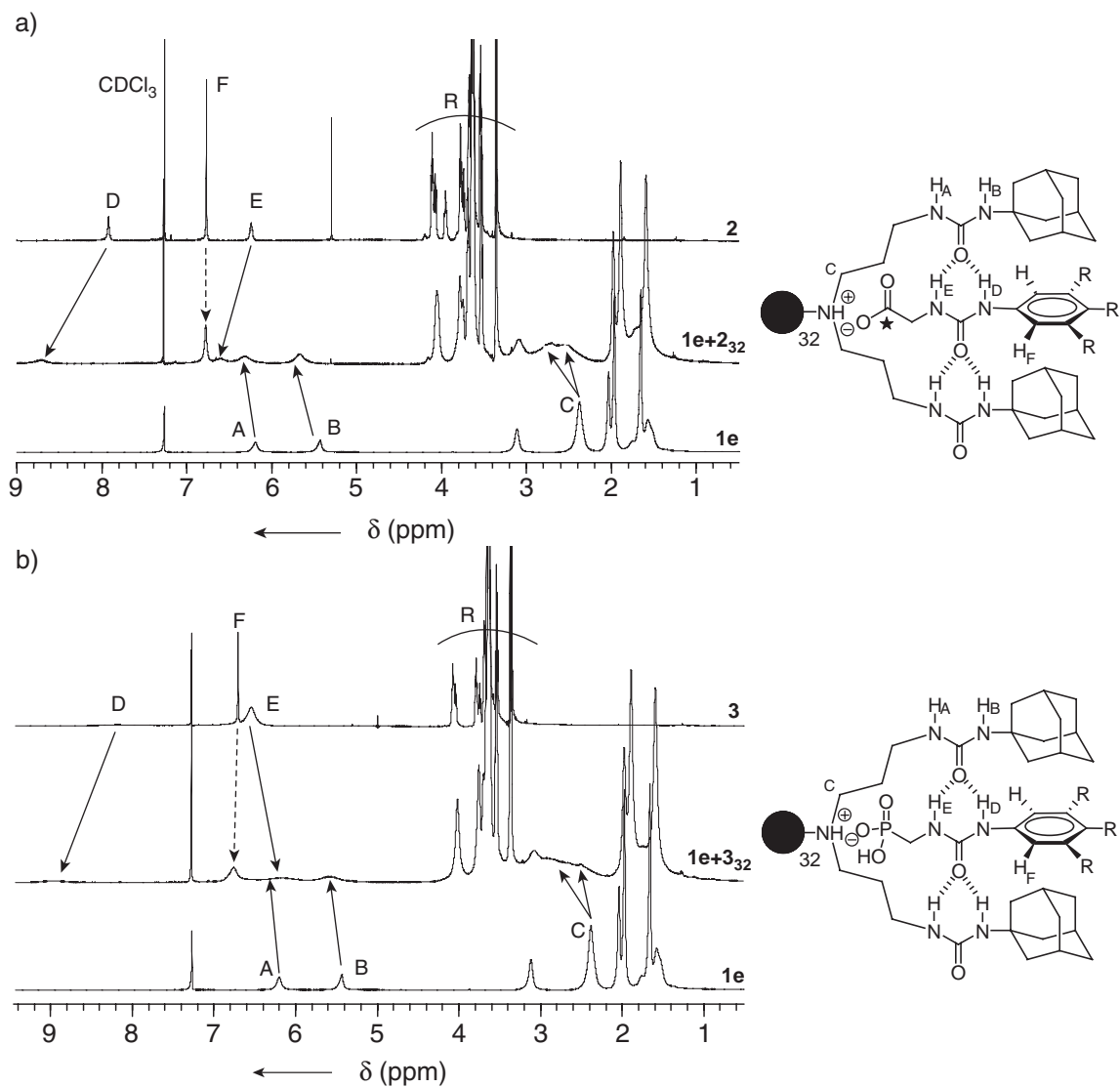


Figure 4.4 ^1H NMR spectra of dendrimer **1e**, guest **2** and **3** and the complexes **1e+2₃₂** and **1e+3₃₂**. The effect of hydrogen bonding and electrostatic interactions on the signals of guest and host are indicated.

If guest and host are bound, they should be in close proximity to each other. As discussed in the beginning of this chapter, this can be examined with ^1H - ^1H NOESY NMR.

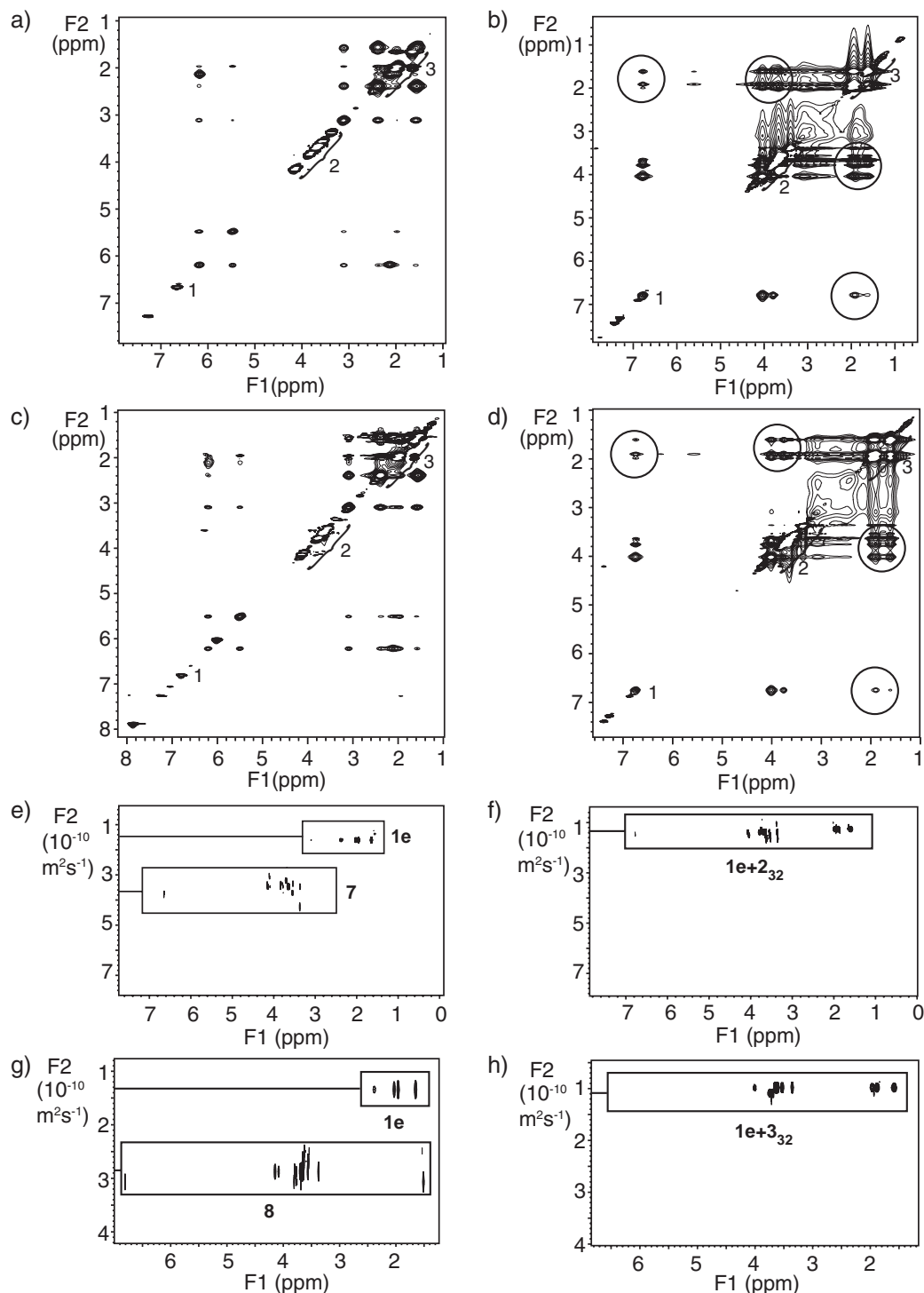


Figure 4.5. ^1H - ^1H NOESY spectra (a-d) and ^1H DOSY spectra (e-h) recorded for a) **1e**+**7**₃₂ b) **1e**+**2**₃₂ c) **1e**+**8**₃₂ d) **1e**+**3**₃₂ e) **1e**+**7**₃₂ f) **1e**+**2**₃₂ g) **1e**+**8**₃₂ and h) **1e**+**3**₃₂ in CDCl_3 at 25°C .

^1H - ^1H NOESY spectra of **1e**+**2**₃₂ and **1e**+**3**₃₂ (Figure 4.5b and d) show cross-peaks between the oligoethylene glycol tails of the guests (in all spectra indicated as 2) and the adamantyl groups (signal 3) of the dendrimer, indicating that these protons are close to each other through space. Also a weak cross-peak is observed between the aromatic protons of guest 2 and 3 (signal 1) and the adamantyl signals of **1e**, which is an indication that the headgroup of the guest is in close proximity

to the periphery of the host and is responsible for complexation, in agreement with the work described in the beginning of this chapter. This is also confirmed by ^1H - ^1H NOESY spectra that have been recorded for **1e+7**₃₂ and **1e+8**₃₂ (Figure 4.5 a and c). In both cases no intermolecular NOE-contacts were observed between the dendrimer and the guests, showing that no complexation occurs.

When a guest molecule binds to fifth generation dendrimer **1e** its diffusion constant should change as the dendrimer has a much higher molecular weight and consequentially diffuses slower. Actually, if binding of a guest to **1e** is strong enough, both guest and host should diffuse with an equal rate as they belong to the same supramolecular aggregate. Therefore, ^1H DOSY NMR has been performed on several complexes. When samples **1e+7**₃₂ and **1e+8**₃₂ are analyzed with ^1H DOSY NMR, different apparent diffusion constants were found for guest and host (Figure 4.5e and g). The apparent diffusion constants of hydantoin **7** and phosphonic ester **8** are higher than of dendrimer **1e**, as they are smaller molecules that diffuse faster. These differences again support the idea that **7** and **8** do not interact with the dendrimer. However, this is not the case for guest molecules **2** and **3** (Figure 4.5f and h). When samples **1e+2**₃₂ and **1e+3**₃₂ are analyzed with ^1H DOSY NMR, the apparent diffusion constants of **2** and **3** are similar to host **1e**. This confirms that guest and host are bound to each other.

4.3.4 Complexation observed by ^{13}C NMR

Having obtained evidence that guest **2** binds to dendrimer **1e** in chloroform, we can analyze the complexation behavior with ^{13}C NMR. This has been done by investigating how the ^{13}C -chemical shift of the guest depends on the composition of the sample. The ^{13}C NMR spectrum of pure **2** in CDCl_3 shows a signal at 172.5 ppm, which corresponds to the carboxylic acid carbon (Figure 4.6).

For the free guest the linewidth of the peak at half height is approx. 3 Hz. For the sample with a guest/host ratio of 8, the peak shifts downfield to 175.6 ppm and broadens slightly. The downfield shift is also observed when an excess of triethylamine is added to guest **2**, but not when hydantoin **7** is added to **1e** (not depicted). Clearly the shift is due to deprotonation of the acid. As in chloroform a tight ion pair is formed between an acid and a base, the downfield shift is a direct measure for complexation of the guest to the dendrimer.

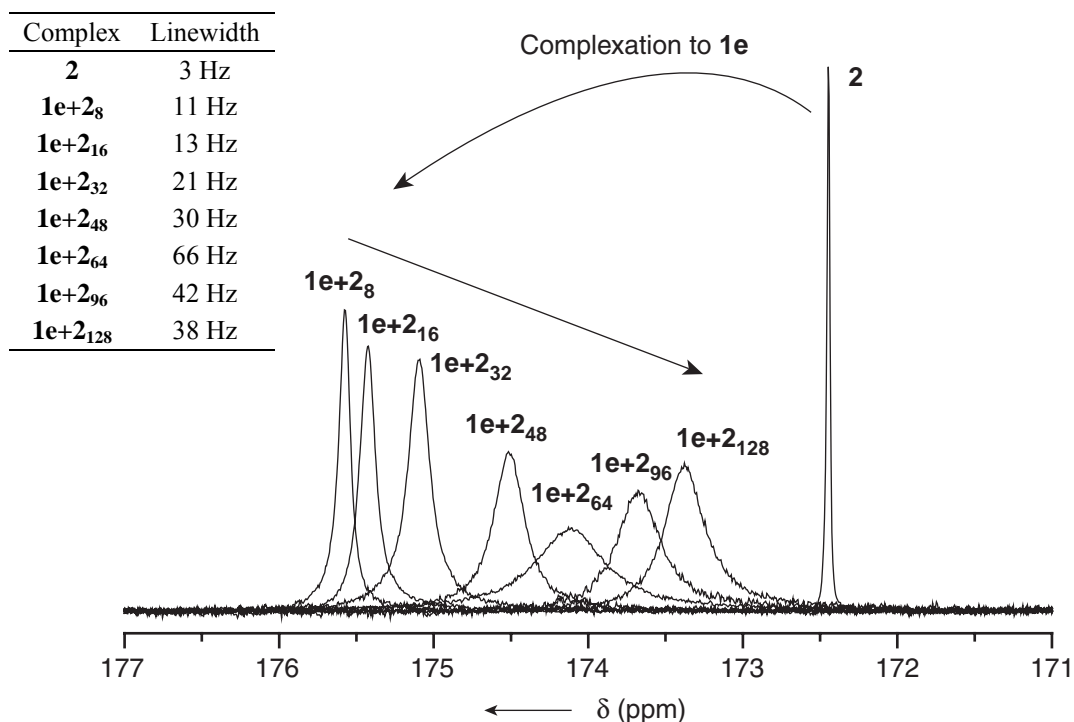


Figure 4.6 ^{13}C NMR spectra of different guest/host ratios of **2** and **1e**. The concentration of guest is kept constant at $2.46 \cdot 10^{-2}$ M. The linewidths of the peaks are indicated in the inset. The intensities are not normalized.

When we look at the results for increasing guest/host ratio, two trends are observed. First of all, the carbonyl signal shifts upfield. The change in chemical shift is small when **1e+2₈** is compared to **1e+2₁₆**, but is clearly present when the guest/host ratio (from now on referred to as G/H) is further increased to 32, 48, 64, 96 and 128. Furthermore, the signal broadens when G/H increases until the value of 64 is reached. A further increase of G/H results in a sharper signal again. We propose that the results can be interpreted in the following manner. Only one peak is observed, and this indicates that the signal is an average signal for both free and bound guest. This shows that exchange between free and bound guest is fast on the spectral timescale.⁴⁴ For increasing G/H the signal shifts back in the direction of the free guest, indicating that the ratio of unbound/bound guests increases.

Two effects govern the broadening of the signal. Complexation to a large macromolecule results in a decrease in mobility of the headgroup of the guest. This causes an increase in T_2 -relaxation, and consequentially in broadening of the signal. However, this is not very plausible as the peak becomes sharper again after 64 equivalents of guest. When the exchange rate between free and bound guest comes close to the spectral timescale, broadening can also occur due to coalescence.⁴⁵ In this case the relative amount of free and bound guest should influence the peak broadness, and this is exactly what happens when G/H is increased. When we start at **1e+2₈**, bound guest is the predominant species. When the relative amount of **2** is increased more unbound guest starts to become present, resulting in a broader signal. At **1e+2₆₄** the linewidth is highest, which

suggests that the amount of free and bound guest is approximately equal in this case. A further increase in G/H results in an excess of unbound guest and thus in a sharper signal.

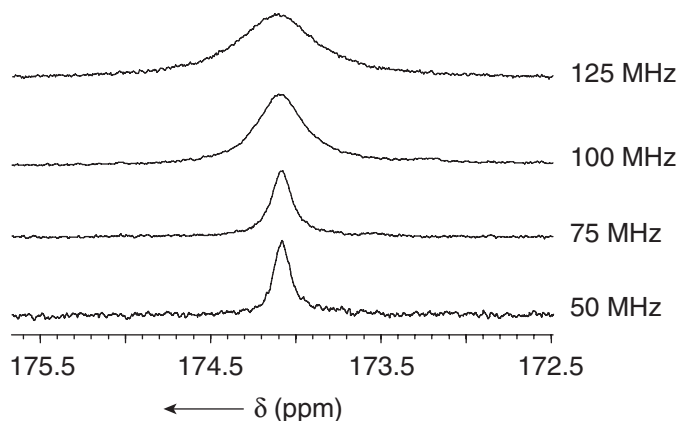


Figure 4.7 Dependency of the signal of $1e+2_{64}$ on the ^{13}C frequency. The signal becomes more narrow when the field strength of the spectrometer decreases.

As spectral lineshape perturbations are dependent on the magnetic field, complex $1e+2_{64}$ was analyzed at different field strengths (Figure 4.7). This resulted in a sharper signal at lower field strength and is an indication that coalescence is indeed taking place. This means that although T_2 -relaxation and coalescence both play a role in line broadening, coalescence is the major contributor of the two.

When guest **2** is added to lower generation dendrimers, the same trend in chemical shift dependency is observed when G/H is increased, and complexation can be followed in exactly the same way (Figure 4.8). Apparently, the method is applicable to all dendrimer generations. Interestingly, the severe broadening of the signal upon increasing G/H has not been observed for lower generation dendrimers, indicating that the exchange kinetics are faster for smaller dendrimers.

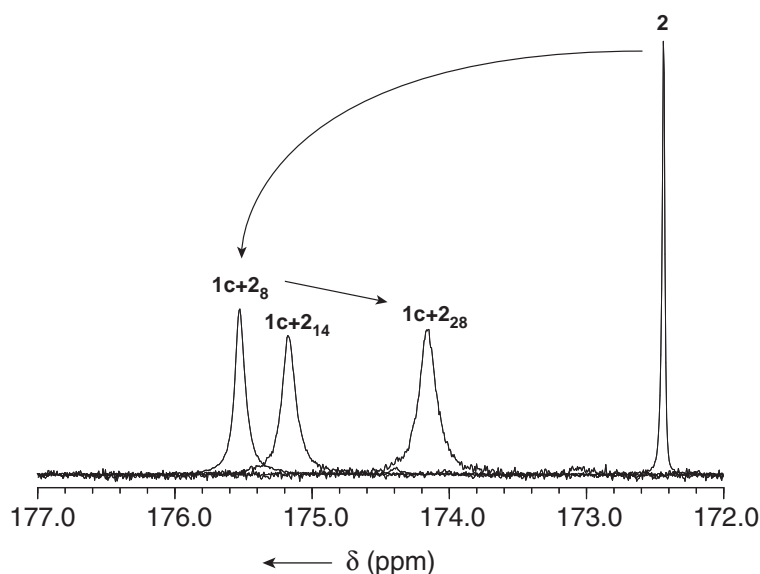


Figure 4.8 ^{13}C NMR spectra of different guest/host ratios of guest **2** with third generation dendrimer **1c**. The linewidths do not change severely upon increasing G/H.

4.3.5 Complexation observed by ^{31}P NMR

In a similar manner to guest **2**, we have investigated the complexation of guest **3** to dendrimer **1e** using ^{31}P NMR (Figure 4.9).

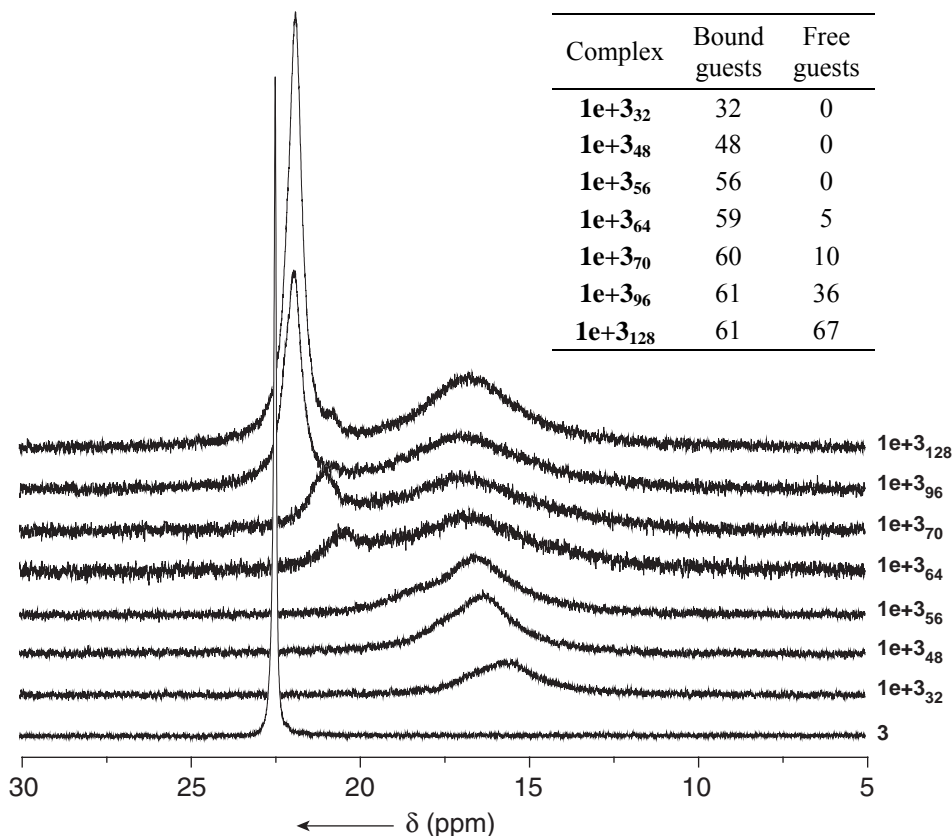


Figure 4.9 ^{31}P NMR spectra of different guest/host ratios of **3** and **1e**. The concentration of guest is kept constant at $2.36 \cdot 10^{-2}$ M. The deconvolution results are depicted in the table.

Free guest **3** gives a sharp peak at 22.5 ppm in CDCl_3 . This peak completely disappears when 16 (not depicted) or 32 guests are added to **1e** and is a broad signal at 16 ppm. When G/H is increased to 56, no big changes occur. At G/H = 64, two distinct signals start to become present: a narrow peak at 21 ppm and the very broad signal at 17 ppm. A further increase of G/H shows that the peak at 21 ppm becomes more intense and shifts a little downfield. The broad peak remains present. These results show completely different trends than the observations for complexation of guest **2** to **1e** in ^{13}C NMR. The chemical shift of the phosphonic acid group shifts upfield instead of downfield due to deprotonation. It is known that the chemical shift of phosphonic acid derivatives strongly depends on the pH. Both upfield and downfield shifts have been reported for different compounds. In our case, deprotonation of the phosphonic acid and the formation of a tight ion pair apparently results in an upfield shift, and this has also been observed when an excess of triethylamine was added to guest **3**. We observe 2 separate signals when G/H is increased, indicating that we now have slow exchange on the spectral timescale.⁴⁶ The signal of the free guest is located

around 22 ppm and relatively sharp, the signal of the bound guest is located around 16 ppm and very broad. It is possible to deconvolute the 2 signals and to directly determine the ratio of free and bound guest. This has been done for $G/H = 64, 70, 96$ and 128 (Figure 4.9, table) and shows that the amount of bound guest remains fairly constant around 60 equivalents. The amount of free guest increases from 5 to 67 guests. The numbers suggest that approx. 60 guests can bind to **1e**. This amount comes very close to the 62 tertiary amines that are present inside the dendrimer.

The signal of the bound guest is very broad. Again, both T_2 -relaxation and coalescence can cause this broadening. However, as we have slow exchange on the spectral timescale coalescence is less likely to be the major contributor. This was confirmed by the observation that measurements at other magnetic field strengths did not show a change in the spectrum. In order to test whether T_2 -relaxation could be the reason for the severe broadening, we examined the phosphorus NMR spectra of guest **3** added to the lower generation dendrimers **1c**, **1a** and pincer molecule **1f** (Figure 4.10). In all cases the stoichiometry of one guest per two endgroups was maintained. The spectrum of **1f+3₁** shows a downfield shift of the phosphorus signal, but no big change in linewidth, in contrast to **1a+3₂**, **1c+3₈** and **1e+3₃₂**. Clearly the linewidth increases upon increasing size of the dendrimer host. A decrease in mobility of the headgroup of the guest due to complexation to such a large molecule could explain the results.

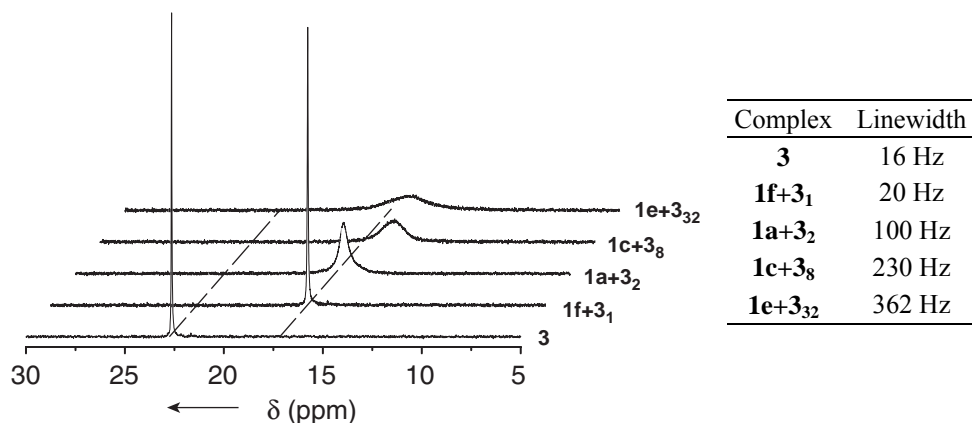


Figure 4.10 The influence of the host on the chemical shift and linewidth of the signal of guest **3** in ^{31}P NMR.

For lower generation hosts a similar chemical shift dependency is observed for different values of G/H , meaning that the signal of the guest shifts upfield upon deprotonation. However, the exchange kinetics also depend on the dendrimer generation and are faster for lower generation dendrimers, as the two different signals for free and bound guest are not always observed. For example, different amounts of guest added to pincer **1f** always result in one signal (Figure 4.11). So, exchange is faster for the pincer. In this case, the broadening is most likely due to coalescence again.

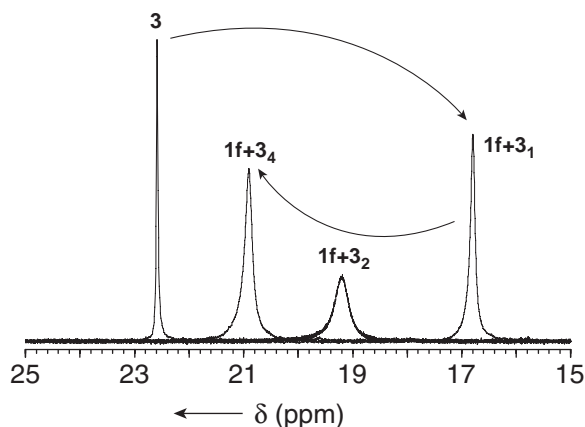


Figure 4.11 ^{31}P NMR spectra of different guest/host ratios of **3** and **1f**. In this case, only one signal is observed, indicating that exchange is fast on the NMR timescale.

4.3.6 Quantitative analysis of binding

The obtained chemical shift values can be used to analyze the binding of guest **2** to dendrimer **1e** in a quantitative manner. The observed chemical shift (δ) can be seen as a mixture of free and bound (deprotonated) guest since we are in a fast exchange situation, and can be represented as:

$$\delta = p_b \delta_b + p_f \delta_f \quad (4.2)$$

with p_b the fraction of bound guest, δ_b the chemical shift of the bound guest, p_f the fraction of free guest and δ_f the chemical shift of the free guest. The chemical shift of the free guest is known ($\delta_f = 172.5$ ppm), but that of the bound guest is not. However, most likely it is very close to the 175.6 ppm obtained for **1e+2g**. We assume there is no cooperativity: all binding sites in the host are identical and do not influence each other. When a 1:1 binding of guest and binding site is assumed, an equation can be derived that gives the fraction of bound guest as a function of G/H (see appendix). Fitting this equation to the measured chemical shift values with a non-linear least-squares fit (Figure 4.12a), gives us values for the number of binding sites (n), the association constant for carboxylic acid guest **2** (K_C) and the chemical shift of the bound guest (δ_b). We find:

$$n = 41 \pm 2$$

$$\delta_b = 175.61 \text{ ppm}$$

$$K_C = 400 \pm 95 \text{ M}^{-1}$$

The obtained association constant is in the same order of magnitude as the association constant found from fluorescence measurements on model host compounds.⁴⁷

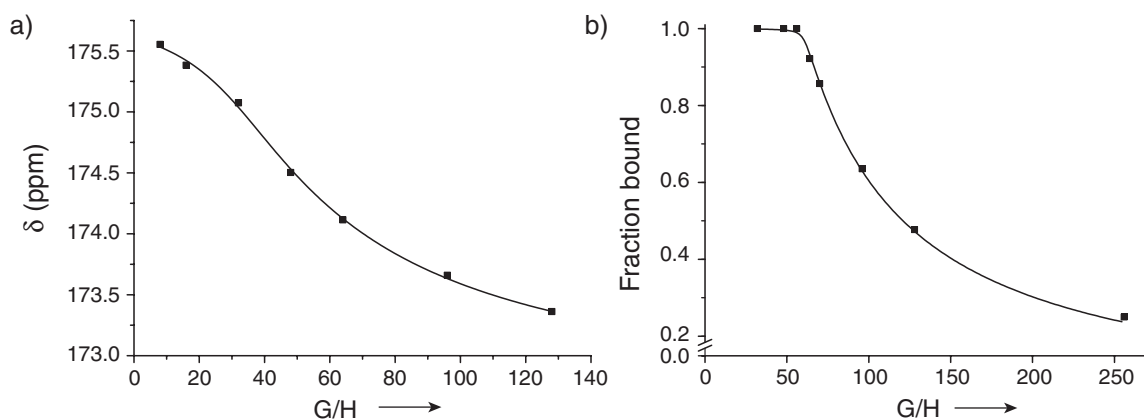


Figure 4.12 a) The chemical shift values of guest **2** as a function of the guest/host ratio (points). The solid line represents the fit. b) The fraction of bound guest **3** to host **1e** as a function of the guest/host ratio. The concentrations of the guests are kept constant at $2.46 \cdot 10^{-2}$ M and $2.36 \cdot 10^{-2}$ M respectively. The solid line represents the fit.

For guest **3** we followed the same reasoning as for guest **2**, but now we have the fraction of bound guest (p_b) directly available from the deconvolution of the spectra. We can directly fit p_b to the equivalents of guest added (Figure 4.12b). We then find:

$$n = 61 \pm 1$$

$$K_p = (4 \pm 3) \times 10^4 \text{ M}^{-1}$$

The fit shows a higher association constant for guest **3** than for guest **2**. This is in agreement with earlier results that show a stronger binding for the phosphonic acid guest. The results are different from the traditional model as more than 32 guests can apparently bind to the dendrimer. The discrimination between guests bound at the periphery or the interior of the dendrimer cannot be made based on ^{31}P NMR.

4.3.7 Exchange

As we are now able to follow complexation of guest **2** and **3** with two orthogonal NMR techniques, we investigated what happens when both guests are simultaneously added to dendrimer **1e**. The amount of carboxylic acid guest **2** was kept constant at $G/H = 32$. To this sample was added 16, 32 and 64 equivalents of phosphonic acid guest **3**, and the results were monitored by both ^{13}C NMR and ^{31}P NMR (Figure 4.13). When 32 equivalents of **2** are added to **1e**, the characteristic downfield shift to 175.1 ppm is observed in ^{13}C NMR. As **3** is not present, the ^{31}P NMR spectrum does not show anything. When 16 equivalents of **3** are added to this sample, resulting in **1e**+(**2**₃₂+**3**₁₆), an upfield shift in ^{13}C NMR is observed to 174.7 ppm, indicating that **2** dissociates partially from the dendrimer. When **1e**+(**2**₃₂+**3**₁₆) is analyzed with ^{31}P NMR, a broad signal at 16 ppm is observed, indicating that all of phosphonic acid guest **3** is bound to **1e**.

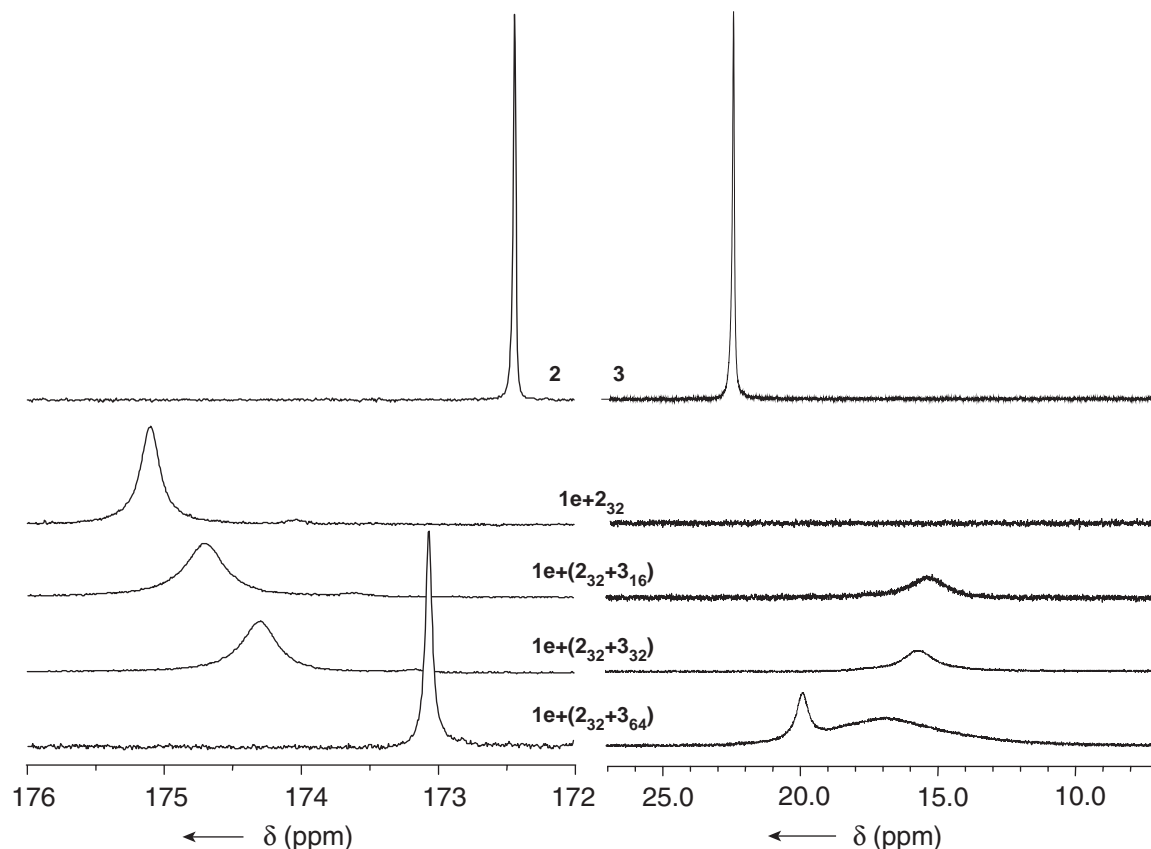


Figure 4.13 Influence of the addition of **3** to $1e+2_{32}$ observed in ^{13}C NMR (left) and ^{31}P NMR (right). The concentration of guest **2** was kept constant at $2.46 \cdot 10^{-2} \text{ M}$.

An increase of the amount of **3** to $1e+(2_{32}+3_{32})$ results in an upfield shift to 174.3 ppm in ^{13}C NMR, so **2** dissociates further from **1e** due to **3**. In ^{31}P NMR we still observe complete complexation of phosphonic acid guest **3** to the dendrimer. When the amount of guest **3** is increased to $1e+(2_{32}+3_{64})$ the signal of guest **2** in ^{13}C NMR shifts to 173.1 ppm. This is much further upfield than observed for $1e+2_{96}$ or $1e+2_{128}$, which give values of 173.7 and 173.4 ppm respectively (Figure 4.6). Also the linewidth of the peak, 10 Hz, is much lower than for $1e+2_{96}$ or $1e+2_{128}$ and indicates the amount of bound **2** is lower. In ^{31}P NMR, we now start to observe two signals, so some free **3** is present.

4.3.8 Interpretation of the NMR data

The results regarding the binding strength and binding stoichiometry of guest **2** and **3** to urea-adamantyl dendrimer **1e** have some major implications for our molecular picture. With the availability of association constant and number of binding sites for both guests, we can calculate the amount of free and bound guest for every guest/host ratio at a certain concentration. This has been done for several guest/host ratios in figure 4.14. Furthermore it is important to realize that not always a monodisperse supramolecular aggregate is present in solution, but a distribution in the number of bound guests. It is possible to calculate how many different complexes can be expected at

a certain guest/host ratio using a binomial distribution. In order to visualize more clearly how the guest/host ratio affects the distributions of guest **2** and **3** bound to dendrimer **1e**, three distributions have been calculated for each guest with $G/H = 32, 64$ and 128 . The results are also depicted in figure 4.13.

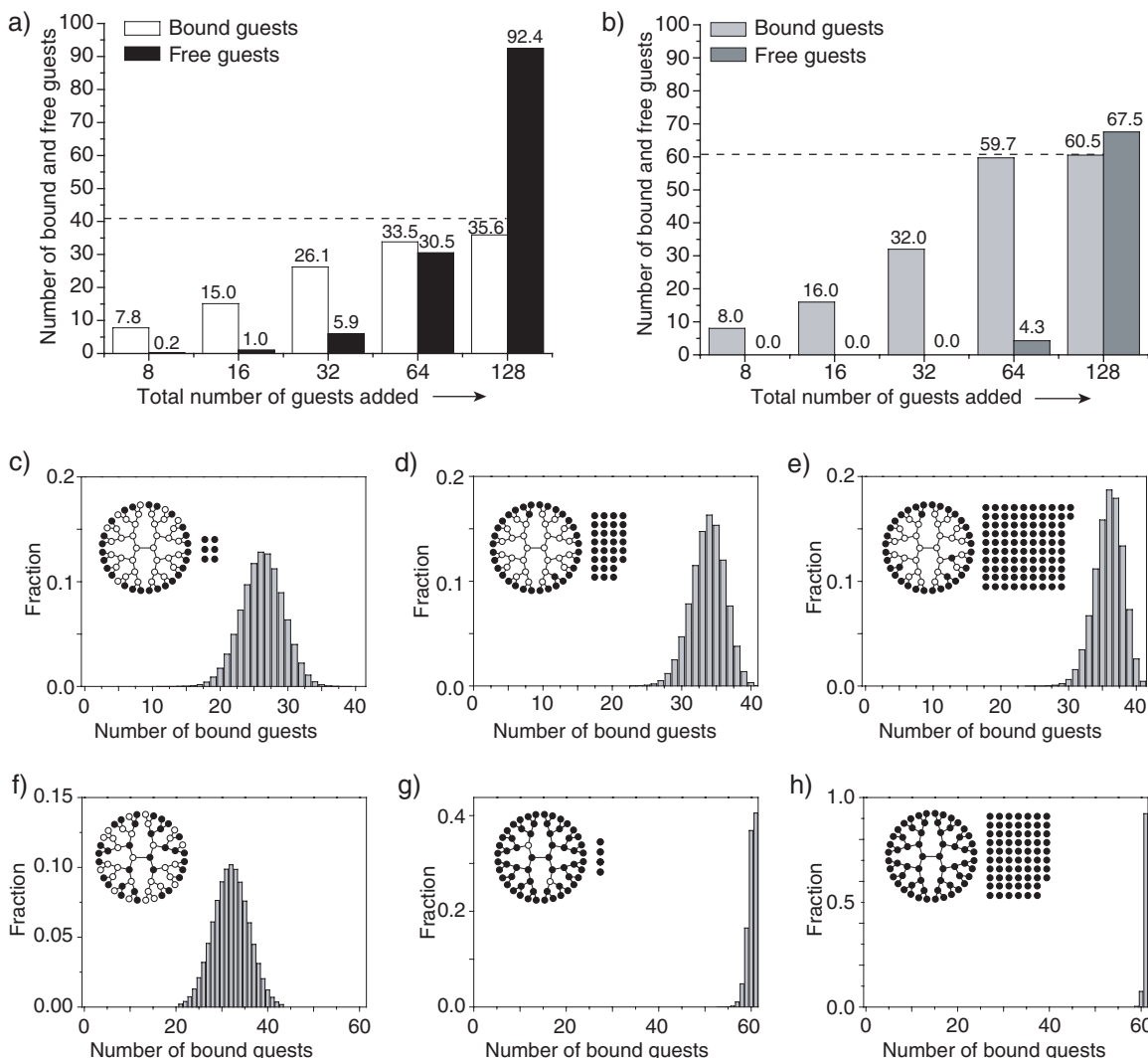


Figure 4.14 Top: the number of free and bound guests **2** (a) and **3** (b) as a function of the total amount of guest as obtained from the fitted data. The dashed line indicates the maximum number of guests that can bind to the dendrimer. Middle: distributions of the number of guests **2** bound to dendrimer **1e** calculated for $G/H = 32$ (c), $G/H = 64$ (d) and $G/H = 128$ (e). Bottom: distributions of the number of guests **3** bound to dendrimer **1e** calculated for $G/H = 32$ (f), $G/H = 64$ (g) and $G/H = 128$ (h). The cartoons reflect the number of free and bound guest at that specific guest/host ratio.

The relatively low association constant of guest **2** has the consequence that when 32 equivalents of guests **2** are added to **1e**, only 26 guests are bound *on average* and also free **2** is present in solution. The term *on average* is deliberately used, as a distribution in the number of bound guests is present. When the amount of **2** is further increased, more guests will be bound on average but the amount of free guest increases significantly too. The distribution of complexes

becomes slightly narrower, but it is clear that a polydisperse supramolecular aggregate is present for $G/H = 128$.

For guest **3** the same statistical rules apply, also resulting in a polydisperse supramolecular aggregate at $G/H = 32$. Interestingly, below $G/H = 60$ virtually all guests are bound to the dendrimer due to the higher association constant. Furthermore, an almost monodisperse supramolecular aggregate can be obtained for guest **3**, but only at high guest/host ratios when a lot of free guest is present (Figure 4.13). The number of bound guests is based on a certain concentration and alters with changes in the concentration.

The differences between guest **2** and **3** are also reflected in the exchange experiment. If we assume that the binding equilibria are independent for **2** and **3**, the amount of free and bound carboxylic acid guest **2** can be determined from the chemical shift, and the amount of free and bound phosphonic acid guest **3** can be determined from deconvolution of the spectra. These values have been determined and are shown in figure 4.15. The numbers show that initially guest **2** and **3** co-exist on the dendrimer. Although the association constant of guest **3** is higher, it does not compete severely with carboxylic acid guest **2** as guest **3** has 61 possible sites to bind to. However, when 64 equivalents of **3** are added to $1e+2_{32}$, **3** competes with all the binding sites of guest **2**, and this results in almost complete dissociation of **2** from **1e**. The amounts of free and bound **2** and **3** that are found in the mixing experiment are in accordance with the expected values based on the obtained association constants. From these experiments we can conclude that it is possible to make mixed aggregates, and that phosphonic acid guest **3** can expel carboxylic acid guest **2** from the dendrimer.

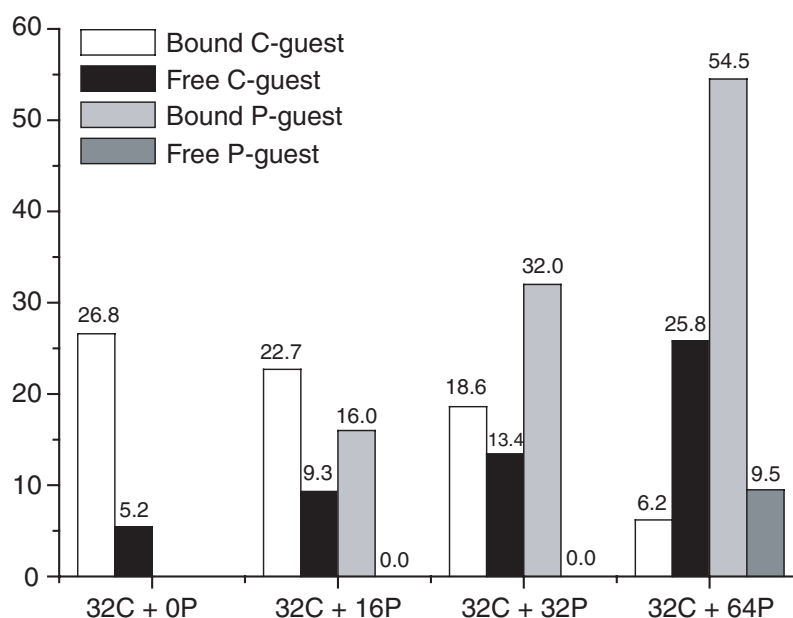


Figure 4.15 The amounts of free and bound guests **2** and **3** as obtained from the exchange experiment depicted in figure 7.

4.3.9 Dynamic light scattering

Scattering techniques are powerful tools to study particle geometry and sizes in solution. Various scattering techniques are known such as X-ray (WAXS, SAXS) and neutron scattering (SANS). In this study dynamic light scattering has been used to investigate whether dendrimer-dendrimer aggregates are present in solution next to dendrimer-guest complexes, in collaboration with the group of prof. George Fytas (IESL/FORTH, Crete, Greece).

Light scattering intensity fluctuations detected in a small volume and in the microsecond time range are related to the Brownian motion of particles in solution due to fluctuations in the number of molecules present in a certain scattering volume. In dynamic light scattering, these intensity fluctuations are measured, and the so-called intensity correlation function $G(q,t)$ is obtained. Via a number of mathematical operations, including inverse Laplace Transformation, characteristic decay times are obtained which are in turn related to the diffusion constant of a particle. The Stokes-Einstein equation (4.3) can then be used to determine the hydrodynamic radius R_H of a particle:

$$R_H = \frac{kT}{6\pi\eta D} \quad (4.3)$$

where k is the Boltzman constant, T is the temperature, η is the solvent viscosity and D is the diffusion constant. From the decay times it is also possible to determine the absolute scattering intensity (also known as the Rayleigh ratio) R_{vv}/c , which is a value related to the molecular weight of a particle.

Dynamic light scattering measurements performed on dendritic host **1e** alone in chloroform and complexes with guest **2** and **3** in different guest/host ratios show one predominant fast process of small particles. The results are displayed in figure 4.16. The hydrodynamic radius (R_H) found for the sample with only dendrimer **1e** is 2.2 nm. This value is in good agreement with the dimensions of a single dendrimer.⁴⁸ For the different host/guest complexes the hydrodynamic radius R_H increases upon increasing G/H, which is expected based on the increasing amount of guests that bind to the dendrimer. Also the absolute scattering intensity R_{vv}/c , normalized to the concentration of dendrimer at large probing lengths ($q \sim 0$), has been determined. It shows an increasing trend upon higher G/H, in agreement with an increase in molecular weight of the complexes. The results also show that no dendrimer aggregation is taking place. It is possible to link the dynamic light scattering experiments with the NMR results discussed in the previous paragraphs. We can plot the absolute scattering intensity R_{vv}/c against the number of guests that are bound to the dendrimer based on the NMR results. A monotonic, almost linear increase is observed for both guest-host systems (Figure 4.16d).

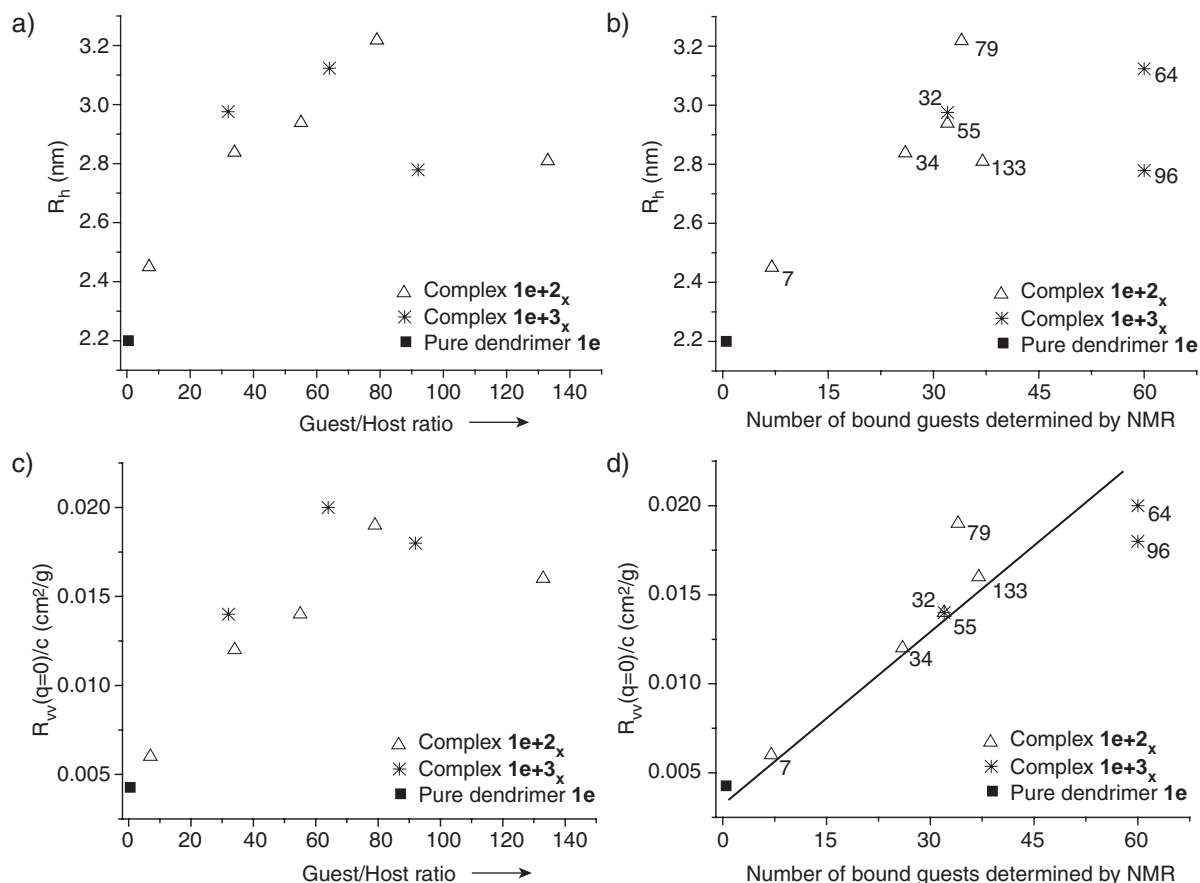


Figure 4.16 a) Hydrodynamic radius as a function of the guest/host ratio (x). b) Hydrodynamic radius as a function of the number of bound guests as determined from the NMR experiments. The numbers correspond to the guest/host ratio of the sample. c) Absolute scattering intensity as a function of the guest/host ratio. d) Absolute scattering intensity as a function of the number of bound guests as determined from the NMR experiments. The numbers correspond to the guest/host ratio of the sample.

This confirms the obtained relations between the number of added guest and the number of bound and free guest found for guests **2** and **3** to dendrimer **1e** by NMR. According to the fitted NMR data, 55 equivalents of guest **2** added to dendrimer **1e** should result in 32 equivalents bound. For guest **3**, addition of 32 equivalents to dendrimer **1e** should also give 32 equivalents bound. These points also overlap in the graph.

4.4 CONCLUSIONS

Knowing all of these details, we can say that the number of guests that bind to the dendrimer in chloroform is mainly governed by the acid–base interaction. When the acid strength is increased, the amount of guests that bind to the dendrimer and the binding strength increases similarly. The hydrogen bonds most likely help to direct and strengthen the binding to the periphery of the dendrimer, as previous ^1H - ^1H NOESY experiments have shown that carboxylic acid based guest molecules are mainly located at the periphery of the dendrimer. However, we must conclude that as

more than 32 equivalents of guest **2** can bind to the dendrimer, some guests should be bound to the inner tertiary amines of the dendrimer. This does not exclude the formation of hydrogen bonds with the dendrimer, as its structure is highly flexible and certainly not always completely stretched, but implies a more chaotic mode of binding than the initial “pincer model” that has been presented in chapter 2. This conclusion is in agreement with the results from the MD simulations and crystal structure analysis, also described in chapter 2.

It is important to stress that the association constant of 400 M^{-1} obtained for guest **2** is not general for every carboxylic acid guest. For the cyanobiphenyl-containing guest **4** the association constant was estimated to be 10^5 M^{-1} in chloroform.¹⁶ The discrepancy in association constant is caused by a difference in solubility. The cyanobiphenyl guest has a low solubility in chloroform, but can be solubilized by complexation to the dendrimer. Therefore the equilibrium (equation 4.1) is shifted in the direction of the complex, resulting in a higher apparent association constant.¹⁷ Clearly the apparent association constant can be influenced over several orders of magnitude by the solubility of guest and complex, as has been nicely demonstrated by Gillies and Fréchet.⁴⁹

For guest **3** we have observed that it can bind to virtually all tertiary amines, indicating that the acid–base interaction dominates the binding to the host.

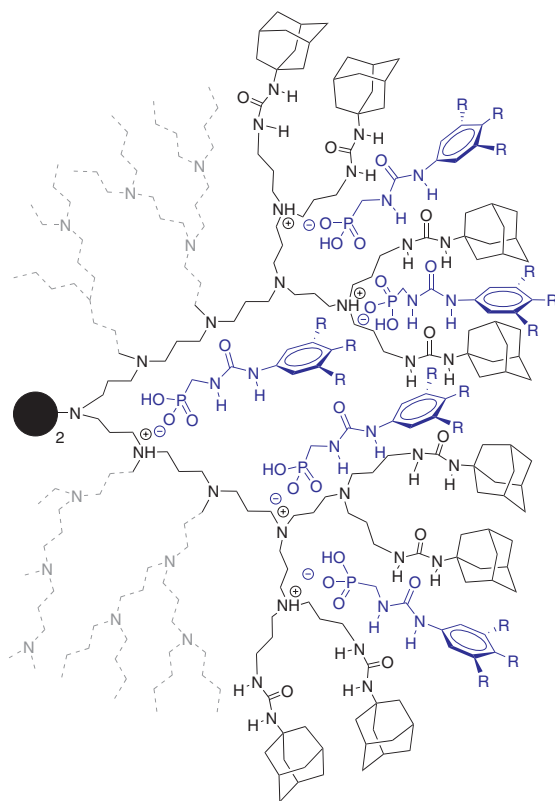


Figure 4.17 Possible representation for the binding of phosphonic acid guests to urea–adamantyl dendrimers that shows that guest molecules can also bind to the inner tertiary amines of the dendrimer. Only a part of the dendrimer structure is depicted. The hydrogen bonds between guest and host have been omitted for clarity.

The urea groups of guest **3** might still help to direct binding to the peripheral tertiary amines of the dendrimer, but this effect is probably weaker than for guest **2**. Actually, based on our

experiments we cannot discriminate between binding to the peripheral tertiary amines and binding to the amines further inside the dendrimer. Especially for guest **3**, figure 4.17 gives a more realistic representation for the binding to dendrimer **1e**. Still, we have to realize that this picture is a static representation of a dynamic, more complex 3D structure, see also the crystal structure analysis and the molecular dynamics simulations described in chapter 2.

4.5 EXPERIMENTAL SECTION

General information and instrumentation

All solvents used were provided by Biosolve, of p.a. quality and used as received unless stated otherwise. 1-¹³C-glycine (Cambridge Isotope Laboratories), benzyl alcohol (Across), p-toluenesulfonic acid monohydrate (Baker), hydrazine monohydrate (Across) and trifluoroacetic acid (Across) were used as received. Standard ¹H NMR, ¹³C NMR and ¹H-¹H COSY spectra were recorded at 25 °C on a Varian Gemini 300 or Varian Mercury 400 MHz spectrometer. Chemical shifts are given in ppm (δ) relative to tetramethylsilane (0 ppm). IR-spectra have been obtained on a Perkin Elmer Spectrum One ATR-FT-IR machine. MALDI-TOF MS spectra were measured in positive mode on a Perspective DE Voyager spectrometer utilizing an α -cyano-4-hydroxycinnamic acid matrix. High resolution electrospray ionization mass spectrometry was performed on a Q-ToF Ultima GLOBAL mass spectrometer (Micromass, Manchester, UK) equipped with a Z-spray source. Electrospray ionization was achieved in the positive ion mode by application of 5 kV on the needle. ¹H NMR, ¹H-¹H NOESY NMR, ¹H DOSY NMR, ¹³C NMR and ³¹P NMR experiments of the dendrimer-guest complexes have been recorded on a Varian Unity Inova 500 spectrometer operating at 500.618 MHz and equipped with a 5-mm 500 SW/PFG probe from Varian. Spectra were referenced to TMS and were obtained at 25 °C. All samples were prepared by adding 10 mg of guest molecule together with the appropriate amount of dendrimer to 0.5 mL of CDCl₃. Prior to Fourier-transformation in the ¹H-¹H NOESY experiments, the f1 and f2 data points were processed with a squared shifted sinebell weighing function. A mixing time of 0.25 s was used. Diffusion ordered spectroscopy was performed on the same Varian Unity Inova 500 spectrometer, employing a Performa II gradient unit capable of a maximum gradient of 70 G cm⁻¹. The apparent diffusion constant was measured with ¹H NMR diffusion measurements⁵⁰ using the bipolar pulsed gradient stimulated echo (BPPSTE) pulse sequence.^{51, 52} A $\pi/2$ pulse of 9.8 μ s and a relaxation delay of 2 s were used. The parameters Δ (diffusion delay) and δ (gradient pulse duration) were determined at $\Delta = 0.05$ – 0.08 s and $\delta = 2$ ms to afford optimal signal decay at increasing gradient strength g . The resulting data was evaluated by the Varian Dosy software in VNMR using the Stejskal-Tanner equation.⁵³ In ¹³C NMR a relaxation delay of 3 s was used, and at least 1400 pulses to obtain a good signal to noise ratio. In ³¹P NMR no relaxation delay was used, and at least 20000 pulses to obtain a good signal to noise ratio. Deconvolution of the ³¹P NMR spectra was performed with standard deconvolution software of Varian.

1-¹³C-Glycine benzylester toluene-4-sulfonate (5)

A solution of p-toluenesulfonic acid monohydrate (6.09 g, 32.0 mmol), 1-¹³C-glycine (2.0 g, 26.3 mmol) and benzyl alcohol (5.75 g, 53.2 mmol) in 35 mL of toluene was refluxed for 5 hours. The flask was connected

to a Dean-Stark setup and a cooler in order to azeotropically remove the water formed during the reaction. The solution was brought to room temperature and 30 mL of diethyl ether was added. White crystals of **4** were formed that could be obtained purely after filtration and drying of the residue (8.75 g, 98%). ^1H NMR (D_2O): δ = 7.68 (2H, d, ArH), 7.46 (5H, m, PhH), 7.35 (2H, d, ArH), 5.29 (2H, d, PhCH_2O , $^3J_{\text{C-H}} = 3$ Hz), 3.95 (d, 2H, $\text{CH}_2\text{C}(\text{O})$, $^2J_{\text{C-H}} = 6$ Hz), 2.38 (s, 3H, CH_3). ^{13}C NMR (D_2O): 167.4 (C(O)O), ^{13}C satellites: $J_{\text{C-C}} = 62$ Hz), 141.8 (ArCSO₃H), 139.1 (ArCCH₃), 134.2 (PhC_{ipso}), 128.9, 128.4, 128.3, 128.0, 124.9 (ArC₂, ArC₃, PhC), 67.8 (d, CH₂-benzyl, $^2J_{\text{C-C}} = 2$ Hz), 39.7 (d, CH₂C(O), $J_{\text{C-C}} = 62$ Hz), 20.0 (CH₃). HRMS: Calculated mass for $[\text{C}_8^{13}\text{CH}_{11}\text{N}_1\text{O}_2 + \text{H}]^+$: 167.090, found 167.080.

1- ^{13}C -Benzyl-2-((3,4,5-tris{2-(2-{2-[2-methoxyethoxy]-ethoxy}-ethoxy)-ethoxy})phenylureido} acetate (6)

The preparation of compound **6** is similar to the unlabeled analog, described in chapter 2. ^1H NMR (CDCl_3): δ = 7.76 (s, 1H, ArNH), 7.32 (m, 5H, PhH), 6.78 (s, 2H, ArH), 6.15 (t, 1H, NHCH₂), 5.15 (d, 2H, PhCH_2O , $^3J_{\text{C-H}} = 3.0$ Hz), 4.1-3.9 (m, 8H, ArOCH₂ {6} + CH₂C(O)O {2}), 3.8-3.4 (m, 42 H, OCH₂CH₂O), 3.36 (s, 3H, OCH₃), 3.34 (s, 6H, OCH₃). ^{13}C NMR (CDCl_3): δ = 170.8 (C(O)O, satellites: $J_{\text{C-C}} = 62$ Hz), 155.9 (NHC(O)NH), 152.3 (ArC₃'), 136.0, 135.5 (PhC_{ipso}, ArC₄'), 133.1 (ArC₁'), 128.5, 128.3, 128.2 (PhC), 99.1 (ArC₂'), 72.3, 71.8, 70.5-70.3, 70.26, 69.54, 68.52 (OCH₂CH₂O), 66.71 (d, CH₂-benzyl, $^2J_{\text{C-C}} = 2.3$ Hz), 59.0 (OCH₃), 58.9 (2 x OCH₃), 41.75 (d, CH₂C(O), $J_{\text{C-C}} = 62$ Hz). ATR-IR: ν (cm^{-1}) = 3356.1, 2872.2, 1696.3, 1605.3, 1551.2, 1502.5, 1455.4, 1422.1, 1350.2, 1292.6, 1216.61, 1026.7, 944.01, 846.8. MALDI-TOF MS: calc. m/z 903.5, found $[\text{M}+\text{H}]^+$: 904.50, $[\text{M}+\text{Na}]^+$: 926.51

1- ^{13}C -2-((3,4,5-tris{2-(2-{2-[2-methoxyethoxy]-ethoxy}-ethoxy)-ethoxy})phenylureido}acetic acid (2)

The preparation of compound **2** is similar to the unlabeled analog described in chapter 2. ^1H NMR (CDCl_3): δ = 7.92 (s, 1H, ArNH), 6.77 (s, 2H, ArH), 6.24 (br t, 1H, NHCH₂), 4.12 (m, 6H, ArOCH₂), 3.95 (t, 2H, CH₂C(O)OH), 3.79-3.4 (m, 42 H, OCH₂CH₂O), 3.36 (s, 3H, CH₃), 3.35 (s, 6H, CH₃). ^{13}C NMR (CDCl_3): δ = 172.6 (C(O)OH), satellites: $J_{\text{C-C}} = 59$ Hz), 156.4 (NHC(O)NH), 152.5 (ArC₃), 135.3 (ArC₄), 133.8 (ArC₁), 99.9 (ArC₂), 72.3, 71.9, 71.8, 70.6-70.3, 69.7, 68.7 (OCH₂CH₂O), 59.0 (CH₃), 58.9 (2 x CH₃), 42.0 (d, CH₂C(O)OH, $J_{\text{C-C}} = 59$ Hz). ATR-IR: ν (cm^{-1}) = 3350.1, 2872.3, 1693.0, 1604.6, 1552.5, 1503.7, 1453.4, 1422.2, 1349.5, 1293.4, 1198.4, 1094.7, 994.42, 845.3. HRMS: Calculated mass for $[\text{C}_{35}^{13}\text{CH}_{64}\text{N}_2\text{O}_{18} + \text{H}]^+$: 814.4266, found 814.4245.

4- ^{13}C -3-((3,4,5-tris{2-(2-{2-[2-methoxyethoxy]-ethoxy}-ethoxy)-ethoxy})imidazolidine-2,4-dione (9)

The crude reaction mixture of ester **6** was washed with 1 M KHSO₄ (2 times 20 mL) and 1 M NaOH (aq) (2 times 20 mL). After the organic phase was dried using MgSO₄ and evaporated in vacuo, ^1H NMR indicated that over 70% of the ester had converted into the hydantoin. Column chromatography (flash silica, dichloromethane/methanol 95/5 v.v. to 90/10 v.v.) was performed to obtain pure **7** (40%). ^1H NMR (CDCl_3): δ = 6.65 (s, 2H, ArH), 6.48 (d, 1H, NH), 4.12 (m, 6H, ArOCH₂), 4.09 (d, 2H, CH₂NH), 3.85-3.44 (m, 42 H, OCH₂CH₂O), 3.37 (s, 9H, CH₃). ^{13}C NMR (CDCl_3): δ = 170.5 (C₄(O)), 157.2 (d, C₂(O), $^2J_{\text{C-C}} = 11$ Hz), 152.7 (ArC₃'), 138.2 (ArC₄'), 126.8 (ArC₁'), 106.4 (ArC₂'), 76.7, 72.4, 71.9, 70.8-70.4, 69.6, 68.9 (OCH₂CH₂O), 59.0 (CH₃), 46.4 (d, CH₂NH, $J_{\text{C-C}} = 48$ Hz). ATR-IR: ν (cm^{-1}) = 3292.8, 2871.4, 1769.0, 1690.1, 1596.2,

1504.3, 1436.8, 1348.6, 1294.4, 1240.7, 1199.7, 1094.0, 944.7, 848.0. HRMS: Calculated mass for $[\text{C}_{35}^{13}\text{CH}_{62}\text{N}_2\text{O}_{17} + \text{H}]^+$: 796.4160; Found 796.4157.

4.6 APPENDIX

We can look at the equilibrium of free guest (G_f) with a free binding site (bs_f) to form a guest bound (G_b) at an individual binding site in the dendrimer:

$$K_C = [G]_b/[G]_f[bs]_f$$

The total amount of guest and dendrimer host (D) is known, but the number of binding sites (n) is not. We assume 1:1 binding of a guest and a binding site, so $[bs]_b = [G]_b$:

$$[G]_f + [G]_b = [G]_t$$

$$[bs]_f + [G]_b = n[D]_t$$

In the experiment, we vary the amount of host and keep the amount of guest constant, so we will use as a variable the equivalents of guest per host (x):

$$x = [G]_t/[D]_t$$

Using for the fractions of bound and free guest: $p_b = [G]_b/[G]_t$, and $p_f = 1 - p_b$, we get:

$$K_C = p_b/\{(1-p_b)(n/x-p_b)[G]_t\}$$

Solving for p_b we get:

$$p_b = \frac{1}{2}(1+n/x+1/K_C[G]_t) - \frac{1}{2}\sqrt{\{(1+n/x+1/K_C[G]_t)^2 - 4n/x\}}$$

With this equation the chemical shift ($\delta = p_b\delta_b + p_f\delta_f$) can be expressed as a function of the number of equivalents of guest **2** added to host **1e** (x). Fitting this equation to the measured values with a non-linear least-squares fit results in the fit shown in figure 6a.

For guest **3**, exchange is slow on the NMR timescale and therefore the fraction of bound and free guest can be obtained from the related peak areas. The same formulas are valid for guest **3**, so

$$K_p = p_b/\{(1-p_b)(n/x-p_b)[G]_t\}$$

Fitting this equation to the measured values results in the fit shown in figure 4.11.

4.7 REFERENCES

- 1 F. Bloch, W. W. Hansen, M. Packard, *Phys. Rev.* **1946**, *69*, 127.
- 2 E. M. Purcell, H. C. Torrey, R. V. Pound, *Phys. Rev.* **1946**, *69*, 37-38.
- 3 M. Chai, Y. Niu, W. J. Youngs, P. L. Rinaldi, *J. Am. Chem. Soc.* **2001**, *123*, 4670-4678.
- 4 M. Chai, Z. Pi, C. Tessier, P. L. Rinaldi, *J. Am. Chem. Soc.* **1999**, *121*, 273-279.
- 5 K. T. Welch, S. Arevalo, J. F. C. Turner, R. Gomez, *Chem. Eur. J.* **2005**, *11*, 1217-1227.
- 6 A. D. Meltzer, D. A. Tirrell, A. A. Jones, P. T. Inglefield, D. M. Hedstrand, D. A. Tomalia, *Macromolecules* **1992**, *25*, 4541-4548.
- 7 J. F. G. A. Jansen, E. M. M. de Brabander van den Berg, E. W. Meijer, *Science* **1994**, *266*, 1226-1229.
- 8 D.-L. Jiang, T. Aida, *J. Am. Chem. Soc.* **1998**, *120*, 10895-10901.
- 9 S. Hecht, J. M. J. Fréchet, *J. Am. Chem. Soc.* **1999**, *121*, 4084-4085.
- 10 H.-J. van Manen, R. H. Fokkens, N. M. M. Nibbering, F. C. J. M. van Veggel, D. N. Reinhoudt, *J. Org. Chem.* **2001**, *66*, 4643-4650.
- 11 J. D. Epperson, L.-J. Ming, G. R. Baker, G. R. Newkome, *J. Am. Chem. Soc.* **2001**, *123*, 8583-8592.
- 12 G. J. M. Koper, M. H. P. van Genderen, C. Elissen-Roman, M. W. P. L. Baars, E. W. Meijer, M. Borkovec, *J. Am. Chem. Soc.* **1997**, *119*, 6512-6521.
- 13 F. Zeng, S. C. Zimmerman, *Chem. Rev.* **1997**, *97*, 1681-1712.
- 14 M. Pons, O. Millet, *Prog. Nucl. Magn. Reson. Spectrosc.* **2001**, *38*, 267-324.
- 15 Y. Cohen, L. Avram, L. Frish, *Angew. Chem. Int. Ed.* **2005**, *44*, 520-554.
- 16 M. W. P. L. Baars, A. J. Karlsson, V. Sorokin, B. F. W. De Waal, E. W. Meijer, *Angew. Chem. Int. Ed.* **2000**, *39*, 4262-4265.
- 17 C. Reichardt, *Solvents and Solvent Effects in Organic Chemistry*, 3rd ed., WILEY-VCH Weinheim Germany, **2003**.
- 18 G. M. Barrow, *J. Am. Chem. Soc.* **1956**, *78*, 5802-5806.
- 19 G. M. Barrow, E. A. Yerger, *J. Am. Chem. Soc.* **1954**, *76*, 5248-5249.
- 20 G. M. Barrow, E. A. Yerger, *J. Am. Chem. Soc.* **1954**, *76*, 5211-5216.
- 21 G. M. Barrow, E. A. Yerger, *J. Am. Chem. Soc.* **1954**, *76*, 5247-5248.
- 22 G. M. Barrow, *J. Am. Chem. Soc.* **1958**, *80*, 86-88.
- 23 E. A. Yerger, G. M. Barrow, *J. Am. Chem. Soc.* **1955**, *77*, 4474-4481.
- 24 E. A. Yerger, G. M. Barrow, *J. Am. Chem. Soc.* **1955**, *77*, 6206-6207.
- 25 D. F. DeTar, R. W. Novak, *J. Am. Chem. Soc.* **1970**, *92*, 1361-1365.
- 26 K. Manabe, K. Okamura, T. Date, K. Koga, *J. Am. Chem. Soc.* **1992**, *114*, 6940-6941.
- 27 K. Manabe, K. Okamura, T. Date, K. Koga, *J. Org. Chem.* **1993**, *58*, 6692-6700.
- 28 K. Manabe, K. Okamura, T. Date, K. Koga, *J. Am. Chem. Soc.* **1993**, *115*, 5324-5325.
- 29 S. P. Zingg, E. M. Arnett, A. T. McPhail, A. A. Bothner-By, W. R. Gilkerson, *J. Am. Chem. Soc.* **1988**, *110*, 1565-1580.
- 30 E. Yashima, K. Maeda, Y. Okamoto, *Nature* **1999**, *399*, 449-451.
- 31 K. Morino, N. Watase, K. Maeda, E. Yashima, *Chem. Eur. J.* **2004**, *10*, 4703-4707.
- 32 Y. Kamikawa, T. Kato, H. Onouchi, D. Kashiwagi, K. Maeda, E. Yashima, *J. Polym. Sci., Part A : Polym. Chem.* **2004**, *42*, 4580-4586.
- 33 H. Onouchi, D. Kashiwagi, K. Hayashi, K. Maeda, E. Yashima, *Macromolecules* **2004**, *37*, 5495-5503.
- 34 K. Maeda, K. Morino, Y. Okamoto, T. Sato, E. Yashima, *J. Am. Chem. Soc.* **2004**, *126*, 4329-4342.

- 35 P. M. Tolstoy, P. Schah-Mohammedi, S. N. Smirnov, N. S. Golubev, G. S. Denisov, H.-H. Limbach, *J. Am. Chem. Soc.* **2004**, *126*, 5621-5634.
- 36 D. L. Holmes, D. A. Lightner, *Tetrahedron* **1995**, *51*, 1607-1622.
- 37 D. L. Holmes, D. A. Lightner, *Tetrahedron* **1996**, *52*, 5319-5338.
- 38 D. P. Cistola, D. M. Small, J. A. Hamilton, *J. Lipid Res.* **1982**, *23*, 795-799.
- 39 R. E. London, *J. Magn. Reson.* **1980**, *38*, 173-177.
- 40 K. Vercruyssen, C. Dejugnat, A. Munoz, G. Etemad-Moghadam, *Eur. J. Org. Chem.* **2000**, 281-289.
- 41 K. Chruszcz, M. Baranska, K. Czarniecki, L. M. Proniewicz, *J. Mol. Struct.* **2003**, *651-653*, 729-737.
- 42 K. Moedritzer, *Inorg. Chem.* **1967**, *6*, 936-939.
- 43 R. P. Carter, Jr., M. M. Crutchfield, R. R. Irani, *Inorg. Chem.* **1967**, *6*, 943-945.
- 44 The spectral timescale represents the inverse width of the NMR spectrum, measured in frequency units. The chemical shift difference between free and bound guest corresponds to 390 Hz (3.1 ppm), which results in a spectral timescale of 2.6 ms. M. H. Levitt, *Spin Dynamics*, John Wiley & Sons, 2002, p. 485.
- 45 J. Sandström, *Dynamic NMR Spectroscopy*, Academic press, **1982**.
- 46 The chemical shift difference of 1315 Hz corresponds to a spectral timescale of 0.76 ms.
- 47 M. Pittelkow, C. B. Nielsen, M. A. C. Broeren, J. L. J. van Dongen, M. H. P. van Genderen, E. W. Meijer, J. B. Christensen, *Chem. Eur. J.* **2005**, *11*, 5126-5135.
- 48 A. W. Bosman, H. M. Janssen, E. W. Meijer, *Chem. Rev.* **1999**, *99*, 1665-1688.
- 49 E. R. Gillies, J. M. J. Fréchet, *J. Org. Chem.* **2004**, *69*, 46-53.
- 50 C. S. Johnson, Jr., *Prog. Nucl. Magn. Reson. Spectrosc.* **1999**, *34*, 203-256.
- 51 D. Wu, A. Chen, C. S. Johnson, Jr., *J. Magn. Res. A* **1995**, *115*, 260-264.
- 52 M. D. Pelta, H. Barjat, G. A. Morris, A. L. Davis, S. J. Hammond, *Magn. Reson. Chem.* **1998**, *36*, 706-714.
- 53 E. O. Stejskal, J. E. Tanner, *J. Chem. Phys.* **1965**, *42*, 288-292.

Chapter 5

Supramolecular dendritic architectures in water*

ABSTRACT: *A supramolecular synthesis has been developed, resulting in stable, dendrimer-based assemblies in water. In this methodology, water-soluble oligoethylene glycol guests are used to solubilize the hydrophobic urea-adamantyl dendrimer in water. These aggregates can only be obtained by preorganization of the complex in chloroform prior to dissolving the architectures in water. NMR experiments confirm that the dendrimer is solubilized by the guests, and that guest and host are in close proximity of each other. Preliminary cryo-TEM and light scattering experiments show that the dendrimers are aggregated, and are not present as single entities solubilized by oligoethylene glycol guests. For carboxylic acid oligoethylene glycol guest 2, sphere-like micelles are obtained at a guest/host ratio of 32, which change into rod-like micelles when the guest/host ratio is increased to 64 and 128. Static and dynamic light scattering experiments confirm the formation of sphere-like micelles, but the sample preparation appears to have a strong influence on the outcome of the structures formed. For phosphonic acid oligoethylene glycol guest 3, disk-like micelles are observed next to sphere-like micelles at a guest/host ratio of 32, which also change into rod-like micelles at a guest/host ratio of 64 and 128. ^{13}C and ^{31}P NMR experiments cannot be used to quantify the binding of guests to the urea-adamantyl dendrimer, but do show that binding to the dendritic scaffold takes place. The NMR measurements also show that exchange can take place between carboxylic and phosphonic acid guests, and that mixed aggregates can be formed. Preliminary dialysis experiments confirm this behavior. NMR experiments also show that it is possible to assemble a functional peptide guest to the dendrimer. Like in chloroform, it should be possible to assemble several functional guest molecules simultaneously to the dendritic scaffold. These results bring the goal of a multicomponent, dynamic library a step closer to reality.*

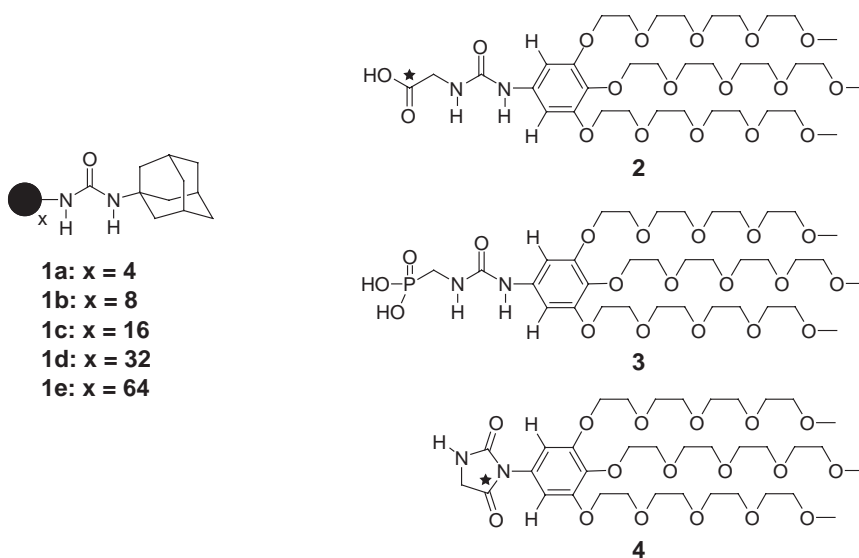
* Part of this work has been published: M.A.C. Broeren, J.G. Linhardt, H. Malda, B.F.M. de Waal, R.M. Versteegen, J.T. Meijer, D.W.P.M. Löwik, J.C.M. van Hest, M.H.P. van Genderen, E.W. Meijer, *J. Polym. Sci., Part A: Polym. Chem.*, accepted for publication.

5.1 INTRODUCTION

The unique properties of dendrimers, such as their well-defined molecular weight, globular architecture and multivalent nature, have made them promising scaffolds for medicinal applications.¹⁻³ Apart from the possibility to attach several drug molecules, imaging agents, targeting groups and solubilizing groups to the periphery of dendrimers in a controlled manner, dendrimers can encapsulate small guest molecules in their interior.⁴⁻⁶ This has made them possible candidates as carriers in drug delivery and gene therapy applications.

The number of supramolecular dendritic architectures in aqueous media is limited though.⁷⁻¹³ This is mainly due to a decrease in strength of hydrogen bonds and electrostatic interactions in polar media. The more polar the solvent is, the weaker the electrostatic interactions and hydrogen bonding due to competitive solvation of the donor and acceptor sites with solvent molecules.¹⁴ Therefore, the formation of stable aggregates in water can be enhanced by combining hydrogen bonds with additional non-covalent interactions like metal coordination, salt bridges, hydrophobic interactions or π - π interactions.

In this chapter, the preparation and analysis of the dendritic host-guest complexes in water is described, using oligoethylene glycol guests **2** and **3** (Scheme 5.1). Hydantoin **4** is used in a control experiment.

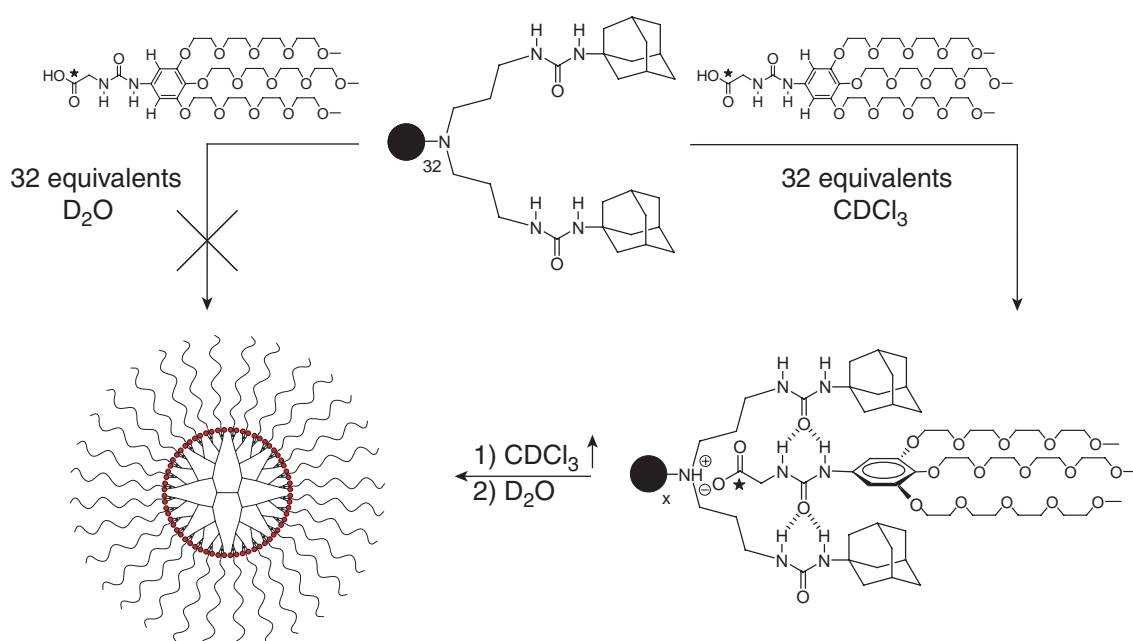


Scheme 5.1 The molecules used in this study.

In section 5.2 the supramolecular synthesis to obtain stable aggregates in water is described. This is a delicate process, since the interactions between dendrimer and guest are very sensitive to water. Preliminary cryogenic transmission electron microscopy (cryo-TEM) and light scattering experiments have been performed to get insights into the structure of the aggregates. The complexation of guests to the dendritic host has been analyzed with ^{13}C and ^{31}P NMR. The synthesis of two functional guest molecules is described, and the binding of these guests with the dendrimer aggregates in water has been investigated.

5.2 THE PREPARATION OF SUPRAMOLECULAR DENDRITIC ARCHITECTURES IN WATER

In chloroform the dendritic host–guest complexes have been prepared by simply mixing the urea–adamantyl dendrimer with the guest molecule of choice. In some cases, e.g. the cyanobiphenyl guest described in chapter 4, the guest molecule itself was not soluble in chloroform, but could be solubilized by means of complexation when it was added to the dendrimer in solution. In water however, the urea–adamantyl dendrimer is not soluble, and consequently water–soluble guests are required to solubilize the dendrimer. Unfortunately, all attempts to form a water–soluble complex by directly mixing the urea–adamantyl dendrimer in water with oligoethylene glycol guest **2** failed (Scheme 5.2, left).



Scheme 5.2 Schematic representation of two possible routes to supramolecular dendritic architectures in water. The addition of any water-soluble guest to the 5th generation urea–adamantyl dendrimer in water (left) does not result in solubilization of the dendrimer. When the complex is preorganized in chloroform (right) prior to the addition of water, a clear solution is obtained. In the ideal case, single dendrimer aggregates are formed in water (cartoon).

Apparently the water–soluble guest molecules are not able to pull the hydrophobic dendrimer into solution. When other water–soluble guests were used, like oligopeptide and carbohydrate guests, a similar result was obtained. When dendrimer **1e** and guest **2** are dissolved in a minimal amount of THF, and the solution is injected in water, some solubilization occurs. However, this method appears to give irreproducible results and partial precipitation of the dendrimer. In another approach, the periphery of the dendrimer was modified with hydrophilic groups, thus making it water–soluble. A clear solution was obtained, but no complexation could be observed with water–soluble guests. This was most likely due to the interference of water with the electrostatic and hydrogen bonding interactions that dictate binding between guest and host. Apparently, hydrophobic interactions are

required to strengthen the interactions between guest and host. These observations led us to conjecture that the urea–adamantyl dendrimer could be solubilized when the complex is formed in chloroform prior to dissolution in water (Scheme 5.2, right). This hypothesis has been tested with oligoethylene glycol guests **2** and **3**, both soluble in chloroform and water. The complexation of guest **2** and **3** to urea–adamantyl dendrimers in chloroform has been investigated in detail with mass spectrometry and NMR in chapter 3 and 4.

A sample containing 32 equivalents of guest **2** added to dendrimer **1e** in 1.5 mL of chloroform has been prepared, with a guest concentration of $1.15 \cdot 10^{-2}$ M. The chloroform was gently evaporated with a stream of air or nitrogen at room temperature. This resulted in a transparent film on the wall of the container. After the addition of 0.5 mL of D₂O and stirring or shaking, a clear solution was obtained (Figure 5.1, inset). When the chloroform is evaporated too quickly, e.g. on a rotavap and at elevated temperature, partial precipitation of the dendrimer will occur when the water is added. ¹H NMR of this solution shows not only the oligoethylene glycol signals of the guest, but also the adamantyl signals of the dendrimer between 1.5 and 2 ppm (the dendrimer by itself is not water–soluble). This clearly demonstrates that the hydrophylic oligoethylene glycol guests solubilize the dendrimer in water, but the complex needs to be preorganized in chloroform in order to be transferred to D₂O.

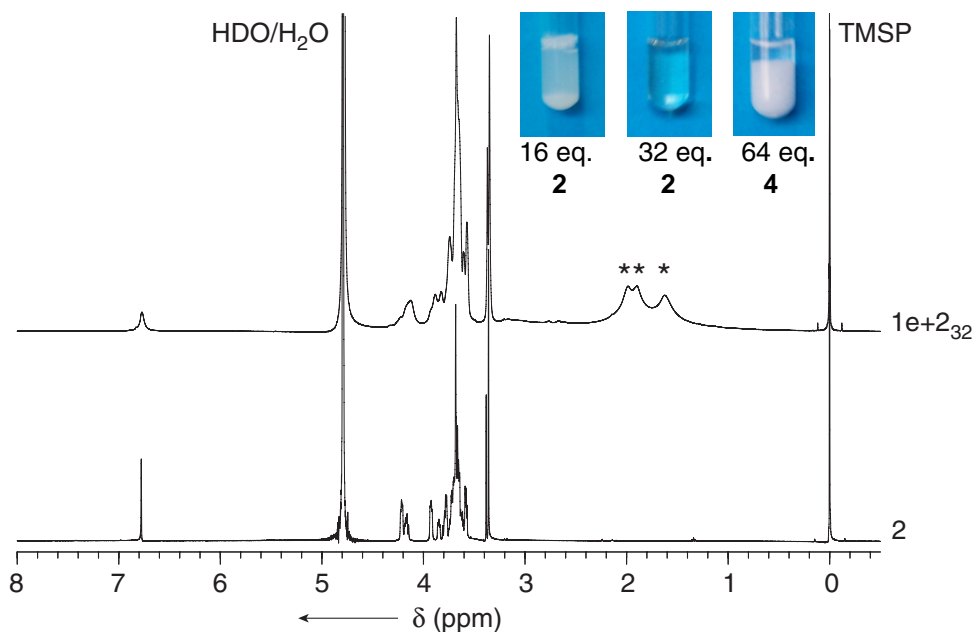


Figure 5.1 ¹H NMR spectra of guest **2** and the complex **1e+2₃₂** in D₂O. The adamantyl signals of the dendrimer are indicated (*). The inset shows three samples containing complexes of **2** (16 and 32 equivalents) and **4** (64 equivalents) with dendrimer **1e**. The concentration of guest is kept constant at $3.46 \cdot 10^{-2}$ M.

In order to determine the amount of guest necessary to solubilize the dendrimer, complexes were prepared with lower ratios of guest to dendrimer. It was determined that when going from 28 to 24 equivalents of guest **2**, the aqueous solution started to become more turbid, and at 16 equivalents of guest the dendrimer clearly precipitated. This means that approximately 26 guest molecules are

necessary to solubilize the dendrimer. Below this number, the hydrophobic parts of the dendrimer aggregate, resulting in larger structures and eventually in precipitation. As a control experiment, the hydantoin guest molecule **4** was added to the dendrimer and the same procedure for complex formation was applied. Immediate precipitation of the dendrimer was observed in D₂O, even when 64 equivalents of **4** were added, indicating that the ureido acetic acid headgroup is necessary for binding in water (Figure 5.1, inset).

¹H-¹H NOESY spectroscopy of the complex in D₂O reveals that guest **2** and dendrimer **1e** are in close proximity of each other, which can be observed from the many cross peaks between the oligoethylene glycol tails and the adamantyl signals of the dendrimer (Figure 5.2). Interestingly, also a small cross peak is observed between the aromatic protons of the guest and the adamantyl groups, which is an indication that the head groups of the guests are located near the periphery of the dendrimer.

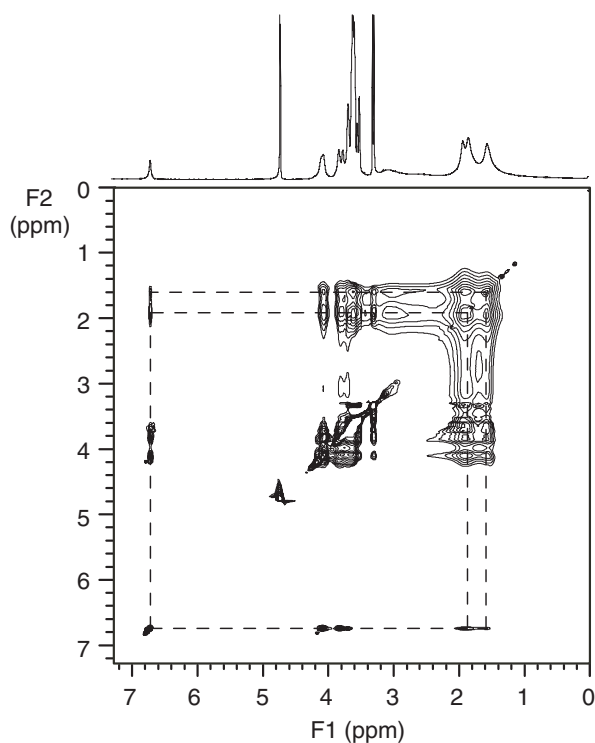


Figure 5.2 ¹H-¹H NOESY spectrum of **1e**+**2**₃₂ in D₂O. The peak at 6.8 ppm corresponds to the aromatic protons of **5**. The signals between 1 and 2 ppm correspond to the adamantyl protons of the dendrimer.

Furthermore, ¹H DOSY NMR shows that guest **2** forms a complex with dendrimer **1e** in water. The CH₃-signals of the oligoethylene glycol tails of guest **2** form two sharp singlets in ¹H NMR at 3.4 ppm, and these signals has been used to determine the diffusion constant of guest **2** using the bipolar pulsed gradient stimulated echo (BPPSTE) pulse sequence. The apparent diffusion constant has been calculated with the Stejskal-Tanner equation:

$$\ln\left(\frac{I}{I_0}\right) = -(\gamma G \delta)^2 D \left(\Delta - \frac{\delta}{3}\right) = -kD \quad (5.1)$$

where I and I_0 are the signal intensities with and without the gradients, γ is the gyromagnetic ratio, G the gradient strength, δ the gradient pulse duration, Δ the diffusion delay, and D the diffusion constant. The apparent diffusion constant D is generally determined as the slope of the linear plot of $\ln(I/I_0)$ versus k , where k is equal to $(\gamma G \delta)^2(\Delta - \delta/3)$. In case of supramolecular structures where the exchange is fast on the NMR timescale, an average diffusion constant is obtained.¹⁵ The plot of the echo-attenuation $\ln(I/I_0)$ versus k for guest **2** in D_2O gives a diffusion constant of $2.9 \cdot 10^{-10} \text{ m}^2/\text{s}$ (Figure 5.3). The diffusion constant of guest **2** in **1e+2₃₂** is significantly lower: $1.1 \cdot 10^{-10} \text{ m}^2/\text{s}$. This indicates that guest **2** binds to dendrimer **1e**, and as a result diffuses slower. When G/H is increased to 128, the diffusion constant of guest **2** is $1.7 \cdot 10^{-10} \text{ m}^2/\text{s}$, which is in between the values for the diffusion constants of free **2** and **2** in **1e+2₃₂**. As the value is an average value, the results suggest that most guests bind to the dendrimer at $G/H = 32$, and that a significant amount of guest is free at $G/H = 128$.

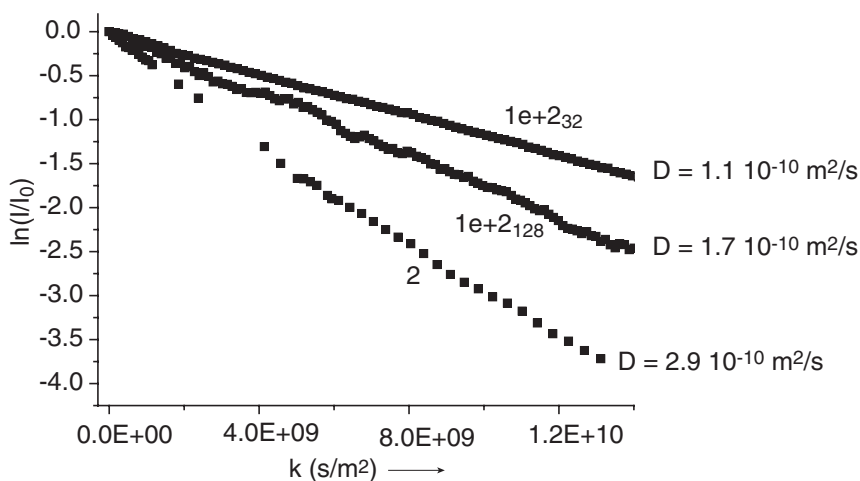


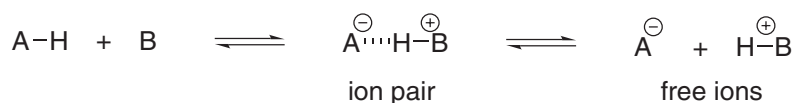
Figure 5.3 Plot of the echo attenuation $\ln(I/I_0)$ versus k for **2**, **1e+2₃₂** and **1e+2₁₂₈**. The diffusion constants are indicated.

Guest **3** is also able to solubilize dendrimer **1e** in water, but surprisingly more than 32 equivalents are required to obtain a completely clear solution. Moreover, complexation appears to give less reproducible results. At a guest/host ratio of 32, a milky, gel-like solution is obtained. When G/H is increased to 48, the solution is still not completely clear, but at $G/H = 64$ it is clear. This observation could indicate that in water the binding strength between guest **2** and dendrimer **1e** is stronger than the binding between guest **3** and dendrimer **1e**, opposite to the binding strengths of both guests in chloroform. It might also be so that the transfer from bulk to aqueous solution is more difficult for the complex of **1e+3₃₂**, which is more viscous in the solid state.

In order to get insights into the stability of the dendritic architectures in water, the influence of ionic strength and pH in water has been examined for complexes of both guest **2** and **3** with dendrimer **1e**. This is discussed in the next section.

5.3 STABILITY OF THE AGGREGATES

In chloroform, the solvent molecules do not participate in acid–base interactions. When an acid–base reaction takes place, a tight ion pair is formed, and this, together with the hydrogen bonding interactions, is the basis for the complexation between a guest and host. Water behaves completely different. First of all, water participates in the acid–base reaction, resulting in a change in the pH. Furthermore, the acid and base can be present in solution as free ions due to solvation of the charges of the deprotonated acid and protonated base (Scheme 5.3).¹⁴ Solvation also allows inorganic salts to dissolve in water, giving rise to a change in the ionic strength of the solvent.



Scheme 5.3. Depending on the polarity of the solvent, acid–base reactions result in ions present in solution as ion pairs or free ions. In chloroform, a tight ion pair is formed. In water, the equilibrium is shifted towards free ions due to solvation of the charges.

In case of the dendritic host–guest complexes in water, the interaction between guest and host cannot be described by the general equilibrium described in scheme 5.3. The dendrimer does not dissolve in water at all, even when water is acidified and heated. This means that the bare dendrimer is not participating in an acid–base reaction with the solvent. The question arises to what extent the basic interior of the dendrimer is capable of being protonated by the water molecules at all. It might be so that due to the hydrophobic, bulky adamantyl groups the interior of the dendrimer is a confined area shielded from water molecules. For water–soluble dendrimers, it is known that the dendritic interior is very basic.²⁸ Amphiphilic dendrimers with palmitoyl chains are very flexible, and refold in such a way that the dendrimer core is exposed to the water, also resulting in protonation. As a result of this flexibility, palmitoyl-modified poly(propylene imine) dendrimers can self-assemble at an air–water interface when the Langmuir technique is applied (see also chapter 1).¹⁶ It is not possible to form well-defined monolayers with adamantyl dendrimers, as the bulky end-groups hamper the dendrimer to effectively change its conformation.

If the bare dendrimer, as well as the solubilized dendrimer, do not participate in acid–base reactions with water, the guests primarily determine the pH of the solution. This has been confirmed by a pH measurement in water of a sample of **1e+3**₃₂. Although 62 tertiary amines are present versus 32 carboxylic acid groups, the solution is acidic (Table 5.1). If the dendrimer (D) does not participate in acid–base reactions (equation 5.4), equation 5.2 and 5.3 can be used to describe the system. In this model, it is assumed that the acid guest only binds to the dendrimer in its neutral form, so it uses proton on the acid (HA).



The influence of pH and ionic strength on the stability of three dendritic host guest–guest complexes has been investigated (Table 5.1). First, the pH of guest **2** and **3** in demineralized water was determined. The pKa values for the first and second deprotonation step of phosphonic acids lie around 1 and 7. The pKa of carboxylic acids lies around 4–5. The first phosphonic acid is clearly more acidic than the carboxylic acid group, and this is reflected in the lower pH found for guest **3**.

Table 5.1 Influence of ionic strength and pH on the dendritic aggregates in water.

Sample	Conc. host (M)	Conc. guest (M)	Starting pH	Stable pH-range ^a	Maximum NaCl conc. (M)
2	-	1.23·10 ⁻²	3.1	-	-
3	-	1.18·10 ⁻²	2.3	-	-
1e+2₃₂	3.69·10 ⁻⁴	1.23·10 ⁻²	4.4	2.2–4.8	0.017
1e+2₆₄	1.84·10 ⁻⁴	1.23·10 ⁻²	3.8	2.2–4.9	0.020
1e+3₆₄	1.92·10 ⁻⁴	1.18·10 ⁻²	3.6	2.2–6.1	0.004

^a No measurements have been performed below pH = 2.2. The complexes might still be stable under more acidic conditions.

In the comparison between the free guests and the complexes, the concentration of guest has been kept constant. As stated above, the pH of 4.4 for sample **1e+2₃₂** indicates that the pH is largely determined by the guest. The higher pH of **1e+2₃₂** can be explained by the lower effective concentration of **2** free in solution as it is partly bound to the dendrimer and therefore not able to affect the pH of the solution. At a guest/host ratio of 64, the pH is lower as more free guest **2** is able to protonate the solvent. For **1e+3₆₄**, the pH of the solution is somewhat lower.

When droplets of pure acetic acid are added to the complexes, the pH of the solution is lowered, but the solutions remain clear. After 0.5 mL of acetic acid, the pH reaches a value of 2.2, and does not change any more when more acetic acid is added. No precipitation of the dendrimer occurs, indicating that the complexes are stable in this pH regime. When the pH is lowered with a stronger acid, the dendrimers will probably precipitate as the salt with the acid.

When the pH of the starting solutions is increased with a diluted ammonia solution, precipitation occurs rapidly. Complex **1e+2₃₂** and **1e+2₆₄** start to precipitate above a pH of 5. Complex **1e+3₆₄** is slightly more tolerant towards base, and precipitates around a pH of 6.1. Clearly, the complexes are tolerant to acid, but sensitive towards base.

Based on the model described in the beginning of this section, the results can possibly be explained by the influence of the pH on the concentration of protonated acid HA. When the pH is lowered, equation 5.2 states that the concentration of HA increases. HA can bind to the solubilized dendrimer, or can remain free in solution, but this does not influence the dendritic host–guest complex. When the pH is increased, more HA is converted into A^- . According to equation 5.3, this results in a withdrawal of HA guests from the dendritic host–guest complex. Eventually, this results in aggregation of the dendrimers, and precipitation. Actually, the pH values at which the complexes start to precipitate come close to the pKa values of the acidic guests.

The complexes seem to be very sensitive to the ionic strength of the solution. When small amounts of sodium chloride are added, all complexes precipitate at a sodium chloride concentration of 0.02 M. The complex with phosphonic acid guest **3** seems to be particularly sensitive to the addition of sodium chloride, and already starts to precipitate at a concentration of 0.004 M. It is not clear at the moment why the complexes are so sensitive towards ions. Perhaps the electrostatic interaction between the guest and the dendrimer are interfered by the ions. Another explanation might be found in the possible binding of cations to the deprotonated acids. Especially phosphonic acids are known to coordinate to cations. This might result in a shift in the equilibrium of equation 5.2 to the right, resulting in a decrease of free acid, and hence in precipitation.

From these results can be concluded that the stability of the aggregates is strongly influenced by pH and ionic strength. Possible explanations are given, but several assumptions are made. More studies are necessary to investigate the factors that influence the stability of these complexes. This can only be done if it is known what kind of aggregates are present in solution, which is discussed in the following section.

5.4 THE STRUCTURE OF DENDRITIC HOST–GUEST COMPLEXES IN WATER

The urea–adamantyl dendrimers have a good solubility in chloroform, and DLS measurements have shown that both the dendrimer and the dendritic host–guest complexes are present as single dendrimer species in chloroform. In water, this is not necessarily the same. It is known that amphiphilic poly(propylene imine) dendrimers can aggregate in aqueous solution, resulting in all kinds of micellar or vesicular architectures.^{1, 10, 13, 16} The shape and size of the dendritic aggregates in water have been investigated using light scattering and cryogenic transmission electron microscopy (cryo-TEM) experiments.

In cryo-TEM, aqueous samples are vitrified in liquid ethane prior to TEM analysis. By this way of fixation, the specimen under investigation remains in its native state, providing a “true vision” of the suspended material as it was in solution.¹⁷ A critical step in cryo-TEM involves the sample preparation. Preparation of thin films in a temperature- and humidity-controlled environment

is essential to prevent artifacts introduced by temperature and osmotic pressure.¹⁸ This, and other advances in cryo-TEM have had a great impact on colloidal chemistry. Also in the field of polymers and dendrimers, cryo-TEM has successfully been applied.^{10, 16, 19-21} The structures of the dendritic guest–host complexes in water, described in the preceding part of this chapter, have been analyzed with cryo-TEM in collaboration with dr. Nico Sommerdijk and the group of dr. Peter Frederik (Maastricht University, Maastricht, The Netherlands).

Figure 5.4a shows a cryo-TEM image of the complex **1e+2₃₂** in water at a guest concentration of $0.82 \cdot 10^{-2}$ M. The picture shows sphere-like micelles with a diameter of 8 ± 2 nm. It is striking to see that the size distribution of the aggregates is very narrow. A cryo-TEM image of pure guest **2** in water at a concentration of $0.82 \cdot 10^{-2}$ M, does not show any aggregates, indicating that the observed aggregates correspond to the dendritic host–guest structures. The diameter of a fifth generation adamantyl dendrimer is roughly 5 nm.¹ Though the oligoethylene glycol tails of guest **2** should give rise to a bigger complex, the observed dimensions suggest that the dendrimers are present as small clusters of dendrimers surrounded by oligoethylene glycol guests, schematically depicted in figure 5.4c.

A sample of **1e+2₁₂₈** at a guest concentration of $3.28 \cdot 10^{-2}$ M was prepared to investigate whether smaller aggregates can be obtained when the guest/host ratio is increased, while keeping the dendrimer concentration constant. Interestingly, figure 5.4b shows that rod-like structures are present, next to sphere-like structures. The diameter of the rods is around 6 ± 1 nm, which comes close to the diameter of a single dendrimer. The spheres are somewhat bigger, around 8 nm in diameter. A sample of guest **2** in water at a concentration of $3.28 \cdot 10^{-2}$ M shows micelles with a diameter of approximately 3 nm. This again implies that the rod-like aggregates correspond to the dendritic host–guest complexes. A possible arrangement is schematically depicted in figure 5.4d. A sample with a guest/host ratio of 64 gave similar results. Why larger instead of smaller aggregates are formed is unclear so far. In order to study this in more detail, light scattering experiments have been performed.

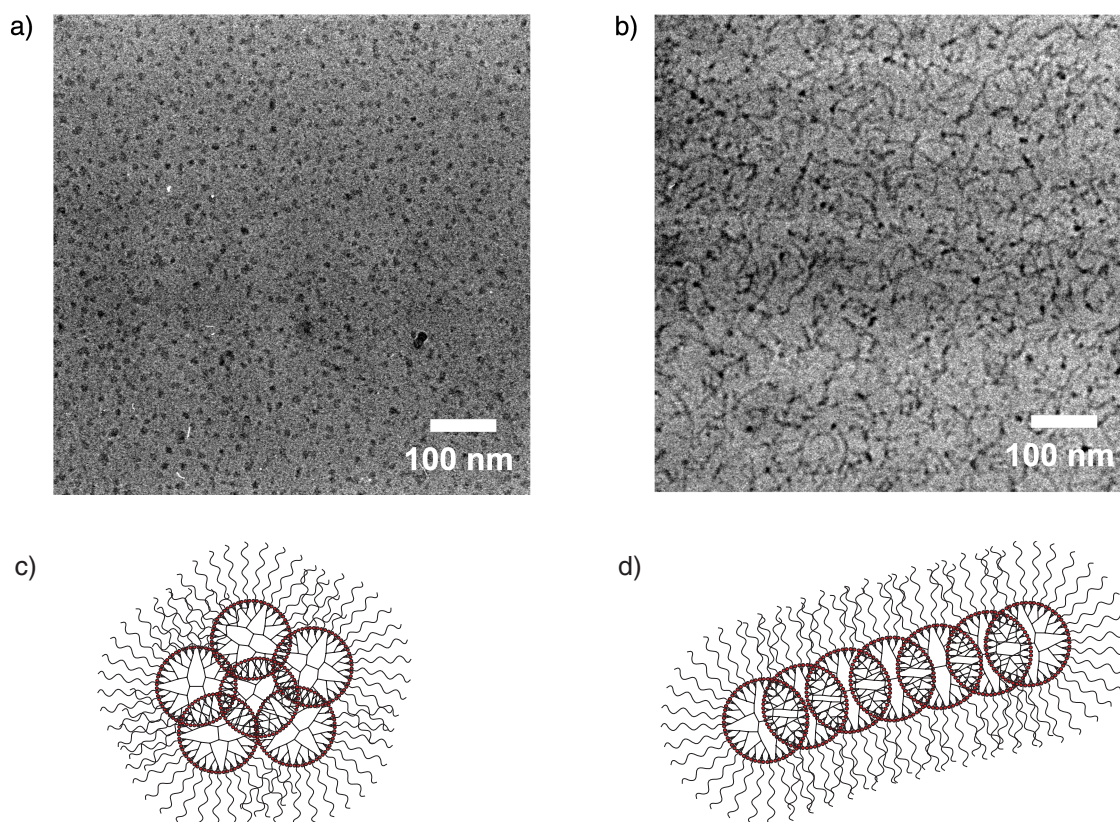


Figure 5.4 Top: Cryo-TEM images of a sample of $1e+2_{32}$ (a) and $1e+2_{128}$ (b) in water, showing the dendrimer aggregates. Bottom: Proposed structures of the globular aggregates observed for $1e+2_{32}$ (c) and the rod-like aggregates observed for $1e+2_{128}$ (d).

Several complexes of **1e** and **2** have been investigated with static and dynamic light scattering. In static light scattering (SLS), the mean scattering intensity is measured under a number of angles between 10° and 150° . In a plot of the average scattering intensity R_w/c as a function of the scattering vector q , the slope of the graph at high q values relates to the shape of the aggregate (Table 5.1).

Table 5.1 Correlation between the slope of R_w/c vs. q at high q values and the aggregate structure in solution.

Structure	Slope
Rigid rod	-1
Chain with excl. vol.	-5/3
Linear Gaussian chain	-2
Swollen branched chain	-2
Smooth 2D objects	-2
Gauss. Chain randomly branched	-16/7
Fractal surface	-3 to -4
3D objects smooth surface	-4

When a plateau is observed at low q -values, the whole aggregate structure can be resolved, meaning that the overall size and molar mass of the particle can be determined from the intensity.

Figure 5.5 shows the SLS results of three complexes of **1e** and **2** with a guest/host ratio of 34, 55 and 79 and a guest concentration around $1.4 \cdot 10^{-2}$ M. No plateau is observed at low q values, indicating that the observed structures are too large to be completely resolved ($> 1 \mu\text{m}$). Hence, no unambiguous information on the overall size and molar mass of the aggregates can be obtained from SLS. The slope at high q -values is -3 in all cases, corresponding to a fractal network.

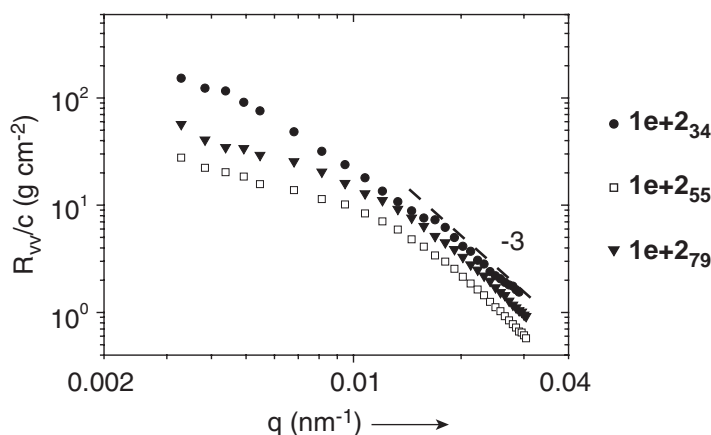


Figure 5.5. Plot of R_w/c versus q for **1e+2₃₄**, **1e+2₅₅** and **1e+2₇₉**. At low q -values no plateau is observed. At high q -values a slope of -3 is found in all cases.

The static light scattering result of sample **1e+2₃₄** does not agree with the cryo-TEM image, where only globular structures are found for **1e+2₃₂**. The results for **1e+2₅₅** and **1e+2₇₉** come closer to the cryo-TEM results, as they might agree with the rod-like aggregates that have been found for **1e+2₆₄**. The dynamic light scattering experiments performed on these large aggregates confirm what was observed with static light scattering. Only one slow process is observed, corresponding to large aggregates (Figure 5.6) with hydrodynamic radii between 171 and 354 nm. Again, as not the whole structure is resolved, and the aggregates seem to be fractals, these values are difficult to interpret. However, the outcome of the light scattering experiments appears to be highly dependent on the sample preparation. In the above described light scattering measurements, the complexes were kept in chloroform for several days before the solvent was evaporated and water was added. When the guest and host are dissolved in chloroform and the chloroform is immediately removed under a nitrogen flow followed by solubilization in water, dynamic light scattering shows a fast dominant process, corresponding to small particles, next to a slow process corresponding to large particles (Figure 5.6). The guest concentration of this sample was $0.82 \cdot 10^{-2}$ M. The hydrodynamic radius calculated for the small particles results in a value of 5.2 nm, which correlates to a diameter of 10.4 nm for a perfect spherical particle. This value is in slightly bigger than the the aggregate size of 8 ± 2 nm obtained from cryo-TEM. The hydrodynamic radius of the large, fractal structures corresponds to approximately 250 nm.

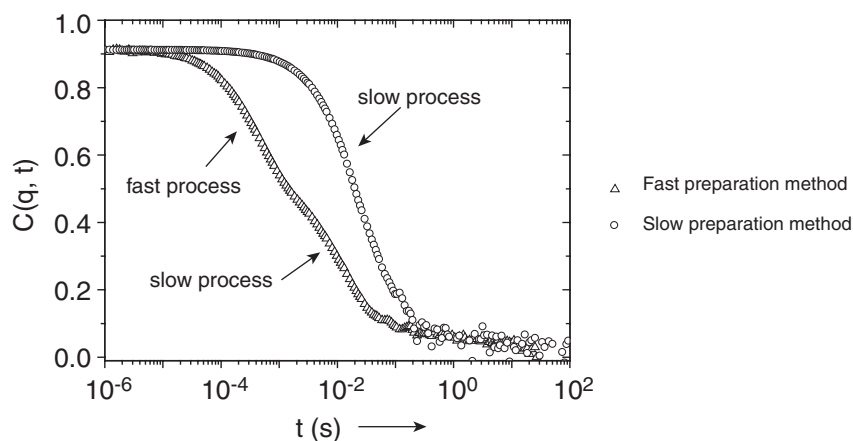


Figure 5.6 DLS spectra showing the influence of the sample preparation on the process that is observed.

It is hard to quantify how much of both aggregates is present in solution. The scattering intensity is proportional to the size of aggregates, meaning that large aggregates can easily dominate the scattering event. This means that if smaller structures, like the single complex, are present in solution they will not or barely be detected by dynamic light scattering due to weak scattering of light relative to the large structures. Therefore, it is very well possible that the large aggregates are only present in 1–5%. In cryo-TEM, the large aggregates are not observed. Much more static and dynamic light scattering experiments will have to be performed in order to determine which parameters influence the structure and size of the aggregates in water.

Complexes of phosphonic acid guest **3** with dendrimer **1e** in water show different aggregates. As has already been explained in the first part of this chapter, the transfer of **1e+3₃₂** from chloroform to water is difficult to achieve, and does not result in a clear but in a milky solution. This suggests that large aggregates are present. Figure 5.7a shows a cryo-TEM image of **1e+3₃₂** in water at a guest concentration of $0.86 \cdot 10^{-2}$ M. Clearly, disc-like aggregates are present with sizes ranging from 30–100 nm together with sphere-like particles with a diameter of 10 ± 2 nm. Some discs are oriented parallel with respect to the surface, observed as disc-like objects with moderate contrast. Others are oriented perpendicular to the surface, and consequently are observed as rod-like structures that correspond to the side of the disks. As the path length of the electron beam through the aggregate is longer in the perpendicular orientation, a stronger contrast is obtained. Several other structures with a tilted orientation with respect to the surface are also observed. When the guest/host ratio is increased to 128 and the dendrimer concentration is kept constant, rod-like micelles are obtained with a diameter of 6 ± 1 nm. These aggregates look completely similar to the aggregates observed for **1e+2₁₂₈**. A cryo-TEM image of guest **3** alone in water shows nothing at a concentration of $1.18 \cdot 10^{-2}$ M, but small micelles of 3 nm at a concentration of $3.53 \cdot 10^{-2}$ M. This indicates that the rod-like aggregates correspond to the dendrimer–guest aggregates. It also shows that the oligoethylene glycol guests aggregate into micelles at higher concentrations, and become visible due to the high local concentration of guest.

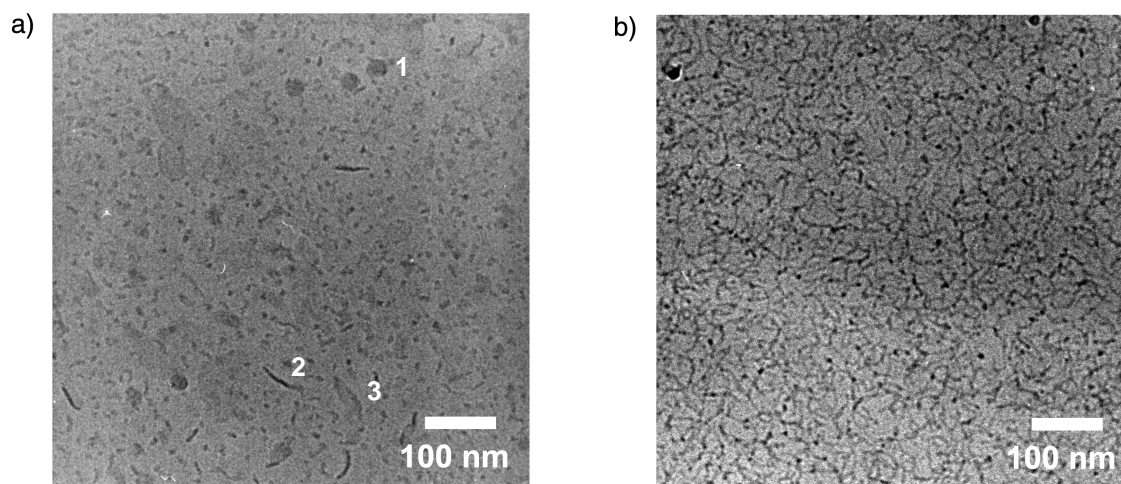


Figure 5.7 a) Cryo-TEM image of $1e+3_{32}$. Disc-like micelles are observed that either lie flat (1), perpendicular (2) or diagonal (3) to the surface. Also sphere-like micelles are observed. b) Cryo-TEM image of $1e+3_{128}$, showing rod-like micelles.

From the cryo-TEM and light scattering experiments it has become clear that the dendrimers are not present in solution as single entities. They are aggregated as globular, disk-like or rod-like assemblies, depending on the guest/host ratio and guest. At this point it is unclear which factors govern the transition from globular to rod-like structures. From literature it is known that many factors can influence this transition.²²⁻²⁷ Keeping the dendrimer concentration constant and increasing the amount of guest also alters the pH of the solution, which becomes more acidic (section 5.3). This might also influence the aggregate structure. As the association of guests and host is concentration dependent, it is possible that the transition between globular architectures and rods is concentration dependent. Measurements of one specific guest/host ratio at different concentrations can give information about this aspect.

Light scattering experiments suggest that the way the complexes are prepared strongly influence the structure in solution. The results clearly show that the solubilization of hydrophobic dendrimers in water is a delicate process, which results in more complicated structures than single dendrimers solubilized by water-soluble guest molecules. With this knowledge in mind, we have investigated to what extent both complexation and exchange of guest molecules to the dendrimer aggregates can be investigated with ^{13}C and ^{31}P NMR.

5.5 ^{13}C NMR AND ^{31}P NMR COMPLEXATION STUDIES IN D_2O

5.5.1 Oligoethylene glycol guests

Although it has been shown that the urea-adamantyl dendrimer forms complicated aggregates in solution, it is still possible to analyze the complexation of guest **2** and **3** to dendrimer **1e** with ^{13}C NMR and ^{31}P NMR. The chemical shift of the ^{13}C -labeled carbonyl group of free **2** in

D₂O is located at approximately 177.7 ppm (Figure 5.8). As an internal standard, sodium-3(trimethylsilyl)propionate-2,2,3,3-d₄ (TMSP) has been used as tetramethylsilane (TMS) is not soluble in water. When sample **1e**+**2**₃₂ in D₂O is analyzed with ¹³C NMR, a downfield shift is observed to 179.8 ppm, and the peak broadens. Complexes of lower guest/host ratio have not been analysed, as precipitation of the dendrimer starts to occur at lower G/H. An increase of G/H to 48, 64, 96 and 128 shows an upfield shift to 178.6. In this process, the peak becomes more narrow again. As we again always observe one signal, we can conclude that exchange is fast on the NMR timescale. As no coalescence effects seem to take place, the exchange is most likely faster in water than in chloroform. Broadening of the signal is most likely due to T₂-relaxation.

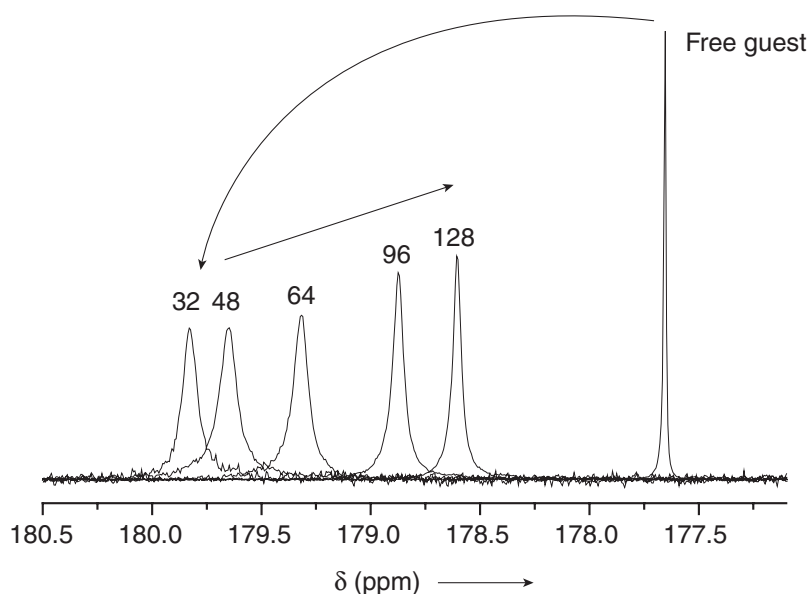


Figure 5.8 ¹³C NMR spectra of different guest/host ratios of guest **2** and dendrimer **1e** in D₂O. The concentration of guest is kept constant at $2.46 \cdot 10^{-2}$ M. The intensities are not normalized.

A quantitative determination of the binding strength of guest **2** to dendrimer **1e** in water is not possible. The chemical shift of the observed signal δ_{obs} can be described as

$$\langle \delta_{\text{obs}} \rangle = p_{\text{HA}} \delta_{\text{HA}} + p_{\text{A}^-} \delta_{\text{A}^-} + p_{\text{HA complex}} \delta_{\text{HA complex}}$$

with p_{HA} , p_{A^-} and $p_{\text{HA complex}}$ the fractions of free acid, deprotonated acid and acid in the complex respectively, and δ_{HA} , δ_{A^-} and δ_{complex} the corresponding chemical shift values of these three situations. Like already stated in section 5.3, the guest can undergo an acid–base reaction with the solvent which influences the pH and the observed chemical shift. This does not have to mean that the guest is bound to the dendrimer. Furthermore, the previous section has shown that the dendrimers are not present in solution as single entities, but as aggregated structures. The guest/host ratio influences the aggregate structure, and therefore most likely also the average number of guests that can bind to the dendrimer as well as the binding strength.

In ^{31}P NMR, the signal of guest **3** in D_2O is located at 20.2 ppm (Figure 5.9). As an internal standard, 80% phosphoric acid has been used in an insert.

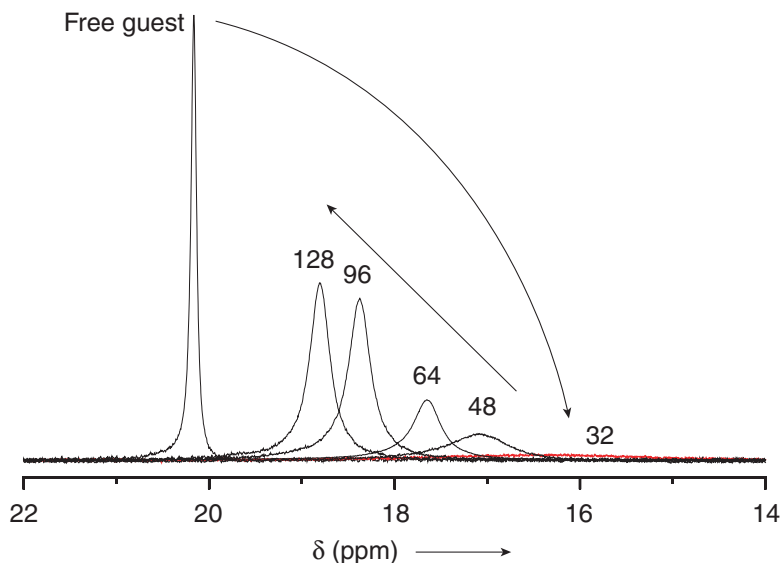


Figure 5.9 ^{31}P NMR spectra of different guest/host ratios of guest **3** to dendrimer **1e** in D_2O . Severe line broadening is observed. The concentration of guest **3** is kept constant at $2.36 \cdot 10^{-2} \text{ M}$.

Although the sample containing **1e+3₃₂** is not completely clear, it is possible to measure the ^{31}P NMR spectrum. An upfield shift to approximately 16 ppm is observed. Apart from this shift, severe line broadening is observed. When G/H is increased to 48, 64, 96 and 128, the peak shifts downfield again and becomes narrower.

In contrast to the results in chloroform, only one peak is observed in all cases, which indicates that exchange is fast on the NMR timescale, and therefore faster than in chloroform. With respect to the association constant the same reasoning holds for this guest. The chemical shift dependency of the peak can be due to both complexation and changes in pH, and a determination of the association constant based on these chemical shift values will give an unreliable value. This is confirmed by a ^{31}P NMR measurement of guest **3** in the presence of an excess of triethylamine at a pH of 10 (not depicted), resulting in a downfield shift of the signal of the guest to 14.6 ppm. Interestingly, the signal remains sharp. This suggests that the severe line broadening is not an effect of pH, but a result of complexation to dendrimer **1e**. Measurements at different field strengths show that the broadening is mostly due to coalescence. A sample of **1e+3₄₈** was prepared in D_2O , and showed a linewidth of 300 Hz at a ^{31}P -frequency of 202 MHz. At a ^{31}P -frequency of 81 MHz, the linewidth was 40 Hz. This clearly shows that the broadening is mainly due to exchange phenomena resulting in coalescence. T_2 -relaxation as a result of a decreased mobility of the phosphonic acid headgroup will be present as well but is less dominant here.

Although the amount of information obtained from ^{13}C NMR and ^{31}P NMR measurements in D_2O is somewhat limited, it is still possible to investigate whether exchange can take place when both guests are added to dendrimer **1e**.

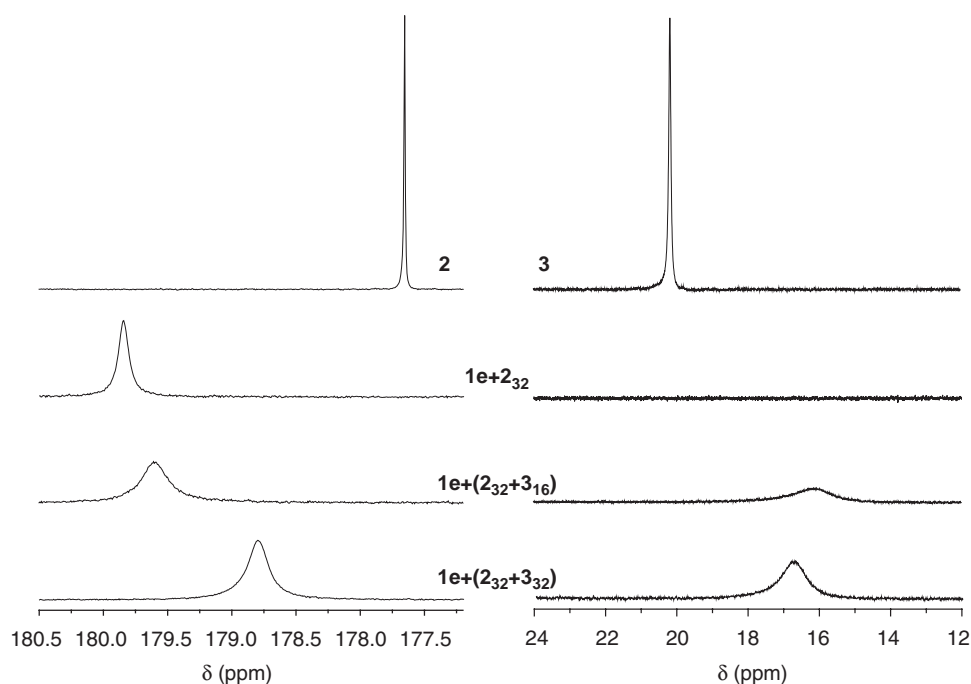


Figure 5.10 ^{13}C and ^{31}P NMR spectra of the different complexes. For clarity, the spectra of guest **2** and **3** are also depicted.

Therefore 16 and 32 equivalents of **3** have been added to a sample of **1e+2₃₂** in D_2O . The results are depicted in figure 5.10. Sample **1e+2₃₂** shows the characteristic downfield shift also observed in figure 5.8. When 16 equivalents of guest **3** are added, the peak of guest **2** shifts upfield, most likely due to a decrease of the pH. The signal of phosphonic acid guest **3** shifts upfield and broadens significantly. Another 16 equivalents of guest **3** results in a further upfield shift in carbon NMR and a slight downfield shift in phosphorus NMR. The signal in phosphorus NMR becomes more narrow. This could indicate that the ratio of bound to free guest **3** decreases. Again, it is impossible to derive any quantitative results from these spectra, but they at least suggest that exchange takes place, and that a mixed aggregate is obtained, as in chloroform.

The dynamics of guest exchange have briefly been investigated with dialysis experiments to arrive at a kind of supramolecular synthetic scheme. Prefabricated dialysis tubes (Spectra/por DispoDialyzer, 500 μL inner volume) containing cellulose ester membranes with a molecular weight cut-off of 3500 g/mol were filled with 0.6 mL of either guest **2** or complex **1e+2₃₂** in water. The amount of guest was kept constant at 5 mg ($10.2 \cdot 10^{-2}$ M). Each DispoDialyzer membrane was put in a Schlenck tube filled with 15 mL of demineralised water. The diffusion of guest **2** through the membrane was followed with UV-spectroscopy. For guest **2**, the extinction coefficient in water was determined to be $15334 \text{ L} \cdot \text{cm}^{-1} \cdot \text{mol}^{-1}$ at 248 nm. Figure 5.11 shows the amount of guest **2** that has

diffused through the membrane as a function of time. Both curves (free **2** and complex **1e+2₃₂**) represent the average values of three experiments.

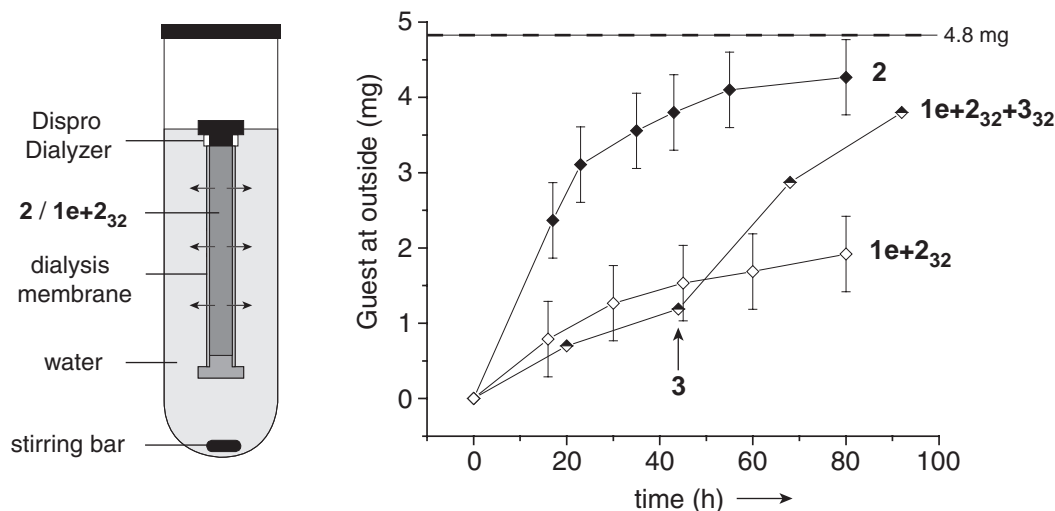
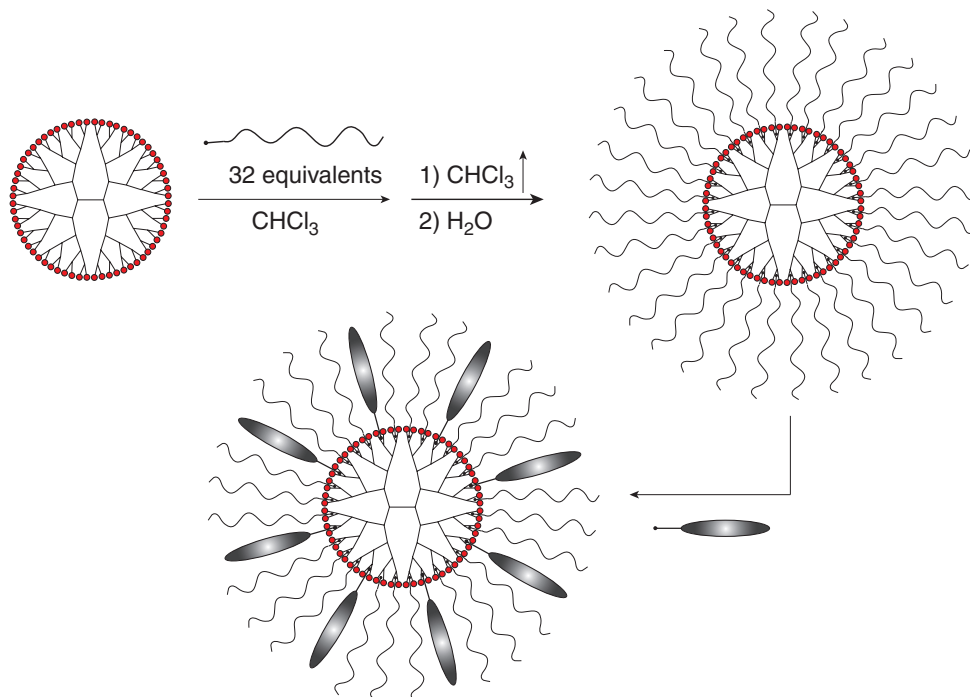


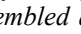
Figure 5.11 The experimental set-up (left) and the diffusion of guest **2** through the membrane as a function of time (right). For the mixed aggregate, guest **3** is added inside the membrane after 44 h.

The diffusion of guest **2** through the membrane goes significantly slower for **1e+2₃₂** than for pure **2**. This is most likely due to complexation to dendrimer **1e**, which results in larger structures. As a result of the constant exchange between free and bound guest, and the difference in inner and outer volume, approximately 4.8 mg of guest **2** should eventually diffuse through the membrane. This also happens, but much slower than in the case of free **2**. No clear precipitation of dendrimer has been observed in the timescale of 80 h. When an additional guest is added inside the dialysis membrane, mixed aggregates should be obtained. Therefore, it should be possible to completely substitute the ethylene glycol guest **2** by another guest if this new guest is added several times. Preliminary results with phosphonic acid guest **3** show that this substitution indeed takes place. Another sample of **1e+2₃₂** was subjected to dialysis for 44 h, and subsequently 5 mg of guest **3** was added to the complex inside the membrane. After the addition of guest **3**, a clear increase in the amount of guest **2** or **3** that has diffused through the membrane is observed through the membrane. Analysis of the inside and outside of the membrane after 92 h shows that the inside contains more of guest **3** and dendrimer, while the outside mostly contains guest **2**. These results suggest that it should be possible to fully substitute guest **2** with guest **3**, especially when guest **3** is added multiple times to the complex inside the dialysis membrane. However, more experiments are required to confirm this hypothesis.

The observed exchange between guests gives the opportunity to test whether the periphery of the adamantyl dendrimer can be functionalized with guest molecules that are only soluble in water. In this supramolecular synthesis, the oligoethylene glycol guest acts as a kind of

“supramolecular protective group”, which is exchanged with the molecule of interest after solubilization of the dendrimer in water (Scheme 5.4).



Scheme 5.4 Idealized representation of the supramolecular synthesis to dendritic architectures with functional guest molecules () assembled at the periphery. In reality, the dendrimers are aggregated, but exchange should still be possible.

The supramolecular synthesis has been investigated for two types of guest molecules, two MRI contrast agents and a peptide.

5.5.2 Guest molecules with MRI labels

Magnetic Resonance Imaging (MRI) contrast agents based on gadolinium(III) complexes are generally applied as diagnostics in medical imaging.³⁰⁻³² Due to its very high magnetic moment and relatively slow electronic relaxation, the Gd^{3+} ion is by far the most frequently chosen ion for MRI contrast agents. The high toxicity of the Gd^{3+} ion in aqueous solution requires the metal ion to be strongly complexed by a chelating agent. Two examples of frequently used chelating agents are DTPA (diethylenetriamine-pentaacetic acid) and DOTA (1,4,7,10-tetraazacyclododecane-1,4,7,10 tetra-acetic acid). Recently, dr. Sander Langereis of our laboratory nicely showed that it is possible to functionalize poly(propylene imine) dendrimers with $Gd(III)DTPA$ moieties.³³ The ionic and molecular relaxivities increased upon increasing the dendrimer generation, and the higher generation dendrimers also showed longer retention times in the blood circulation of rats due to the higher molecular weight.³⁴ We were interested to make a supramolecular dendritic contrast agent based on guest molecules that bind to Gd^{3+} and the urea–adamantyl dendrimer in water. Therefore, guests **4** and **5** have been prepared (Figure 5.13). Guest **5** consists of a DTPA-unit connected to a ^{13}C -labeled

ureido–acetic acid moiety, and guest **6** consists of an N-monosubstituted DO3A-unit (DO3A = 1,4,7,10-tetraazacyclododecane-1,4,7 triacetic acid) modified with a ureido–phosphonic acid group. The relaxivity (a measure for the efficiency of an MRI contrast agent) of the guests might be used as a probe for complexation of the small guest to the larger dendrimer. The paramagnetic nature of the Gd^{3+} ion does hamper NMR measurements. Therefore guests **5** and **6** have also been complexed with yttrium(III). This trivalent ion (Y^{3+}) is commonly used as a diamagnetic probe for lanthanides, since it has a size similar to that of Gd^{3+} .

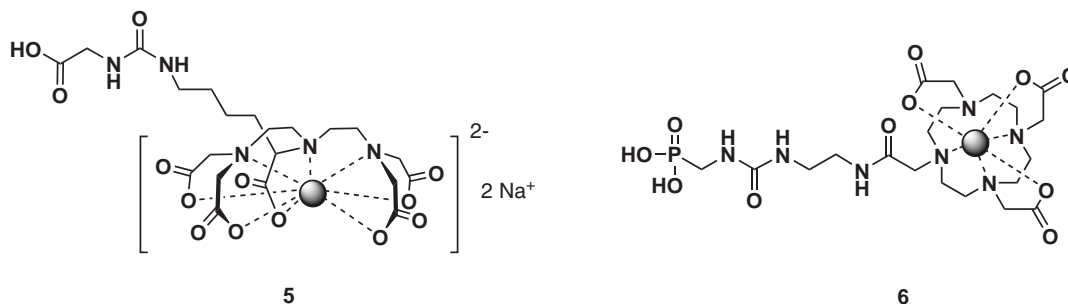


Figure 5.12 The structure of guest **5**, modified with a DTPA unit, and guest **6**, modified with a DO3A-unit. Both guests are able to bind to Gd^{3+} or Y^{3+} , represented by the sphere inside the chelating moiety.

However, when 8 equivalents of $Gd(III)DTPA$ modified guest **5** are added to **1e+2₃₂** in D_2O , immediate precipitation of the dendrimer is observed. This might be due to the charge of the $Gd(III)DTPA$ complex, which is not neutral but has two free sodium carboxylate groups. These groups are also able to interact with the dendrimer, and might interfere with the complex, which results in precipitation of the dendrimer. The precipitation might also be due to the pH of the solution of the guest, which is around 7.

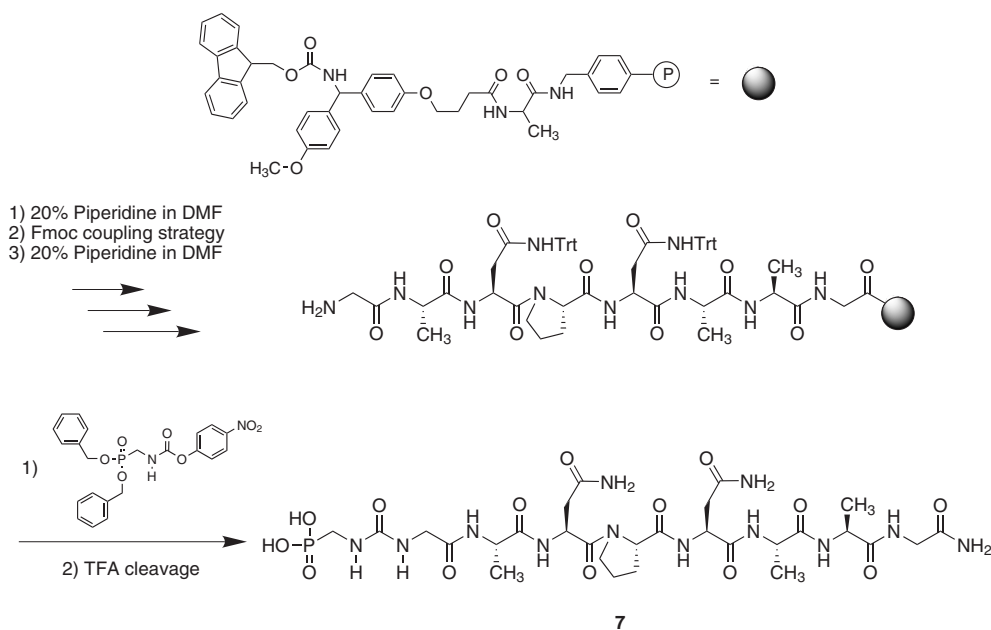
The $Gd(III)DO3A$ -complex is neutral, and does not have free carboxylate groups that can possibly interact with the dendrimer. Addition of 8 equivalents of $Gd(III)DO3A$ -modified guest **6** to **1e+2₃₂** in D_2O does not give rise to precipitation of the dendrimer, but the solution becomes very milky and viscous. When 8 equivalents of the $Y(III)DO3A$ -complex of guest **6** is added, the same changes are observed. ^{31}P NMR shows a sharp peak, indicating that no interaction between the dendrimer and the guest occurs. At this moment it is unclear what causes precipitation of the dendrimer, but from section 5.3 has become clear that the interactions between guest and host are easily distorted by changes in the pH and ionic strength. This might also be the case for the guest molecules with MRI labels.

5.5.3 Peptide guest molecules

Peptide **7** has been synthesized in collaboration with dr. T. Chang and the group of prof. J. van Hest (Radboud University Nijmegen, Nijmegen, The Netherlands). It contains the GANPNAAG-sequence, a β -turn sequence obtained from the CS protein of the malaria parasite

Plasmodium falciparum.³⁵ The folding of this sequence has been investigated in detail, and it was shown that the β -turn could be stabilized by anchoring it into a lipid bilayer. Current studies are investigating the potential of the GANPNAAG- β -turn immobilized on liposomes as synthetic vaccines.³⁶

The peptide has been synthesized according to standard Fmoc chemistry on a Breipohl resin (see scheme 5.5). By reaction of the N-terminal amine with an activated urethane, the peptide is modified with a ureido-phosphonic acid ester. Cleavage from the resin using TFA results in the phosphonic acid **7**. The C-terminus of the peptide is obtained as a primary amide. HPLC analysis indicated that the peptide was completely pure.



Scheme 5.5 The synthesis of the ureido-phosphonic acid modified GANPNAAG peptide **7**.

Figure 5.13 shows the ^{31}P NMR spectrum of guest **7** in D_2O . One peak at 19 ppm is observed. When 8 equivalents of peptide **7** are added to a sample of **1e+2₃₂** in D_2O , the solution becomes slightly opaque, but no precipitation is observed. ^{31}P NMR shows extreme broadening of the signal, suggesting that the peptide indeed binds to the dendrimer. When 16 instead of 8 equivalents are added, the solution becomes more milky. The ^{31}P NMR of this sample shows a slightly sharper signal than in the case of **1e+(2₃₂+7₈)**. Based on the broadness of the peak, it seems that a significant amount of guest **7** is bound. These experiments give a first indication that it is possible to make supramolecular peptide-dendrimer conjugates. The fact that the solution becomes turbid suggests that the aggregate size of the dendrimers becomes bigger. It is important to obtain more proof to confirm this behavior with cryo-TEM and light scattering experiments. Formation of the β -turn should be investigated with CD measurements.

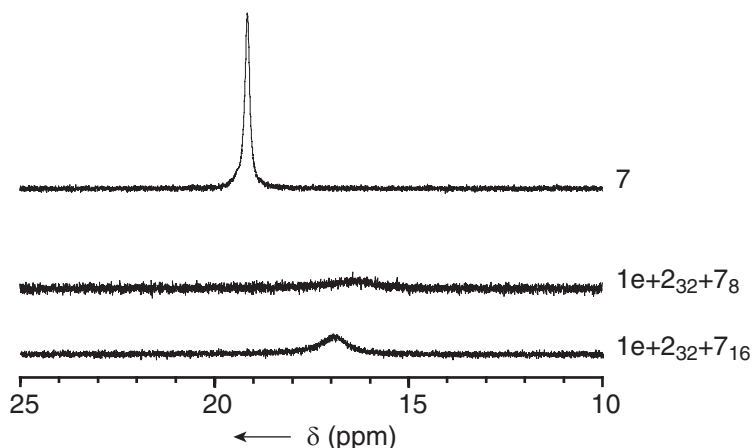


Figure 5.13 ^{31}P NMR spectra of peptide guest **7** added to the solubilized dendrimer in water.

In a similar manner, the GANPNAAG-sequence was prepared with carboxylic acids on both the N-terminus and C-terminus of the peptide. The binding of the peptide to the dendrimer could be enhanced by formation of the β -turn in this case, resulting in 2 interactions with the dendrimer instead of one. Unfortunately, immediate precipitation was observed upon addition of 8 equivalents of the peptide to the dendrimer. This might be due to crosslinking of the dendrimers, followed by precipitation.

5.6 OVERALL CONCLUSIONS

A supramolecular synthesis has been developed to obtain stable, dendrimer-based assemblies in water. The methodology comprises three steps: 1) preorganization of the complex in chloroform with oligoethylene glycol guests, 2) gentle evaporation of the chloroform resulting in a transparent film inside the reaction tube, and 3) addition of the water. NMR experiments confirm that the dendrimer is solubilized by the guests, and that guest and host are in close proximity of each other.

In contrast to the results in chloroform, the aggregates do not consist of single dendrimers surrounded by guests in water. For **1e+2₃₂**, sphere-like micelles are observed which most likely consist of small clusters of dendrimers surrounded by guest molecules. The dendritic host–guest complex can be seen as an amphiphilic structure in which the polar parts are not connected to the apolar parts in a covalent fashion but in a dynamic, non-covalent fashion. At a guest/host ratio of 64 and 128, rod-like micelles are observed. Sphere-to-rod transitions of micelles have been observed frequently for amphiphilic structures. Changes in temperature, concentration of surfactant, additives in the liquid phase and structural groups in the surfactant all may cause change in size, shape and aggregation number of the micelle. More experiments are necessary to determine which factors govern the formation, and transition, of these micellar structures.

A quantitative analysis on the binding of carboxylic and phosphonic acid guest **2** and **3** cannot be performed, but it is possible to investigate exchange between these guests using ^{13}C and

^{31}P NMR. The NMR results indicate that exchange takes place, and that mixed aggregates can be formed. Preliminary dialysis experiments seem to confirm this behavior. This brings the goal of a multicomponent, dynamic library (Figure 5.14) a step closer to reality.

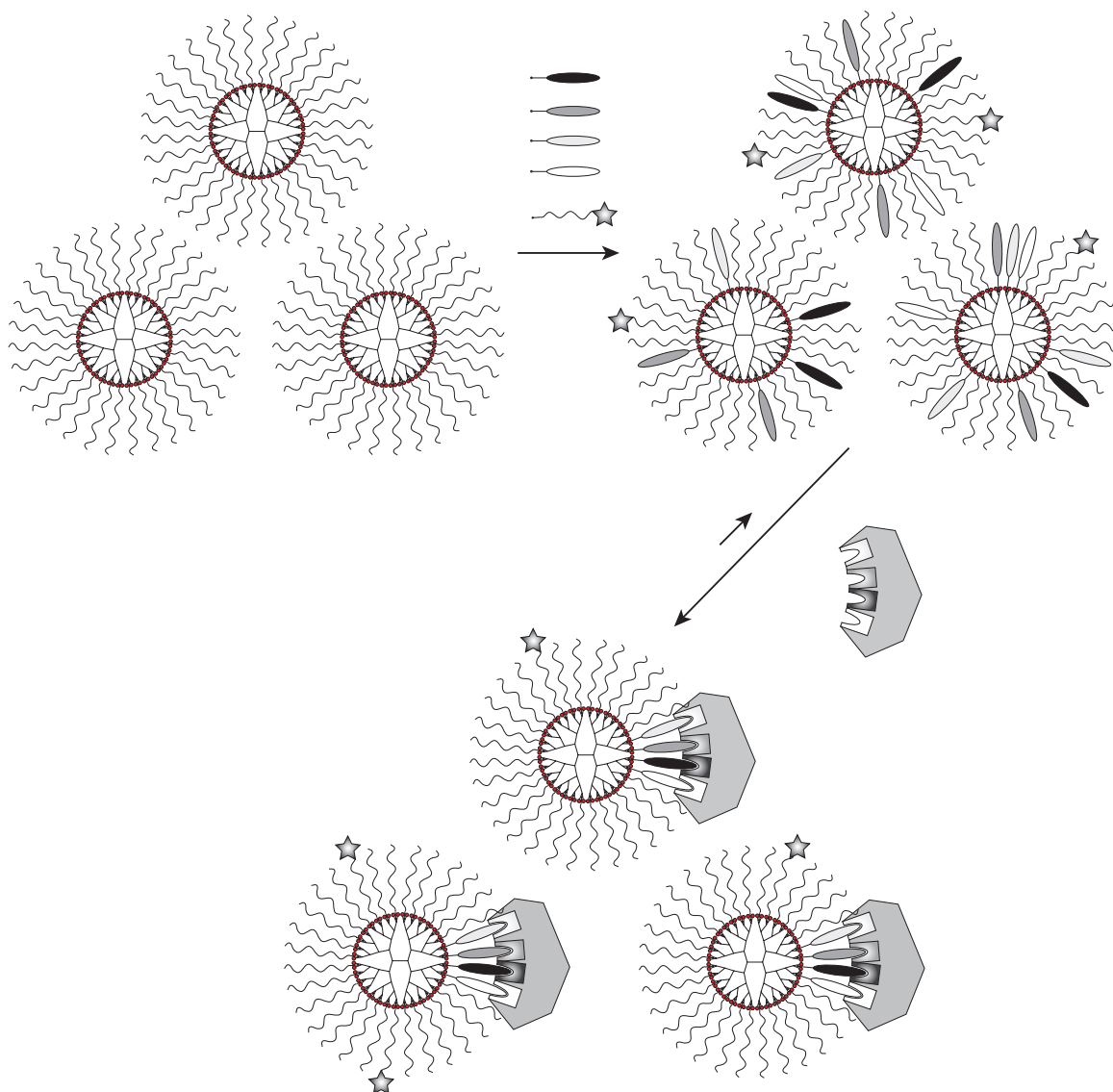


Figure 5.14 The dendritic host–guest system presented as a dynamic combinatorial library. Addition of several different guests to the dendrimer solubilized in water will result in many statistical combinations of guest molecules bound to the dendrimers. Binding to a scaffold, e.g. a protein, results in a shift of the equilibrium towards the best order of guests simultaneously bound to the dendrimer and the scaffold. A guest molecule functionalized with an MR imaging label (indicated with the star) might be useful to follow complexation to the scaffold

The final results described in this chapter show that it seems to be possible to assemble a functional peptide guest to the dendrimer. Like in chloroform, it should be possible to assemble several functional guest molecules simultaneously to the dendritic scaffold. Although much more research is needed to improve the aggregation behavior and stability of the dendritic host–guest system, the results described in this chapter show that a step towards a dynamic combinatorial library in water has been made.

5.7 EPILOGUE

The results described in this chapter clearly illustrate where the challenges of this research for the future lie: control over the supramolecular assemblies in water. In order to achieve this, the research should, in my view, focus on three aspects.

First of all, the interactions between guest and host should become stronger and more specific. We have experienced that the supramolecular interactions that play an important role in chloroform can behave completely different in water. While electrostatic interactions and hydrogen bonding interactions govern the binding between guest and host in chloroform, these interactions are much weaker in water. In contrast, hydrophobic interactions are absent in chloroform, but play a crucial role in water. It is important to realize that stronger binding in chloroform does not mean stronger binding in water.

Although hydrophobic interactions are strong in water, they are nondirectional. When the hydrophobicity of a guest molecule is increased, it might bind stronger to the hydrophobic dendrimer, but it will also tend to aggregate with guest molecules. In a similar manner, the hydrophobic urea–adamantyl dendrimer aggregates. When the hydrophobicity is too high, the compounds will not dissolve. Clearly the adamantyl dendrimer is not the ideal host for applications in water, as it is so hydrophobic that it often precipitates upon small changes in the system.

The acid–base interaction is directional, but weak due to solvation of the charged groups. However, the chelate effect can be used to increase the affinity between guest and a host. When a guest molecule contains multiple acid groups, a multivalent interaction can take place with the tertiary amines of the dendrimer, resulting in a higher overall binding strength. This will only work when the distance between the acid groups is optimized in such a way that all acid groups can simultaneously interact with the tertiary amines. A systematic study into multivalent, water soluble guest molecules with varying spacer lengths between the acid groups can give information about the optimal distance between the acid groups for complexation to the dendritic host. Molecular capsules in aqueous media are an example of supramolecular aggregates based on multiple electrostatic interactions.

Secondly, the influence of the preparation of the complexes, or supramolecular synthesis, on the outcome of the structures formed should be investigated in detail. As discussed in this chapter, the complexes can be formed in water only by preorganization in chloroform, followed by the evaporation of chloroform and addition of water. An injection from THF gave less reproducible results. Sample preparation is clearly an important factor in the formation of the host–guest complexes, and starts to become more complicated than self-assembly, which means that all components are mixed in all at once. Also the speed with which a certain action is performed probably influences the structure formed.

Thirdly, the complexation between guest and host should be analyzed in detail. Both mass spectrometry and NMR spectroscopy are informative analytical tools, also in water. Still, light scattering and cryo-TEM are indispensable in order to get information on the shape and size of the aggregates present in solution. New developments in cryo-TEM, especially 3D-tomography, might give more detailed information on the location of guests and host. These aspects together can give new insights in the formation of supramolecular assemblies in water, as well as a more fundamental understanding of multivalent interactions. This is of general importance in the design of functional nanoscopic assemblies.

5.8 REFERENCES

- 1 A. W. Bosman, H. M. Janssen, E. W. Meijer, *Chem. Rev.* **1999**, *99*, 1665-1688.
- 2 U. Boas, P. M. H. Heegaard, *Chem. Soc. Rev.* **2004**, *33*, 43-63.
- 3 E. R. Gillies, J. M. J. Fréchet, *Drug Discovery Today* **2005**, *10*, 35-43.
- 4 F. Zeng, S. C. Zimmerman, *Chem. Rev.* **1997**, *97*, 1681-1712.
- 5 M. W. P. L. Baars, E. W. Meijer, *Top. Curr. Chem.* **2000**, *210*, 131-182.
- 6 S. C. Zimmerman, L. J. Lawless, *Top. Curr. Chem.* **2001**, *217*, 95-120.
- 7 G. R. Newkome, C. N. Moorefield, G. R. Baker, M. J. Saunders, S. H. Grossman, *Angew. Chem.* **1991**, *103*, 1207-1209.
- 8 C. J. Hawker, K. L. Wooley, J. M. J. Fréchet, *J. Chem. Soc., Perkin Trans. 1* **1993**, 1287-1297.
- 9 S. Mattei, P. Wallimann, B. Kenda, W. Amrein, F. Diederich, *Helv. Chim. Acta* **1997**, *80*, 2391-2417.
- 10 C. Román-Vas, PhD Thesis, Eindhoven University of Technology (The Netherlands), **1999**.
- 11 J. J. Michels, M. W. P. L. Baars, E. W. Meijer, J. Huskens, D. N. Reinhoudt, *Perkin 2* **2000**, 1914-1918.
- 12 M. W. P. L. Baars, R. Kleppinger, M. H. J. Koch, S.-L. Yeu, E. W. Meijer, *Angew. Chem. Int. Ed.* **2000**, *39*, 1285-1288.
- 13 J. J. J. M. Donners, B. R. Heywood, E. W. Meijer, R. J. M. Nolte, N. A. J. M. Sommerdijk, *Chem. Eur. J.* **2002**, *8*, 2561-2567.
- 14 C. Reichardt, *Solvents and Solvent Effects in Organic Chemistry*, 3rd ed., WILEY-VCH Weinheim Germany, **2003**.
- 15 Y. Cohen, L. Avram, L. Frish, *Angew. Chem. Int. Ed.* **2005**, *44*, 520-554.
- 16 A. P. H. J. Schenning, C. Elissen-Roman, J.-W. Weener, M. W. P. L. Baars, S. J. Van der Gaast, E. W. Meijer, *J. Am. Chem. Soc.* **1998**, *120*, 8199-8208.
- 17 M. Adrian, J. Dubochet, J. Lepault, A. W. McDowell, *Nature* **1984**, *308*, 32-36.
- 18 P. M. Frederik, D. H. W. Hubert, *Methods Enzymol.* **2005**, *391*, 431-448.
- 19 C. L. Jackson, H. D. Chanzy, F. P. Booy, B. J. Drake, D. A. Tomalia, B. J. Bauer, E. J. Amis, *Macromolecules* **1998**, *31*, 6259-6265.
- 20 S. Burghardt, A. Hirsch, B. Schade, K. Ludwig, C. Böttcher, *Angew. Chem. Int. Ed.* **2005**, *44*, 2976-2979.
- 21 C. Böttcher, B. Schade, C. Ecker, J. P. Rabe, L. Shu, A. D. Schlüter, *Chem. Eur. J.* **2005**, *11*, 2923-2928.
- 22 P. A. Winsor, *Chem. Rev.* **1968**, *68*, 1-40.
- 23 M. J. Rosen, *Surfactants and interfacial phenomena*, 1st ed., John Wiley & Sons, **1978**.

- 24 C. Tanford, *The Hydrophobic Effect*, 2nd ed., Wiley, New York, **1980**.
- 25 V. Degiorgio, in *Physics of Amphiphiles: Micelles, Vesicles and microemulsions* (Eds.: V. Degiorgio, M. Corti), North-Holland, New York, **1985**, p. 303.
- 26 J. N. Israelachvili, *Intermolecular Forces and Surface Forces. With Applications to Colloidal and Biological Systems*, 1st ed., Academic Press, Inc., **1985**.
- 27 Z. A. Al-Anber, J. B. i Avalos, *J. Chem. Phys.* **2003**, *118*, 3816-3826.
- 28 G. J. M. Koper, M. H. P. van Genderen, C. Elissen-Roman, M. W. P. L. Baars, E. W. Meijer, M. Borkovec, *J. Am. Chem. Soc.* **1997**, *119*, 6512-6521.
- 29 J. J. Michels, M. W. P. L. Baars, E. W. Meijer, J. Huskens, D. N. Reinhoudt, *Perkin 2* **2000**, 1914-1918.
- 30 P. Caravan, J. J. Ellison, T. J. McMurry, R. B. Lauffer, *Chem. Rev.* **1999**, *99*, 2293-2352.
- 31 A. E. Merbach, E. Toth, *The Chemistry of Contrast Agents in Medical Magnetic Resonance Imaging*, John Wiley & Sons, New York, **2001**.
- 32 V. Jacques, J. F. Desreux, *Top. Curr. Chem.* **2002**, *221*, 123-164.
- 33 S. Langereis, Q. G. De Lussanet, M. H. P. Van Genderen, W. H. Backes, E. W. Meijer, *Macromolecules* **2004**, *37*, 3084-3091.
- 34 Q. G. de Lussanet, S. Langereis, R. G. H. Beets-Tan, M. H. P. van Genderen, A. W. Griffioen, J. M. A. van Engelshoven, W. H. Backes, *Radiology* **2005**, *235*, 65-72.
- 35 C. Cerami, U. Frevert, P. Sinnis, B. Takacs, P. Clavijo, M. J. Santos, V. Nussenzweig, *Cell* **1992**, *70*, 1021.
- 36 D. W. P. M. Löwik, J. G. Linhardt, P. J. H. M. Adams, J. C. M. van Hest, *Org. Biomol. Chem.* **2003**, *1*, 1827-1829.

Summary

In the living world, almost all processes are regulated through multiple interactions between molecules. In this way, complex molecular systems are obtained that can perform highly specific functions. The field of supramolecular chemistry aims to understand how the interactions between molecules can be controlled, in order to create complex systems similar to those found in nature. Dendrimers, due to their multivalent and well-defined structure, appeared to be ideal scaffolds for the complexation of molecules through multiple interactions. These branched molecules can host small molecules both at the inside and at the surface of the structure in a similar manner as proteins can interact with substrates.

In our group, a dendritic host–guest system has been developed that allows the binding of multiple guests to a dendritic scaffold in chloroform through a combination of acid–base interactions and hydrogen bonding interactions. The binding between the guests and the host is dynamic, and especially of interest in biomedical applications like drug delivery, synthetic vaccines and dynamic libraries. For these applications, strong binding in aqueous media is required. In order to achieve this, a thorough understanding of the factors that govern binding between guest and host are necessary. This thesis describes the results obtained in the synthesis and analysis of this dendritic host–guest system.

Chapter 1 gives a short introduction into the field of dendrimers, and their role in the area of host–guest chemistry. The concepts of binding valency and cooperativity are introduced, as well as the idea of a supramolecular dynamic library.

In Chapter 2, the synthesis of the dendritic hosts and several guest molecules are described. An *N*-*t*-Boc-*L*-phenylalanine modified guest has been used to probe the mobility of the end groups of guests noncovalently bound to dendrimers. Optical rotation experiments have shown that the conformational freedom of the dangling end groups of the guests does not change significantly upon binding to the dendrimer. X-ray diffraction studies on model compounds have indicated that next to acid–base interactions and urea–urea hydrogen bonding, several other types of hydrogen bonding can take place between the guest and host. These interactions, e.g. hydrogen bonding between the carbonyl oxygen of carboxylic acid groups and the protons of urea groups, have also been found in molecular dynamics (MD) simulations. MD simulations have been used to get insights in the 3D-structure of the dendritic host–guest system in the gas phase.

Chapter 3 describes the analysis of the dendritic host–guest system with mass spectrometry. With electrospray ionization mass spectrometry it is possible to transfer the supramolecular aggregates from solution into the gas phase. Next to the bare dendrimer, complexes of 1–9 guest molecules bound to the dendritic host have been observed. Also statistical mixtures of 2 or 3 guest

molecules simultaneously bound to the dendrimer have been observed. With collision induced dissociation, it has been possible to determine the binding strength of guest molecules in the gas phase in qualitative manner. CID has shown that phosphonic acid guests bind stronger to the dendrimer than carboxylic acid guests, and that sulfonic acid guest bind strongest. These results are in agreement with binding studies performed in chloroform. Molecular dynamics simulations were used to simulate these experiments, and a good agreement between the center of mass energy in the CID experiment and the dissociation temperature in the MD simulations was achieved.

Chapter 4 describes a further analysis of the complexes in chloroform using NMR spectroscopy. ^1H - ^1H NOESY spectroscopy has shown that carboxylic acid guest molecules bind via the acidic headgroup, and mostly bind to the periphery of the dendritic structure. The complexation of carboxylic acid guests has been investigated with ^{13}C NMR on ^{13}C -labeled guest molecules. ^{31}P NMR has been used to investigate the binding of phosphonic acid guests to urea–adamantyl dendrimers. For the carboxylic acid guest, an association constant of $400 \pm 95 \text{ M}^{-1}$ has been obtained with 41 binding sites per dendrimer. For the phosphonic acid guest, an association constant of $(4 \pm 3) \times 10^4 \text{ M}^{-1}$ was found and 61 ± 1 binding sites per dendrimer. The phosphonic acid guest binds stronger, and most likely to all tertiary amines of the dendrimer. A statistical analysis has shown that the carboxylic acid guest always forms a polydisperse supramolecular aggregate, while the phosphonic acid guest is able to form a monodisperse supramolecular aggregate at high guest/host ratios.

In Chapter 5, a supramolecular synthesis is described towards stable dendritic aggregates in water. The hydrophobic urea–adamantyl dendrimers can be solubilized in water by making use of water–soluble oligoethylene glycol guests, but only when the complexes are preorganized in chloroform. Next to several NMR techniques, the complexes have been analyzed with cryogenic transmission electron microscopy and light scattering. The experiments have shown that the dendrimers are present in solution as spherical or rod-like aggregates, depending on the guest/host ratio and concentration. Dialysis experiments and NMR experiments have shown that exchange can take place between the guest molecules that surround the dendritic aggregate. At the end of the chapter, the complexation of guest molecules that contain a peptide sequence or MR imaging labels has been investigated. Although the aggregates are fragile, and often precipitate, there is evidence that the peptide guest can be incorporated in the aggregates. In the epilogue, the author’s personal opinion on the future perspectives of the research is described.

Samenvatting

In de levende wereld vinden bijna alle processen plaats via meervoudige interacties tussen moleculen. Op deze manier worden complexe moleculaire systemen verkregen met zeer specifieke functies. Het vakgebied van de supramoleculaire chemie probeert te begrijpen hoe die interacties tussen moleculen gecontroleerd kunnen worden, om zo complexe systemen te maken vergelijkbaar met systemen in de natuur. Dendrimeren zijn, dankzij hun multivalente en goed gedefinieerde structuur, ideale constructen voor het aangaan van meervoudige interacties met andere moleculen. Gastmoleculen kunnen zowel binnenin als aan het oppervlak van dendrimeren binden op een manier vergelijkbaar met de binding van substraatmoleculen aan eiwitten.

In onze groep is een supramoleculair systeem ontwikkeld waarbij meerdere gastmoleculen kunnen binden aan een dendrimeer in chloroform door een combinatie van zuur–base interacties en waterstofbruggen. De binding tussen gast en gastheer is dynamisch, en met name interessant voor biomedische toepassingen zoals medicijnafgifte, synthetische vaccins en dynamische bibliotheken. Voor deze toepassingen is een sterke binding tussen het dendrimeer en de gastmoleculen in water een vereiste. Om dit doel te bereiken is het van belang een goed begrip te hebben van de factoren die de binding tussen gast en gastheer bepalen. Dit proefschrift bevat de belangrijkste resultaten behaald in de analyse van dit dendritische host–guest systeem.

Hoofdstuk 1 geeft een korte inleiding over dendrimeren en de rol van dendrimeren in de host–guest chemie. Hierin worden ook de concepten bindingsvalentie, cooperativiteit en supramoleculaire dynamische bibliotheken geïntroduceerd.

In hoofdstuk 2 wordt de synthese van verschillende dendrimeren en gastmoleculen beschreven. Een gastmolecuul waarvan het uiteinde bestaat uit een *N*-*t*-Boc-L-fenylalanine groep is gebruikt om de bewegingsvrijheid te onderzoeken van de eindgroepen van gastmoleculen die gebonden zijn aan dendrimeren. Optische rotatie experimenten hebben aangetoond dat de bewegingsvrijheid van de eindgroepen van gasten niet significant verandert als de gastmoleculen binden aan het dendrimeer. Röntgendiffractie-studies aan modelverbindingen hebben aangetoond dat naast de zuur–base interactie en ureum–ureum waterstofbruggen meerdere andere waterstofbruggen plaats kunnen vinden tussen gast en gastheer. Deze interacties zijn ook gevonden in moleculaire dynamica (MD) simulaties. Daarnaast zijn MD-simulaties gebruikt om inzichten te verkrijgen in de 3-dimensionale structuur van de dendritische aggregaten in de gasfase.

Hoofdstuk 3 beschrijft de analyse van de dendritische aggregaten met massaspectrometrie. Met electrospray ionisatie massaspectrometrie is het mogelijk om de complexen intact over te brengen van de vloeistof naar de gasfase. Naast het “kale” dendrimeer zijn complexen gevonden van 1 tot 9 gastmoleculen gebonden aan het dendrimeer. Met botsingsgeïnduceerde dissociatie (CID) is het

mogelijk om de bindingssterkte van gastmoleculen in de gasfase kwalitatief te bepalen. CID experimenten hebben aangetoond dat fosfonzuurgasten sterker binden dan carbonzuurgasten, en dat sulfonzuurgasten het sterkst binden. Deze resultaten zijn in overeenstemming met bindingsstudies uitgevoerd in chloroform. Moleculaire dynamica simulaties zijn uitgevoerd, en hebben geleid tot een goede overeenkomst tussen de “center of mass” energie in het CID experiment en de dissociatietemperatuur in de simulatie experimenten.

In hoofdstuk 4 zijn de complexen in oplossing geanalyseerd met NMR spectroscopie. ^1H - ^1H NOESY spectroscopie heeft aangetoond dat de gastmoleculen binden via de carbonzuurgroep, en met name binden aan de buitenkant van het dendrimeer. De complexatie van carbonzuurgasten is verder onderzocht met ^{13}C NMR aan ^{13}C -gelabelde gastmoleculen. ^{31}P NMR is gebruikt om de binding van fosfonzuren aan ureum–adamantyldendrimeren te onderzoeken. Voor de carbonzuurgast is een associatieconstante van $400 \pm 95 \text{ M}^{-1}$ gevonden met 41 bindingsplaatsen per dendrimeer, en voor de fosfonzuurgast is een associatieconstante van $(4 \pm 3) \times 10^4 \text{ M}^{-1}$ gevonden met 61 ± 1 bindingsplaatsen per dendrimeer. Hieruit blijkt dat de fosfonzuurgast sterker bindt, en waarschijnlijk kan binden aan alle tertiaire amines van het dendrimeer. Een statistische analyse heeft uitgewezen dat de carbonzuurgasten altijd een polydispers supramoleculair aggregaat vormen, maar dat de fosfonzuurgasten een monodispers supramoleculair aggregaat kunnen vormen bij hoge gast/dendrimeer verhoudingen.

In hoofdstuk 5 is de supramoleculaire synthese van stabiele aggregaten in water beschreven. De hydrofobe ureum–adamantyldendrimeren kunnen worden opgelost in water door gebruik te maken van wateroplosbare oligoethyleenglycolgasten. Naast verscheidene NMR technieken zijn de complexen geanalyseerd met cryogene transmissie electronen microscopie en lichtverstrooiing. Deze metingen hebben aangetoond dat de dendrimeren aanwezig zijn in oplossing als bolvormige of cilindrische aggregaten, afhankelijk van de gast/dendrimeer verhouding en concentratie. Dialyse-experimenten en NMR experimenten hebben aangetoond dat uitwisseling kan plaatsvinden tussen de gastmoleculen die de dendrimeren omringen. Aan het einde van het hoofdstuk is de complexatie van gastmoleculen met een peptide-sequentie of MR-imaging label onderzocht. Alhoewel de dendritische aggregaten kwetsbaar zijn en snel neerslaan, lijkt het erop dat de peptidegast kan worden opgenomen in de aggregaten. In de epiloog geeft de auteur zijn persoonlijke mening over de toekomst van het onderzoek.

Curriculum Vitae



Maarten Broeren werd geboren op 20 oktober 1976 te Nijmegen. Na het voltooien van het Atheneum aan het d'Oultremontcollege in Drunen in 1995 werd begonnen aan de studie Scheikundige Technologie van de Technische Universiteit Eindhoven. Tijdens zijn studie liep hij drie maanden stage bij Organon te Oss. De studie werd in 2001 afgerond met een onderzoek naar de niet-covalente modificatie van dendrimeren. Aansluitend trad de auteur in dienst van de Technische Universiteit Eindhoven als promovendus binnen de capaciteitsgroep Macromoleculaire en Organische Chemie van de faculteit Scheikundige Technologie. Onder leiding van prof.dr. E.W. Meijer en dr.ir. M.H.P. van Genderen werkte hij tot november 2005 aan zijn promotieonderzoek. De belangrijkste resultaten hiervan staan beschreven in dit proefschrift.

Maarten Broeren was born in Nijmegen, the Netherlands, on October 20, 1976. He completed high school in 1995 at the d'Oultremont College in Drunen. In the same year, he started studying Chemistry and Chemical Engineering at the Eindhoven University of Technology. During his master study, a traineeship of 3 months was done at Organon in Oss. The master degree was obtained in 2001 with an investigation into the non-covalent modification of dendrimers. Subsequently the author worked as a PhD student at the Eindhoven University of Technology in the laboratory of Macromolecular and Organic Chemistry at the department of Chemistry and Chemical Engineering. Under the supervision of prof.dr. E.W. Meijer and dr.ir. M.H.P. van Genderen, the author has worked on the synthesis and analysis of supramolecular dendritic architectures until November 2005. The most important results of the work are described in this thesis.

List of Publications

Chiral amplification in columns of self-assembled N,N',N''-tris[(S)-3,7-dimethyloctyl]benzene-1,3,5-tricarboxamide in dilute solution

L. Brunsveld, A. P. H. J. Schenning, M. A. C. Broeren, H. M. Janssen, J. A. J. M. Vekemans, E. W. Meijer; *Chem. Lett.*, **2000**, 292-293.

Multivalency in the gas phase: The study of dendritic aggregates by mass spectrometry

M. A. C. Broeren, J. L. J. van Dongen, M. Pittelkow, J. B. Christensen, M. H. P. van Genderen, E. W. Meijer, *Angew. Chem. Int. Ed.* **2004**, *43*, 3557-3562.

An NMR study of the supramolecular chemistry of modified poly(propyleneimine) dendrimers

D. Banerjee, M. A. C. Broeren, M. H. P. van Genderen, E. W. Meijer, P. L. Rinaldi, *Macromolecules* **2004**, *37*, 8313-8318.

Supramolecular dendritic architectures in the gas phase

M. A. C. Broeren, J. L. J. van Dongen, M. H. P. van Genderen, E. W. Meijer, *Polym. Mater. Sci. Eng.* **2004**, *91*, 933-934.

The chirality of dendrimer-based supramolecular complexes

M. A. C. Broeren, B. F. M. de Waal, J. L. J. van Dongen, M. H. P. van Genderen, E. W. Meijer, *Org. Biomol. Chem.* **2005**, *3*, 281-285.

Molecular recognition: comparative study of a tunable host-guest system by using a fluorescent model system and collision-induced dissociation mass spectrometry on dendrimers

M. Pittelkow, C. B. Nielsen, M. A. C. Broeren, J. L. J. van Dongen, M. H. P. van Genderen, E. W. Meijer, J. B. Christensen, *Chem. Eur. J.* **2005**, *11*, 5126-5135.

Multicomponent host-guest chemistry of carboxylic acid and phosphonic acid based guests with dendritic hosts: an NMR study

M. A. C. Broeren, B. F. M. de Waal, M. H. P. van Genderen, H. M. H. F. Sanders, G. Fytas, E. W. Meijer, *J. Am. Chem. Soc.* **2005**, *127*, 10334-10343.

Noncovalent synthesis of supramolecular dendritic architectures in water

M. A. C. Broeren, J. G. Linhardt, H. Malda, B. F. M. de Waal, R. M. Versteegen, J. T. Meijer, D. W. P. M. Löwik, J. C. M. van Hest, M. H. P. van Genderen, E. W. Meijer, *J. Polym. Sci., Part A: Polym. Chem.* **2005**, accepted for publication.

Dankwoord

Met heel veel plezier en voldoening kan ik terugkijken op een fantastische promotietijd. Ik wil heel graag iedereen die een bijdrage heeft geleverd aan mijn onderzoek hartelijk bedanken. Enkele mensen wil ik in het bijzonder bedanken.

Mijn promotor Bert Meijer ben ik zeer erkentelijk voor zijn enthousiaste begeleiding. Bert, je hebt me enorm gemotiveerd. Je deur stond altijd open voor advies en suggesties, zowel over het onderzoek als daarbuiten. Ik heb veel van je geleerd, bedankt! Mijn copromotor Marcel van Genderen wil ik graag bedanken voor alle leerzame discussies en zijn kritische kijk op het onderzoek. Marcel, je kennis van NMR spectroscopie en je wiskundige interpretaties van experimentele resultaten zijn van groot belang geweest in de vooruitgang van het onderzoek, en hebben een grote stempel gedrukt op de inhoud van het boekje.

Ik wil graag prof. Roeland Nolte en prof. Jurriaan Huskens bedanken voor het deelnemen aan de leescommissie en het corrigeren van mijn proefschrift. Prof. Takuzo Aida, I want to thank you for coming all the way to the Netherlands, for taking part in my examination committee and for the suggestions for my manuscript. Ook wil ik dr. Joost Reek en dr. Jef Vekemans bedanken voor hun deelname aan de promotiecommissie.

Joost van Dongen, de analyse van de supramoleculaire aggregaten met massaspectrometrie bleek een schot in de roos te zijn. We hebben heel wat avonden gemeten op de Q/TOF, maar niet zonder succes! In de afgelopen vier jaar heeft het moment dat we voor het eerst de complexen zagen mij de grootste “kick” gegeven. Joost, bedankt voor de leerzame en gezellige samenwerking.

I would like to thank Michael Pittelkow and Jørn B. Christensen for a very pleasant cooperation. Your early explorations on the binding of phosphonic and sulfonic acid guest molecules have been an important basis for the mass spectrometry and NMR work. Prof. Peter Rinaldi and Debasish Banerjee are thanked for the beautiful 2D NOESY study. Jeffrey Linhardt, your work on the complexation of peptide guests in water has been the start of a very challenging part of the research, and is still in progress. Thanks for your help! Hierin wil ik ook de hulp van Hinke Malda en Dennis Löwik betrekken. Theresa Chang, your work on the crystal structures of model compounds, in combination with the molecular dynamics simulations of Koen Pieterse, has given many new insights in the host–guest interactions. Koen, je bent niet alleen een fantastisch ontwerper van covers en proefschriften (met name “onze” Angewandte ziet er toch wel piekfijn uit!), ook het simulatiewerk van jou en Erik Sanders is erg belangrijk geweest. Nico Sommerdijk, Paul Bomans en Peter Frederik ben ik erkentelijk voor de cryo-tem metingen. Bas de Waal, jij bent de enige echte “dendriemeerkoning” van SMO. Bedankt voor al je werk.

Het is een voorrecht geweest als promovendus meerdere studenten te mogen begeleiden. Ik wil Judith Borsboom en Marijn Vlaming graag bedanken voor hun bijdrage in de beginperiode van het onderzoek. Leandra Cornelissen, Erik Sanders en Chantal Loontjens wil ik bedanken voor de nuttige bijdragen van hun afstudeerwerk en de gezellige tijd. Jullie hebben alle drie besloten te gaan promoveren, en dat gaat zeker goed komen. Heel veel succes in de toekomst!

Ik wil Jef Vekemans graag bedanken voor zijn vele adviezen op synthetisch gebied. Het analytisch team bestaande uit Joost van Dongen, Ralf Bovee en Xianwen Lou ben ik dankbaar voor de vele analyses. Henk Eding, bedankt voor de koffie en de gezellige sfeer in de koffiekamer. Je koffie activeerde in de ochtend niet alleen mijn hersenen, maar ook mijn darmen. Hannie van der Lee, bedankt voor je werk en de leuke gesprekken. Het secretariaat bestaande uit Hanneke Veldhoen, Ingrid Dirx, Carine van der Vaart en Joke Rediker ben ik dankbaar voor al hun hulp. Hans Damen, bedankt voor het regelen van de chemicaliën en de gezellige koffiepauzes.

Sander Langereis (mijn onafscheidelijke “chemical brother”), onze interesses voor wetenschap en sportieve uitdagingen hebben inderdaad tot een hechte vriendschap geleid. Naast al het kabaal op lab 1 als “die twee” weer aan het schreeuwen waren hebben we heel wat afgewandeld, gefietst, geklommen, gepraat en vooral gelachen. Onze vriendschap betekent veel voor me, bedankt voor de fantastische tijd! Hierin wil ik natuurlijk ook Muriël Janssens betrekken. Ton Offermans, als stille kracht van STO 4.30 was je een perfecte tegenhangen van mij en Sander. Ik ben vereerd samen met Sander je paranimf te mogen zijn. Verder wil ik Ronald Ligthart, Patricia Dankers, Jos Paulusse, Anouk Dirksen, Arjan Zoombelt, Judith van Gorp, Pauline van Meurs, Serge Söntjens, Tessa ten Cate, René Sinkeldam, Hinke Malda, Jack Donners, Henk Keizer, Jolanda Spiering, Edwin Beckers, Pascal Jonkheijm en Jeroen van Herrikhuizen bedanken voor de vele gezellige gesprekken, etentjes of uitjes.

Het “sick brother” team bestaande uit Kristel Maaywee, Wouter Eckelmans, Simone Meeuwissen, Richard Geurts (alias “de polderkoning”) en Alexander Branderhorst wil ik bedanken voor de gezellige Ardennen-weekendjes en de vele wandelingen. Met name het fierljeppen zal me nog lang bijblijven (het kikkerdril zit nu nog in mijn oren). Kristel en Wouter, veel geluk met jullie kindje. De familie Broeren en de familie Hormes wil ik bedanken voor de altijd aanwezige interesse en gezelligheid, ook als ik weer eens een hele tijd niets van me liet horen.

Ad, ik kan me geen betere broer wensen. Ik ben blij dat jij en Angelique mijn paranimfen willen zijn. Bedankt voor jullie steun en liefde. Als laatste wil ik graag mijn ouders bedanken. Jullie interesse, enthousiasme en onvoorwaardelijke steun hebben veel voor me betekend. Mam, steeds meer merk ik hoeveel karaktereigenschappen ik van jou heb. Pap, ik wil nog vaak die bril zien die bijna verdwijnt in je gezicht als je weer eens helemaal in een deuk ligt om één van je eigen grappen. Maar ik heb gemerkt dat ik dat inmiddels ook al doe...

Maarten